DENSITY DEPENDENT DIFFERENTIATION OF MESENCHYMAL STEM CELLS TO ENDOTHELIAL CELLS

A thesis submitted to the University of Manchester for the degree of Doctor of Philosophy in the Faculty of Life sciences.

2010

Jemima Lois Whyte

CONTENTS

Title page **1**

List of contents **2**

List of figures **7**

Abstract **10**

Declaration **12**

Copyright Statement **12**

List of Abbreviations **13**

Acknowledgements **15**

1. CHAPTER 1: INTRODUCTION **17**

1.1. Adult Stem Cells **17**

1.2 Mesenchymal stem cells (MSCs) **19**

1.2.1. Tissue origin of MSCs **19**

1.2.2. Characterisation of MSCs **20**

1.2.3. Differentiation potential of MSCs **22**

1.2.3.1. Osteogenic differentiation of MSCs **25**

1.2.3.2. Chondrogenic differentiation of MSCs **25**

1.2.3.3. Adipogenic differentiation of MSCs **26**

1.2.3.4. Myogenic and neural differentiation of MSCs **27**

1.2.3.5. Vascular differentiation of MSCs **28**

1.3. Biological Roles of MSCs **28**

1.3.1. Involvement of MSCs during tissue repair **28**

1.3.2. Contribution of MSCs to vasculogenesis **30**

1.4. The vasculature **30**

1.4.1. Endothelial cells (ECs) **31**

1.4.2. Vascular smooth muscle cells (vSMCs) **36**

1.4.3. Vascular extracellular matrix **37**

1.5. Differentiation of MSCs along vascular lineages **38**

1.5.1. Differentiation of MSCs towards ECs **38**

1.5.2. Differentiation of MSCs towards vSMCs **39**

1.6. Regulation of the vascular differentiation of MSCs **40**

1.6.1. Growth factors **41**

1.6.1.1. VEGF and receptors **41**

1.6.1.2. PDGF and receptors **42**

1.6.2. Extracellular matrix **46**

1.6.3. Oxygen tension **46**

1.6.4. Mechanical strain **47**

1.6.5. Cell-to-cell contact **48**

1.6.5.1. Notch signalling **48**

1.7. Summary **51**

1.8. Aims **52**

2. CHAPTER 2: MATERIALS AND METHODS **54**

2.1. MATERIALS **54**

2.1.1. Cell lines **54**

2.1.2. Growth factors and inhibitors **54**

2.1.3. Primer Sequences **55**

2.1.4. Antibodies **56**

2.2. METHODS **57**

2.2.1. Cell plating **57**

2.2.2. MSC differentiation assay **57**

2.2.3. Polymerase chain reaction **58**

2.2.4. Immunoblot analysis **60**

2.2.5. Immunofluorescence microscopy **61**

2.2.6. Immunoprecipitation analysis **61**

2.2.7. Proteome array analysis **62**

2.2.8. Enzyme linked immunosorbent assays (ELISAs) **62**

2.2.9. Flow cytometry **62**

2.2.10. siRNA transfections **63**

2.2.11. VEGFR1 activation **63**

2.2.12. Notch activation **63**

2.2.13. DiI-Ac-LDL uptake **63**

2.2.14. Matrigel network formation assay **64**

2.2.15 Chorioallantoic membrane (CAM) assay **64**

2.2.16. Microscopy **66**

2.2.17. Transmission Electron Microscopy **66**

2.2.18. Statistics **66**

3. CHAPTER 3: RESULTS **69**

3.1. High cell density induced endothelial characteristics in MSCs **69**

3.2. MSC characterisation **71**

3.2.1. Morphological characterisation of MSCs **71**

3.2.2. Immunophenotypical characterisation of MSCs **71**

3.2.3. Differentiation capacity of MSCs **74**

3.3. MSCs cultured at high density had the potential to differentiate to ECs **76**

3.3.1. MSCs cultured at high density developed a cobblestone-like morphology **76**

3.3.2. High cell density induced MSCs to express VEGFR1 **76**

3.3.2.1. High cell density induced MSCs to express VEGFR1 transcripts **76**

3.3.2.2. High cell density induced MSCs to express VEGFR1 protein **78**

3.3.2.3. Localisation of VEGFR1 in MSCs cultured at high density **80**

3.3.3. High density enhanced VEGF-A secretion in MSCs **82**

3.3.4. High density enhanced vWF expression in MSCs **86**

3.3.4.1. High cell density enhanced vWF transcripts in MSCs **86**

3.3.4.2. High cell density enhanced vWF protein in MSCs **86**

3.3.4.3. Distribution of vWF in MSCs cultured at high density **88**

3.3.4.4. Transmission electron microscopy of MSCs cultured at high density **88**

3.3.5. High density induced VE-cadherin expression in MSC **91**

3.3.5.1. High density induced VE-cadherin expression in MSCs **91**

3.3.5.2. Distribution of VE-cadherin in MSCs cultured at high density **91**

3.3.6. High density enhanced PECAM-1 expression in MSCs **93**

3.3.6.1. High density enhanced PECAM-1 protein expression in MSCs **93**

3.3.6.2. Distribution of PECAM-1 in MSCs cultured at high density **96**

3.3.7. Functional properties of MSCs cultured at high density **96**

3.3.7.1. MSCs cultured at high density uptake ac-LDL **96**

3.3.7.2. MSCs pre-cultured at high density displayed enhanced networks **98**

3.3.7.3. High density MSCs induced VCAM-1 following TNFα exposure **98**

3.3.7.4. High cell density did not stimulate EC markers in HDFs **101**
3.4. High density MSCs maintained a moderately stable phenotype **101**
3.4.1. Re-plating at low density largely maintained EC marker expression **101**
3.4.2. MSC characterisation markers were decreased in MSCs at high density **104**
3.4.3. MSC density did not up-regulate other cell lineage differentiation markers **104**
3.4.4. High density MSCs could not be induced to differentiate to adipocytes **107**
3.4.5. High density MSCs could not be induced to differentiate to osteoblasts **107**
3.5. Discussion **111**
3.6. Summary **116**

4. CHAPTER 4: RESULTS **118**

4.1. Mechanisms regulating the differentiation of MSC to ECs **118**
4.2. MSC density-dependent differentiation to ECs occurred in two phases **119**
4.3. Involvement of VEGF-A in initiating MSC commitment to ECs **121**
4.3.1. Exposure to VEGF-A did not induce MSCs to express EC markers **121**
4.3.2. VEGF-A neutralisation did not alter EC marker expression **123**
4.3.3. VEGF-A siRNA knockdown did not alter EC marker expression **123**
4.4. Involvement of Notch signalling in initiating MSC commitment to ECs **126**
4.4.1. MSCs expressed Notch Receptors 1, 2 and 3 **126**
4.4.2. High density culture increased Notch signalling components in MSCs **126**
4.4.3. Notch signalling components fluctuated at high density **128**
4.3.4. Notch signalling inhibition decreased EC markers and VEGF-A secretion **128**
4.4.5. Notch receptor siRNA knockdown inhibited EC marker expression **131**
4.4.6. Notch activation stimulated MSCs at low density to express EC markers **134**
4.5. Involvement of VEGF-A in consolidating the EC fate. **136**
4.5.1. Sustained exposure to VEGF-A enhanced VEGFR1 expression **136**
4.5.2. Sustained VEGF stimulation regulated EC marker expression **138**
4.5.3. Notch and VEGF-A stimulated MSC differentiation to ECs over 14 days **138**
4.5.4. VEGF-A up-regulated PECAM-1 expression **140**
4.5.5. MSCs at high density up-regulated PDGFR expression and signalling **140**
4.5.6. VEGF-A-PDGFR signalling up-regulated PECAM-1 expression **143**
4.5.7. PDGFRα mediated PECAM-1 expression **143**
4.5.8. VEGF-A did not regulate Notch signalling **146**

4.6. Involvement of other mechanisms in density-dependent differentiation **146**

4.7. Discussion **153**

4.8. Summary **159**

CHAPTER 5: RESULTS **161**

5.1. Behaviour of Endothelialised MSCs in angiogenic environments **161**

5.2. Effects of in vitro Matrigel culture on MSC differentiation to ECs **162**

5.2.1. Endothelialised MSCs enhanced VE-cadherin in Matrigel **162**

5.2.2. Endothelialised MSCs expressed VEGFR2 in Matrigel **163**

5.2.3. Endothelialised MSCs decreased PECAM-1 in Matrigel **165**

5.3. Effect of *in ovo* Matrigel culture on MSC differentiation to ECs **165**

5.3.1. Endothelialised MSCs formed enhanced networks within the CAM **168**

5.3.2. Endothelialised MSCs promoted CAM vascularisation **168**

5.3.3. MSCs integrated into pre-formed endothelial networks **175**

5.4. Discussion **175**

5.5. Summary **181**

CHAPTER 6: FINAL DISCUSSION **183**

6.1. Potential therapeutic strategies **183**

6.2. Stem cell therapy **183**

6.3. Therapeutic manipulation **185**

6.4. Notch regulation of stem cell differentiation **186**

6.5. MSCs as a vascular progenitor cell **187**

6.6. Density dependent differentiation of MSCs to ECs *in vivo* **187**

6.7. Summary **191**

7.0. References **192**

Word count: 51,417

LIST OF FIGURES

CHAPTER 1: INTRODUCTION

1.1. Bone marrow MSCs differentiate to a number of different cell lineages *in vitro* **18**

1.2. MSCs are recuited from the bone marrow to sites of neovascularisation **21**

1.3. MSCs are heterogenous in terms of their multilineage differentiation potential **23**

1.4. Schematic diagram of the structure of blood vessels **32**

1.5. Specification pathways during generation of endothelium and blood cells **33**

1.6. Organisation of endothelial cell–cell junctions **35**

1.7. Structure of the VEGF receptors **43**

1.8. Structure of the PDGF receptors **45**

1.9. Model of the Notch signalling pathway **50**

CHAPTER 2: MATERIALS AND METHODS

2.1. The coverslip method for immunostaining cultured cells in the CAM assay **65**

CHAPTER 3: RESULTS

3.1. Morphological characterisation of MSCs **72**

3.2. Immunophenotypical characterisation of MSCs **73**

3.3. Differentiation capacity of MSCs **75**

3.4. MSCs cultured at high cell density developed a cobblestone-like morphology **77**

3.5. High cell density induced MSCs to express VEGFR1 transcripts **79**

3.6. High cell density induced MSCs to express VEGFR1 protein **81**

3.7. Localisation of VEGFR1 in MSCs cultured at high density **83**

3.8. VEGFR1 was localised to the Golgi apparatus in MSCs cultured at high density **84**

3.9. High density enhanced VEGF-A secretion in MSCs **85**

3.10. High density enhanced vWF expression in MSCs **87**

3.11. Distribution of vWF in MSCs cultured at high density **89**

3.12. Transmission electron microscopy of MSCs cultured at high density **90**

3.13. High density induced VE-cadherin expression in MSCs **92**

3.14. Distribution of VE-cadherin in MSCs cultured at high density **94**

3.15. High density enhanced PECAM-1expression in MSCs **95**

3.16. Distribution of PECAM-1 in MSCs cultured at high density **97**

3.17. MSCs cultured at high density uptake ac-LDL **99**

3.18. MSCs pre-cultured at high density displayed enhanced networks **100**

3.19. High density culture induced VCAM-1 following TNFα exposure in MSCs **102**

3.20. High cell density did not stimulate EC markers in HDFs **103**

3.21. High density MSCs maintained a stable phenotype **105**

3.22. MSC characterisation markers were decreased in MSCs cultured at high density **106**

3.23. MSC density did not up-regulate other cell lineage differentiation markers **108**

3.24. High density MSCs could not be induced to differentiate to adipocytes **109**

3.25. High density MSCs could not be induced to differentiate to osteoblasts **110**

CHAPTER 4: RESULTS

4.1. MSC density dependent differentiation to ECs occurred in two phases **120**

4.2 Exposure to VEGF-A did not induce MSCs to express EC markers **122**

4.3. VEGF-A neutralisation did not alter EC marker expression **124**

4.4. VEGF-A siRNA knockdown did not alter EC marker expression **125**

4.5. MSCs expressed Notch receptors 1, 2 and 3 **127**

4.6. High density MSC culture increased Notch signalling components **129**

4.7. Notch signalling components fluctuatuated at high density **130**

4.8. Notch signalling inhibition decreased EC markers and VEGF-A secretion **132**

4.9. Notch receptor siRNA knockdown inhibited EC marker expression **133**

4.10. Notch activation stimulated MSCs at low density to express EC markers **135**

4.11. Sustained exposure to VEGF-A enhanced VEGFR1 expression **137**

4.12. Sustained VEGF stimulation up-regulated EC markers **139**

4.13. Notch and VEGF-A stimulated MSC differentiation to ECs over 14 days **141**

4.14. VEGF-A up-regulated PECAM-1 expression **142**

4.15. MSC at high density up-regulated PDGFR expression and signalling **144**

4.16. VEGF-A-PDGFR signalling up-regulated PECAM-1 expression **145**

4.17. PDGFRα mediated PECAM-1 expression **147**

4.18. VEGF-A did not regulate Notch signalling **148**

4.19. Involvement of other mechanisms in density-dependent differentiation **149**

4.20. VEGFR signalling controls **150**

4.21. PDGFR signalling controls **151**

4.22. Notch signalling controls **152**

CHAPTER 5: RESULTS

5.1. Endotheliallised MSCs enhanced VE-cadherin in Matrigel **164**

5.2. Endothelialised MSCs potentially expressed VEGFR2 in Matrigel **166**

5.3. Endothelialised MSCs decreased PECAM-1 expression in Matrigel **167**

5.4. Endothelialised MSCs formed enhanced networks within the CAM **169**

5.5. VE-cadherin expression in endothelialised MSC networks within the chick CAM **170**

5.6. VE-cadherin localised to the cell surface in endothelialised MSCs within the CAM **171**

5.7. PECAM-expression in endothelialised MSCs within the chick CAM **172**

5.8. VEGFR2 expression in endothelialised MSCs within the chick CAM **173**

5.9. Endothelialised MSCs promoted CAM vascularisation **174**

5.10. MSCs integrated into preformed endothelial networks **176**

5.11. Endothelialised MSCs were detected on the CAM surface **177**

CHAPTER 6: FINAL DISCUSSION

6.1. Model of how Notch signalling initiates MSCs to EC commitment **190**

THE UNIVERSITY OF MANCHESTER

Abstract of thesis submitted by Jemima Lois Whyte for the degree of Doctor of Philosophy entitled 'Density dependent differentiation of mesenchymal stem cells to endothelial cells' September 2010.

The differentiation of mesenchymal stem cells (MSCs) to endothelium is a critical but poorly understood feature of tissue vascularisation and considerable scepticism still remains surrounding this important differentiation event. Defining features of endothelial cells (ECs) are their ability to exist as contact-inhibited polarised monolayers that are stabilised by intercellular junctions, and the expression and activity of endothelial markers.

During vasculogenesis, communication between MSCs and differentiated ECs or vascular smooth muscle cells, or between MSCs themselves is likely to influence MSC differentiation. In this study, the possibility that cell density can influence MSC differentiation along the EC lineage was examined. High density plating of human bone marrow-derived MSCs induced prominent endothelial characteristics including cobblestone-like morphology, enhanced endothelial networks, acetylated-low density lipoprotein uptake, vascular growth and stimulated expression of characteristic endothelial markers.

Mechanistically, this density-dependent process has been defined. Cell-cell contact-induced Notch signalling was a key initiating step regulating commitment towards an EC lineage, whilst VEGF-A stimulation was required to consolidate the EC fate. Thus, this study not only provides evidence that MSC density is an essential microenvironmental factor stimulating the *in vitro* differentiation of MSCs to ECs but also demonstrates that MSCs can be differentiated to a functional EC. Taken together, defining how these crucial MSC differentiation events are regulated *in vitro*, provides an insight into how MSCs differentiate to ECs during postnatal neovascularisation and an opportunity for the

therapeutic manipulation of MSCs *in vivo*, enabling targeted modulation of neovascularisation in ischaemia, wound healing and tumourigenesis.

Declaration

No portion of the work referred to in the thesis has been submitted in support of an application for another degree or qualification of this or any other university or other institute of learning.

Copyright Statement

i. The author of this thesis (including any appendices and/or schedules to this thesis) owns any copyright in it (the "Copyright") and she has given The University of Manchester the right to use such Copyright for any administrative, promotional, educational and/or teaching purposes.

ii. Copies of this thesis, either in full or in extracts, may be made **only** in accordance with the regulations of the John Rylands University Library of Manchester. Details of these regulations may be obtained from the Librarian. This page must form part of any such copies made.

iii. The ownership of any patents, designs, trade marks and any and all other intellectual property rights except for the Copyright (the "Intellectual Property Rights") and any reproductions of copyright works, for example graphs and tables ("Reproductions"), which may be described in this thesis, may not be owned by the author and may be owned by third parties. Such Intellectual Property Rights and Reproductions cannot and must not be made available for use without the prior written permission of the owner(s) of the relevant Intellectual Property Rights and/or Reproductions.

iv. Further information on the conditions under which disclosure, publication and exploitation of this thesis, the Copyright and any Intellectual Property Rights and/or Reproductions described in it may take place is available from the Dean of the Faculty of Life Sciences.

List of Abbreviations

α SMA	Smooth muscle alpha actin
Ac-LDL	Acetylated low density lipoprotein
AlkP	Alkaline phosphatase
AP2	Adipocyte protein 2
Bodipy	Boron-dipyrromethene
BM	Bone marrow
BMP	Bone morphogenetic proteins
CAM	Chorioallantoic membrane
Col2A1	Type 2 collagen alpha 1
Col9A2	Type 9 collagen alpha 2
DAPI	4'6-diamidino-2-phenylindole
DAPT	N-[N-(3,5-Difluorophenacetyl-L-alanyl)]-S-phenylglycine t-butyl ester.
DiI	1,1'-dioctadecyl-3,3,3',3'-tetramethyl-indocarbocyanine perchlorate
DLL	Delta-like
ECs	Endothelial cells
ECM	Extracellular matrix
EDTA	Ethylene-diamine tetra-acetic acid
EGF	Epidermal growth factor
ESCs	Embryonic stem cells
EPCs	Endothelial progenitor cells
FABP-4	Fatty acid binding protein 4
FITC	Fluorescein Isothiocyanate
GAPDH	Glyceraldehyde-3-phosphate dehydrogenase
g	Centrifugal force (gravity)
HCAECs	Human coronary artery endothelial cells
HDFs	Human dermal fibroblasts
HES	Hairy/enhancer of split
HEY	Hairy/enhancer-of-split related with YRPW motif 1
HIF	Hypoxia inducible factor
HUVECs	Human umbilical vein endothelial cells
HSCs	Haematopoietic stem cells
ICAM	Intracellular adhesion molecule
JAG	Jagged
MSC	Mesenchymal stem cells
mM	Millimolar
NICD	Notch intracellular domain
NRP	Neuropilin
PBS	Phosphate buffered saline
PCR	Polymerase chain reaction
PDGF	Platelet derived growth factor
PDGFR	Platelet derived growth factor receptor

PE	Phycoerythrin
PECAM-1	Platelet/endothelial cell adhesion molecule 1(CD31)
PPAR-γ	Peroxisome proliferator-activated receptor-gamma
RPM	Revolutions per minute
RTK	Receptor tyrosine kinase
RT-PCR	Reverse transcription polymerase chain reaction
Scr	Scrambled
siRNA	Small interfering RNA
SMC	Smooth muscle Cell
SM-MHC-1	Vascular smooth muscle myosin heavy chain 1
TGFβ	Transforming growth factor beta
TNFα	Tumour necrosis factor alpha
VCAM	Vascular cell adhesion molecule
VE-Cadherin	Vascular endothelial cadherin (CD144)
VEGF	Vascular endothelial growth factor
VEGFR	Vascular endothelial growth factor receptor
vSMC	Vascular smooth muscle cell
vWF	Von Willebrand factor
μg	Microgram
μl	Microlitres
μM	Micromolar
WP bodies	Weibel Palade bodies
QPCR	Quantitative RT-PCR

Acknowledgements

Firstly I would like to thank my supervisor Professor Cay Kielty for her guidance, all her time and her continual support throughout my PhD. I am indebted to Steve Ball for his expert training and his limitless advice and encouragement. I am extremely grateful to Adrian Shuttleworth, Keith Brennan and my advisor Stephen Taylor for all their very helpful discussions, their enthusiasm and their novel ideas about my project. Thank you to the Manchester University flow cytometry, bioimaging and electron microscopy facilities for providing an excellent service. I would also like to thank all Kielty lab members past and present for making my four years such a memorable experience. Lastly I would like to thank my parents for the endless amount of love and support they gave me throughout my PhD.

I would like to acknowledge the Wellcome Trust for their funding of the project.

CHAPTER 1

INTRODUCTION

CHAPTER 1: INTRODUCTION

1.1. Adult stem cells

Stem cells are generally defined as clonogenic, undifferentiated cells capable of self-renewal and able to give rise to one or more types of differentiated cell progeny (Barry *et al* 2003). Embryonic stem cells (ESCs) are pluripotent, that is, they have the ability to give rise to cell types and tissues of all three germ layers of the body (ectodermal, mesodermal and endodermal origins) and they are capable of unlimited proliferation in an undifferentiated state (Stojkovic *et al* ., 2004). Adult mesenchymal stem cells (MSCs) however are much more committed, persisting throughout life and capable of differentiating into a more restricted number of cell lineages and subsequent tissues of predominantly mesodermal origin (Kolf *et al*., 2007). Such tissues include bone (Friedman *et al* ., 2007), cartilage (Baksh *et al* ., 2004; Tuan *et al* ., 2003; Hardingham *et al* ., 2006; Oldershaw *et al*., 2008), fat (Hong *et al* ., 2005; Jakkaraju *et al* ., 2005; McBeath *et al* ., 2004), tendon (Altman *et al* ., 2002) and muscle, for example vascular smooth muscle (Dezawa *et al* ., 2005; Li *et al* ., 2006). More recently however, MSCs were shown to be capable of differentiating along neural (ectodermal) (Dezawa *et al* ., 2004) and endothelial lineages (Al-Khaldi *et al* ., 2003; Alviano *et al* ., 2007; Bai *et al* ., 2009; Chen *et al* ., 2009; Chung *et al* ., 2009; Lozito *et al* ., 2009a; b; Ohata *et al*., 2009; Oswald *et al* ., 2004; Silva *et al* ., 2005; Wu *et al* ., 2005; Xu *et al* ., 2009; Yue *et al* ., 2008; Zhang *et al* ., 2008) (Figure 1.1).

Adult stem cells have been shown to occupy specific niches within most human tissues and organs, including bone marrow (BM), heart, brain, adipose tissues, muscles, skin, eyes, kidneys, lungs, liver, gastrointestinal tract, pancreas, breast, ovaries, prostate, testis, umbilical cord and vascular walls (Baksh *et al* ., 2004; Chen *et al* ., 2009; Crisan *et al* ., 2008; Mimeault *et al* ., 2006; 2007). The best characterised adult stem cells are the BM-derived stem cells, which mainly comprise haematopoietic stem cells (HSCs) and MSCs, as well as cardiac stem cells and neural stem cells that are localised in heart and brain, respectively (Mimeault *et al* ., 2006). This introduction focuses on

Figure 1.1

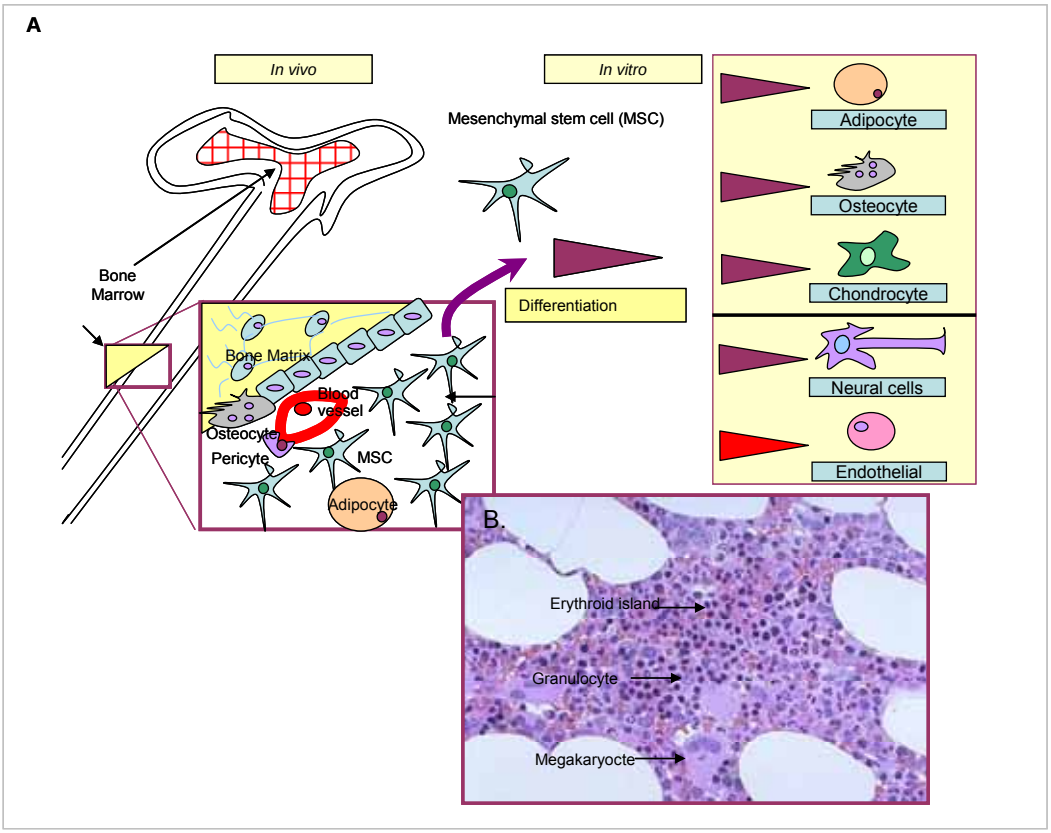

Figure 1.1. *Bone marrow MSCs can be induced to a number of different cell lineages in vitro*

(A) Schematic showing how MSCs can be isolated from a number of different cell types within the bone marrow stroma (black arrow) and induced either chemically or following exposure to vascular growth factors to differentiate to a number of different cell types *in vitro*. A micrograph of red bone marrow containing haematopoietic tissue is depicted in **B** and is taken from www.aamdsglossary.co.uk.

current understanding of the differentiation of adult MSCs along vascular cell lineages.

1.2. Mesenchymal stem cells (MSCs)

1.2.1. Tissue origin of MSCs

Considerable inconsistency has occurred between the nomenclature and biological properties of MSCs. Recently the terms multipotent mesenchymal stromal cells and mesenchymal progenitor cells have also been coined as alternative nomenclature for MSCs. (Erices *et al*, 2000; Horwitz *et al*, 2005). In this thesis, MSCs refers to the plastic-adherent cells isolated from BM with multipotent differentiation capacity *in vitro* as defined by Caplan *et al*, 1991 and Dominici *et al*, 2006.

MSCs have been located in BM, umbilical vein, muscle, trabecular bone, adipose tissue, dermis, periosteum, adult peripheral blood, synovial membrane, periodontal ligament, liver, lung, deciduous teeth and vascular walls (van Vliet *et al* ., 2007; Schaffler *et al* ., 2007; Dhawan *et al* ., 2005; Peault *et al* ., 2007; Beltrami *et al*., 2003; Leri *et al* ., 2005; Kim *et al* ., 2005a; Brittan *et al* ., 2002; Griffiths *et al* ., 2005; Bussolati *et al* ., 2005; Herrera *et al* ., 2006; Koblas *et al* ., 2007). MSCs are typically isolated from the stromal fraction of adult BM, and most insights into their biological properties and characteristics have been obtained from BM-derived MSCs. Aside from being one of the first documented sources of MSCs, BM is considered to be one of the most enriched and accessible stem cell sources. Murine MSCs are obtained from the femurs and tibias of mice by flushing the marrow out of these bones with culture medium, then selecting and expanding the MSC population by cell culture techniques. Human MSCs can similarly be obtained by taking aspirates of BM from the iliac crest of donors (Barry *et al*, 2003).

BM is the flexible tissue found in the hollow interior of bones. There are two types of BM: yellow BM (a complex heterogeneous cellular milieu forming a niche comprising HSCs, adipocytes, osteoblasts, endothelial cells (ECs), endothelial progenitor cells (EPCs), vascular smooth muscle cells (vSMCs), and MSCs) and red BM (comprising red blood

cells, platelets and most white blood cells). Both types of BM contain numerous blood vessels and capillaries (see Figure 1.1). The stroma of the BM is all tissue not directly involved in haematopoiesis (The formation of blood cell components) which includes the yellow BM, in addition to stromal cells located in the red BM (Wilson *et al* ., 2006). In fresh BM, MSCs account for only 0.01-0.0001% of nucleated marrow cells (Barry *et al*, 2003). However the BM is still considered the most accessible and enriched source of MSCs. Although rare, MSCs serve many important functions within the BM, including providing mechanical support for the differentiating HSCs in marrow, and regulating the maturation of haematopoietic cells. In addition, MSCs also play a role in the maintenance of tissues in the adult organism, being involved in the repair of microfractures of bone that occur on a daily basis, as well as repairing more occasional bone fractures (Shanti *et al*., 2007). In response to injury, a number of studies have shown how MSCs can be mobilised from the BM leading to subsequent migration, engraftment and differentiation at sites of postnatal neovascularisation. Growth factors and cytokines such as vascular endothelial growth factor (VEGF) have been strongly implicated as signals that mediate this response (Figure 1.2) (Mace *et al* ., 2009; Moore *et al* ., 2001; Raafi *et al* ., 2002)

1.2.2. Characterisation of MSCs

The cellular heterogeneity of the BM means that, in order to isolate populations of MSCs, other contaminating cell types must be removed. One simple method of isolating MSCs relies on the fact that MSCs selectively adhere to plastic surfaces, whereas haematopoietic cells do not adhere and can therefore be removed through culture medium changes. Alternatively, mononuclear cells can be sorted based on their density and enriched by centrifugation over a Percoll gradient (Barry *et al*, 2003). However these methods are relatively crude; and more specific methodologies employ antibodies directed against defined cell surface expressed antigens to isolate selected populations of MSCs. These techniques may involve sorting BM populations by fluorescence activated cell sorting, or magnetic bead based sorting applications, either by positively

Figure 1.2

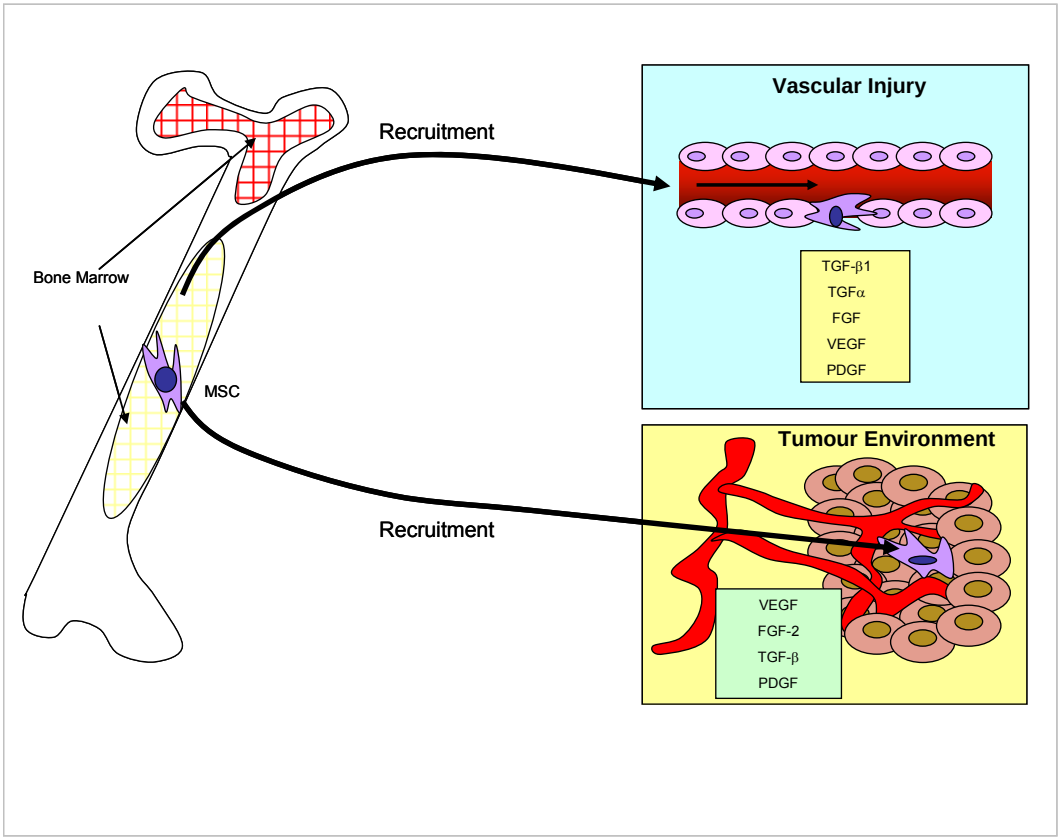

Figure 1.2. *MSCs are recuited from the bone marrow to sites of neovascularisation.*

Schematic diagram showing MSC recruitment from the bone marrow to sites of postnatal neovascularisation. Once MSCs reach these sites it is thought that they differentiate to ECs and such differentiation events are largely controlled by microenvironmental factors present within these environments including vascular growth factors.

selecting for MSC cell surface antigens and/or by immuno-depletion of cells expressing haematopoietic and/or other lineage antigens (Baksh *et al* ., 2004). Typically, cell surface markers used to identify the MSC fraction include CD13, CD29, CD44, CD54, CD63, CD73, CD105, CD106, CD140b, CD166 and Stro-1 (Dominici *et al* ., 2006; Delorme *et al* ., 2008). However, none of these epitopes individually is considered a specific marker for MSCs since they have also been detected in a range of differentiated mesenchymal cell types. To date, no single marker that definitively designates MSCs *in vivo* or *in vitro* has been identified, leading to significant difficulties in identifying MSCs during their isolation and purification. Many groups have reported varying degrees of heterogeneity in their MSC cultures after isolation and purification, resulting in different expansion and differentiation capabilities (Ho *et al* ., 2008; Shanti *et al* ., 2007; Phinney *et al* ., 2007b).

1.2.3. Differentiation potential of MSCs

As previously mentioned, MSCs have the potential to differentiate into a restricted number of cell lineages of mesodermal origin including bone, cartilage, fat and muscle (Figure 1.1). It is important to note that different populations of MSCs are heterogenous in terms of their multilineage differentiation potential. For instance, it has been reported (Baksh *et al* ., 2004) that only one-third of BM-derived MSC clones are multipotent, having the capacity to differentiate to osteogenic, chondrogenic and adipogenic lineages, whilst the remainder displayed a bi-lineage (osteogenic/chondrogenic) or uni-lineage osteogenic potential (Figure 1.3). In addition, a subset of MSCs has been identified which appeared to possess pluripotency, giving rise to adipocytes, osteoblasts, chondrocytes, endothelial cells, skeletal and cardiac muscle cells, neural cells, hepatocytes and epithelial cells (Baksh *et al* ., 2004; Charbord et al., 2010). However, these cells are extremely rare and may arise from fusion with cells in contact with MSCs, cell reprogramming or the selection of rare vestigial embryonic stem cells that have homed to the bone marrow (Charbord et al., 2010). Recent data indicates that proliferating MSCs may be primed to the adipogenic, osteogenic, chondrogenic and

Figure 1.3

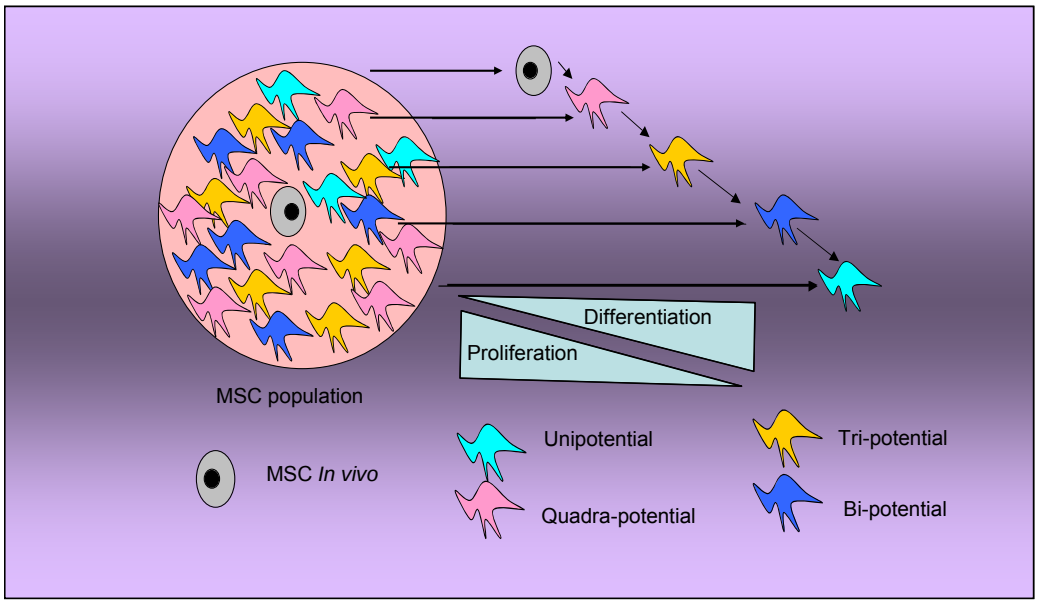

Figure 1.3. *MSCs are heterogenous in terms of their multilineage differentiation potential.*

MSCs comprise cell populations which have different differentiation potentials (i.e., quadrapotential, tripotential, bipotential or uni-potential) (Baksh *et al* ., 2004). Using appropriate *in vitro* differentiation culture conditions, all or a subset of these MSCs may be isolated.

vascular lineages, endogenously expressing a subset of genes associated to the differentiation pathways to which they can commit (Delorme et al., 2009). The differentiation potential of MSCs can vary throughout life, with older cells generally having a more limited differentiation potential. In addition, species differences, such as human cells compared to murine cells, the tissue source of the cells, such as BM compared to umbilical vein, and variations in isolation and culture techniques can all contribute to differences in MSC differentiation capacity. There are currently no culture conditions that have been described which can maintain MSC multipotency over time. Because of the lack of ability to distinguish and separate multi, bi and unipotent cells, directed differentiation currently is unlikely to give homogenous populations for regenerative purposes **(**Kaltz et al., 2010)**.** Recently, genome wide gene expression analysis identified novel markers enriched in unipotent MSCs capable of differentiating only to osteoblasts (integrin subunit alpha II) or in bipotent MSCs capable of differentiating to both adipocytes and osteoblasts (Notch3). These studies may facilitate the development of more homogenous MSC populations for cell therapy (Kaltz et al., 2010). The intrinsic ability of MSCs to self-renew or to differentiate into different cell types, has generated much excitement and promise as a potential source of cells for cell-based therapeutic strategies. Stem cell therapy can be defined as the treatment of disease by the mobilisation or transplantation of autologous (donor and host (recipient) are the same) or allogeneic (donor and host are different) stem cells into a host. It is noteworthy that neither autologous nor allogeneic MSCs induce any significant immunoreactivity in the host upon local transplantation or systemic administration, since studies indicate that MSCs are immune-privileged with low major Histocompatibility Complex I and no major Histocompatibility Complex II (Uccelli *et al*., 2007). Some striking examples of the therapeutic use of MSCs have been reported, both in mammals and in humans covering a broad spectrum of disorders (Mimeault *et al* ., 2006; Li *et al*., 2009a; Sasaki *et al* ., 2008; Shoji *et al*., 2010; Xu *et al* ., 2010; Wakabayashi *et al* ., 2010; Zhang *et al* ., 2010)).

1.2.3.1. Osteogenic differentiation of MSCs

Bone formation (osteogenesis) is a complex process involving three main steps: the production of the extracellular organic matrix (osteoid); mineralisation of the matrix to form bone; and bone remodelling by resorption and reformation. The cellular activities of osteoblasts, osteoblasts, and osteoclasts are essential to the process. Osteoblasts synthesise the collagenous precursors of bone matrix and also regulate its mineralisation (Caplan *et al* ., 2001). Osteogenic differentiation of MSCs can be induced *in vitro* by treating a monolayer culture with osteogenic differentiation media, standardly composed of dexamethasone, ascorbic acid-2-phosphate and β-glycerophosphate. Mineralised deposits and an osteoblastic morphology can appear after a week, accompanied by an increase in bone-specific alkaline phosphatase (ALKP) activity and the activation of bone-specific genes such as osterix, core binding factor α1, osteopontin, osteocalcin and bone sialoprotein (Barry *et al*, 2003). Recently, osteogenic differentiation has also shown to be regulated by the bone morphogenetic proteins (BMPs) 2 and 6 (Caplan *et al* ., 2001; Friedman *et al* ., 2006), as well as environmental factors including morphogenetic signals from chondrocytes, (Zachos *et al* ., 2006; Solursh *et al* ., 1975; Gerstenfeld *et al* ., 2002; 2003) exposure to hypoxia (1% oxygen) (Potier *et al* ., 2007) and collagen types I and III (Kundu *et al* ., 2006; Jager ., 2005). Osteogenic differentiation can be demonstrated by von Kossa staining, a stain for calcium in mineralised tissue which utilises silver nitrate solution followed by sodium thiosulphate. Calcified bone but not osteoid is stained brown to black. Alternatively alizarin red staining can be utilised to detect calcium deposits (Zachos *et al* ., 2006).

1.2.3.2. Chondrogenic differentiation of MSCs

The formation of cartilage, or chondrogenesis, is an orchestrated molecular and cellular process that shapes musculoskeletal tissues during embryogenesis (Goldring *et al* ., 2006). This complex process is controlled by cellular interactions with the surrounding matrix, growth and morphogenetic factors, and other environmental cues that modulate

cellular signalling pathways and transcription of specific genes in a temporal-spatial manner. Chondrogenesis can be chemically induced by forcing aggregation of 200,000 to 300,000 MSCs in chondrogenic medium, usually containing the presence of dexamethasone, ascorbic acid phosphate, bovine insulin, transferrin, selenous acid, linoleic acid and bovine serum albumin (Barry *et al*, 2003). Further additives to the medium include sodium pyruvate, proline, L-glutamine and transforming growth factor (TGF-β) 1 (Goessler *et al* ., 2005; Mauck *et al* ., 2006). The TGF-β superfamily such as TGF-β1, TGF-β2, insulin-like growth factor-1 (Longobardi *et al* ., 2003) and the BMPs seem to play a crucial role in inducing and maintaining chondrogenic differentiation (Reddi *et al*, 1994; Hunziker *et al*, 2000; Worster *et al* ., 2000). Environmental factors such as morphogenetic signals from chondrocytes (Hwang *et al* ., 2007) and hyaluronan (Grigolo *et al* ., 2003) have also been shown to be involved in chondrogenic differentiation. In the majority of these studies, chondrogenic differentiation has been characterised by the emergence of cartilage-specific markers, such as the expression and deposition of collagen type II (Col2A1), collagen type IX (Col9A2), aggrecan, and other sulphated proteoglycans (Mauck *et al* ., 2006).

1.2.3.3. Adipogenic differentiation of MSCs

Adipogenesis can be chemically induced by treating MSCs twice weekly for three weeks, with a medium supplemented with dexamethasone, isobutylmethylxanthine, insulin and a peroxisome proliferation activated receptor gamma (PPARγ) agonist. Alternatively, adipogenesis can be stimulated by three cycles of three days in culture with induction medium (contains indomethacin), followed by three days in maintenance media (contains insulin) (Jackson *et al* ., 2007). BMP7 has also been shown to stimulate adipogenesis using a serum-free high-density micro-mass culture, a differentiation system that favours chondrogenic development (Neumann *et al* ., 2007). Adipogenic differentiation can be determined by screening for a series of genes shown to increase with adipogenic differentiation, including PPARγ, CCAAT enhancer-binding protein-α, acylCoA synthetase, lipoprotein lipase, and Adipocyte protein 4 and 2 (AP2/AP4). The

formation of lipid droplets can also be specifically stained with fresh Oil Red-O solution or Sudan Red. Alternatively, staining can be performed for Bodipy493/503 which stains lipid droplets green and immunostaining for fatty acid binding protein 4 (FABP-4) (Sekiya *et al* ., 2004).

1.2.3.4. Myogenic and neural differentiation of MSCs

MSC differentiation towards muscle and neural cells has been less well characterised, however, MSCs can be chemically differentiated *in vitro* to a cardiomyocyte-like phenotype by treatment with medium containing 5-azacytidine (10 µmol/l), basic fibroblast growth factor (10 µg/l), and amphotericin (0.25 mg/l) for two weeks (Barry *et al*, 2003). In addition, Wnt3a (Shang *et al* ., 2007) and a muscle-specific micro-RNA, miRNA206 (Kim *et al* ., 2006), have also been shown to be sufficient to induce myogenic differentiation in MSCs by activating the muscular regulatory genes Pax3, Pax7, MyoD, Myf5, myogenin and the major Histocompatibility Complex. Damaged rat skeletal muscle is endowed with the capacity to induce myogenic differentiation of BM-derived mesenchymal progenitors. Conditioned medium prepared from skeletal muscle previously damaged by a barium chloride injection, resulted in a time-dependent change from fibroblast-like into elongated multinucleated cells. A transient increase in the number of MyoD positive cells, and the subsequent onset of myogenin, α-actinin, and myosin heavy chain expression occurred (Santa Maria *et al* ., 2004). Direct cell-cell contact of rat MSCs with either cardiomyocytes or SMCs also invoked MSC differentiation, as judged by their expression of a panel of cardiomyocyte markers including α-actin, desmin and cardiac Troponin T (Wang *et al* ., 2006; Xu *et al*., 2004). These findings indicate that either physical contact or soluble chemical factors can determine the differentiation fate of MSCs.

Mesenchymal-like cells from umbilical cord blood have been shown to be capable of differentiation towards neural cells, with this capability being mediated through the protein kinase A signal transduction pathway. Whilst activation of protein kinase A via

experimental cyclic adenosine monophosphate-activated protein up-regulation led to outgrowth of neurite-like structures as well as expression of neural marker genes, blocking protein kinase A activity completely abolished all these features (Wang *et al* ., 2007a). Neuron-like morphologic changes and neuronal markers (growth-associated protein-43, neuron-specific nuclear protein and neurofilament 200 kDa) have also been shown in MSCs cultured for ten days with different neurotrophic factors, including brain-derived neurotrophic factor, epidermal growth factor and neural growth factor (Choong *et al* ., 2007).

1.2.3.5. Vascular differentiation of MSCs

MSC differentiation towards vascular cell lineages is controversial and the mechanisms regulating MSC differentiation to vascular cells are ill defined, however it is becoming increasingly recognised that MSCs make an important contribution to promoting postnatal vascularisation during ischaemic myocardial tissue regeneration, wound healing and tumour vasculogenesis. It is therefore crucial to understand mechanisms controlling MSC differentiation into vascular cells to enable their therapeutic manipulation. The vasculature and its resident cells will be described (see Chapter 1: Introduction; section 1.4), followed by the current understanding of the vascular differentiation potential of MSCs.

1.3. Biological roles of MSCs

1.3.1. Involvement of MSCs during tissue repair

It has been well documented that MSCs are involved in revascularisation of injured tissues such as in a wound site, during ischaemic myocardial tissue regeneration and also during pathological situations such as in tumour neovascularisation (Liechty *et al*., 2000; Toma *et al*., 2002; Nagaya *et al*., 2004). Myocardial infarction or coronary artery occlusion induces tissue ischaemia, resulting in the permanent loss of a proportion of cardiomyocytes and a compromised contractile function of the remaining cells. Several

studies have shown that local administration of human MSCs into the infarcted myocardium resulted in their differentiation towards cardiomyocytes, mediated by platelet derived growth factors (PDGFs) signalling through the PDGF receptors (PDGFRs), (PDGF-AB induced PDGFR$\alpha\alpha$ and/or PDGFR$\alpha\beta$), which improved cardiac function (Liechty *et al* ., 2000; Toma *et al* ., 2002). Furthermore, MSC administration also stimulated revascularisation of the injured myocardium, presumably influenced by VEGF-A released from the ischaemic tissue (Nagaya *et al* ., 2004). Thus VEGF-A signalling is a crucial determinant in regulating the recruitment and incorporation of MSCs into new blood vessel walls, which may also subsequently control the differentiation of MSC into ECs. As well as MSCs being regulated by VEGF-A, MSCs may also be an important source of VEGF-A during neovascularisation. MSCs can secrete several arteriogenic factors, such as VEGF, which may stimulate neovascularisation from pre-existing arterial vessels (Kinnaird *et al* ., 2004).

During pathological situations such as tumour vasculogenesis, the formation of tumour blood vessels and associated connective tissue stroma is regulated by VEGF-A, which is expressed by the majority of human tumours. As the tumour enlarges above one to two millimetres in size, an increase in the level of hypoxia leads to increased VEGF-A expression, which stimulates blood vessel formation to provide nutrients and oxygen for growth. Several studies have documented that MSCs are involved in tumour vasculogenesis, being actively recruited to areas of blood vessel growth (neovascularisation), and differentiating into platelet endothelial adhesion molecule-1 (PECAM-1) positive, von Willebrand factor (vWF) positive endothelial-like cells (Annabi *et al* ., 2004). MSCs have been shown to significantly enhance vascularisation in a murine tumour models, engrafting into tumour lesions and becoming incorporated into the tumour stroma (Studeny *et al* ., 2002; Hung *et al* ., 2005).

1.3.2. Contribution of MSCs to vasculogenesis

In the adult, two separate mechanisms are responsible for driving neovascularisation. In the first, differentiated vascular cells derived from pre-existing vessels are utilised, a process known an angiogenesis. The second involves the recruitment of undifferentiated BM-derived cells and is known as vasculogenesis. During angiogenesis, ECs in pre-existing blood vessels are activated by VEGF, and such activation leads to local EC proliferation and migration to form new vessel sprouts, then primitive tubular vascular structures. These immature vascular structures subsequently secrete PDGF-BB, inducing proliferation and recruitment of PDGFRβ-positive mural cells (vSMCs or pericytes), from vessel walls (Ball *et al* ., 2007a). These mural cells surround and coat the immature endothelial tubes, promoting EC survival, stability and maturation (Hellstrom *et al* ., 1999).

Adult vasculogenesis in contrast is driven by local tissue hypoxia and this is presumed to be mediated by increased VEGF release (Tepper *et al*., 2005). Local VEGF release creates a chemoattractive gradient, which has been shown to mobilise BM-derived EPCs into the circulation, where they form tubular vessels and connect to the existing vasculature (Asahara *et al*., 1999). During severe hypoxia, such as at a wound site, within a tumour environment or in ischaemic tissue disease, it is proposed that a proportion of neovascularisation occurs by vasculogenesis and may involve MSCs.

During vasculogenesis, MSC recruitment and differentiation has been demonstrated to be mediated by VEGF-induced signalling. However as previously reported, MSCs may not express cell surface VEGF receptors (VEGFRs) (Asahara *et al* ., 1999), therefore such signalling is likely to occur by VEGF-induced PDGFR signalling (Ball *et al* ., 2007c).

1.4. The vasculature

The adult vascular system is composed of arterial, venous and lymphatic compartments, which together provide oxygen and nutrients to peripheral organs, remove carbon

dioxide and waste products and maintain an immune barrier to defend the host against foreign organisms. The vascular system comprises an organised hierarchical structure of arteries, capillaries and veins. The capillary bed is composed solely of ECs, occasionally associated with an outer covering of pericytes. These simple capillary tubes are surrounded by a basement membrane. Larger blood vessels such as arteries have three distinct cellular layers (Figure 1.4). ECs and the subendothelial extracellular matrix (ECM) form the intimal layer (tunica intima), which is surrounded by an outer ring of vSMCs interspersed with elastic fibres that is known as the medial layer (tunica media). An outer adventitial layer (tunica adventitia) encases the blood vessel and is composed primarily of fibroblasts and collagen-rich connective tissue (Eichmann *et al* ., 2005). The size of the vessel wall varies according to the location and function, for example the aorta is subject to high intra-vessel pressures hence there is a need for elastic recoil and thick vessel walls. In comparison, veins are subject to low intra-vessel pressure and therefore have thin vessel walls.

1.4.1. Endothelial cells (ECs)

All blood vessels are lined with ECs and these cells are thought to derive from a common Flk-1 +ve/ E-cadherin +ve mesodermal precursor (Figure 1.5). Haemogenic endothelial cells are specified from cells already expressing endothelial markers, which in turn generate blood cells (Eilken et al., 2009). EPCs are thought to derive from a non haematopoietic origin (Urbich *et al* ., 2004; Khakoo *et al* ., 2005; Ribatti *et al* ., 2007). However, controversy exists with respect to the identification and the origin of ECPs, which are isolated from peripheral blood mononuclear cells by cultivation in medium favouring endothelial differentiation (Urbich *et al* ., 2004; Khakoo *et al* ., 2005). Overall, there is consensus that EPCs can derive from the BM and that CD133/VEGFR2 cells represent a population with endothelial progenitor capacity. However, evidence suggest that there are additional BM-derived cell populations (e.g. myeloid cells) within the blood, which also can give rise to ECs (Schmeisser ., 2001). Moreover, non-bone marrow-derived cells with endothelial characteristic were isolated from the peripheral blood. This

Figure 1.4

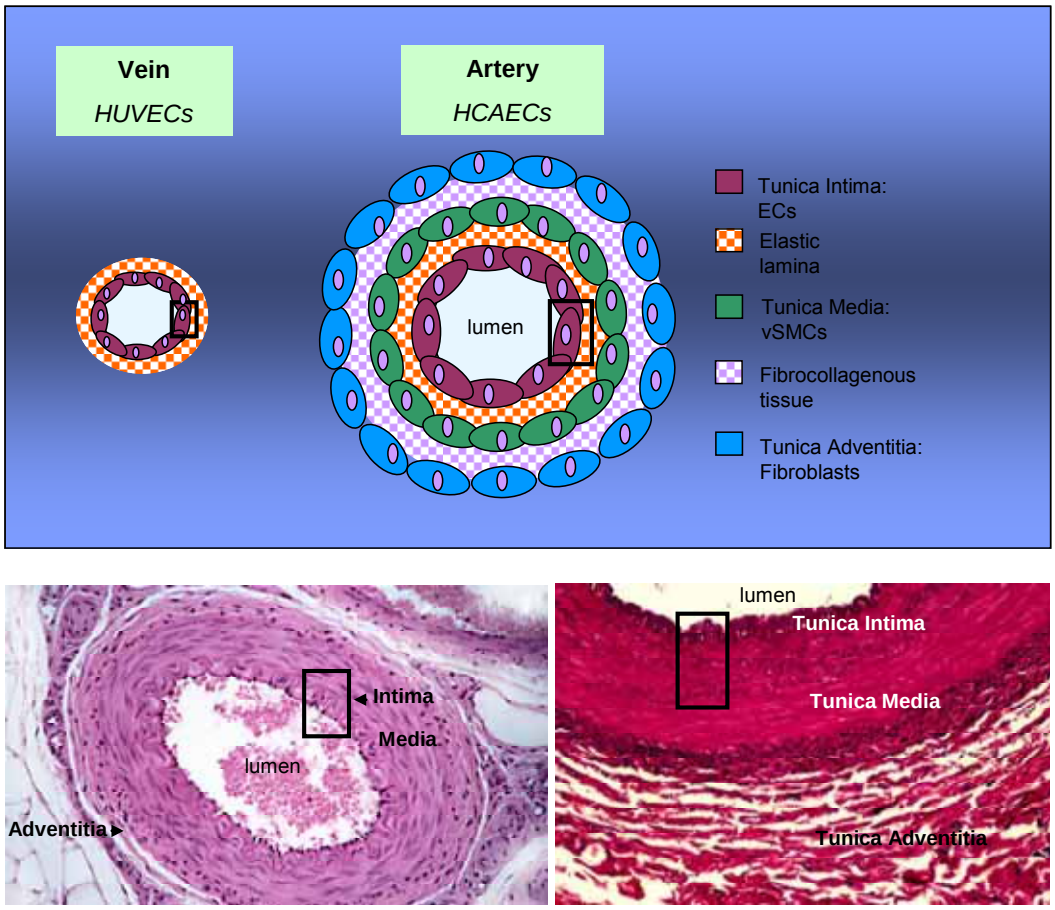

Figure 1.4. *Schematic diagram of the structure of blood vessels.*

ECs form a lumen in blood vessels. They can either exist in a simple organisation surrounded by a basal lamina as in a vein (examples include the human umbilical vein endothelial cells (HUVECs) or as a relatively more complex organisation surrounded by layers of mural cells as in an artery (examples include the human coronary artery endothelial cells (HCAECs). The ECs and basement membrane constitute the tunica intima, the thick ring of vSMCs encasing the endothelial layer constitutes the tunica media while the outer layer of fibroblasts and connective tissue constitutes the tunica adventitia. The black box depicts ECs. The lower panels depict two different cross sectional images of arteries, one at low magnification (taken from http://blog.lib.umn.edu) and one at high magnification (taken from http://cccla.hostrocket.com) depicting the different intimal, medial and adventitial layers.

Figure 1.5

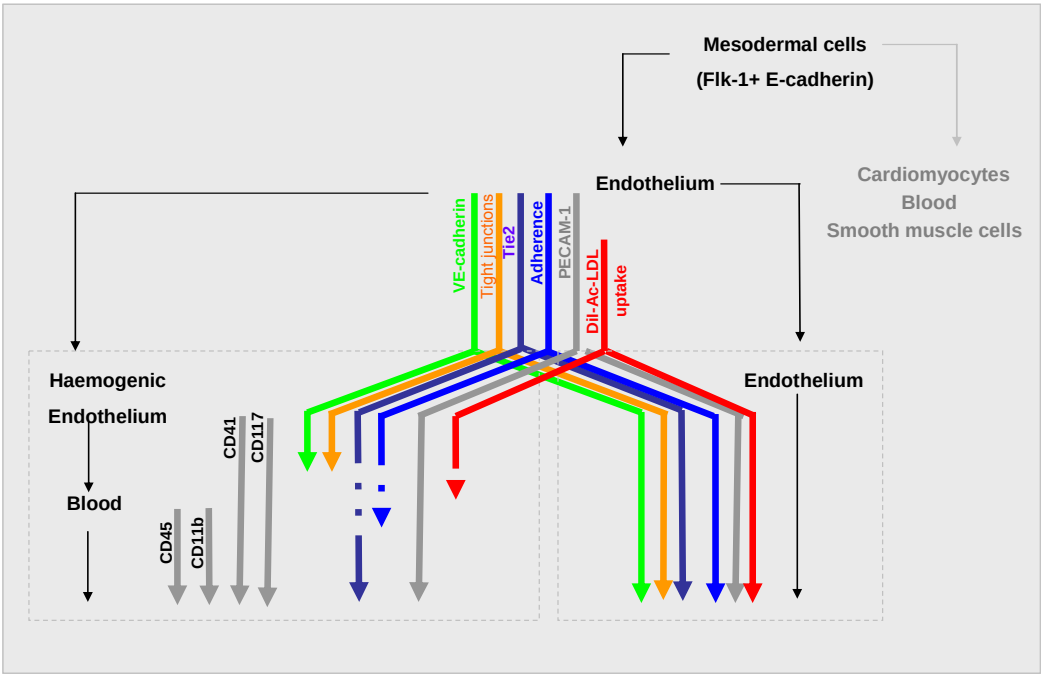

Figure 1.5. *Specification pathways during generation of endothelium and blood cells*

Upon appropriate cytokine stimulation, Flk1 +ve/ E-cadherin +ve mesodermal cells differentiate into endothelium. Haemogenic endothelial cells are specified from cells already expressing endothelial markers, which in turn generate blood cells (Adapted from Eilken et al., 2009)

might represent shed mature ECs or other ECs deriving from other progenitor cell populations (Urbich 2004; Ribatti ., 2007).The functions of ECs are diverse; they do not just form a passive barrier. They can actively transport small molecules, macromolecules and hormones such as insulin, and degrade lipoprotein particles (Bouis ., 2001; Pinkney ., 1997). Furthermore, ECs play major roles in blood pressure regulation, blood coagulation and fibrinolysis (Cines ., 1998), adhesion and transmigration of inflammatory cells out of the vessel into the target tissue. Additionally, ECs are the primary cell type responsible for angiogenesis, the formation of new blood vessels from pre-existing vasculature, during physiological and pathological neovascularisation. EC functions can vary considerably depending on their localisation and the size of the blood vessels they constitute. Human umbilical vein endothelial cells (HUVECs) found in a venous environment will differ considerably from human coronary artery endothelial cells (HCAECs) found in an arterial environment, in their morphology, expression of markers and ability to perform endothelial functional tests.

Whilst ECs may have heterogeneous characteristics, they also display a “typical” phenotype and function (Figure 1.6). Firstly, most form monolayers that are stablilised by cell-cell junctions giving them a characteristic ‘cobble-stone’ morpology (Bazzoni et al., 2004). They contain Weibel-Palade bodies, which are large rod-shaped organelles specific to ECs. Weibel-Palade bodies store large amounts of vWF, also known as factor VIII related antigen; that can quickly be released upon activation of the cells. vWF is a large adhesive glycoprotein specific to ECs, which serves as a stabilising carrier for factor VIII with which it circulates as a complex. vWF secretion can be constitutive or regulated, and may occur in the absence of Weibel Palade bodies. Secretion of vWF is a key characteristic of ECs (Weibel *et al* ., 1964; Ewenstein *et al* ., 1987; Edgell *et al* . 1983). Secondly, the expression of intracellular adhesion molecules (ICAMs), vascular cell adhesion molecule (VCAM) and E-selectin are also up-regulated upon EC activation, and vascular endothelial cadherin (VE-cadherin) and PECAM-1 are expressed at the cellular junctions (Pober *et al* ., 1986; Dejana *et al*, 2004). In addition, the expression of specific cell surface receptor tyrosine kinase (RTK) receptors can serve to identify ECs.

Figure 1.6

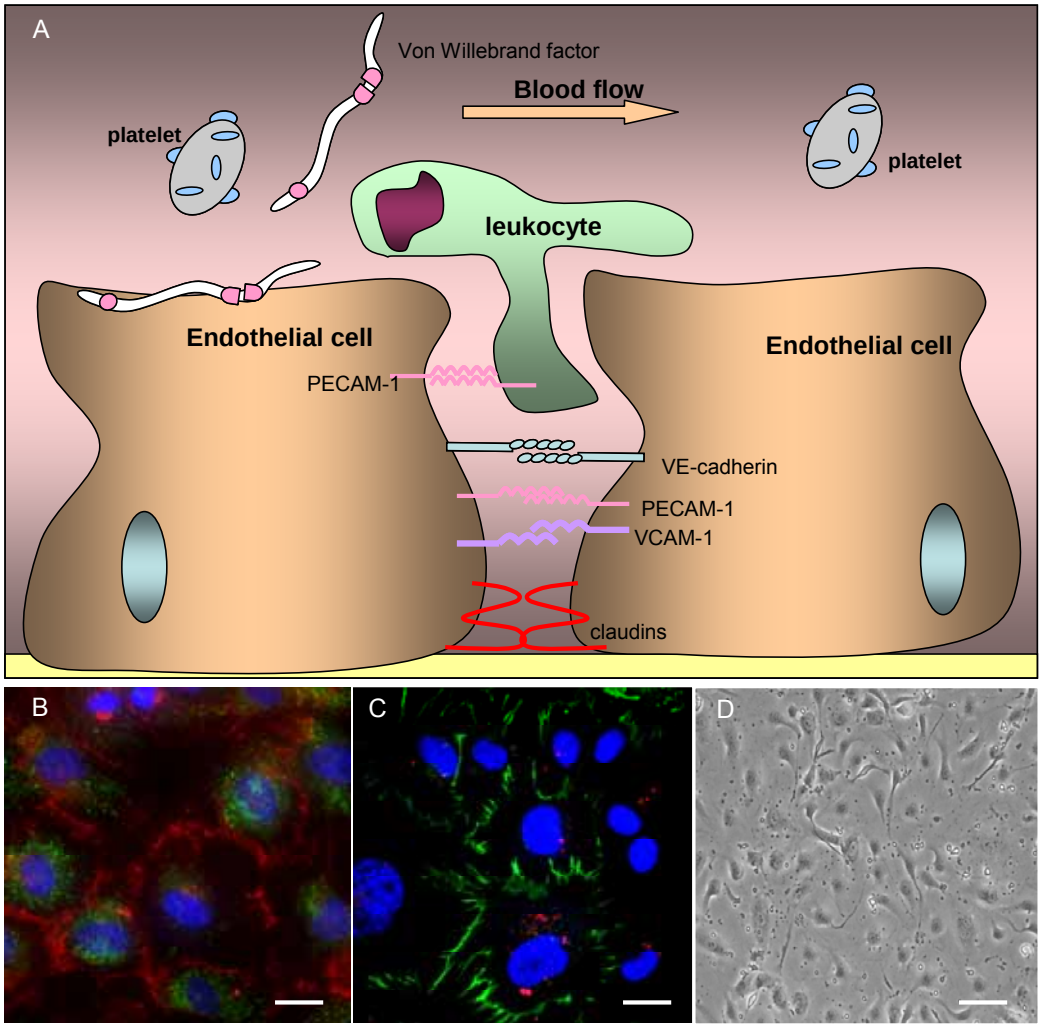

Figure 1.6. *Organisation of endothelial cell–cell junctions.*

(A) ECs adhesion is mediated by transmembrane proteins that promote homophilic interactions and form a pericellular zipper-like structure along the cell border. ECs express cell-type-specific transmembrane adhesion proteins, such as VE-cadherin at adherens junctions, shown by red immunostaning in **B** and claudin-5 at tight junctions, the glycoprotein vWF involved in factor VIII binding is depicted in green. Outside specialised junctional structures, ECs express other cell-specific homophilic adhesion proteins including PECAM-1, shown by green immunostaining in **C**. Scale bar = 7μm. PECAM-1 is also present in leukocytes and platelets and mediates leukocyte diapedesis. Together these cell-cell contacts stabilise ECs forming monolayers displaying a typical cobblestone morphology shown in D. Scale bar = 100μm. Images were taken using a Nikon upright C1 confocal microscope (60× objective) or an Olympus (CK X41 microscope (10× objective).

For instance, the receptor Tie2 is expressed by ECs as well as HSCs and, together with its ligand angiopoietin-1, is essential for both angiogenesis and EC survival (Claesson-Welsh., 2003). ECs also express three different VEGFRs, named VEGFR1 (Flt-1), VEGFR2 (KDR/Flk-1) and VEGFR3 (Flt-4). The expression of the VEGFRs is almost exclusively restricted to ECs, but VEGFR1 can also be expressed on many other cells including monocytes (Salmonsson *et al* ., 2003), humal dermal fibroblasts (HDFs) as well as some populations of vSMCs (Ishida ., 2001). Specific functions which may serve to identify ECs include binding of the *Ulex europaeus* lectin agglutinin 1 (Holthofer *et al* ., 1982), uptake of acetylated low-density lipoprotein (ac-LDL) (Voyta *et al* ., 1984), histamine induced release of vWF, angiotensin converting enzyme activity, induction of VCAM-1 in response to tumour necrosis factor α (TNFα) and nitric oxide release (Johnson *et al* ., 1977).

1.4.2. Vascular smooth muscle cells (vSMCs)

Vascular smooth muscle refers to a specific type of smooth muscle found within blood vessels and the gut. In blood vessels, SMCs comprise the major cell type within the medial layer. vSMCs maintain blood vessel tone by pulsatile contraction, to both change the volume of blood vessels and the local blood pressure, a mechanism that is responsible for redistributing blood within the body to areas where it is needed (i.e. areas with temporarily enhanced oxygen consumption) (Conway et al., 2001). Thus the main function of vascular smooth muscle tonus is to regulate the calibre of the blood vessels in the body. Excessive vasoconstriction leads to hypertension, while excessive vasodilation leads to hypotension. Unlike most other adult cells, vSMCs are not terminally differentiated, but exist as a continuum of phenotypes ranging from synthetic to contractile. Synthetic vSMCs are proliferative, migratory and express abundant ECM molecules, but few contractile proteins, representing an immature phenotype commonly found in pathology (Ball *et al* ., 2007a; Owens *et al*, 1995). In contrast, contractile vSMCs are quiescent, contractile and express few ECM molecules but abundant contractile proteins, representing a more differentiated phenotype as found in the medial

layer of adult blood vessels (Ball *et al* ., 2004). Vascular smooth muscle profoundly differs from SMCs of digestive, respiratory and urogenital tract, in that it contains a number of different SMC contractile proteins, such as smooth muscle alpha actin (α-SMA), vascular smooth muscle-myosin heavy chain 1 (SM-MHC-1) and smoothelin-B (Ball *et al* ., 2004; Stephan *et al* ., 2006). Whilst there is no individual protein that defines vSMCs, the complement of contractile proteins characterises the vSMC phenotype. As the cell becomes more differentiated, it acquires an increasingly complex array of contractile components (Ball *et al* ., 2007a).

1.4.3. Vascular extracellular matrix

The ECM is a highly organised structural network of proteins and polysaccharides, that provides a set of instructive molecular signals to cells that are attached to it. Much of the information content of the vascular ECM resides in the insoluble collagenous and non-collagenous glycoproteins (e.g., collagens VIII, VI, XV, elastin, vitronectin, proteoglycans and fibronectin) and together with the basement membrane is known as the subendothelial extracellular matrix. ECs reside on basement membranes in which the primary components are laminin, collagen type IV and perlecan, a heparan sulphate proteoglycan, whilst vSMCs interact with elastic fibers in the medial layer indicating these ECM molecules may be important in mediating MSC differentiation towards vascular cells (Hayden *et al* ., 2005).

Cellular interactions with ECM molecules are primarily mediated by integrins, a family of heterodimeric cell adhesion receptors that provide both a physical bridge and a biochemical link integrating the outside and inside of the cell. Integrins are composed of an α and β chain, and different α and β chain combinations facilitate selective binding to different ECM ligands. The level of integrin-mediated receptor signalling regulation will depend on the local ECM composition, together with the abundance and type of cell surface integrins expressed. Specific ECM-integrin interactions have been shown to modulate RTK signalling. For instance, vitronectin induced αvβ3/PDGFRβ and

αvβ3/PDGFRα complexes (Woodard *et al* ., 1998; Baron *et al* ., 2002), whilst collagen type I induced a α2β1/PDGFRβ complex (Hollenbeck ., 2004), all of which increased PDGF stimulated responses. In addition, membrane associated proteins such as sphingosine-1-phosphate (Tanimoto *et al* .,2004) and membrane-type 1 matrix metalloproteinase 14 (Lehti *et al* ., 2005) have been shown to modulate PDGF/PDGFR signalling. It is therefore possible for a particular RTK, such as PDGFR, to transmodulate its signalling by forming different complexes with other membrane associated proteins. Furthermore, ligand stimulation of either PDGFRα or PDGFRβ can induce the recruitment, activation and interaction with different complements of intracellular signalling molecules (Klinghoffer *et al* ., 2001). Thus, different vascular ECM molecules can modulate RTK signalling and may regulate the activity of effectors such as intracellular enzymes and transcription factors, resulting in distinct cellular responses.

1.5. Differentiation of MSCs along vascular lineages

Several studies have indicated that MSCs are involved in revascularisation of tissues after vascular injury. MSCs have been documented to be involved in revascularisation of the injured myocardium in myocardial ischaemia (Tang *et al*, 2005a), wound healing (Satoh *et al* ., 2004), and to contribute to tumour neovascularisation, where they may also engraft into tumour lesions and become incorporated into the tumour stroma (Ball *et al* ., 2007a). Many of these studies have suggested that, at these sites of injury, MSC differentiation is regulated by local microenvironmental factors such as the composition of the ECM, the bioavailability of growth factors and cytokines, and local mechanical forces.

1.5.1. Differentiation of MSCs towards ECs

The contribution of BM-derived cells to tumour neovascularisation in animal models is highly variable, ranging from near to 100% to virtually negligible (Annabi *et al*., 2004). In a murine tumour model, VEGFR2-negative MSCs were shown to be actively recruited to

areas of neovascularisation, where they differentiated into PECAM-1-positive endothelial-like cells and increased vascularisation (Annabi *et al* ., 2004). In addition, MSCs systemically administered into a murine tumour model were shown to localise and engraft into tumor lesions, where they proliferated, differentiated into vWF and PECAM-1-positive endothelial-like cells, and formed a significant fraction of the tumour stroma (Hung *et al* ., 2005).

Previous studies have reported that differentiation can be induced by cultivation of confluent human MSCs following exposure to VEGF (Al-Khaldi *et al* ., 2003; Alviano *et al* ., 2007; Bai *et al* ., 2009; Chen *et al* ., 2009; Chung *et al* ., 2009; Oswald *et al*., 2004; Wu *et al* ., 2005; Xu *et al*., 2009; Zhang *et al* ., 2008). One group demonstrated that human BM-derived MSCs positive for CD105, CD73, CD166, CD90 and CD44, but negative for CD34, CD133, VEGFR1, VEGFR2, VE-cadherin, VCAM-1 and vWF could be induced to differentiate towards ECs after seven days culture in 2% fetal calf serum supplemented with VEGF-A (Oswald *et al* ., 2004). A second study using human term amniotic membrane MSCs positive for CD105, CD73, CD29, CD44, CD166 and negative for CD14, CD34, CD45, demonstrated a spontaneous differentiation into endothelial-like cells induced by *in vitro* culture on Matrigel, a basement membrane extract derived from the Engelbreth-Holm-Swarm mouse tumour on which MSCs spontaneously form networks and this differentiation was enhanced by VEGF-A exposure (Alviano *et al* ., 2007). Similarly, in a third study, human BM-derived MSCs, positive for CD105, CD166, but negative for CD34, VEGFR2 and vWF, expressed the endothelial marker vWF following five days culture in 10% fetal calf serum supplemented with VEGF-A (Wu *et al* ., 2005). However, these *in vitro* studies have not convincingly demonstrated MSC differentiation to ECs only analysing the expression of a limited number of markers or functional tests. Thus, MSC differentiation to ECs is not widely accepted and remains controversial.

1.5.2. Differentiation of MSCs towards vSMCs

As mentioned above, vSMCs profoundly differ from SMCs of digestive, respiratory and urogenital tract by the presence of additional SMC-specific contractile component proteins, such as α-SMA, SM-MHC-1 and smoothelin-B. Several studies have demonstrated that MSCs can possess some inherent SMC-like characteristics. Human MSCs are similar to synthetic state vSMCs in their expression of several early contractile markers, α-SMA and calponin, as well as smoothelin-B, a novel marker for the mid differentiated contractile phenotype (Stephan *et al*., 2006). The transcription cofactor for serum response factor, myocardin, selectively binds to regions found in the promoters for several SMC genes, including α-SMA and SM-MHC-1, but not smoothelin-B (Du *et al* ., 2003; Yoshida *et al* ., 2003). MSCs normally contain low levels of myocardin transcript, however when a myocardin adenovirus was transfected into MSCs, SM-MHC-1 was induced. Furthermore, serum response factor has also been shown to activate the small GTPase RhoA thereby promoting α-SMA gene expression (van Tuyn *et al* ., 2005). Recently PDGFR signalling has been implicated in determining vSMC fate of MSCs (Ball *et al* ., 2007b). MSCs have a high ratio of PDGFRα:PDGFRβ, and PDGFRα signalling can activate RhoA through Rho-associated kinase dependent cofilin phosphorylation and myosin light chain kinase dependent pathways, resulting in enhanced α-SMA transcription and filament polymerisation. PDGF-BB mediated PDGFRβ signalling, however, was found to up-regulate RhoE, inhibiting RhoA-associated kinase and α-SMA filaments and inducing cofilin-mediated actin filament destabilisation (Ball *et al* ., 2007b).

1.6. Regulation of the vascular differentiation of MSCs

An important approach to elucidating the mechanisms involved in regulating MSC differentiation towards vascular cells is to selectively identify and examine *in vitro* specific environmental factors which may control MSC differentiation events. During neovascularisation in a wound, tumour or ischaemic injury, cellular exposure to local environmental factors *en route* or *in situ* or at these sites will be key elements in regulating the differentiation process. Such environmental factors will likely include

exposure to different types of cytokines and growth factors, vascular ECM molecules, cell-matrix and cell-cell interactions, cell density, mechanical strain, and oxygen tension.

1.6.1. Growth factors

1.6.1.1. VEGF and receptors

VEGF is a homodimeric 34-42 kDa heparin-binding glycoprotein with potent angiogenic, mitogenic and vascular-permeability enhancing activities. The VEGF family consists of seven members, termed; VEGF-A, VEGF-B, VEGF-C, VEGF-D, VEGF-E, VEGF-F and placental growth factor, which share a common structure of eight characteristically spaced cysteine residues in a VEGF homology domain. The main VEGF family member documented is VEGF-A, which induces angiogenesis and vasculogenesis *in vivo* and causes EC proliferation, sprouting, migration and tube formation (Li *et al* ., 2008a). VEGF-A has also been shown to stimulate vWF factor release from ECs and to be chemotactic for monocytes and osteoblasts *in vitro* (Cross *et al* ., 2003). In addition, VEGF-A induces angiogenesis in a variety of physiological and pathological conditions including embryogenesis, corpus luteum formation, tumour growth, wound healing, and compensatory angiogenesis in the heart (Ferrara et al., 2005). Furthermore, VEGF-A is known to promote EC survival by inducing the expression of the anti-apoptotic protein Bcl-2. VEGF-A mRNA expression is regulated by hypoxia, as it contains a hypoxic responsive element in its promoter (Matsumoto *et al*., 2001).

VEGF-A mediates its responses primarily by activating the class III RTKs, VEGFR1 and VEGFR2 (expressed in ECs, as well as pericytes, placental trophoblasts, osteoblasts, monocytes/macrophages, renal mesangial cells and also in some HSCs) (Ferrara et al., 2005). Two important alternatively spliced VEGF-A isoforms are VEGF-$A_{165,}$ which contains a heparin-binding domain, and VEGF-A_{121} which does not bind heparin. VEGF-A_{165} binds to accessory neuropilin (NRP) co-receptors, NRP1 and NRP2, which are cell surface transmembrane glycoprotein receptors. Binding of VEGF-A_{165} to NRPs has been

shown to facilitate enhanced VEGFR mediated signalling (Claesson-Welsh *et al*, 2003) A novel VEGF-A signalling mechanism has been identified, whereby VEGF-A can directly stimulate PDGFR activation in BM-derived human adult MSCs that did not express VEGFRs (Ball *et al* ., 2007c).

VEGFRs have seven extracellular immunoglobulin-like domains, a transmembrane region and a split intracellular kinase domain, which form receptor homodimers on ligand binding (Figure 1.7). Whilst VEGF-A binding to VEGFR1 induces only weak mitogenic signals in ECs, VEGF-A binding to VEGFR2 elicits strong signalling properties. As such, VEGFR2 is thought to be the primary receptor, which mediates VEGF-A induced signalling. However, VEGFR1 is associated with the recruitment and survival of BM-derived progenitor cells. VEGFR1 expression has also been shown to be up- regulated during angiogenesis and by hypoxia, unlike that of VEGFR2 and VEGFR3 (Gerwins *et al* ., 2000). The VEGF-A growth factor and its receptors act to facilitate neovascularisation, however the cellular response to these growth factors can vary according to growth factor availability, the duration of receptor exposure to the growth factor, and expression of different growth factor isoforms. Furthermore, growth factors can bind to and be sequestered by specific ECM molecules. Growth factor deposition within the ECM may create short range concentration gradients to facilitate chemotaxis. The composition of the ECM may therefore regulate the retention and presentation of bioactive ligands at the pericellular interface, thereby acting to modulate the intensity and/or duration of receptor signalling, resulting in distinct biological responses.

1.6.1.2. PDGF and receptors

The PDGF family consists of four ligands PDGFA-D, that form disulphide-linked homodimers (AA-DD). In addition, PDGF-A and PDGF-B can also form a heterodimer (AB). PDGF mediated biological actions occur via two structurally related but distinct RTKs, PDGFRα (170kDa) and PDGFRβ (190kDa), both comprising five immunoglobulin domains, a transmembrane region and a split intracellular kinase domain (Figure 1.8).

Figure 1.7

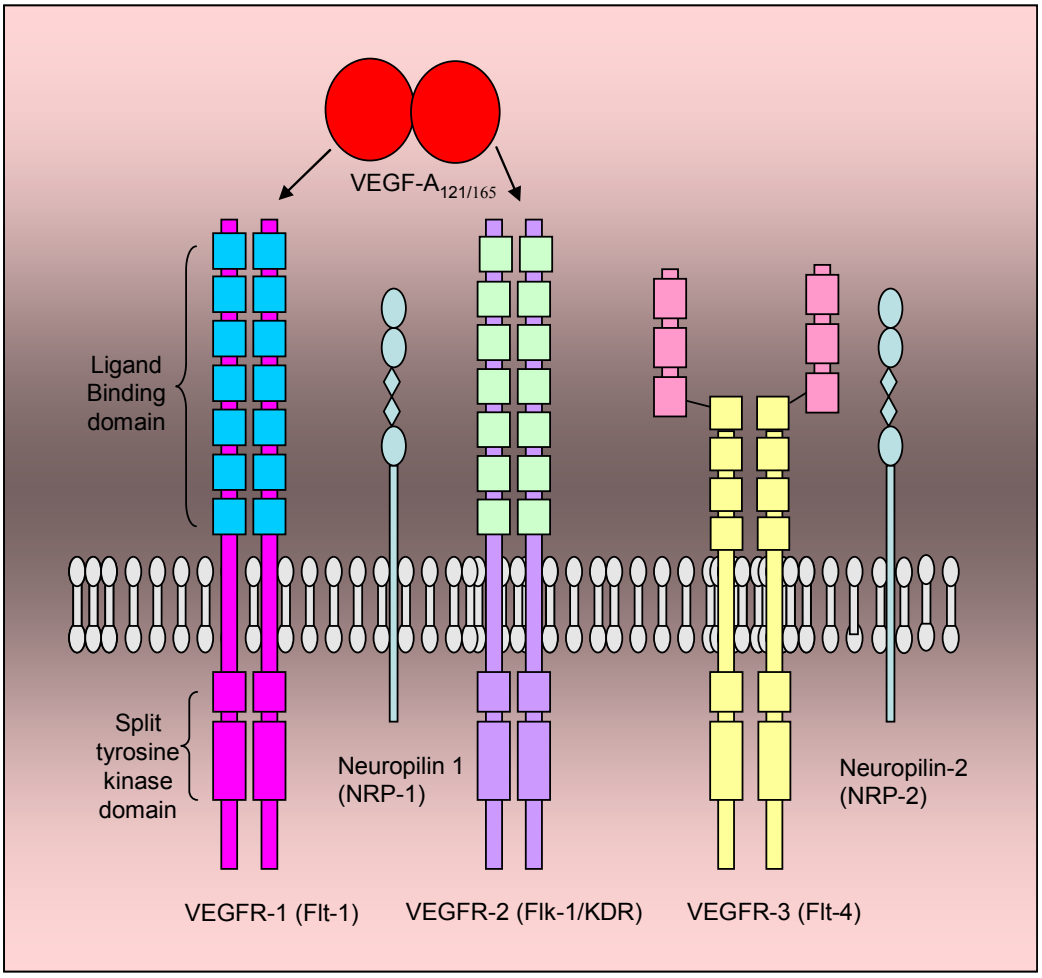

Figure 1.7. *Structure of the VEGF receptors*

VEGF receptors are shown spanning the plasma membrane. VEGFR1, VEGFR2, and VEGFR3 are structurally homologous and consist of seven immunoglobulin homology domains in the extracellular region and a tyrosine kinase domain in the intracellular portion that is interrupted by a tyrosine kinase insert domain. A soluble form of VEGFR1 exists but is not shown. The extracellular domain of VEGFR3 is proteolytically cleaved in the fifth immunoglobulin-like domain and the fragments remain associated by disulfide bonds. Neuropilin 1 (NRP1) consists of a short intracellular domain and an extracellular domain containing two complement C1r/s homology domains, two domains with homology to coagulation factors V and VIII, and a single MAM domain. NRP2, also binds VEGF. The VEGF family members (represented as dimers) that interact with each receptor are indicated at the top of the figure and are represented in the diagram as dimers bound to the receptors.

On ligand binding, the receptors α and β can either homo- or hetero-dimerise into αα, αβ, and ββ combinations. Since the extracellular portion of these two receptors are only 31% identical, ligands have varying affinities for these different receptor combinations: PDGF-AA binds only PDGFRαα, PDGF-CC and PDGF-AB bind either PDGFRαα or PDGFRαβ, PDGF-DD binds PDGFRαβ and PDGFRββ, while PDGF-BB binds all three receptor types. Binding of ligand causes receptor dimerisation and subsequent auto-phosphorylation of tyrosine residues in the cytoplasmic domain of the receptor. This activated form of the receptor can then serve as docking sites for multiple protein complexes, leading to the initiation of signalling pathways including Ras-GTPase Activated Protein phosphatidylinositol 3-kinase, Src family kinases, and phospholipase-Cγ pathways (Claesson-Welsh *et al*, 1994; 1996; Westermark *et al*., 1990). PDGF-B/PDGFRβ signalling is essential for regulating the migration and proliferation of mural (vSMC, pericyte) progenitor cells during vascular development (Hellstrom *et al* ., 1999). In addition, PDGF-B/PDGFRβ knockout studies revealed severe defects in vascular development, and subsequent death during the late embryonic stage (Leveen *et al* ., 1994; Soriano *et al*, 1994). PDGF-A/PDGFRα signalling however is crucial for a wider variety of functions during both embryogenesis and organogenesis (Betsholtz *et al*, 2004). PDGF-A/PDGFRα knockout mice are embryonic lethal, due to a range of mesenchymal tissue defects including vascular abnormalities (Betsholtz *et al* ., 2001). The PDGFR heterodimer (PDGFRαβ) may have a crucial role in mediating MSC differentiation events, since both *in vitro* and *in vivo* studies have demonstrated that PDGF-AB stimulation promoted the differentiation of adult BM-derived cells to cardiomyocytes (Xaymardan *et al* ., 2004). Furthermore, PDGF-CC, which can also stimulate PDGFRαβ, has been shown to be a potent angiogenic factor similar to VEGF-A (Cao *et al* ., 2002). It has been demonstrated that MSCs *in vitro* are defined by a high PDGFRα:β ratio, which could be a characteristic of relatively undifferentiated cells (Ball *et al* ., 2007a). Thus the cell surface PDGFR expression is likely to be an important determinant in mediating the fate of MSCs. Furthermore, recently it has been shown that NRP1 associates with phosphorylated PDGFRs, thereby regulating cell signalling, migration, proliferation and network assembly (Ball *et al* ., 2010a).

Figure 1.8

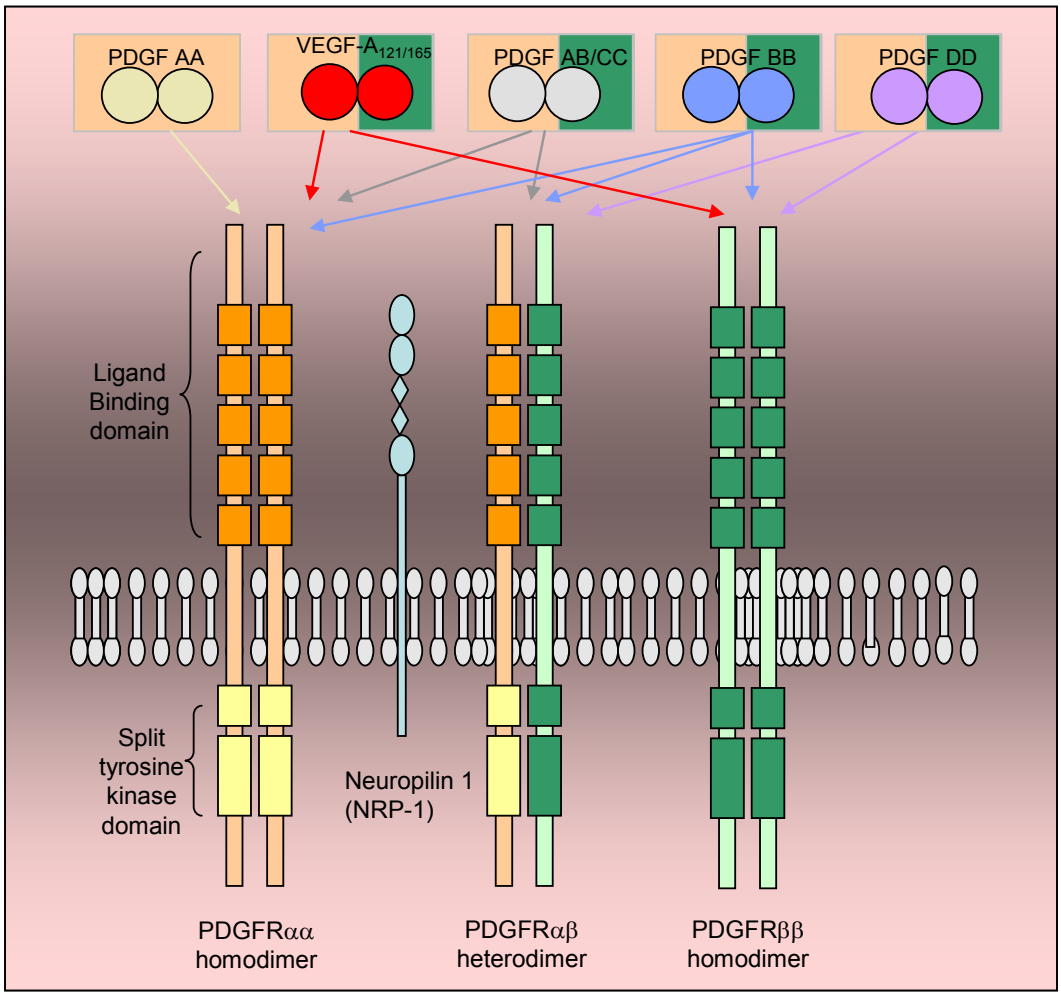

Figure 1.8. *Structure of the PDGF receptors.*

These receptors are transmembrane proteins that have an extracellular ligand-binding domain, a transmembrane domain, and a cytoplasmic tyrosine kinase domain. Extracellularly, each receptor contains 5 immunoglobulin-like domains, and intracellularly, there is a tyrosine kinase domain that contains a characteristic inserted sequence without homology to kinases. On ligand binding, PDGF receptors homodimerise or heterodimerise and phosphorylate each other on specific tyrosine residues, initiating signalling cascades. The binding interaction of mammalian PDGF ligands and PDGF receptors is shown, along with the receptor-binding specificity of the 5 PDGF and VEGF-A isoforms (rectangles). The ability of the five different dimeric isoforms of PDGF to bind and activate homodimeric and heterodimeric complexes of receptors are indicated with arrows.

1.6.2. Extracellular matrix

The rigidity or elasticity of the matrix has been shown to play a key role in modulating MSC differentiation. Recently it has been shown that human MSCs grown on collagen I coated acrylamide gels (a soft extracellular environment) favours development of a neuronal phenotype, whereas moderate elasticity (compliance) promotes myogenic differentiation and a rigid extracellular environment results in osteogenic differentiation. Cells 'sense' matrix rigidity through their ability to transmit extracellular tension, mediated by focal adhesions and integrins which modulate intracellular tension within actin structures (Engler *et al* ., 2006). It is important to recognise that an *in vitro* two-dimensional culture environment may modulate MSC differentiation differently, compared to a three-dimensional *in vivo* environment. As such, MSCs cultured within matrigel or fibrin gels may be useful *in vitro* model systems, more representive of three-dimensional *in vivo* environments. Thus an important caveat to consider is that, since the majority of published MSC *in vitro* differentiation events have utilised two-dimensional tissue culture techniques, these studies are not fully representative of differentiation mechanisms occurring *in vivo*.

1.6.3. Oxygen tension

Low oxygen (hypoxic 1% O_2) conditions within the BM provide an ideal niche for stem cells to proliferate and to maintain their stem cell phenotype (Ren *et al* ., 2006). Hypoxic conditions however, are also prevalent in the adult during vascular remodelling, such as angiogenesis in cancer (the formation of new blood vessels from a pre-existing vasculature), wound healing and ischaemic tissue disease.

The molecular mechanisms of the cellular response to hypoxia are reasonably well understood. Under normoxia, the basic helix loop helix proteins designated hypoxia inducible factors (HIFs) HIF1α and HIF2α are hydroxylated at internal proline residues, and this hydroxylation creates a recognition site for binding of the Von-Hippel Lindau

protein. Following binding of Von-Hippel Lindau, HIFα subunits are rapidly degraded via the 26S proteosome, thereby preventing transactivation of HIF target genes under normoxia. During hypoxia however, prolyl hydroxylase enzymes which hydroxylate internal proline residues are inhibited since they utilise oxygen as a co-substrate. Unhydroxylated HIFα proteins escape recognition by Von-Hippel Lindau, and stabilised HIFα translocates to the nucleus where it binds its dimerisation partner to form an active transcription complex, thereby activating the transcription of close to 200 different genes. The resulting proteins are involved in a broad range of cellular processes, including cell proliferation and apoptosis (Insulin growth factor-2, TGF-α, TGF-β), gene expression and control of angiogenesis and vascular tone (VEGF, VEGFR2, Ang-2, Tie-2, and endothelin-1) (Hickey *et al* ., 2006).

1.6.4. Mechanical strain

The phenotype and morphology of MSCs are regulated not only by chemical factors, but also by mechanical forces such as fluid flow, shear stress and mechanical strain (Kobayashi *et al* ., 2004; Stohlberg *et al* ., 2009). The blood vessel wall is constantly subjected to cyclic mechanical strain in the circumferential direction due to the pulsatile nature of blood flow. Specific mechanical and chemical factors in the vascular microenvironment therefore may promote the differentiation of perivascular MSCs towards vascular cells (Ball *et al* ., 2010b; Buxboim *et al* ., 2010). Previous studies have shown that mechanical strain plays an important role in the remodelling of the vessel wall *in vivo,* and in the remodelling of tissue-engineered vascular grafts *in vitro* (Nerem *et al* ., 2001). Both equiaxial and uniaxial mechanical strain devices have been used to study cellular responses. One study investigated different modes of strain and showed that mechanical strain regulated gene expression in MSCs, with different modes of mechanical strain inducing different responses (Park *et al* ., 2004). Cyclic equiaxial strain downregulated α-SMA and smooth muscle protein 22-α in MSCs and decreased α-SMA filaments in stress fibers. In contrast, cyclic uniaxial strain transiently increased the expression of α-SMA and smooth muscle protein 22-α, which subsequently returned to

basal level after the cells aligned in the direction perpendicular to the strain direction (Park *et al* ., 2004). This study therefore shows that MSCs can sense the subtle difference between various types of mechanical loading in the microenvironment, and respond accordingly. Since the major mechanical stretch in the vessel wall is in the circumferential direction, uniaxial strain better simulates the *in vivo* condition, and thus may promote the differentiation of MSCs towards vascular cells.

1.6.5. Cell-to-cell contact

During vasculogenesis, contact and communication between differentiated ECs and uncommitted MSCs or between MSCs themselves may influence MSC differentiation. Although in healthy blood vessels, ECs are separated from other vascular cells by the internal elastic lamina, in injury and development ECs can be in direct contact with cells of mesenchymal origin. MSCs may “home” to specific repair sites in the vasculature where contact with local vascular cells may influence their phenotypic state.

Direct co-cultures of human MSCs with ECs have previously been shown to lead to disruption of α-SMA filament organisation, suggesting decreased MSC contractility. Interestingly, co-culture of MSCs with fibroblasts leads to differentiation into myofibroblast-like cells (Ball *et al* ., 2004). Furthermore, direct cell-to-cell contact between rat MSCs and adult cardiomyocytes or SMCs is crucial in the differentiation of MSC into cardiomyocytes or SMCs (Xu *et al* ., 2004).

These studies suggest that the local environment and resident cellular populations are major factors in determining MSC fate, with MSCs being specifically influenced by contact with differentiated cells or between MSCs themselves. A signalling pathway that may be crucial in mediating such cell-to-cell contact differentiation events is Notch signalling (Figure 1.9).

1.6.5.1. Notch signalling

Notch signalling is characterised by transmembrane ligands and receptors, therefore signalling only occurs when cells are in close contact. Four mammalian Notch receptors (Notch 1–4) have been characterised in mammals. They bind to five ligands (Jagged (JAG) 1 and 2 and Delta-like (Dll) 1, 3 and 4) (Bray *et al*, 2006). The interaction between ligand and receptor leads to proteolytic cleavage and shedding of the extracellular portion of the Notch receptor. This process is followed by a second cleavage event by the enzyme gamma secretase resulting in membrane proteolysis that releases the intracellular part of the Notch molecule (NICD) from the cell membrane. The resulting intracellular Notch translocates to the nucleus, where it modulates transcription factor activity including hairy enhanced of split-1 (HES-1) and Hairy/enhancer-of-split related with YRPW motif 1 (HEY) by binding to the transcription factor recombination signal sequence-binding protein (also known as CBF-1/RJBk in mammals) (Yanjie *et al* ., 2007; Chiba *et al*, 2006; Bray *et al*, 2006) (Figure 1.9). Interestingly, many studies have reported that hypoxia can activate Notch-responsive promoters through interactions between the Notch intracellular domain and HIF-1 leading to increased expression of Notch downstream genes (Sainson *et al* ., 2006; Gustafsson *et al* ., 2005).

Notch signalling has been demonstrated to play a critical role in both the differentiation and specification of the vasculature during development and homeostasis of vessels in the adult. Deletion of several Notch receptors and ligands by homologous recombination in mice results in embryonic lethality due to vascular and cardiac defects. In addition, several vascular abnormalities have been linked to Notch receptors and ligands (Alva *et al* ., 2004; Bray *et al*, 2006; Opherk *et al* ., 2009) Notch signalling has been demonstrated to play a key role in enhancing MSC differentiation towards chondrocytes (Hardingham *et al* ., 2006) in defined differentiation medium. In addition, Notch signalling may, by modulating VEGF signalling, direct EC fate and coordinate the specification of arterial and venous ECs (Zhang *et al* ., 2008; Siekmann *et al* ., 2008). Furthermore, Notch activated experimentally over days in culture (Xu *et al* ., 2009), or during vascular development (Ohata *et al* ., 2009) can enhance endothelial differentiation from mesenchymal precursors.

Figure 1.9

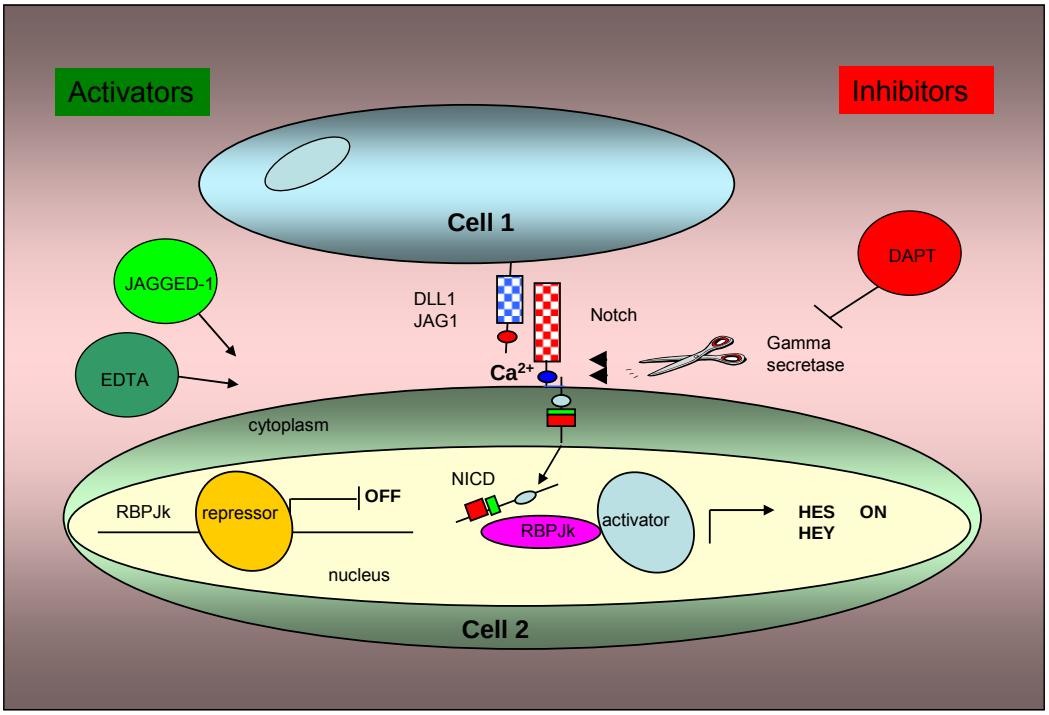

Figure 1.9. *Model of the Notch signalling pathway.*

Four mammalian Notch receptors (Notch 1–4) have been characterised in mammals. They bind to five ligands (Jagged (JAG) 1 and 2 and Delta-like (Dll) 1, 3 and 4) (Bray *et al*, 2006). The interaction between ligand and receptor leads to proteolytic cleavage and shedding of the extracellular portion of the Notch receptor. This process is followed by a second cleavage event by the enzyme gamma secretase resulting in membrane proteolysis that releases the intracellular part of the Notch molecule (NICD) from the cell membrane. The resulting intracellular Notch translocates to the nucleus, where it modulates transcription factor activity including hairy enhanced of split-1 (HES-1) and Hairy/enhancer-of-split related with YRPW motif 1 (HEY) by binding to the transcription factor recombination signal sequence-binding protein (also known as CBF-1/RJBk in mammals). The Notch signalling inhibitor N-[N-(3,5-Difluorophenacetyl-L-alanyl)]-S-phenylglycine t-butyl ester (DAPT) which inhibits gamma secretase and the Notch activators recombinant Jagged-1 and EDTA are also depicted.

1.7. Summary

Currently very little is known about the differentiation of MSC along vascular cell lineages. While several studies provide evidence for the differentiation of MSCs towards vSMCs and differentiation to ECs, it is now increasingly accepted that MSCs also make a significant contribution to postnatal vasculogenesis in many *in vivo* situations. A major determinant in regulating the differentiation of MSCs to vascular cells is the *in vivo* micro environment, with growth factors, vascular ECM molecules, cell to cell contact, mechanical stress and oxygen tension likely to be the key mediators. By selectively examining these *in vivo* environmental elements *in vitro*, it should be possible to identify the key factors involved in modulating MSC differentiation towards vascular cells. Identifying influential environmental constituents which regulate the differentiation of MSCs to vascular cells and the mechanisms involved, will provide new opportunities for *in vitro* engineering of artificial vascularised tissues based on autologous MSCs. Furthermore, the *in vitro* definition of crucial regulatory components, will contribute to the therapeutic manipulation of MSCs within *in vivo* environments, potentially enabling the regulation of neovascularisation during ischaemia, wound healing and tumourigenesis. Thus to advance current therapeutic strategies towards controlling postnatal vasculogenesis, an understanding of how the micro-environmental niche can modulate MSC differentiation is essential.

1.8. AIMS

The aim of this project is to investigate the differentiation of MSCs along the EC lineage, and to identify specific factors modulating this process and the mechanisms involved.

Specific aims are:

- To provide extensive evidence to show that MSCs can be induced to differentiate into a functional EC by examining:

    1. their morphology
    2. their expression of known EC markers, vWF, VEGFR1, VEGFR2, VE-cadherin and PECAM-1
    3. EC functional tests including ac-LDL uptake, network formation on Matrigel and induction of VCAM-1 in response to TNFα
    4. the stability of the EC phenotype.

- To investigate the roles of VEGF-A and cell density in inducing MSC differentiation to ECs.

- To describe the mechanisms regulating MSC differentiation to ECs, specifically focussing on the involvement of the Notch signalling pathway.

- To determine how 'endothelialised MSCs' respond in pro-angiogenic environments utilising three dimensional *in vitro* Matrigel culture and the chick chorioallantoic membrane (CAM) assay.

CHAPTER 2

MATERIALS AND METHODS

CHAPTER 2: MATERALS AND METHODS

2.1. MATERIALS

2.1.1. Cell lines

All cell lines and growth medium, unless otherwise stated, were obtained from Lonza (Cambrex Bio Science, Wokingham, UK). Human MSCs were obtained from the normal human bone marrow of a 28 year old female (lot number 6F3974.) All experiments were repeated using MSCs obtained from bone marrow of a second individual (a 21-year-old male; lot number 6F3502). The MSCs had been confirmed to have the potential to differentiate into osteoblast, chondrocyte, and adipocyte lineages (McBeath *et al* ., 2004), and they were positive for CD29, CD44, CD105, and CD166, but negative for hematopoietic cell markers CD14, CD34, and CD45. MSCs were routinely maintained in MSC basal medium containing batch selected 10% foetal bovine serum, 2% L-glutamine and 0.1% penicillin/streptomycin. MSCs were cultured under standard conditions i.e. in a humidified atmosphere of 20% O_2, 5% CO_2, and 37 ^{o}C at 70% confluence and used at passage 5. HUVECs from a 43-year-old and 29-year old female Caucasians (Cascade Biologics), were maintained on 5% gelatin in phosphate buffered saline (PBS) (Sigma) in endothelial cell basal medium containing 5% fetal bovine serum, 0.4% fibroblast growth factor, 0.1% VEGF, 0.1% Epidermal growth factor (EGF), 0.1% Insulin-like growth factor, 0.1% gentamycin/amphotericin solution, 0.1% ascorbic acid and 0.04% hydrocortisone, and used at passage 6. HDFs from a 51-year-old male, obtained from the European Collection of Cell Cultures (CAMR, Porton Down, UK), were maintained in Dulbecco's minimal essential medium (Gibco, Paisley, UK) containing 10% fetal bovine serum, 1% L-glutamine, 0.2% penicillin/ streptomycin and used at passage 6.

2.1.2. Growth factors and inhibitors

VEGF-A_{165} (50 ng/ml) was obtained from R&D Systems (298-VS). To inhibit VEGFR signalling, VEGFR tyrosine kinase inhibitor III (Calbiochem, KRN633) was used at a concentration of 0.5 μM (designated VEGFR-I). The inhibitor is a cell-permeable, reversible, ATP-competitive inhibitor of VEGFR kinase activity (IC_{50} = 170 nM, 160 nM, and 125 nM for VEGFR1, VEGFR2, VEGFR3, respectively) and inhibits PDGFR-α and c-Kit only at higher concentrations (IC_{50} = 0.97 μM and 4.33 μM, respectively). VEGFR-I is inactive towards a panel of 17 other kinases (IC_{50} ≥ 10 μM). A VEGF neutralising monoclonal antibody (designated (VEGF-I) was purchased from R&D Systems (clone 26503), and used at a concentration of 1 μg/ml. PDGFR tyrosine kinase inhibitor V (Calbiochem, 521234) was used at a concentration of 0.1 μM (designated PDGFR-I). This inhibitor is a cell-permeable quinolinyl-thiourea compound that acts a potent, ATP-competitive, and reversible inhibitor of PDGFR (IC_{50} = 4 and 7.6 nM in ligand-induced cellular PDGFR phosphorylation and in *in vitro* kinase activity, respectively). Inhibits c-kit receptor only at higher concentrations (IC_{50} = 434 and 234 nM in receptor phosphorylation and kinase activity, respectively. Affinity purified goat anti human PDGFRα (AF-307-NA) and PDGFRβ (AF385) neutralising antibodies were purchased from R&D Systems and used at a concentration of 10 μg/ml. The gamma secretase inhibitor N-[N-(3,5-Difluorophenacetyl-L-alanyl)]-S-phenylglycine t-butyl ester (DAPT) (Sigma) was resuspended in DMSO and used at a concentration of 50 μM. DMSO alone was used as a control. Recombinant human TNF-α (10 ng/ml) was purchased from R&D Systems (210-TA-010). Fresh growth factors and inhibitors were re-applied to cells every two days throughout experiments.

2.1.3. Primer sequences

Oligonucleotide primers for PCR were designed using Primer3 software (Rozen & Skaletsky, 2000). Each primer pair were designed using the same parameters (70-100 base pair product size and an optimum Tm of 60 ^{o}C, resulting in similar Tm values and product lengths, as shown: Glyceraldehyde-3-phosphate dehydrogenase (GAPDH) (71-bp), forward (5'-AAGGGCATCCTGGGCTAC-3') and reverse (5'-

GTGGAGGAGTGGGTGTCG-3'); VEGFR1 (99-bp), forward (5'-GCGACGTGTGGTCTTACG-3') and reverse (5'-GGCGACTGCAAAAGTCCT-3'); VEGFR2 (81-bp) forward (5'-CATCCAGTGGGCTGATGA-3') and reverse (5'-TGCCACTTCCAAAAGCAA–3'); VEGFR3 (87-bp), forward (5'-GATGCGGGACCGTATCTG-3') and reverse (5'-ATCCTCGGAGCCTTCCAC-3'); vWF (95-bp), forward (5'-GGTGTCCCTGCTTTCATC-3') and reverse (5'-GTTCCACTTCCGGTCCTG-3'); VEGF-A (98-bp), forward (5'-CACCCATGGCAGAAGGAG-3') and reverse (5'- CACCAGGGTCTCGATTGG–3') Notch 1 (75-bp), forward (5'-GAGGCATGCATCAGCAAC-3') and reverse (5'-GATGGCCTTGCCATTGAC-3'); Notch 2 (84-bp), forward (5'-CAGCCTCTGTGGGCAAGT-3') and reverse (5'-TGACTGGGTGTTCGCTCA-3'), Notch 3 (82-bp), forward (5'-GGCACCTGTACCGACCAC3'-) and reverse (5'-GCAGGTCTTGTTCGCAGT-3'); Jagged-1 (90-bp), forward (5'-TGTGGTTGGCTGGGAAAT-3') and reverse (5'-GCAAGGGGACACACAACC-3'), DLL3 (72-bp), forward (5'-CACGGTCCCTGTCTCCAC-3') and reverse (5'-ACAAGGCATCTGGTGGTA-3'); HES1 (91-bp), forward (5'-CCAAAGACAGCATCTGAGCA-3') and reverse (5'-TCAGCTGGCTCAGACTTTCA-3'); HES5 (85-bp), forward (5'-ACATCCTGGAGATGGCTGTC-3') and reverse (5'-TAGTCCTGGTGCAGGCTCTT-3'); VE-cadherin (74-bp), forward (5'-GGAGCCGAGCATGTGTCT-3') and reverse (5'-TCTGCAAGGTGTGCCTGA-3').2. 2.

2.1.4. Antibodies

Primary antibodies used for immunoblot and immunofluorescence analysis were goat anti-human VEGFR1 (AF321); rabbit anti-human phospho-VEGF R1/Flt-1 (Y1213) (AF4170), Goat anti human HES-1 (AF3317), Goat anti human Jagged-1 (AF1277) (R&D Systems); mouse anti-human vWF (3H3126) (sc-73267); mouse anti-human Notch 1 (mN1A) (sc-32745) and rabbit anti-human Notch 2 (25-255) (sc-5545); rabbit anti-human Notch 3 (M-134) (sc-5593), mouse anti human VCAM-1 (P3C4) (sc-20070) rabbit anti-human PDGFRβ (P-20) (sc-339), rabbit anti human PDGFRα (C-20) (sc-338),

anti-phosphotyrosine (Tyr-P) (PY99; sc-7020) (all from Santa Cruz Biotechnology), rabbit anti-human VEGFR2 (55B11) (2479), rabbit anti-human Notch1 (C37C7), rabbit anti human and Notch2 (8A1), mouse anti-human PECAM-1 (89C2) (3528), rabbit anti-human VE-cadherin (2158) (all from Cell Signalling Technology), anti-GM130 (35/GM130) antibody (BD Transduction Laboratories). All immunoblot HRP and FITC conjugated secondary antibodies and anti–IgG_1 antibody, (X093101) were purchased from DAKO. Secondary antibodies used for Immunofluorescence were Alexa-Fluor 488 conjugated or Alexa-Fluor 546/555 conjugated (Invitrogen). Primary antibodies used for flow cytometry were mouse anti–human VE-cadherin-PE (555511) and PECAM-1-PE (555446) (BD Pharmingen), CD73 (550256), CD29-PE (555443), CD44-PE (555479), CD51-PE (550037) CD14 (347460), CD45 (347490 BD Pharmingen), CD105-PE (FAB10971P R&D Systems), CD34 (CBL555 Chemicon).

2.2. METHODS

2.2.1. Cell Plating

For standard plating density experiments, cells were seeded at 70,000 cells in 9.6 cm^2 at initial plating (corresponding to 70% confluence). For high cell density experiments, MSCs were seeded at 100,000 cells in 9.6 cm^2 at initial plating. For low density experiments, MSCs were seeded at 10,000 cells in 9.6 cm^2 at initial plating.

2.2.2. MSC differentiation assay

The ability of MSCs to differentiate into adipogenic or osteogenic lineages was assessed using the MSC functional Identification kit (R&D systems).

For adipogenic differentiation, MSCs were seeded into 24 well plates at 100% confluence (2.1×10^4 cells/cm^2). Adipogenic medium containing hydrocortisone, isobutylmethylxanthine, and indomethacin in 10% serum α-MEM was added to cells

every 3-4 days. After 14 days, adipocytes were fixed in 4% paraformaldehyde and staining performed for Bodipy 493/503 (1:1000 dilution) (Invitrogen) and immunostaining performed for FABP-4 (10μg/ml) (R&D Systems).

For osteogenic differentiation, MSCs were seeded into 24 plates at 50-70% confluency (7.4×10^3 cells/well). Osteogenic medium containing dexamethasone, ascorbate-phosphate, and β-glycerolphosphate in 10% serum α-MEM was added to cells every 3-4 days. After 14 days, osteoblasts were fixed in 4% paraformaldehyde and Alizarin red staining performed (2g/100ml Alizarin red in ddH_20) by staining cells for 1 hour at room temperature. Following Alizarin red staining cells images were captured using an Olympus (CK X41) phase contrast microscope.

2.2.3. Polymerase chain reaction

Total RNA was isolated from cultured cells using Trizol reagent. In brief, Trizol was added to cells and rocked for up to 1 hour. Flasks were vortexed for 1 minute and solution transfered to 15 ml falcon tubes. $1/5^{th}$ volume chloroform was added to solution, the solution was shaken vigorously for 15 seconds, incubated for 3 minutes at room temperature and centrifuged at 12,000 × g for 15 minutes at 4 ^oC. Following centrifugation the aqueous phase was isolated and RNA precipitated by mixing with ½ volume propanol. Samples were incubated at room temperature for 10 minutes and centrifuged at 12,000 × g for 15 minutes at 4 ^oC. Supernatants were removed completely and RNA pellet washed once with 1 volume 75% ethanol the centrifuged at 7500 × g for 15 minutes. Residual ethanol was removed and RNA pellet air dried at 80 ^oC for 5 minutes. RNA was dissolved in 50 μl DEPC treated water then quantitated by diluting 5 μl RNA in 50 μl elution buffer (Qiagen)and using a Genequant pro RNA/DNA calculator (Amersham Pharmacia, Cambridge, UK). For reverse transcription, 1 μg total RNA and 1 μl diluted oligo dT primer (500μg/ml Promega) (4 μl oligo dT primer, 6 μl elution buffer, were incubated for 10 minutes at 65 ^oC, then reverse transcribed using 1 μl 25U/μl AMV reverse transcriptase (Roche Diagnostics, Lewes, UK) in a mix of 4 μl 5×

RT buffer (Roche), 2 μl 100 mM DTT (Promega), 2 μl 10 mM dNTP (Promega), 0.5 μl 40U/μl RNAse inhibitor (Roche) and ddH20 up to 9.5 μl and incubating for 10 minutes at 30 ^{o}C, then 90 minutes at 42 ^{o}C.

For reverse transcription polymerase chain reaction (RT-PCR), 50 μl reactions containing 5 μl cDNA, 1 μl dNTP, 1 μl primer mix (equal volumes of 100μM forward and reverse primer stocks), 5 μl 10× PCR buffer (Roche), 1 μl 3.5U/μl Enzyme (Roche) and dd$H_2$0 up to 37 μl were incubated for 3 minutes at 94 ^{o}C, immediately followed by 35 cycles of 30 seconds at 94 ^{o}C, 1 minute at 60 ^{o}C, and 1 minute at 72 ^{o}C for 35 cycles, then a 7 minute incubation at 72 ^{o}C. Each set of RT-PCR experiments was performed using the same stock solutions, using the same GeneAmp PCR System 2700 thermocycler (Applied Biosystems, California, USA). Following PCR, 1× DNA loading buffer (Bioline) was added to reaction products and products resolved using a 2.5% ultrapure agarose (Gibco, Paisley, UK) gel run at 100V for 2 hours in 1× TAE buffer (1 litre: 50× TAE buffer: 242g Tris Base, 57.1ml glacial acetic acid, 100mls 0.5M EDTA pH 8.0). 2.5 μl gene red (Biotium) was added to agarose to visualise products and a 25 base pair DNA ladder (Promega) was used to determine product size.

Quantitative PCR (QPCR) was performed using a Sybr green QPCR core kit No ROX reference dye (Eurogentec RT-SN10-05NR). Amplifications were performed as 25 μl reactions by making an initial QPCR Mastermix (1 ml master mix: 250 μl Buffer, 175 μl $MgCl_2$, 100 μl dNTP, 12.5 μl Goldstar Taq polymerase, 75 μl Sybr green and 387 μl $H_2$0) and adding 10 μl of this mix to 2.5 μl primer mix and 11.5 μl H_2O. 24 μl of this mix was then added to 1 μl cDNA and aliquoted into Low-Profile 96-Well Unskirted White PCR Plates (Biorad MLL-9651). Reaction mixtures were incubated for 50 ^{o}C for 2 minutes, 95 ^{o}C for 10 minutes, followed by 39 cycles of 95 ^{o}C for 15 seconds and 60 ^{o}C for 1 minute. Melting curves were calculated from 70 ^{o}C to 94 ^{o}C, reading every 0.2 ^{o}C. QPCR was performed using the ABI PRISM 7000 thermocycler and Opticon Monitor 2 software. Data were normalised to glyceraldehyde-3-phosphate dehydrogenase (GAPDH).

Relative expression was calculated according to the 2-[Delta]CT formula (Potier *et al*., 2007).

2.2.4. Immunoblot analysis

Cells were washed with phosphate buffered saline (PBS), incubated with lysis buffer (To make 200mls 10 × sodium vanadate (Na_3V0_4): Na_3Vo_4 in 200mls 1 × PBS (10mM) was boiled until dissolved. The solution was adjusted to pH 10 until it turned yellow and re-boiled until colourless. The solution was cooled on ice and re-adjusted to pH 10. The cycle was repeated until after cooling the pH remained at 10. The solution was stored at 4^{o}C. To make 300mls lysis buffer (pH 8: 0.727g Tris (20 mM), 0.28g ethylene diamine tetra-acetic acid (EDTA) (2.5 mM), 2.63g sodium chloride (150 mM), 3mls phenylmethanesulphonylfluoride (PMSF) (1 mM (0.1742g/10mls methanol)), a serine protease inhibitor, 30mls 10 × Na_3V0_4 solution (1 mM), 3mls Tergitol-type nonyl phenoxylpolyethoxylethanol (NP) 40 (1%) 500μl aprotinin (trypsin inhibitor (Sigma) (10 μg/ml from 5mg/ml stock) 500μl leupeptin (protease inhibitor (Sigma)) (10 μg/ml from 5mg/ml stock) and 30mls glycerol (10%)) for 15 minutes on ice, vortexed for 1 minute, scraped gently from the tissue culture flask, then incubated for 30 minutes rotating at 4^{o}C. Supernatants were collected after centrifugation at 12,000 rpm, then total protein was quantitated using a BCA protein assay kit (Pierce, Perbio Science, Tattenhall, UK).

Samples (100-200 μg) were electrophoresed using NuPAGE 3-8% Tris acetate or 4-12% Bis-Tris gel systems (Invitrogen, Groningen, The Netherlands) in 1× NUPAGE Tris-acetate or MES SDS running buffer (Invitrogen) run at 150V or 200V (For Tris acetate or Bis Tris respectively) for 1.5 hours. 5 μl Precision plus dual colour protein standard (BioRad) was used as a size marker. Protein was transferred to a nitrocellulose membrane using a NuPAGE western transfer system (Invitrogen, Groningen, The Netherlands) in 1× NUPAGE Transfer buffer (Invitrogen) run at 35V for 1.5 hours. Membranes were blocked with 4% Marvel skimmed milk in 1× TBST (1 litre 10× TBST: 12.114g Tris (0.01 M), 87.66g NaCl (0.15 M), 50mls (w/v) Tween 20 (0.5%)) pH 7.4) for

1 hour, then incubated overnight at 4°C with the primary antibody (1:500-1:1000 dilution). Membranes were washed 3× in 1× TBST, incubated with HRP-conjugated secondary antibody (Dako, Ely, UK) (1:2000 dilution) for 2 hours, washed 3× with 1× TBST, then developed with Supersignal west dura enhanced chemiluminescence kit (Thermo scientific). Proteins were visualised using Kodak X-AR or Kodak-MR film and density of bands determined using Gene Tools software (Syngene) and normalisation to the corresponding loading control.

2.2.5. Immunofluorescence microscopy

After culturing cells on gelatin-coated 1.7 cm^2 chamber slides (Becton Dickinson, Oxford, UK), cells were washed with PBS and fixed in 4% paraformaldehyde (To make 4% paraformaldehyde, 2 g paraformaldehyde was added to 25 ml 1× PBS and heated to 50°C with constant stirring, 1M sodium hydroxide was added dropwise until solution cleared. 5 ml 10× PBS was added to the solution and the volume brought up to 50mls with ddH_20 then the solution was allowed to cool to 37°C and pH adjusted to 7.4) for 20 minutes at room temperature, then washed again with PBS. Paraformaldehyde was quenched in 0.1M glycine/PBS (Fisher Chemicals) for 20 minutes, washed 2× and cells permeabilised in 0.5% Triton-X-100 (Sigma) for 30 minutes. Non-specific binding was blocked with 2% fish gelatin in PBS (Sigma, Poole, UK) for 1 hour, then slides incubated overnight at 4°C with primary antibodies (1:50-100 dilution) contained in a 2% fish gelatin solution. After washing with PBS, diluted secondary antibodies (1:200) were added for 2 hours. F-actin was visualised using tetramethyl rhodamine isothiocyanate labeled Rhodamine Phalloidin (1:500 dilution) (Molecular Probes R-415), then slides washed and coverslips mounted using Prolong gold Antifade solution containing DAPI (Invitrogen).

2.2.6. Immunoprecipitation analysis

Lysates were pre-cleared using 40 µl protein A–Sepharose (GE Healthcare) for 1 hour, protein A-Sepharose was removed by centrifugation at 2000 × g for 3 minutes and supernatants incubated with primary antibodies overnight at 4 ^{o}C (1:500 dilution). Immune complexes were isolated by incubation with 80 µl protein A–Sepharose for 2 hours. Protein A-Sepharose beads were washed 3× with 500 µl ice cold lysis buffer, the supernatant removed and 25 µl loading buffer added for immuno-blot analysis.

2.2.7. Proteome array analysis

A human phosphorylated RTK array Kit (ARY001; R&D Systems) was used to simultaneously detect the relative tyrosine phosphorylation levels of 42 different RTKs. Each array contains duplicate validated control and capture antibodies for specific RTKs. In brief, array membranes were blocked, incubated with 500 µg MSC lysate overnight at 4^{o}C, washed and incubated with anti-phosphotyrosine-HRP for 2 hours at room temperature, washed again, and developed with enhanced chemi luminescent western blotting detection reagent (GE healthcare), and RTK spots were visualised using Kodak MR or XAR film.

2.2.8. Enzyme linked immunosorbent assays (ELISAs)

ELISAs were performed using the Quantikine human VEGF, PDGF-AA, BB, AB immunoassays (R&D Systems) according to the manufacturer's protocol.

2.2.9. Flow cytometry

MSCs, HUVECs, or HDFs were trypsinised, resuspended in 1ml media and allowed to recover for 1 hour. Cells were washed 2 × in 5 ml wash buffer, (0.5% BSA (Sigma)/PBS) and 1×10^{5} cells incubated with either phycoerythrin (PE) or un-conjugated antibodies for 1 hour (1:5 dilution). After primary antibody incubation, cells were washed 3 × in 0.5% BSA/PBS wash buffer and unconjugated antibodies incubated with fluoroscein

isothiocyanate (FITC) secondary antibody (1:200 dilution) (Dako Cytomation) for 45 minutes, washed twice in 0.5% bovine serum albumin in PBS and sent for analysis in Manchester University flow cytometry facility.

2.2.10. siRNA transfections

MSCs (5×10^5 cells), together with 3 μg siRNAs, were transfected by electroporation with a human Nucleofector kit (Amaxa) and cultured overnight in growth medium. Validated siRNAs, which were functionally tested to provide ≥70% target gene knockdown, were used for VEGF-A knockdown (QIAGEN). For Notch knockdowns, siRNAs for Notch1 (sc-36095), Notch2 (sc-40135) and Notch3 (sc-37135) (Santa Cruz) were employed, with scrambled siRNA as a control (QIAGEN).

2.2.11. VEGFR1 activation

100 μM Pervanadate (30 mM sodium orthovanadate, 1× PBS, 0.18% (w/v) hydrogen peroxide in PBS) was added to MSCs or HUVECs for 5 minutes, washed 2× with calcium-free magnesium-free 1× PBS, and cell lysates extracted for VEGFR1 phosphorylation analysis.

2.2.12. Notch activation

For EDTA experiments, cells were stimulated for 15 minutes with 5 mM EDTA, washed twice with MSC basal medium, left to recover overnight, and cell lysates extracted. Recombinant human Jagged-1/Fc chimera (R&D Systems, 1277-JG) was immobilised on culture plates by incubating plates with a solution of Jagged-1 (5 μg/ml) in PBS for 2 hours at 37°C. MSCs were seeded onto plates and cultured for 24 hours.

2.2.13. DiI-Ac-LDL uptake

Cells were incubated with 10 µg/ml 1,1'-dioctadecyl-3,3,3',3'-tetramethylindocarbocyanine-labelled acetylated LDL (DiI-Ac-LDL) (Biomedical technologies Ltd (BT-906) for 3 hours at 37 °C to allow uptake, and immunofluorescence performed as above.

2.2.14. Matrigel network formation assay

200 µl growth factor reduced Matrigel (BD biosciences) was added to each well of a 24 well plate on ice, then removed and plates incubated for 30 minutes at 37 ^{o}C. 25000 cells in 0.5% fetal calf serum Dulbecco's minimal essential medium were added to each well of the 24 well plate and plates visualised after 4 hours and 24 hours at 37^{o}C for network formation. For Matrigel protein extraction, 2 ml growth factor reduced Matrigel (BD biosciences) was added to a 25cm^{2} flask on ice, Matrigel removed and plates incubated for 30 minutes at 37^{o}C. After this time flasks were seeded with cells and protein extracted after 48 hours as previously described.

2.2.15. Chorioallantoic membrane (CAM) assay

Fertilized white chicken eggs (Henry Stewart company) were incubated for five days at 37.5 ^{o}C and 43% humidity in a specialised egg incubator (R.Com King Suro 20 Digital Incubator). Under aseptic conditions in a laminar flow cabinet, cells were labelled with 10 µg/ml DiI (Sigma 42364-100MG) for 30 minutes at 37 ^{o}C and the Matrigel assay prepared as above in 24 well plates on 13 mm diameter glass coverslips (Scientific Laboratory Supplies Ltd). Eggs were cleaned with 70% ethanol and a square window cut into the shell with dissecting scissors to reveal the underlying embryo and CAM blood vessels. The membrane covering the CAM surface was removed with forceps and coverslips placed gently on the CAM. The window was sealed with transparent tape and the egg returned to the incubator for 48 hours at 37.5 ^{o}C and 65% humidity, following which time coverslips were removed and prepared for immunofluorescence as previously described. Figure 2.1 shows a schematic of the coverslip method.

Figure 2.1

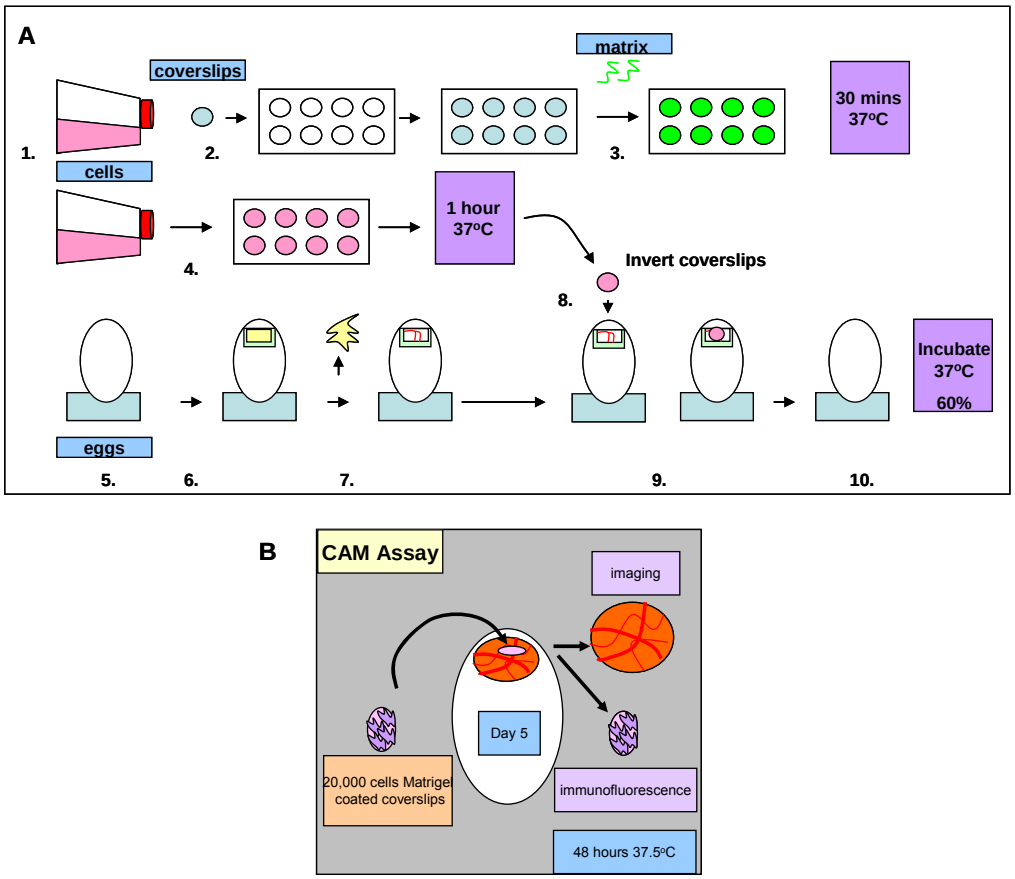

Figure 2.1. *The coverslip method for immunostaining cultured cells in the CAM assay*

(A) Stepwise procedure of the method. 1) Set up cells; 2) Carefully place coverslips in wells of tissue culture plates using curved tip forceps; 3) Apply 200μl matrix protein of interest to coverslips in dishes; 4) Apply cells to coverslips applying 1ml media to each well of tissue culture plate and allow cell to adhere to matrix by culturing at 37°C for 1 hour; 5) incubate eggs until desired stage 6) Carefully cut hole in egg and remove membrane covering the CAM surface 7) Remove media from prepared cells, and carefully dislodge coverslip with two bent end needles; 8) invert coverslip to allow direct contact of cells with chick CAM. 9) Place coverslips gently onto CAM; 10) Seal the window with transparent tape and return the egg to the incubator. Incubate eggs for desired length of time.

(B) Either 20,000 DiI labelled control standard cultured MSCs (MSC-S), or endothelialised MSCs (MSC-H) were seeded on Matrigel, then placed into the chick CAM of a day 5 chick embryo for 48 hours. Coverslips were then removed and processed for Immunofluorescence analysis. The underlying CAM blood vessels were imaged following coverslip removal.

2.2.16. Microscopy

All light microscopy images were taken using an Olympus (CK X41) phase contrast microscope with attached digital camera using ×4, ×10 and ×20 objectives. CAM vascularisation was imaged using a Nikon stereo microscope.

For fluorescence microscopy images were collected on an Olympus Widefield BX51 upright microscope using a 20×/ UPlanFLN objective and captured using a Coolsnap HQ camera (Photometrics) through MetaVue Software (Molecular Devices). Specific band pass filter sets for DAPI, FITC, TRITC were used to prevent bleed through from one channel to the next.

For confocal microscopy, images were collected using a Nikon C1 confocal on an upright 90i microscope with a 60×/ 1.40 Plan Apo objective and 3× confocal zoom. Images for DAPI, FITC and Texas red were excited with the 405nm, 488nm and 543nm laser lines respectively. Different sample images detecting the same antibodies were aquired under constant acquisition settings. Images were then processed using Nikon EZ-C1 Freeviewer v3.3 software.

For Delta Vision microscopy, a Delta Vision RT (Applied Precision) restoration microscope 40×/ 0.85 UPlan Apo objective and Coolsnap HQ (Photometrics) camera was utilised. Raw images were deconvolved using the Softworx software; maximum intensity projections of these deconvolved images are shown**.** At least twenty representative images of each sample were taken.

2.2.17. Transmission Electron Microscopy

Samples were processed by University of Manchester electron microscopy facility, briefly samples were chemically fixed, dehydrated with solvent, embedded in special resins, sectioned with an ultramicrotome and stained using heavy metal salts. Imaging was performed using a Philips 400 Transmission Electron Microscope**:**

2.2.18. Statistics

In all quantitation experiments, results are expressed as the mean ± the SD. Statistical differences between sets of data were determined by using a student *t* test on SigmaPlot 8.0 software, with $P < 0.05$ considered significant.

CHAPTER 3

RESULTS

High cell density induced endothelial characteristics in MSCs

CHAPTER 3: RESULTS

3.1. High cell density induced endothelial characteristics in MSCs

An increasing number of studies have now demonstrated that MSCs can differentiate to ECs (Al-Khaldi *et al* ., 2003; Alviano *et al* ., 2007; Bai *et al*., 2009; Chen *et al* ., 2009; Chung *et al* ., 2009; Lozito *et al* ., 2009a;b; Ohata *et al*., 2009; Oswald *et al* ., 2004; Silva *et al* ., 2005; Wu *et al* ., 2005; Xu *et al* ., 2009; Yue *et al* ., 2008; Zhang *et al* ., 2008) and contribute to postnatal vasculogenesis (Aghi and Chiocca, 2005; Hung *et al* ., 2005; Tang *et al* ., 2006; Xin *et al* ., 2007; Roorda *et al* ., 2009). The environmental cues that MSCs sense when at sites of repair or regeneration, such as exposure to growth factors, ECM composition, cell-cell contact, shear stress or mechanical stretch are likely to be critical mediators in regulating their differentiation to an EC fate.

A defining feature of ECs in growing blood vessels is their ability to switch from a migratory phenotype to a contact-inhibited phenotype within polarised monolayers which are stabilised by intercellular junctions (Dejana *et al.,* 2004 Hordijk *et al* ., 1999). Both VE-cadherin and PECAM-1 are expressed constitutively at cellular junctions and induce rapid cellular responses to cell-cell contact (Newman *et al* ., 2003; Vestweber *et al*, 2008; Vestweber *et al* ., 2009; Vincent *et al* ., 2004; Woodfin *et al* ., 2007). The adhesion molecules VCAM-1 and ICAM-1 are inducible by TNF-α in ECs (McHale *et al* ., 1999). Furthermore, the expression of specific cell surface RTKs can serve to identify ECs (Kliche *et al* ; 2001; Munoz-Chapuli *et al* ; 2004; Olsson *et al* ., 2006). The primary RTKs expressed by ECs are the VEGFRs, VEGFR1 (Flt-1), VEGFR2 (KDR/Flk-1) and VEGFR3 (Flt-4) (Olsson *et al* ., 2006). Their expression is almost exclusively restricted to ECs, but they can be expressed by other cell types, for example, VEGFR1 can be expressed on monocytes (Schmeisser *et al* ., 2001; 2003) and both VEGFR1 and VEGFR2 can be expressed by some populations of vSMCs (Banerjee *et al* ., 2008; Greenberg *et al* ., 2008). In addition, ECs can also be identified by their expression of vWF, a large multimeric glycoprotein present in blood plasma and produced constitutively in endothelium, megakaryocytes and subendothelial connective tissue

(Sadler *et al*, 1998) and by functional assays such as uptake of ac-LDL and tubular network forming ability in semi-solid media (Voyta *et al* ., 1984; Baatout *et al*, 1996;1997).

As previously discussed, exogenous VEGF-A_{165} profoundly influences the endothelial differentiation of MSCs (Al-Khaldi *et al* ., 2003; Alviano *et al* ., 2007; Bai *et al* ., 2009; Chen *et al* ., 2009; Chung *et al* ., 2009; Oswald *et al* ., 2004; Wu *et al* ., 2005; Xu *et al* ., 2009; Zhang *et al* ., 2008). However, the addition of exogenous VEGF-A in MSCs cultured at subconfluence for 5 hours was insufficient to induce endothelial marker expression (Ball *et al* ., 2007c), suggesting that VEGF-A alone is insufficient to induce endothelial marker expression in MSCs.

Direct cell-cell interaction has also been shown to influence MSC differentiation events (Ball *et al* ., 2004; McBeath *et al* 2004). MSCs co-cultured with neonatal cardiomyocytes mediated MSC differentiation into cardiomyocytes (Xu *et al* ., 2004), whilst MSCs cocultured with ECs severely disrupted αSMA organisation and thus contractile function (Ball *et al* ., 2004; 2007a). In addition, cell density has been shown to modulate MSC morphology and induced differentiation of MSCs into adipogenic or osteogenic lineages (McBeath *et al*., 2004).

Studies have shown that endothelial markers are strongly regulated by EC density, with PECAM-1 only being expressed when ECs form stable monolayers and not when the cells are sparsely distributed (RayChaudhury *et al* ., 2001; Lampugnani *et al* ., 1997). VEGFR2 activity has also been shown to be regulated by cell density, with high levels of VEGF dependent tyrosine phosphorylation detected in sparse cells, whilst confluent monolayers only exhibited very low levels of tyrosine phosphorylation (Rahimi *et al* ., 1999). Furthermore, in subconfluent ECs, VE-cadherin phosphorylation was only enriched at areas of cell-cell contact (Lampugnani *et al* ., 1997).

In this chapter, the effect of cell density on influencing MSC differentiation to an EC fate

was examined.

3.2. MSC characterisation

3.2.1. Morphological characterisation of MSCs

MSCs are characterised morphologically by having a small cell body with long thin processes, often referred to as a spindle-shaped morphology (Baksh *et al* ., 2004). Figure 3.1 shows phase contrast images of human MSCs cultured for 24 hours at 10% confluence (Figure 3.1 (A); 3.1 (AI)), in standard conditions (70% confluency) (Figure 3.1 (B); 3.1 (BI)), or at 100% confluence (Figure 3.1 (C); 3.1(CI)) showing small adherent cells displaying a spindle-shaped morphology. All experiments were performed on MSCs obtained from the normal human BM of a 28 year old female and repeated using MSCs obtained from BM of a a 21-year-old male (*see* Chapter 2: Materials and Methods section 2.1.1).

3.2.2. Immunophenotypical characterisation of MSCs

MSCs were characterised to ensure their immunophenotypic profile was consistent with the minimum criteria reported in the literature for human BM-derived MSCs in standard culture conditions (Dominici *et al* ., 2006; Huang *et al* 2009, Phinney and Prokop 2007a). Furthermore, it was necessary to verify that the MSCs were not contaminated by haematopoietic cells. Flow cytometry (Figure 3.2) revealed that the MSCs were positive for the characteristic MSC markers CD73 (ecto-5'-nucleotidase), CD29 (integrin β1 chain), CD44 (hyaluronan receptor), CD51 (αV integrin) and CD105 (endoglin), whilst being negative for the haematopoietic cell marker CD34. In addition, these MSCs have been shown to be negative for the leukocytic markers CD14 and CD45 (McBeath *et al* ., 2004).

Figure 3.1

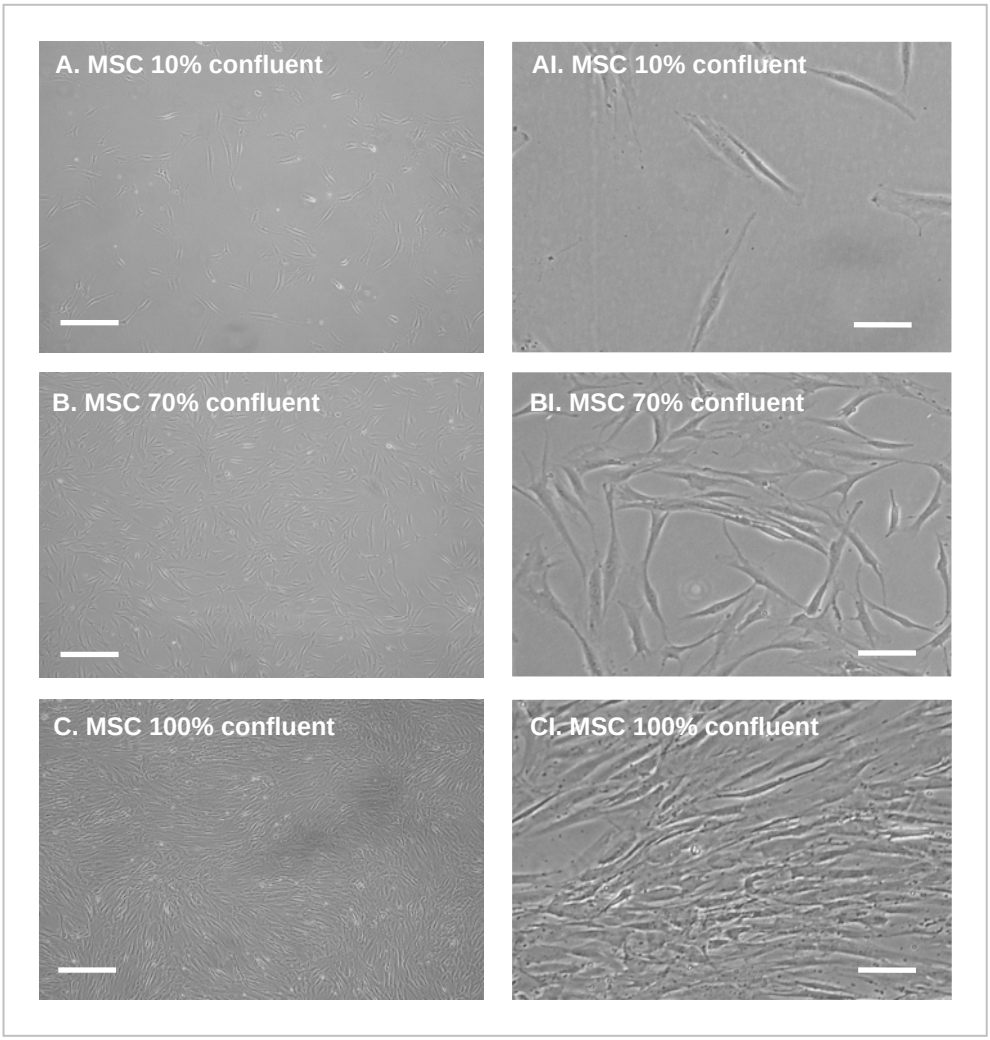

Figure 3.1. *Morphological characterisation of MSCs*

Representative phase contrast images of MSCs cultured at 10% confluence (A,), 70% confluence (B) or 100% confluence (C) for 24 hours. Images were obtained using an Olympus (CK X41) microscope with attached digital camera (4× objective). Scale bars = 100μm. Figures AI-CI represent an enlarged region of A-C. Scale bars = 25μm. 10 representative images were taken for each analysis.

Figure 3.2

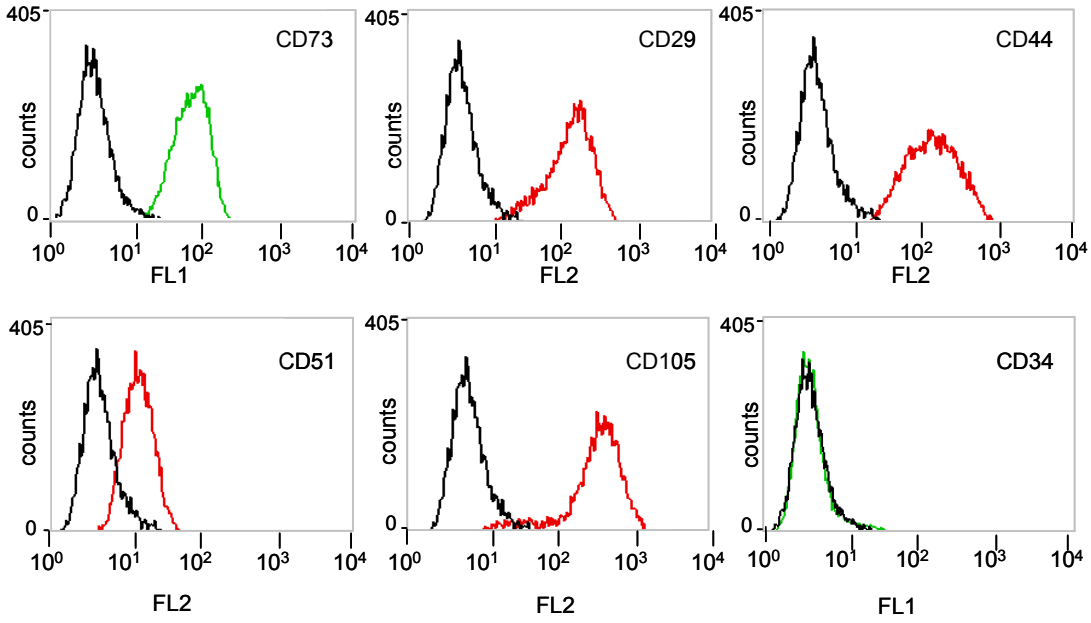

Figure 3.2. *Immunophenotypical characterisation of MSCs*

Flow cytometry of MSCs cultured under standard conditions (70% confluency) for 48 hours using phycoerythrin (PE) or FITC-conjugated antibodies. The MSC markers CD73 (ecto 5' nucleotidase), CD29 (integrin β1 chain), CD44 (hyaluronan receptor), CD105 (endoglin) and CD51 (αV integrin) and the haemoatopoietic marker (CD34) are represented by coloured peaks (either green for FITC conjugated antibodies (FL1) or red for PE-conjugated antibodies (FL2). Black peaks represent the control IgG_1. Data are representative of two independent experiments for each analysis.

3.2.3. Differentiation capacity of MSCs

MSCs have the capacity to differentiate into multiple cell types including osteoblasts, chondrocytes and adipocytes (Huang *et al* 2009, Phinney and Prokop 2007a; Pittenger *et al*., 1999). To confirm MSC multipotency, MSCs are induced to differentiate to osteoblasts, chondrocytes or adipocytes, following culture using defined differentiation media.

MSCs were cultured in standard conditions using MSC basal medium for 14 days, or induced to differentiate to adipogenic or osteogenic lineages using defined differentiation media (Chapter 2: Materials and Methods, section 2.2.2) (Figure 3.3). Chondrogenic differentiation was not analysed due to the large number of cells needed for this assay. Adipogenic differentiation was detected by immunofluorescence microscopy using Bodipy 493/503, which stains lipid droplets, and FABP-4, which is characteristically present in adipocytes. Osteogenic differentiation was detected using Alizarin red staining which stains calcium rich deposits.

Control non-induced MSCs cultured in MSC basal medium for 14 days (Figure 3.3 (A)) were negative for Bodipy 493/503 and FABP-4, suggesting no lipid containing vacuoles or FABP-4 were present. In contrast, confluent MSCs cultured in adipogenic media for 14 days (Figure 3.3 (B)) exhibited a rounded morphology, and large lipid filled vacuoles were evident within the cells as detected by positive Bodipy 493/503 staining. In addition, positive FABP-4 immunoreactivity was apparent at the cell periphery. In contrast, MSCs induced to differentiate towards osteoblasts for 14 days adopted a more flattened morphology, and mineralised deposits could be detected with alizarin red staining (Figure 3.3 (D)). Alizarin red staining of MSCs cultured in MSC basal medium for 14 days which had a spindle shaped morphology, resulted in no detectable positive staining, suggesting mineralised deposits were not present (Figure 3.3 (C)).

Figure 3.3

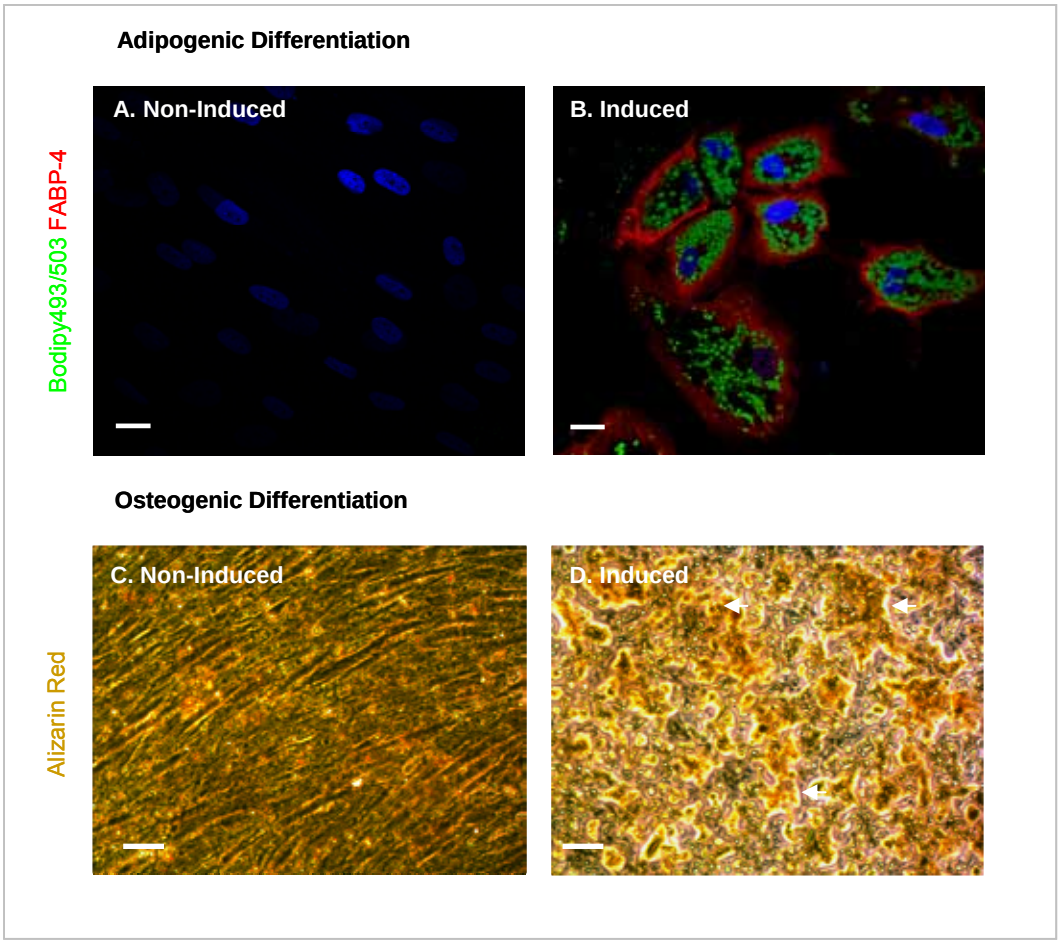

Figure 3.3. *Differentiation capacity of MSCs*

MSCs cultured in standard conditions for 24 hours (70% confluence) were induced to differentiate to adipogenic or osteogenic lineages by culture using defined differentiation media over 14 days. As non-induced MSC controls, **(A, C)** MSCs were cultured in standard conditions in MSC basal media over 14 days. **(B, D)** Induced MSCs. Adipocytes were detected by staining for Bodipy 493/503 (green) and immunostaining for FABP-4 (red), using a Nikon C1 upright confocal microscope (60× objective). Nuclei are stained with DAPI (blue). Scale bars = 7μm. Osteoblasts were detected by alizarin red staining and phase contrast microscopy using an Olympus (CK X41) phase contrast microscope (20× objective). Calcium deposits are marked with white arrows. Scale Bars = 20μm. Each image is representative of ten random images captured for each treatment, with each analysis performed in triplicate.

Thus, MSCs in standard culture conditions maintained their potential to differentiate towards adipogenic and osteogenic lineages.

3.3. MSCs cultured at high density had the potential to differentiate to ECs

3.3.1. MSCs cultured at high cell density developed a cobblestone-like morphology

Cell density can regulate the morphology and differentiation of MSCs (Ball *et al* ., 2004; McBeath *et al* ., 2004). For experiments examining the effects of cell density on endothelial marker expression, it is first necessary to define low cell density and high cell density in these studies. As mentioned in Chapter 2: Materials and Methods, section 2.2.1 and above section 3.2.1, the term standard culture conditions, refers to MSCs plated and cultured up to 70% confluency. However, at 70% confluency, invariably a small proportion of MSCs will be in contact. Therefore at low cell density, MSCs were plated sparsely at 10% confluency to ensure minimal cell contact during culture. High cell density was defined as MSCs plated and cultured at 100% confluency, to ensure maximal cell contact from the moment of plating (*see also* Figure 3.1). After 48 hours in culture, MSCs at standard cell density (70% confluent at plating) (Figure 3.4 (A)), or at low cell density (10% confluent at plating) for 14 days (Figure 3.4 (B)), maintained a spindle-shaped morphology. In contrast, MSCs in close contact at high cell density (100% confluent at plating) for 14 days (Figure 3.4 (C)) developed a more rounded cobblestone-like morphology that was similar to HUVECs in standard culture conditions (Figure 3.4 (D)) and as reported in other EC lines (Hutley *et al* ., 2001).

3.3.2. High cell density induced MSCs to express VEGFR1

3.3.2.1. High cell density induced MSCs to express VEGFR1 transcripts

MSCs cultured at high density for 14 days adopted a cobble-stone morphology similar to cultured ECs. To determine if MSCs cultured at high density were differentiating towards

Figure 3.4

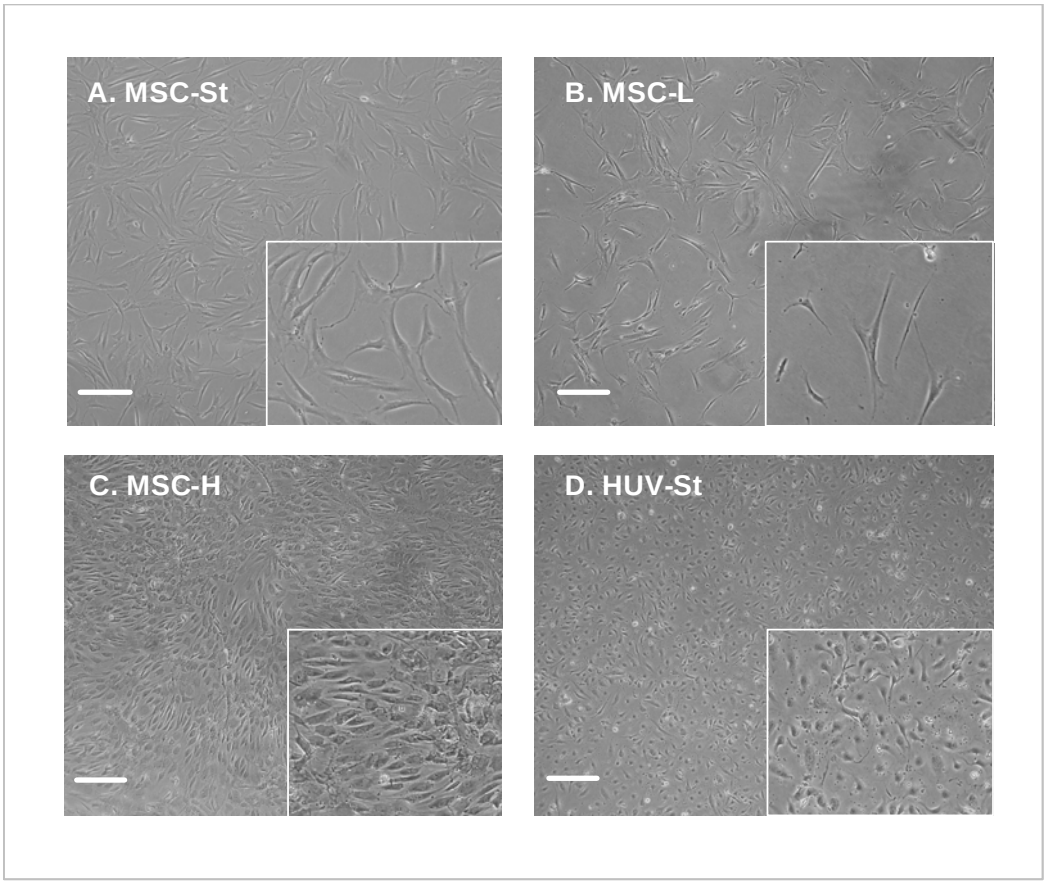

Figure 3.4. *MSCs cultured at high cell density developed a cobblestone-like morphology*

Representative phase contrast images of **(A)** MSCs in standard culture conditions (MSC-St) for 48 hours, **(B)** MSCs cultured at low density (MSC-L) for 14 days or **(C)** MSCs cultured at high density (MSC-H) for 14 days. **(D)** HUVECs in standard culture conditions (HUV-St) were used as a positive cellular control. Images were obtained using an Olympus (CK X41) microscope with attached digital camera (4× objective). Inserts represent an enlarged region of each image. Each image is representative of two independent experiments with ten representative images taken for each analysis. Scale bars = 100μm.

an EC lineage, the expression of the endothelial markers VEGFR1, vWF, VE-cadherin and PECAM-1 were assessed. VEGFR1 is a RTK expressed on ECs (Kliche *et al* ., 2001) as well as on some populations of vSMCs, HDFs, monocytes and macrophages (Banerjee *et al* ., 2008; Salmonsson *et al* ., 2003). VEGFR1 functions in vascular development as a "decoy receptor" to bind and sequester VEGF-A thereby regulating signalling through VEGFR2 (Shibuya *et al*, 2006a). Expression of VEGFR transcripts was determined using RT-PCR. HUVECs cultured in standard conditions, which were used as positive control cells, expressed VEGFR1 (Figure 3.5 (A); lane 1) and VEGFR2 (Figure 3.5 (A); lane 2) but did not express VEGFR3 (Figure 3.5 (A); lane 3), as previously shown (Ball *et al* ., 2007c). MSCs cultured after plating at low cell density for 14 days expressed no detectable VEGFR transcripts (Figure. 3.5 (A)), as reported (Ball *et al* ., 2007c), whilst MSCs cultured after plating at high cell density for 14 days expressed VEGFR1 (Figure 3.5 (A); lane 1) but no detectable VEGFR2 or VEGFR3 transcripts (Figure 3.5 (A); lanes 2-3 respectively). Verification by quantitative PCR analysis of VEGFR1 transcripts expressed by MSCs cultured for 14 days revealed a low level of VEGFR1 transcripts in MSCs cultured at low cell density, but a significant increase (5.0±0.7 fold) in VEGFR1 transcripts in MSCs cultured at high cell density (Figure 3.5 (B)).

3.3.2.2. High cell density induced MSCs to express VEGFR1 protein

Immunoblotting analysis was used to detect VEGFR1 protein levels in MSCs that had been plated at low, standard or high cell density and cultured for 14 days. HUVECs in standard culture conditions were used as a positive control, which resulted in an immunopositive band at 180-kDa (Figure 3.6 (A); lane 1), corresponding to the expected size of VEGFR1. HDFs in standard culture conditions were used as negative control cells, which did not produce any detectable VEGFR1 immunoreactivity (Figure 3.6 (A); lane 2). In addition, minus primary (Figure 3.6 (A); lane 3), minus secondary (Figure 3.6 (A); lane 4) or isotype specific IgG_1 (Figure 3.6 (A); lane 5) controls displayed no binding.

Figure 3.5

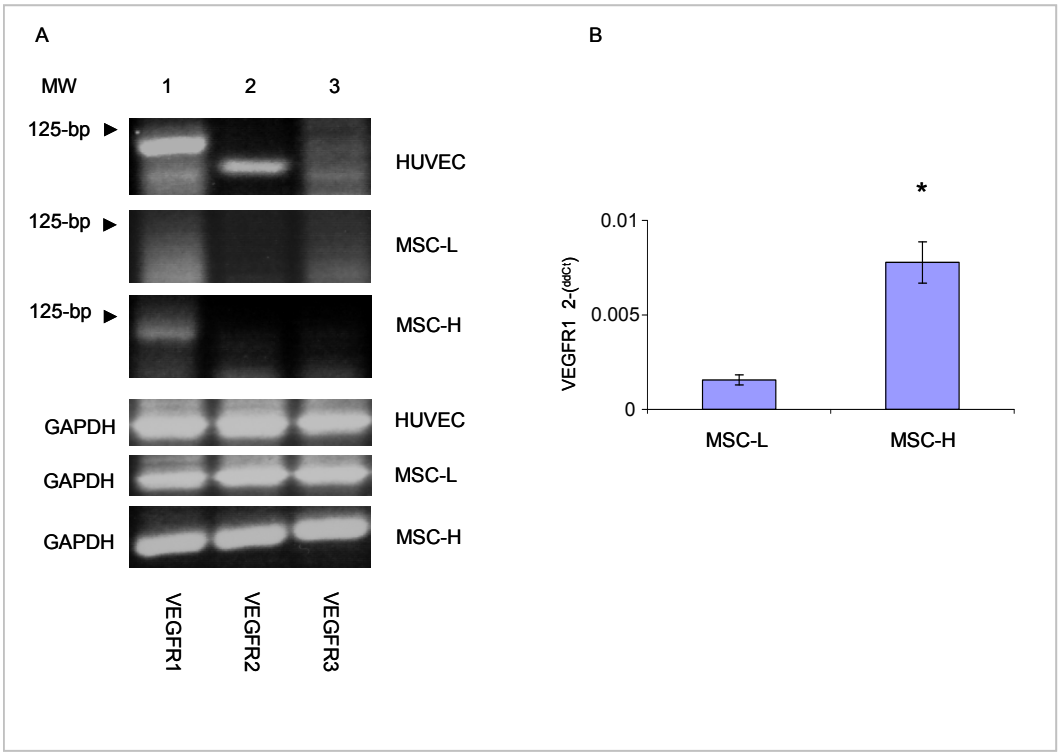

Figure 3.5. H*igh cell density induced MSCs to express VEGFR1 transcripts*

(A) VEGFR expression was examined by semi-quantitative RT-PCR analysis. HUVECs plated at standard cell density, and MSCs at low cell density (MSC-L) or at high cell density (MSC-H), were cultured for 14 days. Lane 1 is VEGFR1 (99-bp); lane 2 is VEGFR2 (81-bp); lane 3 is VEGFR3 (87-bp). Two different primer pairs for VEGFRs 1-3 gave similar results, and GAPDH (71-bp) was a loading control.

(B) Quantitative PCR analysis of VEGFR1 mRNA from MSCs cultured for 14 days after plating at low cell density (MSC-L) or at high cell density (MSC-H), each sample was run in triplicate. * represents $p<0.05$ compared to MSCs cultured after plating at low cell density. Data are representative of two independent experiments.

MSCs cultured under standard conditions (Figure 3.6 (A); lane 6) or at low density for 14 days (Figure 3.6 (A); lane 7) produced no detectable VEGFR1 protein. In contrast, MSCs cultured at high density for 14 days expressed readily detectable VEGFR1 protein at 180-kDa (Figure 3.6 (A); lane 8).

Having detected VEGFR1 transcript and protein expression in MSCs cultured at high density for 14 days, experiments were conducted to establish whether the induced VEGFR1 was capable of signalling (Figure 3.6 (B)). The phosphorylation status of VEGFR1 was analysed in unstimulated HUVECs and MSCs cultured at high density, or upon pervanadate stimulation, a potent inducer of tyrosine phosphorylation (Figure 3.6 (B)) (Vecchi *et al* ., 1998). Immunoprecipitation then immunoblotting for VEGFR1 in unstimulated HUVECs and MSCs (Figure 3.6 (B); lanes 1 and 3) detected low levels of phosphorylated VEGFR1. In contrast, HUVECs and MSCs stimulated with pervanadate revealed prominent VEGFR1 tyrosine phosphorylation (Figure 3.6 (B); lanes 2 and 4 respectively). Thus, VEGFR1 induced by MSCs cultured after plating at high cell density was capable of signalling.

To determine whether the induced VEGFR1 was expressed on the MSC surface or had an intracellular distribution, single cell flow cytometry (Figure 3.6 (C)) was performed. MSCs cultured at low density for 14 days showed no apparent cell surface VEGFR1, whilst MSCs cultured at high density displayed only minimal levels of cell surface VEGFR1 expression, suggesting VEGFR1 expression may be predominantly intracellular. Following culture of MSCs at high density for 14 days it was difficult to obtain a homogenous single cell suspension, which may be reflected in the presence of a second peak on the histogram.

3.3.2.3. Localisation of VEGFR1 in MSCs cultured at high density

Immunofluorescence analysis was performed to establish whether the induced VEGFR1 showed an intracellular distribution in MSCs. MSCs cultured at low or high density for 14

Figure 3.6

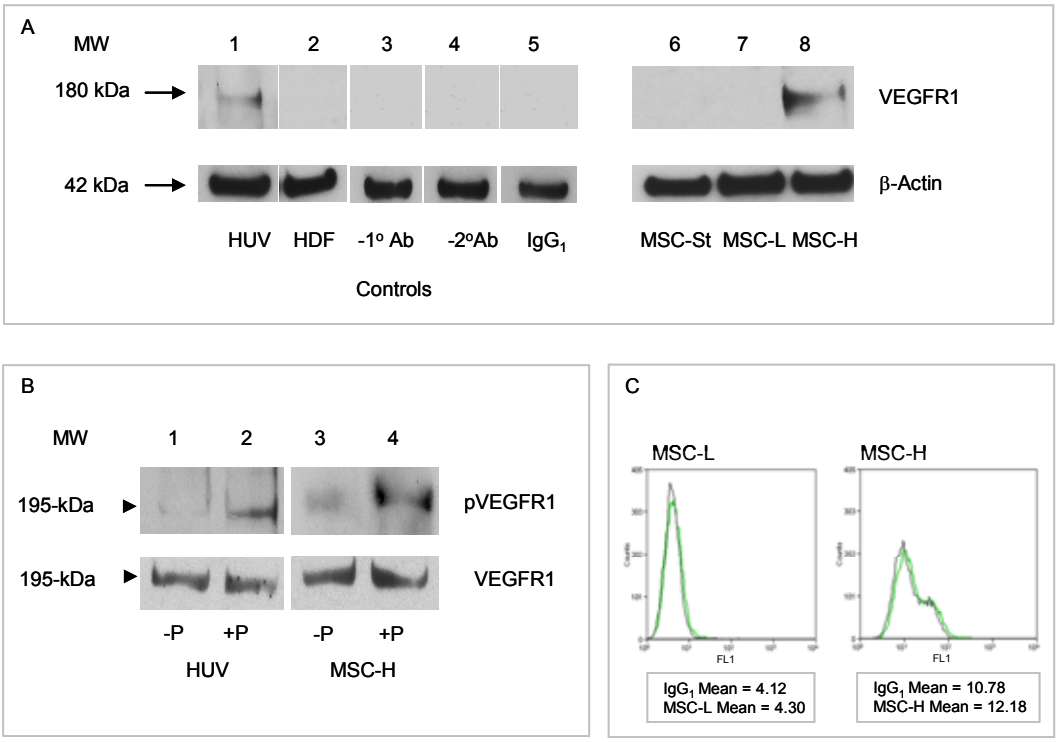

Figure 3.6. H*igh cell density induced MSCs to express VEGFR1 protein*

(A) Immunoblot analysis for VEGFR1 in 14 day total protein lysates. Lane 1, HUVECs (HUV) as a VEGFR positive-cell after plating at standard cell density; lane 2, HDFs as a VEGFR-negative cell after plating at standard cell density; lanes 3-5 are minus primary antibody (-1°Ab), minus secondary antibody (-2°Ab) and isotype specific (IgG_1) negative controls, respectively; lane 6, MSCs at standard cell density (MSC-St); lane 7, MSCs at low cell density (MSC-L); lane 8, MSCs at high cell density (MSC-H). Membranes were reprobed with β-actin as loading controls. **(B)** Tyrosine phosphorylation analysis of VEGFR1 after immunoprecipitation in 14 day total protein lysates. HUVECs (HUV) were used as a VEGFR1 positive control and were stimulated with 100 μM pervanadate (+P) (lanes 2 and 4) for 5 minutes at 37°C, or unstimulated (-P) (lanes 1 and 3). VEGFR1 was immunoprecipitated using an anti-VEGFR1 antibody, and phosphorylation detected by immunoblot using an anti-phosphoVEGFR1 antibody. Membranes were reprobed with anti-VEGFR1 as loading controls. **(C)** Single colour flow cytometry analysis for VEGFR1 (green) using an unconjugated VEGFR1 primary antibody (AF321) and a FITC conjugated secondary antibody (FL1) in MSCs cultured at low density (MSC-L) or MSCs cultured at high density (MSC-H) for 14 days. Black curves=IgG_1. A representative of two independent experiments is shown for each analysis.

days were examined for total VEGFR1 and phosphorylated VEGFR1 (tyrosine residue Y1213) by immunofluorescence analysis (Figure 3.7), with HUVECs used as a VEGFR1 positive cellular control. The isotype specific IgG_1 was used as a negative control. HUVECs (Figure 3.7 (A)) were shown to express a large proportion of total VEGFR1 resident within a compact juxtanuclear compartment that has been previously identified as the Golgi apparatus (Mittar *et al* ., 2009). In addition, variable amounts of total and phosphorylated (Y1213) VEGFR1 were found to be present within a diffuse punctate pattern, consistent with relatively small cytoplasmic vesicles documented previously (Mittar *et al* ., 2009) as well as present on the surface of the plasma membrane. Here, MSCs cultured at low density (Figure 3.7 (B)) exhibited only trace levels of immunostaining. However, in contrast, MSCs cultured at high density (Figure 3.7 (C)) displayed prominent VEGFR1 immunoreactivity (total and phosphorylated). However, it must be noted that the phosphorylated VEGFR1 immunostaining would be expected to overlap completely with the total VEGFR1 immunostaining. This result is unexplained and needs further validation. No binding of control IgG_1 was detected (Figure 3.7 (D)).

To determine whether the induced VEGFR1 in MSCs cultured at high density localised predominantly to the Golgi apparatus, immunofluorescence co-localisation analysis of total VEGFR1 and the Golgi marker GM130 (Figure 3.8 (A-D)) was determined. Co-localisation analysis revealed total VEGFR1 was localised to the Golgi apparatus in MSCs cultured at high density.

3.3.3. High density enhanced VEGF-A secretion in MSCs

Since high MSC density induced prominent VEGFR1 phosphorylation (Y1213), ELISA assays were performed to establish whether autocrine secretion of the VEGFR1 ligand VEGF-A_{165} also increased in response to density (Figure 3.9).

VEGF-A concentration significantly increased 3.5-fold ($p=0.0009$) in MSCs cultured at high density (Figure 3.9 (A)) compared to low density. In contrast, MSC density

Figure 3.7

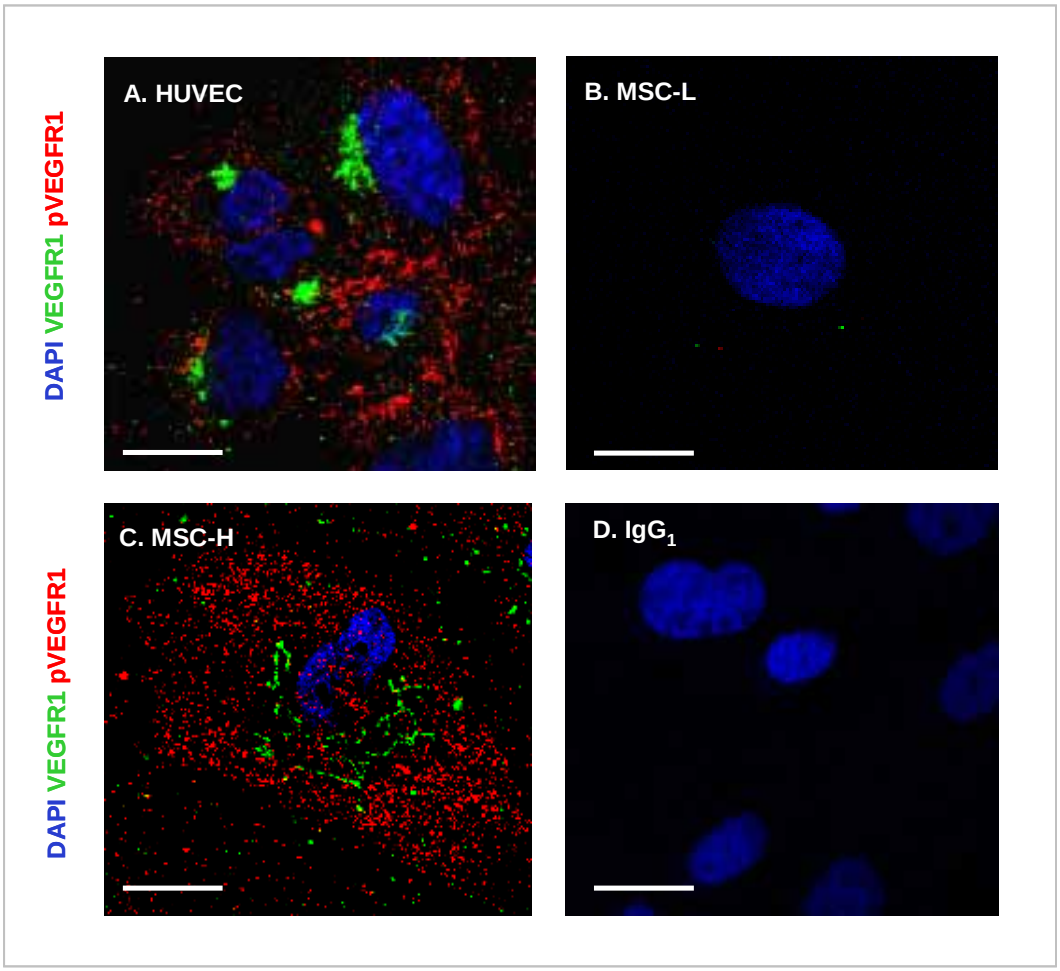

Figure 3.7. *Localisation of VEGFR1 in MSCs cultured at high density*

Immunofluorescence analysis of VEGFR1 (green) and phosphorylated (Y1213) VEGFR1 (pVEGFR1) (red) in **(A)** HUVECs cultured in standard conditions for 48 hours, **(B)** MSCs cultured at low density for 14 days or **(C)** MSCs cultured at high density for 14 days. Nuclei are visualised with DAPI (blue). **(D)** The isotype specific (IgG_1) negative control is shown for MSC-H. A representative of two independent experiments is shown for each analysis with ten representative images taken for each experiment using a Nikon C1 upright confocal microscope (60× objective). Scale bars = 7μm.

Figure 3.8

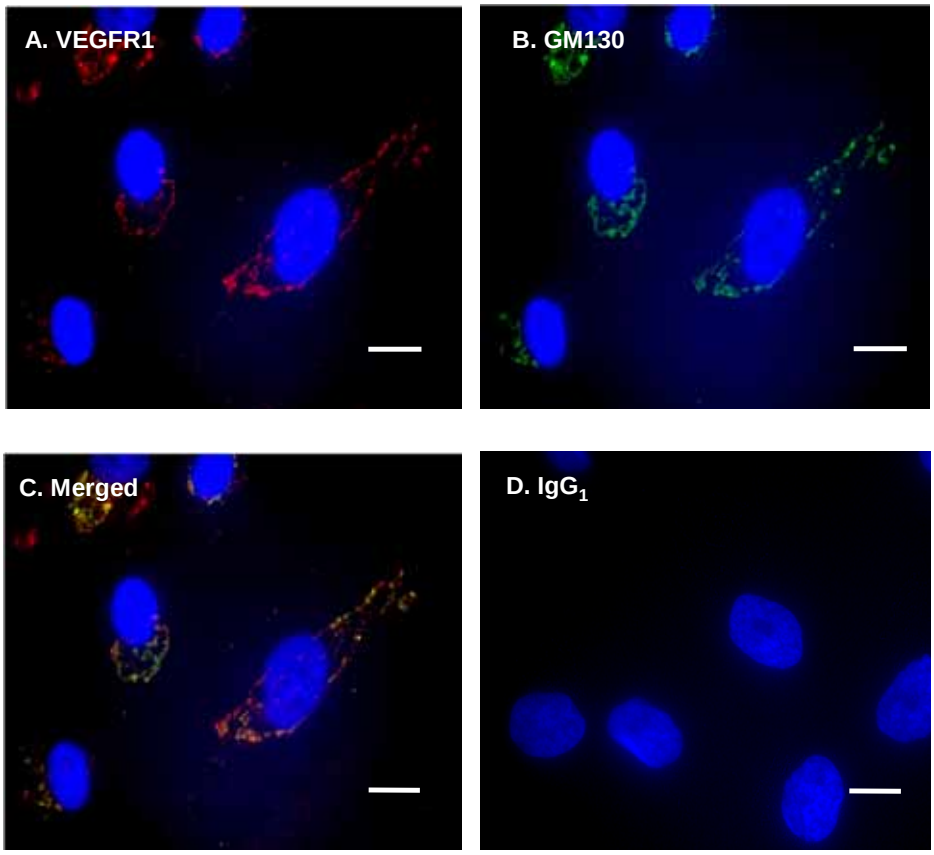

Figure 3.8. *VEGFR1 was localised to the Golgi apparatus in MSCs cultured at high density.*

Co-localisation analysis of VEGFR1 and the Golgi marker GM130 in MSCs cultured at high density for 14 days is depicted in A-D. **(A)** MSCs immunostained for VEGFR1; **(B)** MSCs immunostained for GM130; **(C)** Merged image of VEGFR1 and GM130; **(D)** isotype specific IgG_1 negative control. A representative of two independent experiments is shown for each analysis with ten representative images taken for each experiment using a Olympus IX71 Deltavision microscope (40× objective). Scale bars = 10μm.

Figure 3.9

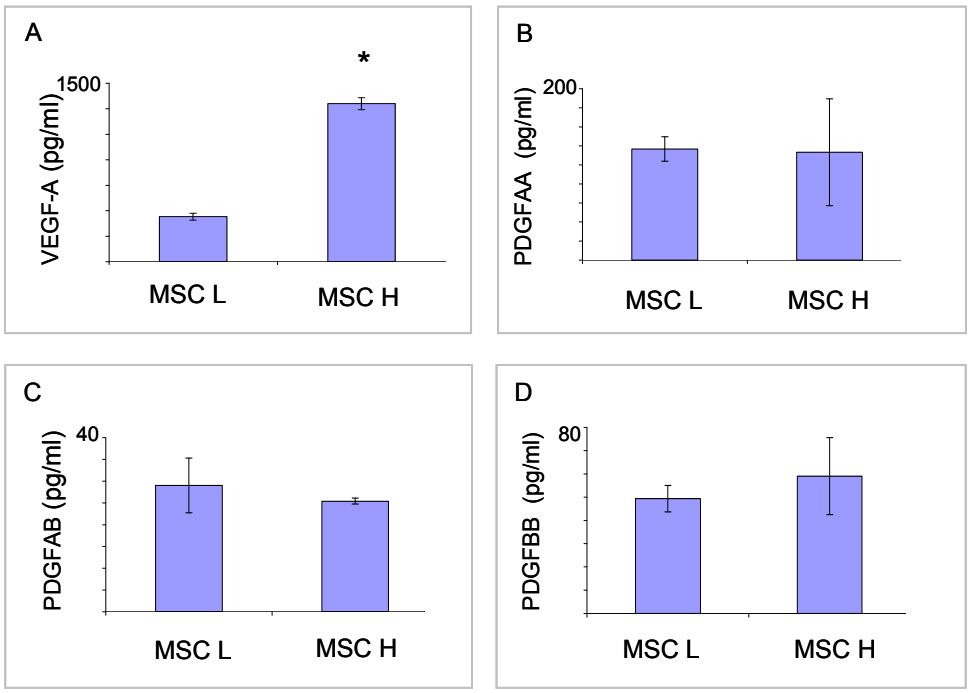

Figure 3.9. *High density enhanced VEGF-A secretion in MSCs*

Enzyme linked immunosorbant assay (ELISA) showing **(A)** VEGF-A, **(B)** PDGF-AA, **(C)** PDGF-AB, or **(D)** PDGFBB isolated from media derived from MSCs cultured at low density or high density for 48 hours. * represents $p<0.05$ compared to growth factor secretion in MSCs cultured at low density. A representative of two independent experiments is shown for each analysis, with each analysis performed in duplicate.

produced no detectable change in the concetration of PDGF ligands (Figure 3.9 (B-D)). Thus, MSC exposure to VEGF-A was significantly increased at high cell density. It must be noted that the production of VEGF-A on a per cell basis may be unchanged as the data is not normalised to the total number of cells within the population. This increased VEGF-A exposure may account for the high levels of phosphorylated VEGFR1 seen in MSCs cultured at high density.

3.3.4. High density enhanced vWF expression in MSCs

3.3.4.1. High density enhanced vWF transcript expression in MSCs

vWF is a multimeric glycoprotein produced constitutively in endothelium within rod shaped organelles called Weibel-Palade bodies (Sadler *et al*, 1998) which has been shown to be a characteristic marker for ECs. However, vWF is also expressed in megakaryocytes within α-granules of platelets (Schick *et al* ., 1997). Therefore to further define the role of MSCs density in directing an EC fate, vWF expression was also examined (Figure 3.10).

RT-PCR was used to determine vWF transcript expression, by MSCs initially seeded at low or high cell density then cultured for 14 days (Figure 3.10 (A)). HUVECs, used as a positive control, demonstrated prominent vWF transcript expression (Figure 3.10 (A); lane 1). While MSCs cultured at low cell density displayed a low levels of vWF transcript (Figure 3.10 (A); lane 2), in comparison, MSCs cultured at high cell density exhibited enhanced vWF transcript expression (Figure 3.10 (A); lane 3). Quantitative PCR analysis revealed that MSCs cultured at high cell density produced a significant increase in vWF transcript expression (2.9 ± 0.4 fold), compared with MSCs cultured at low cell density (Figure 3.10 (B)).

3.3.4.2. High density enhanced vWF protein expression in MSCs

Figure 3.10

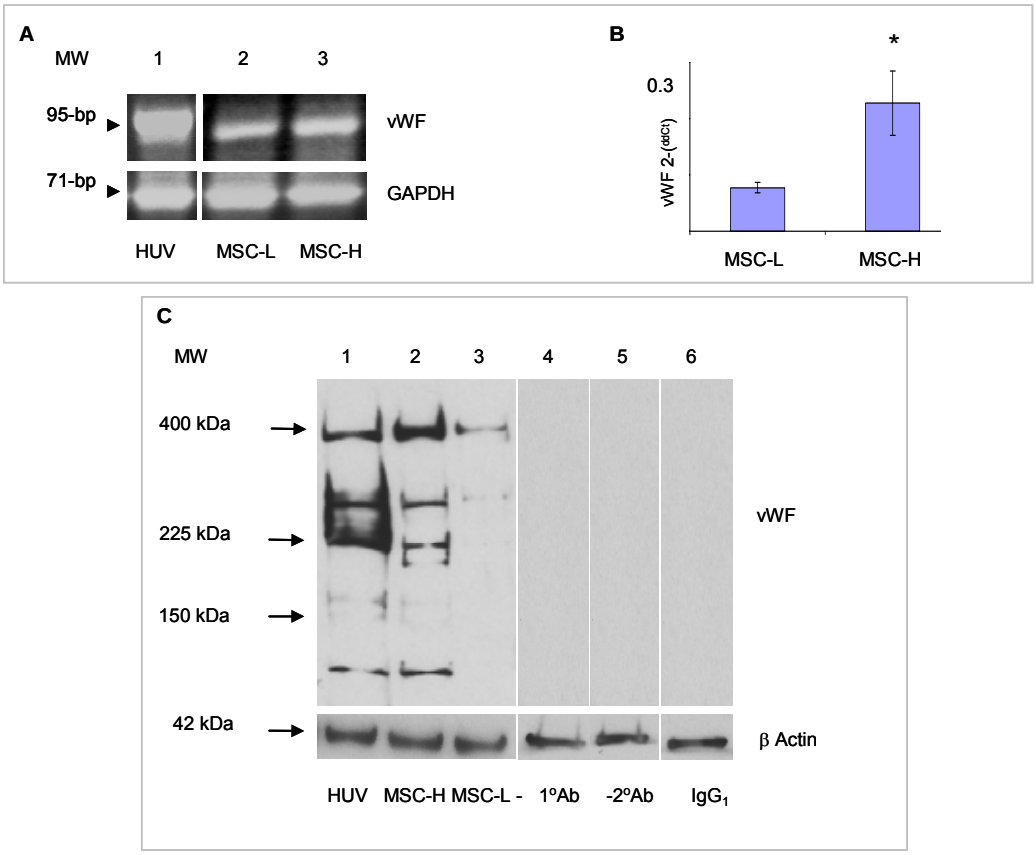

Figure 3.10. *High density enhanced vWF expression in MSCs*

vWF expression was examined by **(A)** RT-PCR analysis or **(B)** Quantitative PCR analysis. HUVECs (HUV) plated at standard density, or MSCs plated at low cell density (MSC-L) or high cell density (MSC-H) were cultured for 14 days and RNA extracted. **(A)** Lane 1, vWF transcript (95-bp) in HUVECs; lane 2, vWF transcript in MSC-L; lane 3, vWF transcripts in MSC-H. Two different primer pairs for vWF produced similar results, GAPDH (71-bp) was used as a loading control. **(B)** Quantitative PCR analysis of vWF transcript expression in MSC-L or MSC-H. Each sample was run in triplicate. * represents $p<0.05$ compared to MSC-L. **(C)** Immunoblot analysis of vWF protein after 14 days in culture. Lane 1, HUVECs as a positive control cell; lane 2, MSC-H; lane 3, MSC-L; lanes 4-6, minus primary antibody (-1^{o}Ab), minus secondary antibody (-2^{o}Ab) and isotype specific (IgG_1) negative controls, respectively. vWF typically displays a ladder of bands representing the different sized vWF multimers, with the mature vWF subunit corresponding to the 225-kDa band (Zimmerman et al., 1986). Membranes were reprobed with β-actin as loading controls.

Immunoblotting analysis was used to detect vWF protein levels, following 14 days culture of MSCs after plating at low or high cell density. HUVECs, used as a positive control, displayed a characteristic ladder of bands of vWF multimers, with the mature vWF subunit represented by the 225-kDa band (Figure 3.10 (C); lane 1) (Zimmerman *et al* ., 1986). In this respect, while the mature vWF subunit was prominently expressed in MSCs cultured at high density (Figure 3.10 (C); lane 2), it was barely detectable in MSCs cultured at low density (Figure 3.10 (C); lane 3). Antibody controls were all immunonegative (Figure 3.10 (C); lanes 4-6).

3.3.4.3. Distribution of vWF in MSCs cultured at high density

Cell density dependent expression of vWF protein by MSCs was confirmed by immunofluorescence analysis after culture for 14 days (Figure 3.11). Using HUVECs as vWF-positive control cells, all HUVECs per field of view exhibited characteristic punctate vWF immunoreactivity, together with a perinuclear ring of vWF immunoreactivity (Figure 3.11 (A) see arrows). MSCs cultured after plating at low cell density exhibited only minimal levels of vWF immunoreactivity (Figure 3.11 (B)), in contrast however, MSCs cultured at high cell density showed widespread punctate vWF immunoreactivity, together with a prominent perinuclear ring of vWF immunoreactivity similar to the HUVEC control (Figure 3.11 (C)). An isotype-specific IgG_1 antibody, used as a negative control (Figure 3.11 (D)), displayed only minimal binding.

3.3.4.4. Transmission electron microscopy of MSCs cultured at high density

Having shown vWF transcript and protein expression in MSCs cultured at high density after 14 days, transmission electron microscopy was performed to determine if vWF storage organelles, known as Weibel-Palade bodies could be detected (Figure 3.12). Weibel-Palade bodies are described as having a single membrane in HUVECs, with a dense interior and rod-shaped, rounded or oval profile (Ewenstein *et al* ., 1987). Transmission electron microscopy analysis of MSCs cultured at low density showed no

Figure 3.11

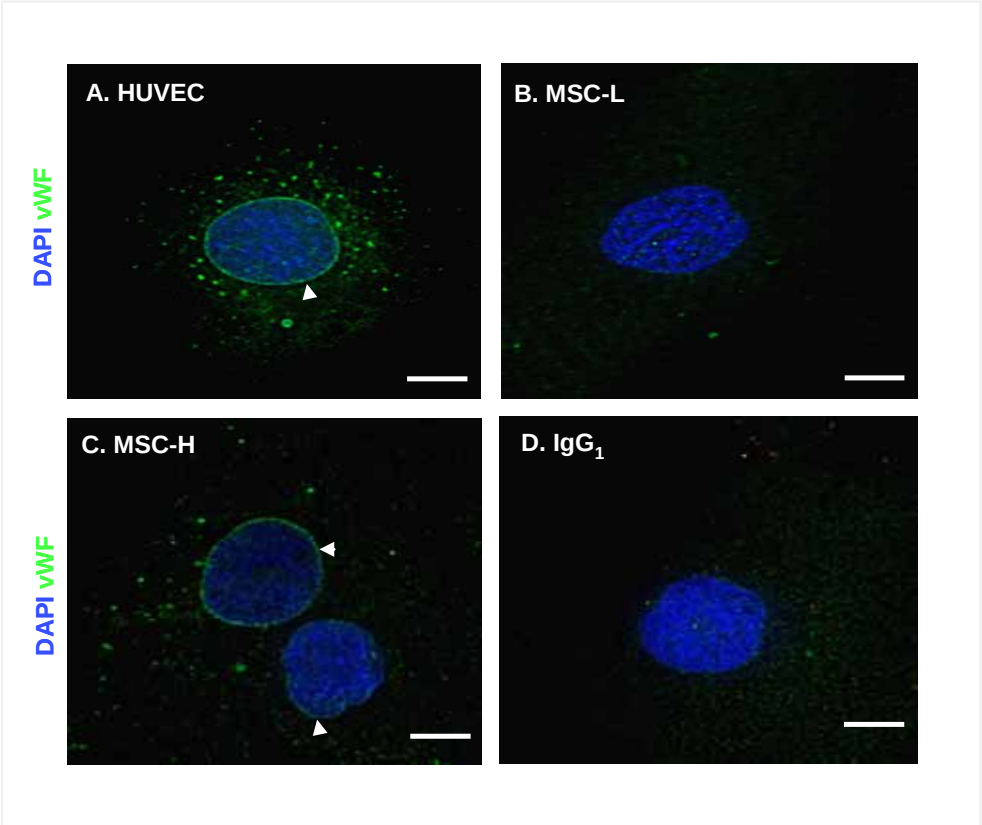

Figure 3.11. *Distribution of vWF in MSCs cultured at high density*

Immunofluorescence analysis of vWF in **(A)** HUVECs, **(B)** MSCs cultured at low density (MSC-L) or **(C)** MSCs cultured at high density (MSC-H) for 14 days. **(D)** Isotype specific IgG_1 negative control. A representative of two independent experiments is shown with ten representative images taken for each experiment using an Olympus IX71 Deltavision microscope (40× objective). Arrows delineate perinuclear vWF staining. Scale bars = 10μm.

Figure 3.12

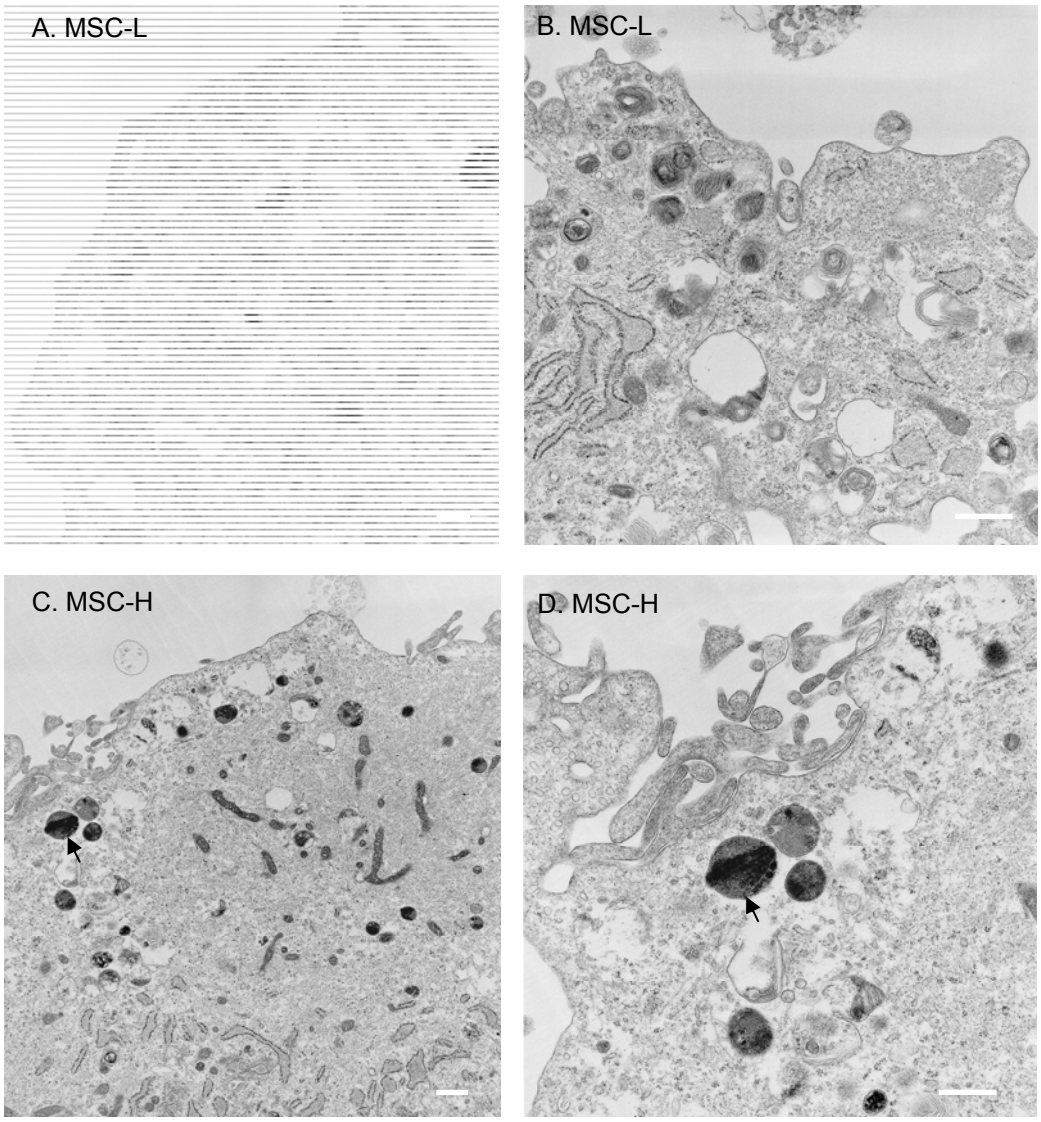

Figure 3.12. *Transmission electron microscopy of MSCs cultured at high density*

Representative micrographs of **(A, B)** MSCs cultured at low density (MSC-L) or **(C, D)** MSCs cultured at high density (MSC-H) for 14 days. Arrows depict possible Weibel-Palade like structures. Scale Bars = 500nm. D represents an enlargement of C.

evidence of Weibel-Palade body-like structures (Figure 3.12 (A, B)). In contrast, transmission electron microscopy of MSCs cultured at high density for 14 days, identified possible Weibel-Palade body-like structures (Figure 3.12 (C,D)).

3.3.5. High MSC density induced VE-cadherin expression

3.3.5.1. High density induced VE-cadherin expression in MSCs

VE-cadherin is an endothelial specific adhesion molecule involved in regulating vascular permeability and leukocyte trafficking. In addition, VE-cadherin has been shown to regulate cell proliferation, apoptosis and modulates VEGF receptor functions (Gavard *et al* ., 2008; Hodijk *et al* ., 1999; Lampugnani *et al*., 2006; Vestweber *et al*, 2008). RT-PCR and immunoblotting were used to determine the levels of VE-cadherin expressed by MSCs cultured at low or high cell density for 14 days (Figure 3.13 (A)). RT-PCR demonstrated HUVECs, used as a positive control, expressed a high level of VE-cadherin transcript. In comparison, MSCs cultured at high cell density expressed a lower level of VE-cadherin transcript, but no expression was detected in MSCs cultured at low cell density (Figure 3.13 (A)). Similarly, immunoblot analysis of HUVECs demonstrated prominent VE-cadherin protein at 130-kDa, while MSCs at high cell density expressed a lower level of VE-cadherin, but no VE-cadherin protein was observed in MSCs cultured at low cell density (Figure 3.13 (B))

3.3.5.2. Distribution of VE-cadherin in MSCs cultured at high density

To determine if the induced VE-cadherin expression in MSCs cultured at high density demonstrated a cell surface or intracellular distribution, single cell flow cytometry was employed to detect cell surface VE-cadherin expression (Figure 3.13 (C)). While MSCs cultured at low density showed no apparent cell surface VE-cadherin expression (mean=3.89), MSCs cultured at high density displayed a minimal level of cell surface VE-cadherin (mean=14.5).

Figure 3.13

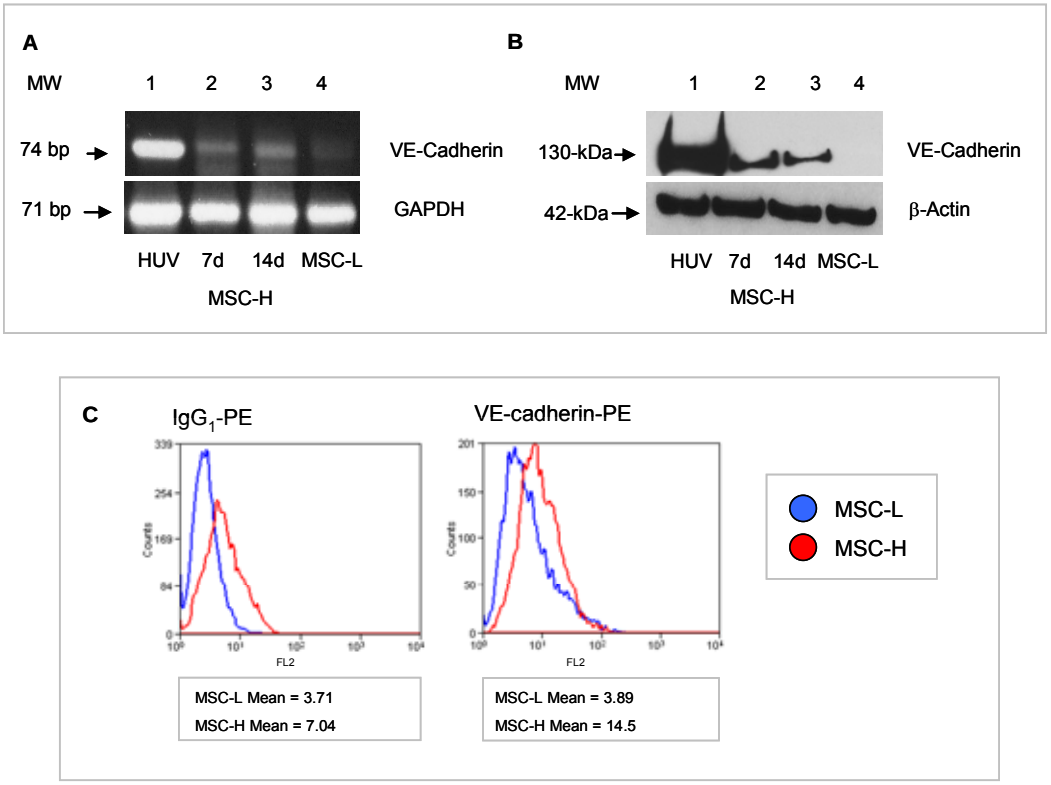

Figure 3.13. *High density induced VE-cadherin expression in MSCs*

VE-cadherin expression in MSCs cultured at low (MSC-L) or high density (MSC-H) up to 14 days was determined by **(A)** semi-quantitative RT-PCR and **(B)** immunoblot analysis. HUVECs (HUV) in standard culture conditions for 48 hours were used as a positive control. Lane 1, HUVECs; lane 2, MSC-H cultured at for 7 days; lane 3, MSC-H cultured for 14 days; lane 4, MSC-H cultured for 14 days. GAPDH or β-actin, were used as loading controls. **(C)** Single colour flow cytometry analysis of VE-cadherin cell surface expression in MSC-L (blue curves) or MSC-H (red curves) cultured for 7 days. Isotype specific IgG_1 was used as a negative control. PE=phycoerythrin conjugated antibodies (FL2). A representative of two independent experiments is shown for each analysis.

Cell density dependent expression of VE-cadherin protein by MSCs cultured for 14 days was confirmed by immunofluorescence analysis (Figure 3.14). Using HUVECs as VE-cadherin-positive control cells, all HUVECs per field of view exhibited VE-cadherin localisation at the cell membrane as well as displaying punctate intracellular immunoreactivity (Figure 3.14 (A)). VE-cadherin could not be detected in MSCs in standard culture conditions (Figure 3.14 (B)), but MSCs cultured at high cell density exhibited punctate intracellular VE-cadherin immunoreactivity at a lower level but similar to HUVEC controls (Figure 3.14 (C)). An isotype-specific IgG_1 antibody, used as a negative control (Figure 3.14 (D)), displayed only minimal binding.

3.3.6. High density enhanced PECAM-1 expression in MSCs

3.3.6.1. High density enhanced PECAM-1 protein expression in MSCs

PECAM-1 is an adhesion molecule belonging to the immunoglobulin superfamily. It is a transmembrane glycoprotein and is constitutively expressed on the surface of all ECs, monocytes, neutrophils and platelets (Newman *et al* . 2003; Raychaudhury *et al* ., 2001; Rival *et al*., 1996; Woodfin *et al*., 2007). Immunoblotting for PECAM-1 in lysates derived from HUVECs as a positive cellular control, demonstrated an immunopositive band of 130-kDa, which was the expected size of PECAM-1 (Figure 3.15 (A); lane 1). Immunoprecipitation then immunoblotting for PECAM-1 in lysates derived from MSCs cultured at high density for 14 days, revealed PECAM-1 immunoreactivity at 130-kDa (Figure 3.15 (A); lane 2). In contrast, MSCs cultured at low density for 14 days displayed only minimal levels of PECAM-1 immunoreactivity (Figure 3.15 (A); lane 3). As previously discussed and reported, PECAM-1 predominantly exists as a membrane receptor in cultured ECs (Newman *et al* ., 2003; Woodfin *et al* ., 2007). Single colour flow cytometry was therefore performed to determine the expression of PECAM-1 on the surface of MSCs following culture at low or high density for 14 days. However, flow cytometry analysis was unable to detect PECAM-1 on the surface of MSCs after 14 days culture at low or high density (Figure 3.15 (B)).

Figure 3.14

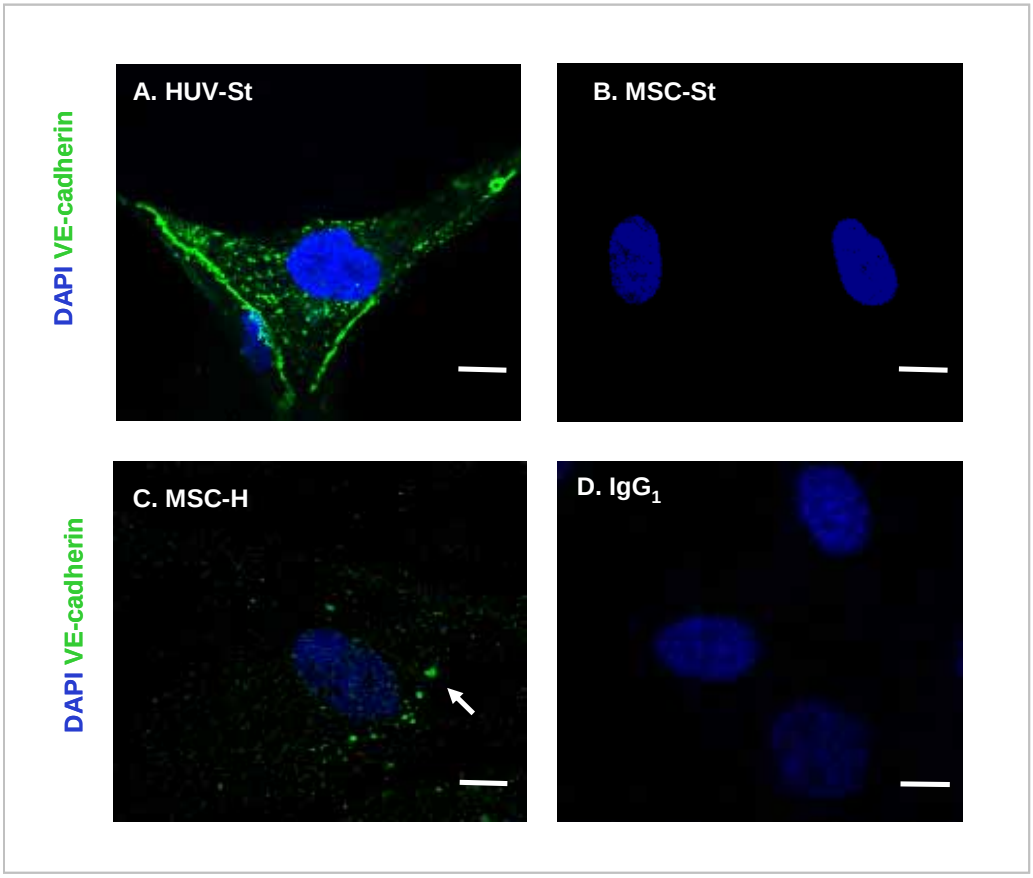

Figure 3.14. *Distribution of VE-cadherin in MSCs cultured at high density*

Immunofluorescence analysis of VE-cadherin in **(A)** HUVECs in standard conditions for 48 hours, **(B)** MSCs in standard culture conditions for 48 hours, or **(C)** MSCs cultured at high density (MSC-H) for 28 days. **(D)** Isotype specific IgG_1 negative control for MSC-H. VE-cadherin = green, nuclei were stained with DAPI = blue. A representative of two independent experiments is shown with ten representative images taken for each experiment using a Nikon C1 upright confocal microscope (60× objective). Scale bars = 7μm.

Figure 3.15

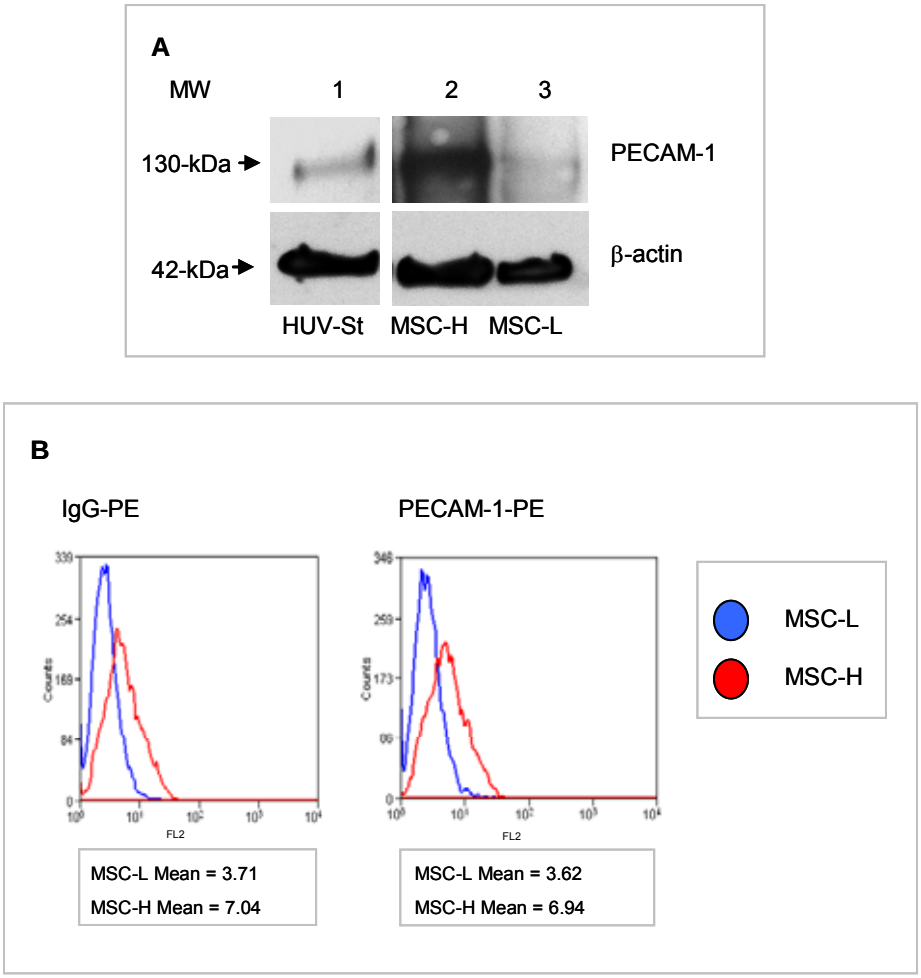

Figure 3.15. *High density enhanced PECAM-1expression in MSCs*

(A) PECAM-1 expression in MSCs cultured at low (MSC-L) or high density (MSC-H) for 14 days was determined by immunoprecipitation and immunoblot analysis. Total cell lysates were extracted from MSC-L or MSC-H, then PECAM-1 immunoprecipitated followed by PECAM-1 immunoblot analysis. Lysate (40μg) extracted from HUVECs (HUV) in standard culture conditions for 48 hours was used as a positive control. Lane 1, HUVECs cultured in standard conditions for 48 hours; lane 2, MSC-H cultured for 14 days; lane 3, MSC-L cultured for 14 days. Equal volumes of lysate were immunoblotted for β-actin to determine equal loadings. **(B)** Cell surface PECAM-1 expression was determined by single colour flow cytometry. Isotype specific IgG_1 was used as a negative control. MSC-L (blue curves) MSC-H (red curves) cultured for 7 days. PE = phycoerythrin conjugated antibodies (FL2). A representative of two independent experiments is shown for each analysis.

3.3.6.2. Distribution of PECAM-1 in MSCs cultured at high density

To further investigate the density-dependent expression of PECAM-1 in MSCs, immunofluorescence analysis was performed (Figure 3.16). HUVECs, as previously reported, expressed PECAM-1 predominantly as a broad ribbon of sub-plasma-lemmal staining at cell-cell contact sites (Figure 3.16 (A)) (Woodfin *et al* ., 2007). In addition, fine intracellular PECAM-1 immunofluorescence was also detected. In comparison, MSCs cultured in standard conditions for 48 hours exhibited a low level of intracellular PECAM-1 immunoreactivity (Figure 3.16 (B)). In contrast however, MSCs cultured at high density for 28 days displayed prominent intracellular punctuate PECAM-1 immunoreactivity (Figure 3.16 (C)).

3.3.7. Functional properties of MSCs cultured at high density

3.3.7.1. MSCs cultured at high density uptake ac-LDL

Having established that MSCs cultured at high density adopt an endothelial-like cell morphology and express endothelial markers after 14 days of culture, MSCs cultured at high density for 28 days were subjected to endothelial functional tests.

DiI-Ac-LDL is commonly used to label and isolate ECs from a mixed cell population (Voyta *et al* ., 1984). ECs or macrophages labelled with DiI-Ac-LDL take up the lipoprotein within 4 hours then the lipoprotein is subsequently degraded by lysosomal enzymes (Voyta *et al* ., 1984; Schmeisser *et al* 2001; 2003). The fluorescent probe (DiI) accumulates within intracellular membranes enabling fluorescent detection. However, other cell types such as HDFs, pericytes, vSMCs and epithelial cells, do not take up DiI-Ac-LDL and are not labelled.

The ability of MSCs to uptake DiI-ac-LDL was therefore established. Using HUVECs as a positive cellular control, MSCs in standard culture conditions for 48 hours or MSCs

Figure 3.16

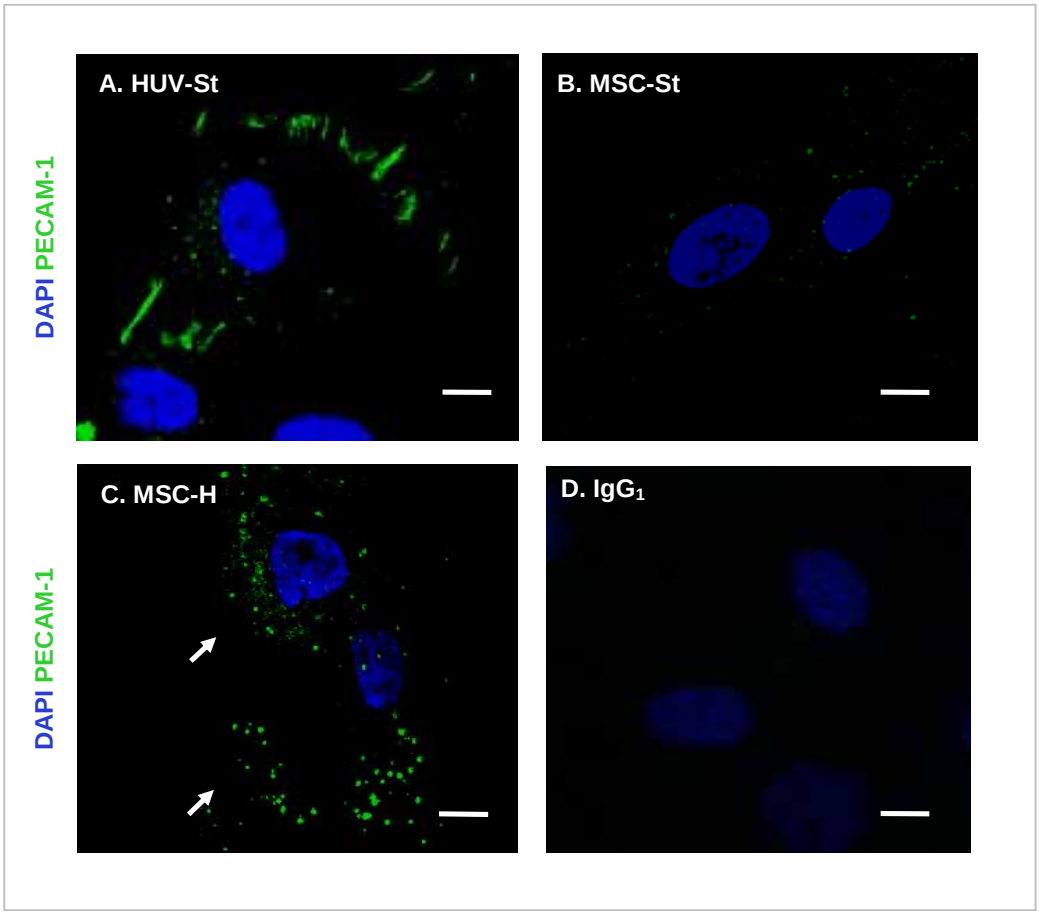

Figure 3.16. *Distribution of PECAM-1 in MSCs cultured at high density*

Immunofluorescence analysis of PECAM-1 expression in **(A)** HUVECs in standard culture conditions for 48 hours, **(B)** MSCs in standard culture conditions for 48 hours, or **(C)** MSCs cultured at high density (MSC-H) for 28 days. **(D)** Isotype specific IgG_1 negative control for MSC-H. PECAM-1=green, nuclei were stained with DAPI=blue. A representative of two independent experiments is shown with ten representative images were taken for each experiment using a Nikon C1 upright confocal microscope (60× objective). Scale bars = 7μm.

cultured at high density for 28 days were cultured for four hours with 10μg/ml DiI-ac-LDL, then uptake determined by fluorescence microscopy. HUVECs in standard culture conditions for 48 hours displayed virtually 100% uptake of DiI-ac-LDL (Figure 3.17 (A)). In comparison, MSCs cultured in standard conditions for 48 hours did not take up DiI-ac-LDL (Figure 3.17 (B)). However, in contrast, MSCs cultured at high density for 28 days exhibited DiI-ac-LDL uptake in approximately 53% of cells analysed (Figure 3.17 (C) and Figure 3.17 (D)).

3.3.7.2. MSCs pre-cultured at high density displayed enhanced networks

Matrigel, an extract of the basement membrane from the Englebreth-Holm-Swarm tumour, is liquid at 4°C and forms a gel at 37°C (Baatout *et al* ., 1996; 1997). When plated on Matrigel, ECs rapidly form capillary-like structures within 24 hours *in vitro* (Figure 3.18 (A)). The functional behaviour of MSCs which had been cultured at high density was further tested by seeding these cells on Matrigel (Figure 3.18). MSCs pre-cultured in standard conditions for 48 hours then seeded onto Matrigel, formed thin elongated branched networks within 24 hours (Figure 3.18 (B)). In contrast, MSCs pre-cultured at high density for 28 days, then seeded onto Matrigel formed a significantly enhanced number of branch points within 24 hours (Figure 3.18 (C) and Figure 3.18 (D)). Further analysis of endothelialised MSCs in Matrigel culture is shown in Chapter 5.

3.3.7.3. High density MSCs induced VCAM-1 following TNFα exposure

The adhesion molecule VCAM-1 is inducible by TNF-α in ECs (Figure 3.19 (A and B)), (McHale *et al* ., 1999). To determine whether VCAM-1 could be induced in MSCs cultured at high density for 28 days exposed to 10ng/ml TNF-α, immunofluorescence microscopy was performed. MSCs cultured in standard conditions detectected no VCAM-1 immunoreactivity in the presence or absence of 10ng/ml TNF-α (Figure 3.19 (C, D)). MSCs cultured at high density detected no VCAM-1 immunoreactivity in unstimulated cells (Figure 3.19 (E)), but in contrast, VCAM-1 immunoreactivity was

Figure 3.17

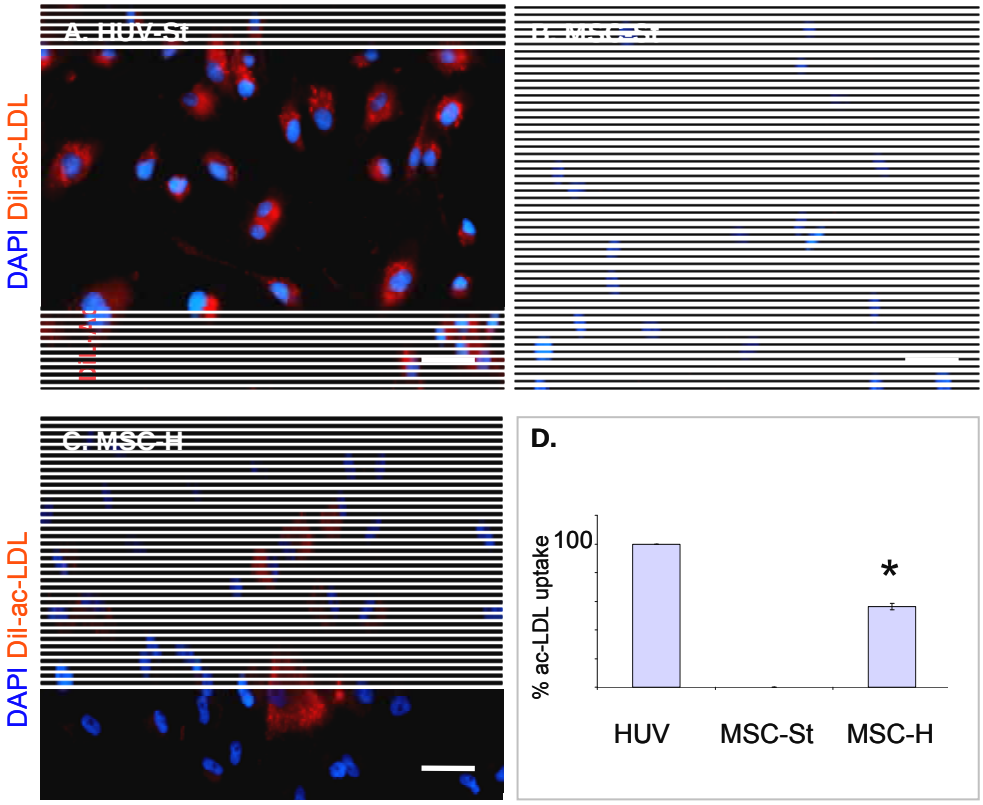

Figure 3.17. *MSCs cultured at high density uptake ac-LDL*

Immunofluorescence analysis showing DiI-Ac-LDL uptake in **(A)** HUVECs, **(B)** MSCs in standard culture conditions (MSC-St) for 48 hours and **(C)** MSCs cultured at high density (MSC-H) for 28 days. DAPI=blue, DiI-Ac-LDL uptake=Red. Images were taken on a Olympus upright widefield fluorescence microscope (BX51) using a 20× objective. Scale bars = 20μm. A representative of two independent experiments is shown. Insets show a second representative image. **(D)** The total number of cells exhibiting DiI-ac-LDL uptake were calculated as a percentage and plotted as a bar graph. * = $p<0.05$ compared to MSC-St.

Figure 3.18

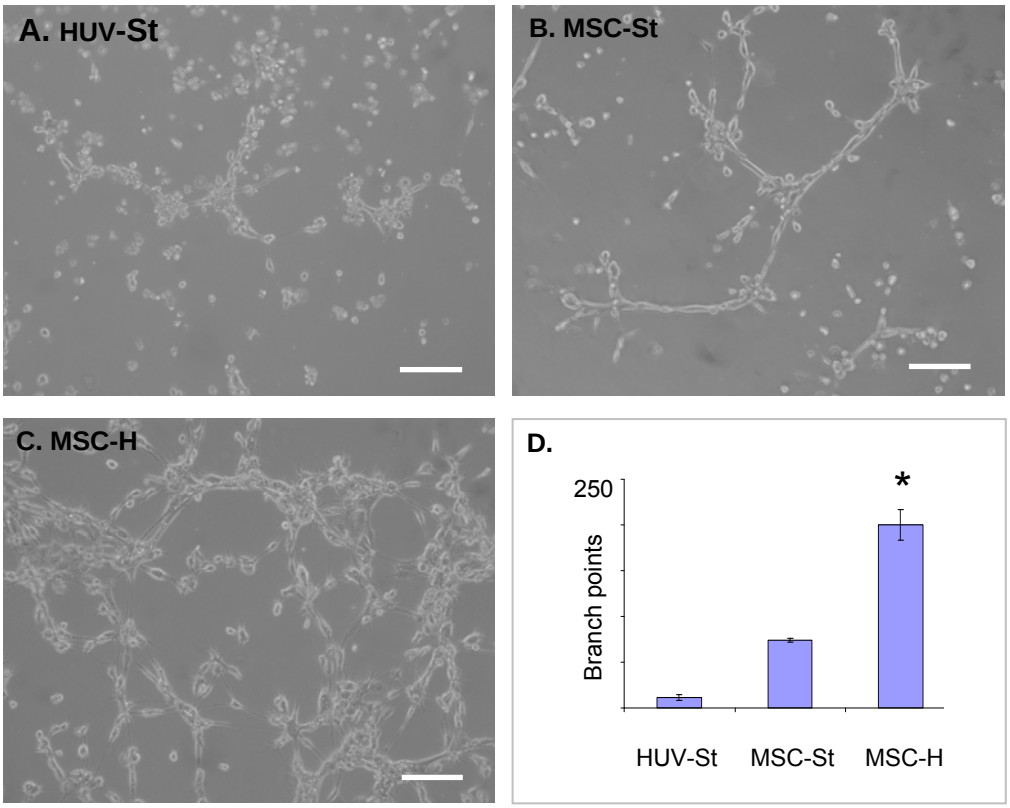

Figure 3.18. *MSCs pre-cultured at high density displayed enhanced networks*

(A) HUVECs cultured in standard conditions for 48 hours (HUV-St), **(B)** MSCs cultured in standard conditions for 48 hours (MSC-St) or **(C)** MSCs cultured at high density for 28 days (MSC-H), were seeded onto growth factor reduced Matrigel in 0.5% serum DMEM for 48 hours. Images were obtained using an Olympus (CK X41) microscope with attached digital camera (10× objective). Scale bars = 40 μm. **(D)** Average number of branch points was determined and plotted as a bar graph. * = $p<0.05$ compared to MSC-St.

induced in response to 10ng/ml TNF-α stimulation (Figure 3.19 (F)). Thus, VCAM-1 could be induced in MSCs cultured at high density in response to exogenous TNF-α stimulation.

3.3.7.4. High cell density did not stimulate EC markers in HDFs

To determine whether high cell density induced other cell types to express EC markers, the effects of cell density on HDFs was examined by immunofluorescence analysis. While HDFs cultured for 14 days were immunopositive for VEGFR1, which predominantly localised to the Golgi apparatus as judged by GM130 colocalisation analysis, (Figure 3.20 (A, B), Figure 3.8) no detectable difference in immunofluorescence was observed at either low or high HDF cell density. Furthermore, HDFs were immunonegative for vWF (Figure 3.20 (C, D)) and VE-cadherin (Figure 3.20 (E, F)) at either low or high cell density. Thus, HDF cell density does not regulate the expression of the EC markers VEGFR1, vWF or VE-cadherin.

3.4. High density MSCs maintained a moderately stable phenotype

3.4.1. Re-plating at low density largely maintained EC marker expression

To assess the stability of the MSC density-dependent EC like phenotype, MSCs that had been pre-cultured at high density for 28 days were seeded back at low density for 7 days (Figure 3.21). While MSCs cultured at high density for 28 days maintained a cobble-stone morphology (Figure 3.21 (A)), when these cells were then re-seeded at low density for 7 days, they adopted a flattened morphology very different to their original morphology (Figure 3.21 (B), Figure 3.1). Immunoblot analysis for VEGFR1 and vWF in the cells seeded at low density demonstrated that they still largely maintained a high level of vWF and VEGFR1 expression, similar to MSCs cultured at high density (Figure 3.21 (C, D)).

Figure 3.19

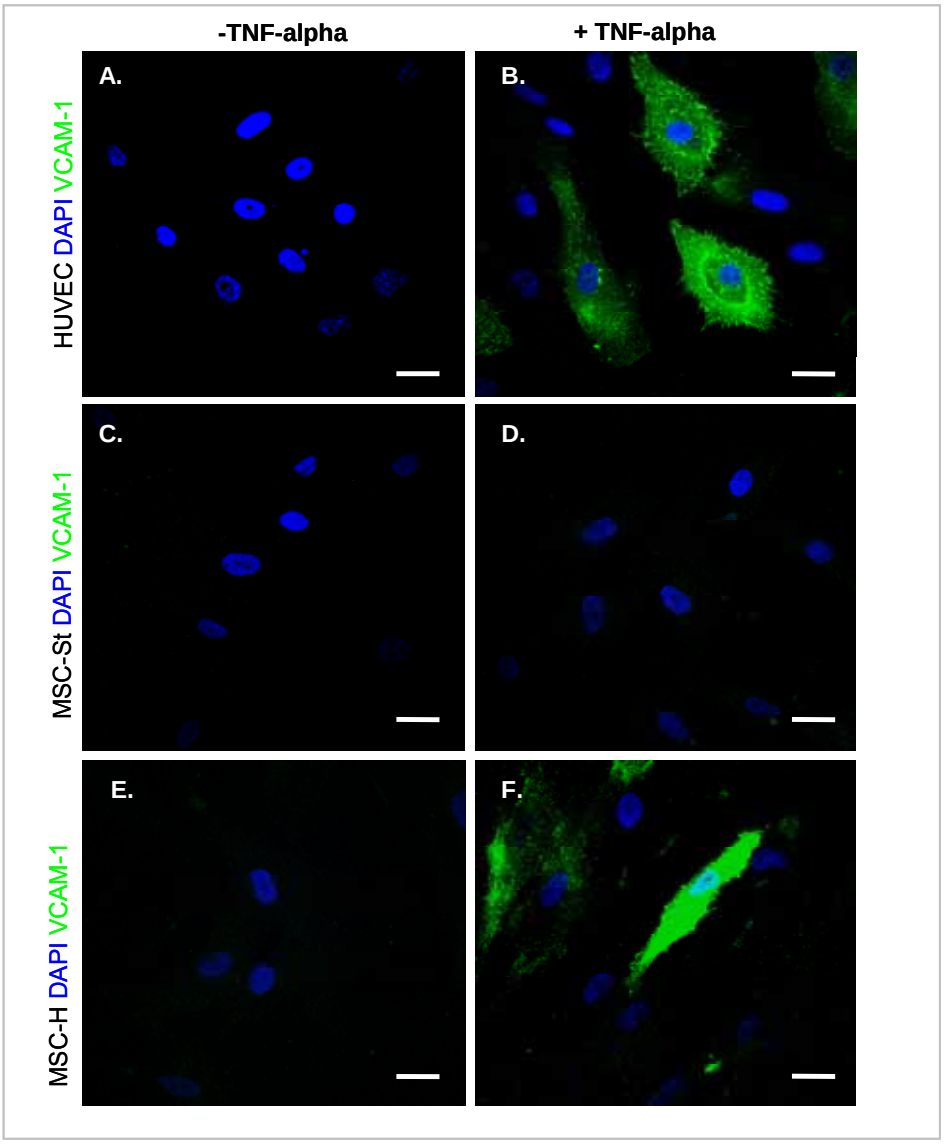

Figure 3.19. High density MSC culture induced VCAM-1 following TNFα exposure

Immunofluorescence analysis of VCAM-1 in **(A, B)** HUVECs in standard culture conditions for 48 hours, **(C,D)** MSCs in standard culture conditions (MSC-St) for 48 hours **(E,F)** MSCs at high density (MSC-H) for 28 days. **(A, C, E)** unstimulated cells; **(B, D, F)** cells stimulated with 10ng/ml TNFα for 24 hours. VCAM-1 = green, nuclei were stained with DAPI = blue. A representative of two independent experiments is shown and ten representative images were taken for each experiment using a Nikon C1 upright confocal microscope (60$\times$ objective). Scale bars = 7μm.

Figure 3.20

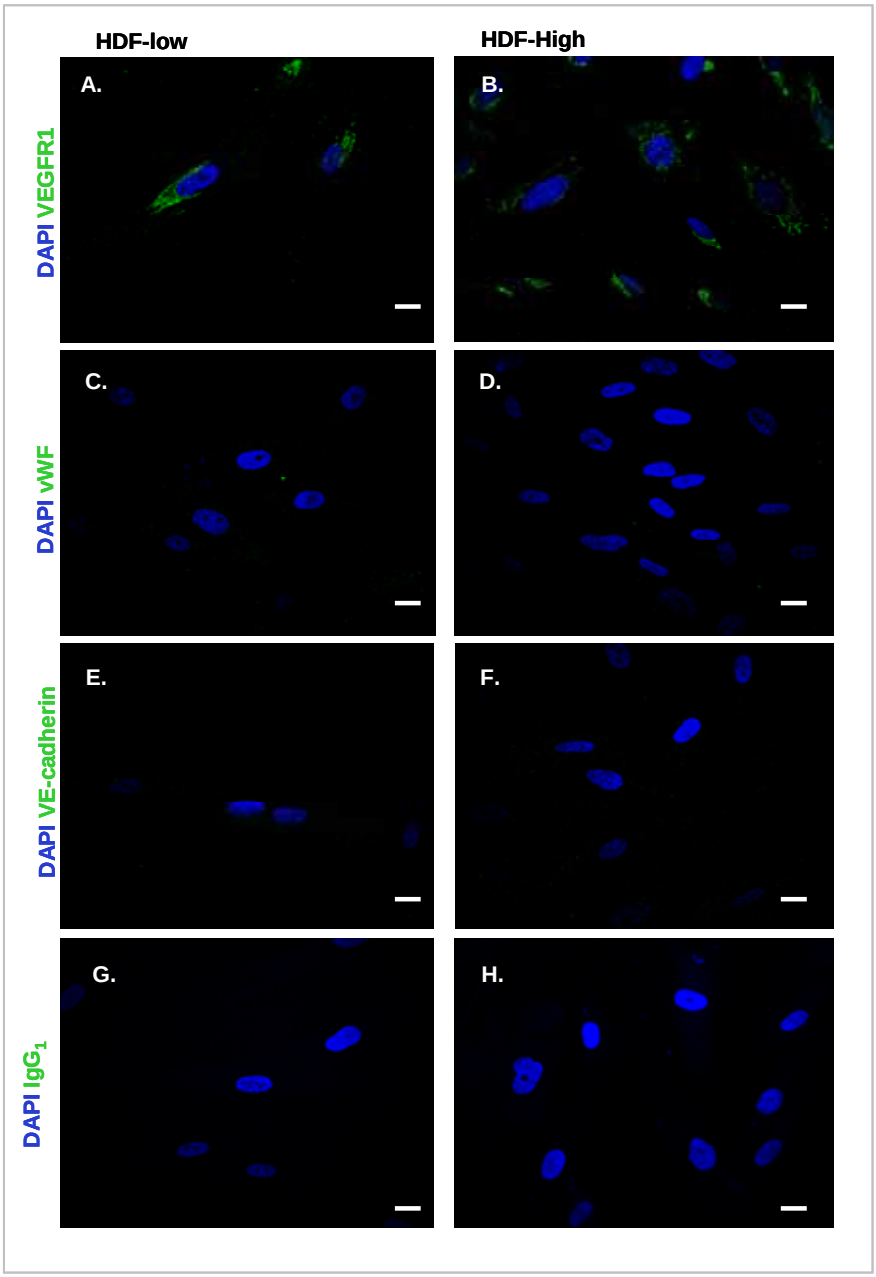

Figure 3.20. *High cell density did not stimulate EC markers in HDFs*

Immunofluorescence analysis of EC markers VEGFR1, vWF and VE-cadherin in HDFs cultured at low density (HDF-low) (A, C, E, G) or high density (HDF-High) for 14 days (B, D, F, H). (G,H) Isotype specific IgG_1 negative controls. EC markers = green, nuclei were stained with DAPI = blue. A representative of two independent experiments are shown, with ten representative images were taken for each experiment using a Nikon C1 upright confocal microscope (60× objective). Scale bars = 7μm.

3.4.2. MSC characterisation markers were decreased in MSCs at high density

As previously discussed, MSCs are typically characterised by their expression of the surface antigens CD29, CD44, CD51, CD105 and CD73 as well as their induced differentiation potential into osteoblasts, chondrocytes and adipocytes (Huang *et al* 2009, Phinney and Prokop 2007a; Pittenger *et al* . ,1999). To establish whether differentiation of MSCs to ECs resulted in a concomitant decrease or loss of characteristic MSC surface antigens, their expression was determined by single colour flow cytometry following MSC culture at high density for 7 days (Figure 3.22). MSCs cultured at high density showed a decrease in surface antigens CD29 (mean = 124.98), CD105 (mean = 144.88) and CD44 (mean = 242.39) compared to MSCs cultured at low density (means =230.02, 224.56 and 389.41 respectively). Since leukocytes have previously been shown to express vWF and VEGFR1 and to form networks in Matrigel (Schmeisser *et al* ., 2001), expression of the leukocyte marker CD45 was also determined following MSC culture at low or high density. Flow cytometry confirmed that MSCs cultured at high or low density for 7 days did not express cell surface CD45, demonstrating the MSCs were not differentiating towards a leukocyte lineage.

3.4.3. MSC density did not up-regulate other cell lineage differentiation markers

To establish whether MSC density regulated the expression of other lineage markers, the effects of cell density on adipogenic, chondrogenic or osteogenic markers were also examined (Figure 3.23). Quantitative PCR was used to determine MSC transcript expression for adipogenic markers; PPAR γ and AP2, osteogenic markers; osteopontin and ALKP as well as chondrogenic markers; Col2A1 and Col9A2 (see Chapter 1: introduction section 1.2.3) . Analysis of adipogenic differentiation marker AP2 (Figure 3.23 (A)) and PPAR-Gamma (Figure 3.23 (B)) or chondrogenic marker Col2A1 (Figure3.23 (E)) and Col9A2 (Figure 3.23 (F)) expression at low or high MSC density, demonstrated that their expression did not significantly change. In contrast, the

Figure 3.21

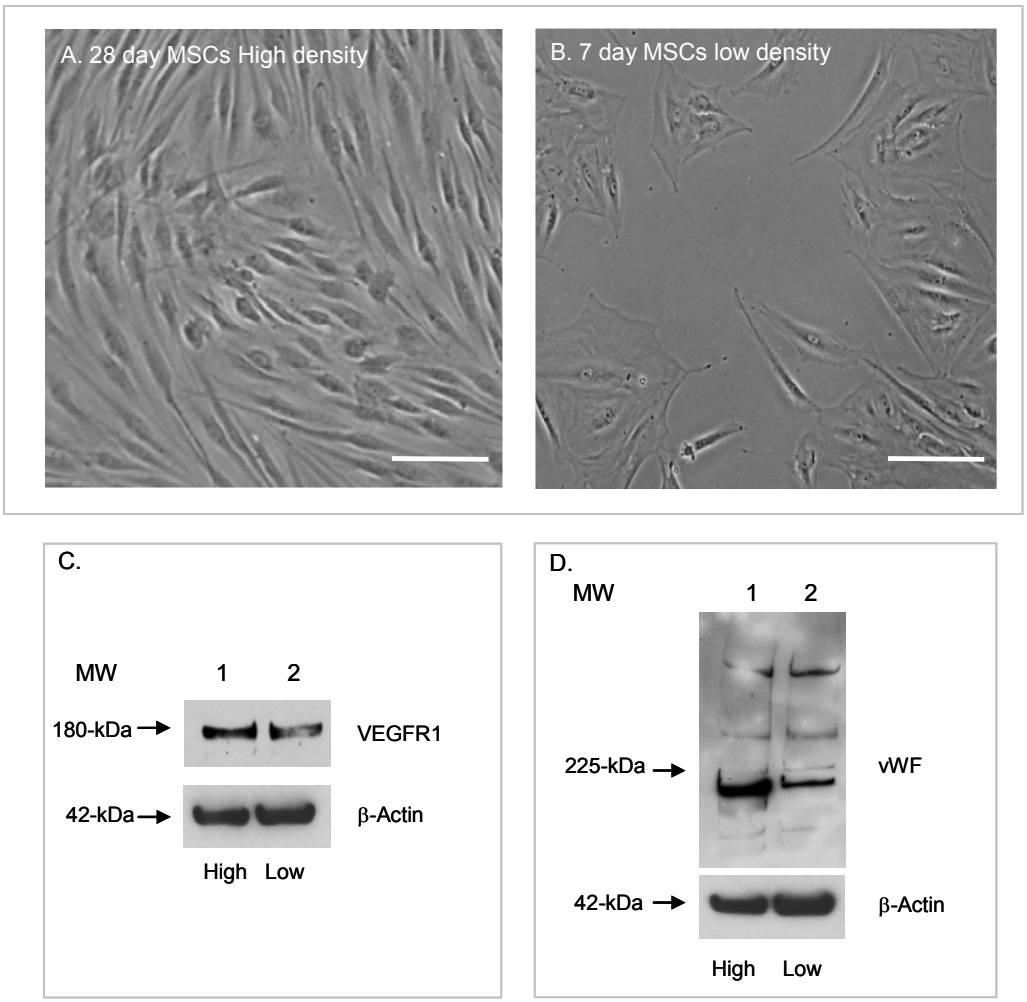

Figure 3.21. *High density MSCs maintained a moderately stable phenotype*

To determine the stability of MSC density dependent EC-like phenotype, MSCs cultured at high density for 28 days were seeded back at low density for 7 days. **(A)** MSCs cultured at high density for 28 days or **(B)** the same MSCs seeded at low density for 7 days. Representative phase contrast images using a 20× objective lens. Scale bars = 50μm. Immunoblot analysis of **(C)** VEGFR1 or **(D)** vWF expression, in MSCs cultured at high density for 28 days (high) or the same MSCs seeded at low density for 7 days (low). Membranes were reprobed with β-Actin as loading controls.

Figure 3.22

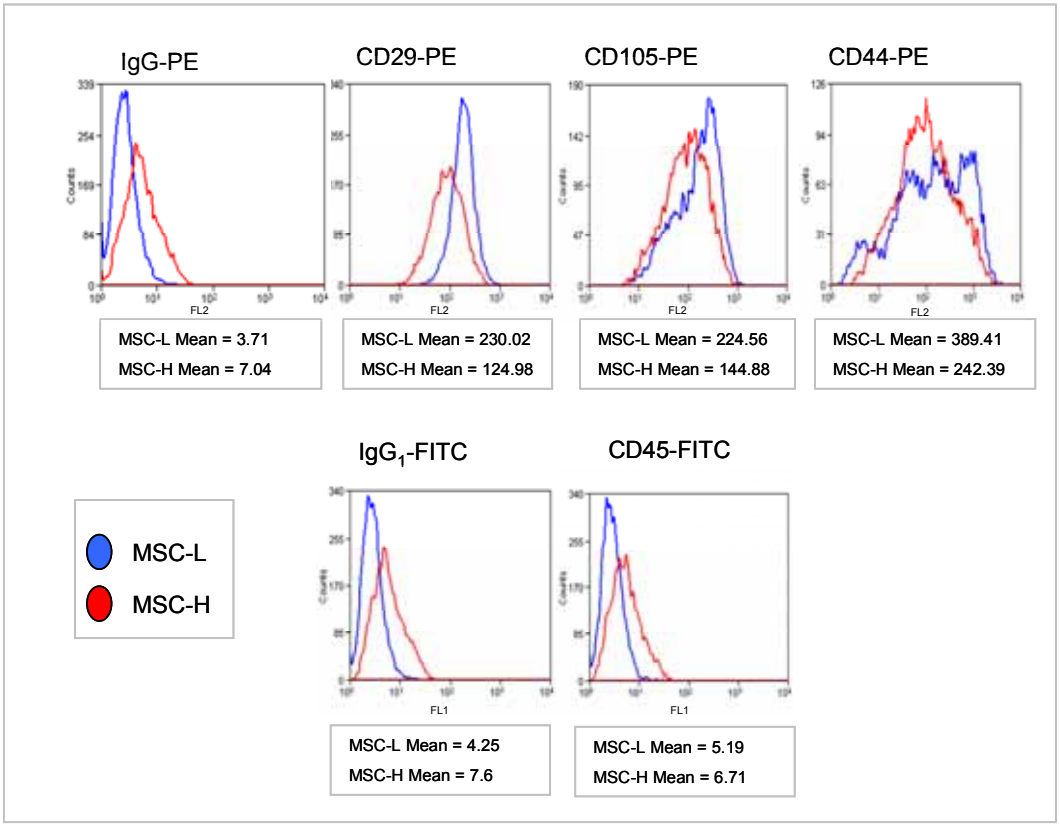

Figure 3.22. *High density MSCs decreased MSC characterisation markers*

Flow cytometry analysis of characteristic MSC surface antigens CD29 (integrin β1 chain), CD105 (endoglin), CD44 (hyaluronan receptor) and the leukocytic marker CD45 using PE (FL2) conjugated or FITC labeled (FL1) antibodies, in MSCs cultured at low (MSC-L = blue curves) or high density (MSC-H = red curves) for 7 days. IgG_1 was used as a negative control.

osteogenic marker osteopontin significantly (p=0.0077) increased in MSCs at high density (Figure 3.23 (C)), However, since the melting curve shows two peaks for osteopontin, the increase may be over-estimated. In comparison, the osteogenic marker AlkP (Figure 3.23 (D)) significantly (p=0.0200) decreased in MSCs at high density.

3.4.4. High density MSCs could not be induced to differentiate to adipocytes

To establish further whether MSCs cultured at high density for 28 days were displaying lineage commitment, their potential to be induced towards adipogenic and osteogenic lineages was evaluated. These experiments were performed at the same time as those in Figure 3.3. In contrast to the un-induced control cells (Figure 3.24 (A), also shown in Figure 3.3), MSCs cultured in standard conditions exposed to adipogenic media for 14 days exhibited a rounded morphology and detected prominent Bodipy 493/503 staining and FABP-4 positive immunoreactivity was detected, (characteristic for lipid droplets) (Figure 3.24 (B) also shown in Figure 3.3). However, similar to the un-induced control (Figure 3.24 (C)), MSCs cultured at high density for 28 days then exposed to adipogenic media for 14 days demonstrated no discernible Bodipy 493/503 positive vesicles or FABP-4 immunoreactivity (Figure 3.24 (D)), suggesting that these MSCs could not be differentiated towards adipocytes.

3.4.5. High density MSCs could not be induced to differentiate to osteoblasts

Similarly, in contrast to the un-induced control cells (Figure 3.25 (A), also shown in Figure 3.3), MSCs cultured in standard conditions exposed to osteogenic media for 14 days exhibited a flattened morphology and produced alizarin red positive staining indicative for calcium deposits (Figure 3.25 (B), also shown in Figure 3.3). However, similar to the un-induced control (Figure 3.25 (C)), MSCs cultured at high density for 28 days, then exposed to osteogenic differentiation media for 14 days displayed no discernible alizarin red positive staining (Figure 3.25 (D)), indicating that these MSCs

Figure 3.23

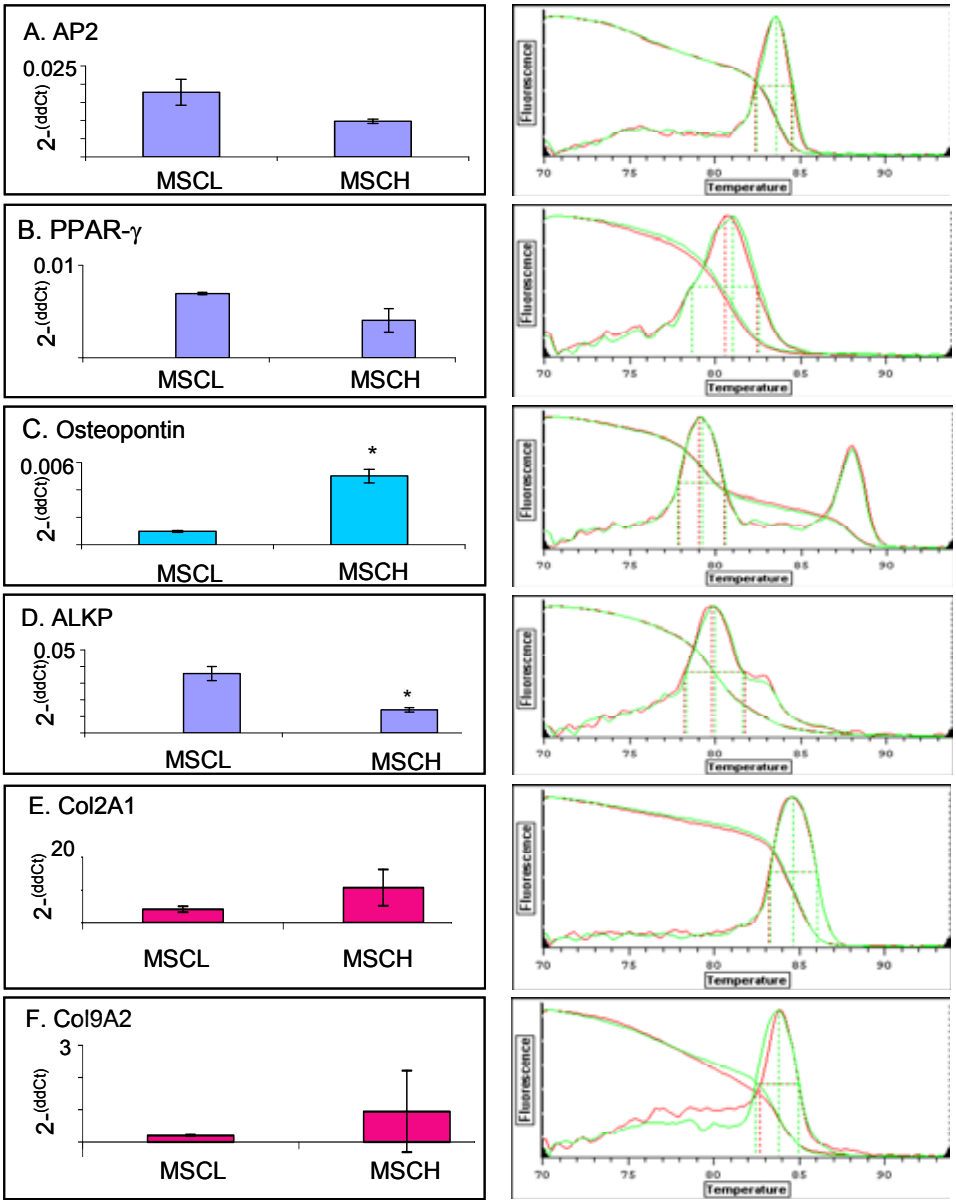

Figure 3.23. *MSC density did not up-regulate other cell lineage differentiation markers*

Quantitative PCR analysis of adipocyte differentiation markers **(A)** AP2, **(B)** PPARγ osteoblast markers **(C)** Osteopontin, **(D)** AlkP and chondrocyte markers **(E)** Col2A1, **(F)** Col9A2 using RNA taken from MSCs cultured at low density (MSC-L) or high density (MSC-H) for 3 days. The double delta Ct method was used to transform Ct values into relative quantities with standard deviations. Minus RT (–RT) and minus cDNA (-cDNA) reactions were also performed for each reaction to verify there was no genomic DNA or reagent contamination. * represents $p<0.005$ compared with MSC-L. For each analysis, a representative of two independent experiments is shown with each sample run in triplicate. Melting curves are shown on right.

Figure 3.24

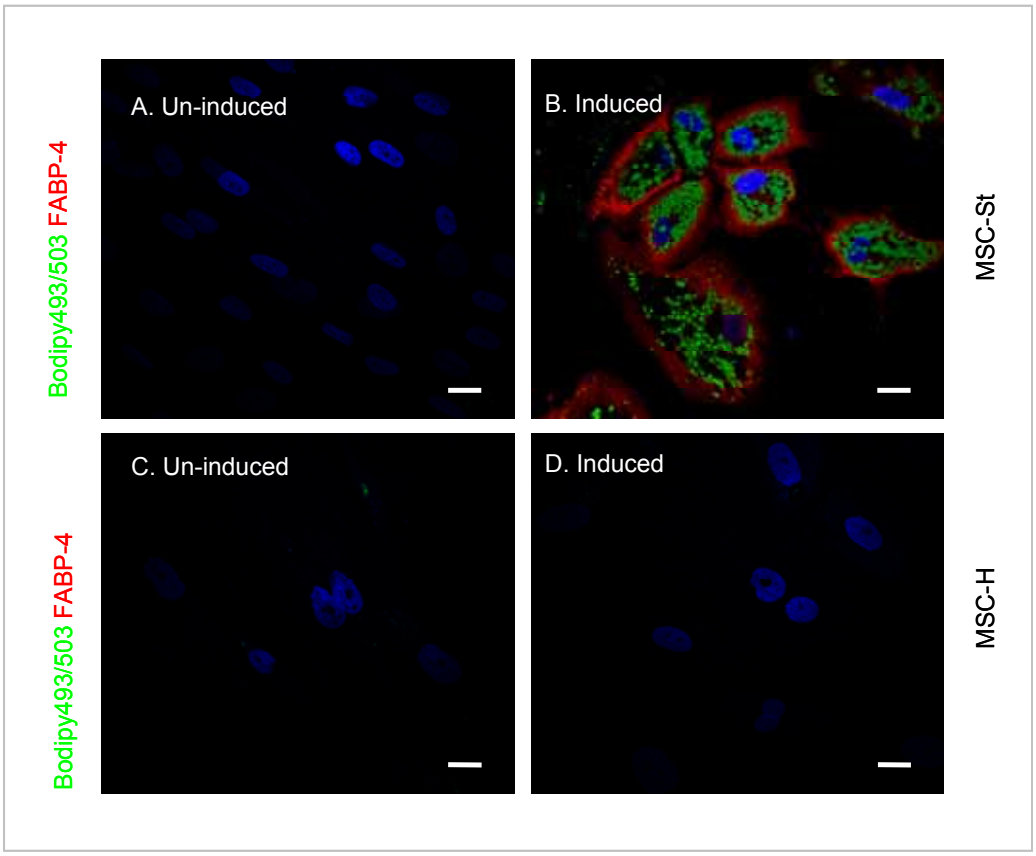

Figure 3.24. *High density MSCs could not be induced to differentiate to adipocytes*

MSCs cultured in standard conditions for 24 hours or cultured a high density for 28 days were induced to differentiate to adipocytes by exposure to adipogenic differentiation media over 14 days. Adipocytes were detected by staining for Bodipy 493/503 (green) and immunostaining for FABP-4 (red) using a Nikon C1 upright confocal microscope (60× objective). Nuclei are stained with DAPI (blue). **(A)** MSCs in standard culture conditions in basal media for 14 days; **(B)** MSCs in standard culture conditions exposed to adipogenic differentiation media for 14 days; **(C)** MSCs at high density in basal media for 14 days; **(D)** MSCs at high density exposed to adipogenic differentiation media for 14 days. Figures A and B are also shown in Figure 3.3. Ten representative images were taken for each treatment with each analysis performed in triplicate. Scale bars = 7μm

Figure 3.25

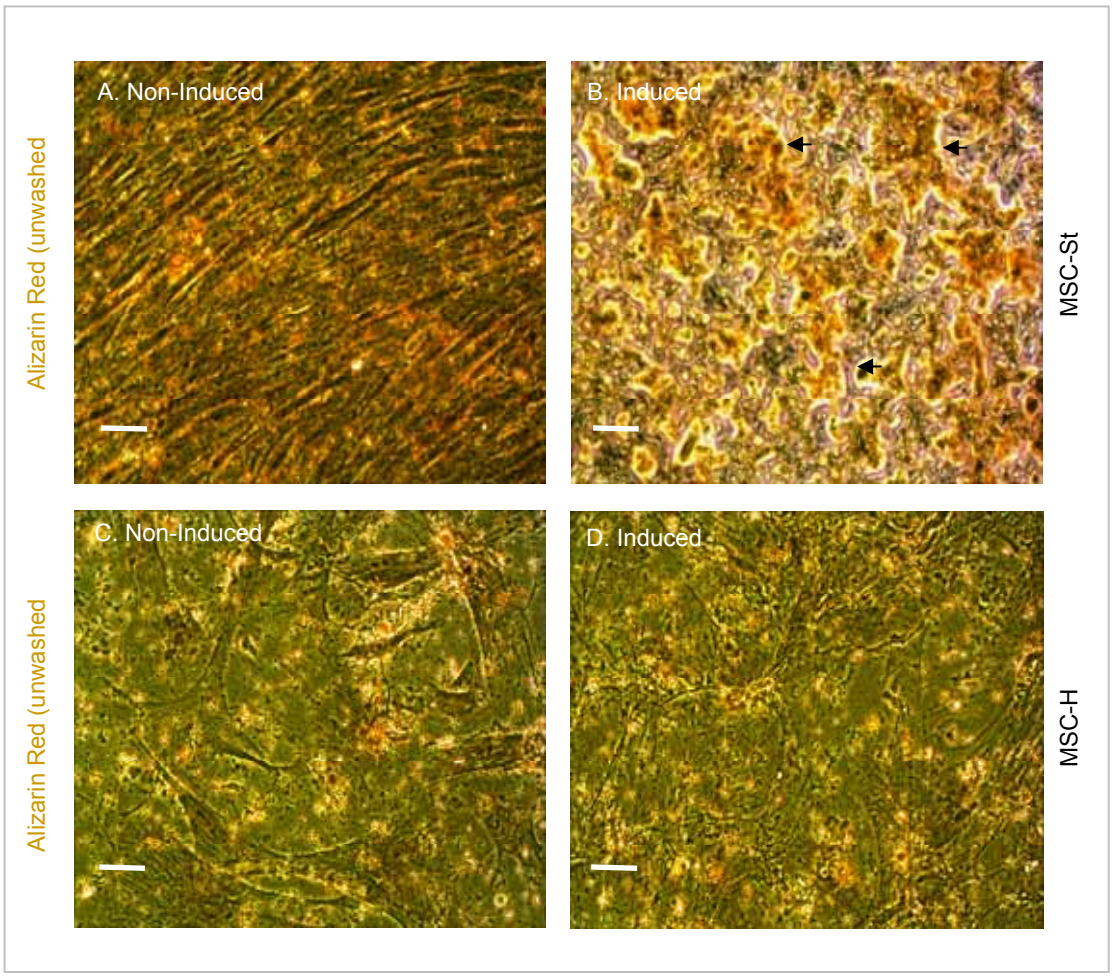

Figure 3.25. High density MSCs could not be induced to differentiate to osteoblasts

MSCs cultured in standard conditions for 24 hours or at high density for 28 days were induced to differentiate to osteoblasts by exposure to osteogenic differentiation media over 14 days. Osteoblasts were detected by alizarin red staining using an Olympus (CK X41) phase contrast microscope (20× objective) and images captured. **(A)** MSCs in standard culture conditions in basal media for 14 days; **(B)** MSCs in standard culture conditions exposed to osteogenic differentiation media for 14 days; **(C)** MSCs at high density in MSC basal media for 14 days; **(D)** MSCs at high density exposed to osteogenic differentiation media for 14 days. Figures A and B are also shown in Figure 3.3. Ten representative images were taken for each treatment with each analysis performed in triplicate. Black arrows depict calcium deposits. Scale Bars = 20μm.

were unable to differentiate to osteoblasts. These experiments were performed at the same time as those in Figure 3.3.

3.5. Discussion

The potential for adult bone marrow-derived MSCs to differentiate into ECs is a critical determinant which may direct many postnatal vascularisation events (Aghi and Chiocca, 2005; Hung *et al* ., 2005; Tang *et al* ., 2006; Xin *et al* ., 2007). In this study, human BM-derived MSCs, plated and cultured at high cell density developed a cobblestone-like morphology that was similar to ECs in culture. Moreover, MSCs cultured at high cell density began to express EC markers and a proportion of these cells acquired the ability to perform endothelial functional tests. These cellular changes appeared to be differentiation events specific to MSCs, since HDFs cultured at high density did not express EC markers.

It has been proposed that, during embryogenesis haematopoietic cells and ECs are both derived from a common mesoderm precursor (Bailey *et al* ., 2003; Eilken et al., 2009; Lancrin *et al* ., 2009; Lacaud *et al* ., 2009; Vogeli *et al* ., 2006) (see also Chapter 1: introduction section 1.4.1 and Figure 1.5). Thus, the identification of unique markers that define ECs has generated much controversy, and a universally accepted functional assay or specific endothelial marker for ECs is lacking. The close embryonic relationship between the haematopoietic and vascular systems has consequently resulted in overlapping marker expression, common to both leukocytic lineages and vSMCs/pericytes (Bailey *et al* ., 2006; Schlingemann *et al* ., 1991; Reddy *et al* ., 2008; Schmeisser *et al* ., 2003; Zovein *et al* ., 2006). VE-cadherin, thought to be exclusively expressed on ECs, has now been detected on fetal HSCs (Kim *et al* ., 2005b). More recently, evidence has been shown that the cell type consistent with current definitions of a blood derived EPC phenotype may arise from an uptake of platelet microparticles by mononuclear cells resulting in a gross misinterpretation of their cellular progeny (Prokopi *et al* ., 2009). In addition, vSMCs and macrophages have been shown to express VEGFR1 and VEGFR2, generally defined as EC specific markers (Banerjee *et al* .,

2008; Salmonsson *et al* ., 2003), whilst monocytes have been documented to express endothelial markers and form networks in Matrigel in the presence of angiogenic stimuli (Bailey *et al* ., 2006., Schmeisser *et al* ., 2001; 2003). Interestingly, HUVECs exposed to equilaxial stretch *in vitro* can express MHC-1, most probably reflecting the adaptability of vascular cells during normal physiological and aberrant pathological events (Cevallos *et al* ., 2006). Thus verification of ECs requires the expression of a complement of EC markers, EC functional assays and lack of non-EC cell lineage markers. In this study, the absence of leukocytic markers by MSCs cultured at high density, together with the appearance of a subset of EC markers and the ability to perform EC functional tests in a small proportion of MSCs, may indicate that a subpopulation of MSCs cultured at high density were differentiating to an EC fate. To help give a more definitive identification, further indicators of a fully functional EC could be tested including prostacylin and nitric oxide release, E-cadherin expression as well as determining whether leukocytes could transmigrate across a monolayer of these 'endothelialised cells'.

It should be noted that HUVECs, a relatively specialised embryonic EC population derived from the umbilical vein, were used throughout this study as a EC standard, primarily due to their availability and ease of culture *in vitro*. However, fully differentiated ECs derived from MSCs may be more similar to adult mature ECs such as HCAECs, microvascular ECs or even tumour endothelium. These different ECs all display distinct differences from HUVECs in terms of their morphology, abundance of endothelial markers and functional endothelial behaviour (Aird *et al*, 2003; Garlanda *et al* ., 1997). Such differences are largely pre-determined by EC position within the vascular tree and blood flow velocity which all play important roles during EC differentiation. ECs incorporated into larger blood vessels interact with a specialised basement membrane derived from surrounding contractile vSMCs or pericytes, which also regulate EC differentiation events. Thus, ECs derived from MSCs during postnatal vasculogenesis, may prove to be more similar to HCAECs than HUVECs.

Following MSC culture at high density, the same cells then re-seeded at low density only lost a small proportion of their expression of vWF and VEGFR1, which may suggest that these cells could be sub-cultured. However, the expression of these markers was only monitored in reseeded cells for 7 days and ideally these cells would need to be monitored for longer time periods. MSCs cultured at high density showed a decrease in the stem cell markers CD29, CD44 and CD105 together with a complete loss of their potential to differentiate towards osteogenic or adipogenic lineages. It is important to consider that only a small decrease in MSC associated markers was observed in MSCs cultured at high density which may reflect that perhaps only a subpopulation is changing and/or the change elicited is only partially towards a fully committed EC or that these markers are also expressed on ECs. The osteogenic marker osteopontin was up-regulated during high density culture. Interestingly, it has recently been shown that osteopontin can also function as an intrinsic marker of hypoxia (Zhou *et al* ., 2009). This study demonstrated that high cell density-mediated pericellular hypoxia was an important factor in inducing expression of osteopontin in human prostate tumour cells and may explain the significant up-regulation of osteopontin in MSCs cultured at high density.

The MSC density induced cobble-stone morphology was lost when these cells were re-seeded at low density when a more flattened cell morphology was adopted. The change in cellular morphology may not indicate a dramatic loss of EC differentiation, but may well reflect the immaturity of the EC phenotype. While fully differentiated ECs maintained their cobblestone morphology, immature ECs may well have a less defined morphology, displaying a range of phenotypes, with the majority displaying rounded cobblestone morphologies but also exhibiting spindle shaped and flattened morphologies (Aird *et al*, 2003; Garlanda *et al* ., 1997). These differences in morphology may reflect different stages of maturity, with rounded reflecting fully differentiated ECs, while spindle and flattened morphologies may be indicative of an immature phenotype. Alternatively, these MSCs cultured for up to 28 days at high density could have entered replicative senescence; this could be determined by testing for beta galactosidase activity, a biomarker of senescence. In

addition, a number of studies have shown how migratory ECs typically display a fibroblast-like phenotype whilst confluent ECs adopt a cobble-stone morphology within polarised monolayers (Dejana *et al*, 2004). Thus re-seeding MSC-derived ECs at low density directly onto tissue culture plastic may not be the ideal situation for maintaining a cobble-stone morphology, and for example, re-seeding the differentiated cells onto Matrigel may be more appropriate.

Interestingly, the main EC signalling receptor VEGFR2 was not expressed by MSCs cultured at high density. It has previously been established that VEGFR1 and VEGFR2 play different roles during physiological and pathological angiogenesis (Kliche *et al* ., 2001; Huusko *et al* ., 2009; Matsumoto *et al* ., 2006; Olsson *et al* ., 2006; Takahashi *et al* ., 2001; 2005). VEGFR1 plays a negative role during embryonic vasculogenesis where it acts as a "decoy receptor" for VEGF-A, preventing growth factor binding to VEGFR2. In contrast, VEGFR1 has been shown to play a positive role in adulthood during postnatal vascular remodelling, activating EC proliferation and promoting tumour growth, metastasis and inflammation (Shibuya *et al*, 2006a, b; Takahashi *et al* ., 2005). In contrast, VEGFR2 is considered the major inducer of vascular remodelling. VEGFR2 gene knock-out mice die at E8.0-8.5 due to a lack of vasculogenesis and VEGFR2 was shown to have a major role in tumor angiogenesis and diabetic retinopathy using animal models (Shalaby *et al* ., 1995; 1997, Shibuya *et al*, 2006c). VEGFR2 is also known to interact with VE-cadherin and integrins, to regulate many steps of angiogenesis (Shay-Salit *et al*., 2002; Stupack *et al*.,, 2004). While the MSC-derived endothelial-like cells generated in this study, exhibited a wide range of characteristics indicative for ECs, the lack of VEGFR2 further supports the concept of an immature EC phenotype, with a more mature phenotype represented by VEGFR2 expression (see Chapter 5).

Immunofluorescence analysis of the EC markers VEGFR1, VE-cadherin and PECAM-1 showed a predominantly intracellular distribution. Total cellular VEGFR1 predominantly localised within the Golgi apparatus as previously demonstrated (Mittar *et al*., 2009). These authors postulated that compartmentalisation of VEGFR1 may regulate VEGF-A

mediated responses, by preventing VEGFR1 from sequestering circulating VEGF-A. High levels of internalised phosphorylated VEGFR1 were detected within the cytoplasm of MSCs at high density, suggesting that VEGFR1 was signalling, presumably through the up-regulated autocrine VEGF-A, and cycling to intracellular storage compartments. In this study, both VE-cadherin and PECAM-1 exhibited a punctate intracellular distribution. The biosynthesis, processing and turnover of the adhesion molecules VE-cadherin and PECAM-1, has previously been shown to have distinct cellular localisations (Goldberger *et al* ., 1994; Mamdouh *et al* ., 2003; Rival *et al* ., 1996; Xiao ., 2003). VE-cadherin is constitutively internalised from cell borders and internalised VE-cadherin has been shown to localise to cytoplasmic vesicles (Xiao *et al* ., 2003). VE-cadherin internalisation has been shown to be tightly controlled by VEGF-A abundance. In ECs, VEGF-A binding to VEGFR2 led to VE-cadherin phosphorylation, promoting VE-cadherin internalisation (Mukherjee *et al* ., 2006; Gavard *et al* ., 2006; Wallez *et al* ., 2006; 2007). Therefore in this study, the levels of VEGF-A secreted by MSCs at high density may activate VEGFR1 signalling to promote VEGFR1, VE-cadherin and PECAM-1 internalisation.

As previously discussed, non-clonal MSCs are heterogenous with regard to their differentiation potential (Ho *et al* ., 2008; Huang *et al* ., 2009; Phinney *et al*, 2007b). This heterogeneity may give rise to MSC populations that have higher EC potential and may explain the low proportion (~50%) of MSCs amenable to taking up ac-LDL and the lower expression levels of vWF, PECAM-1 and VE-cadherin compared with HUVECs. Immunofluorescence analysis suggested that most MSCs were expressing EC markers, but at varying levels. It has recently been reported that single-cell-derived clonal populations could be isolated from human umbilical cord derived perivascular cells, known as HUCPVCs (Sarugaser *et al* ., 2009). Definitive parent and daughter clones were isolated from mixed suspensions and then assayed for their ability to differentiate into one or more of five mesenchymal lineages. These single cell-derived clones maintained extensive self-renewal capacity *in vitro* and clonally produced daughter populations of cells with different differentiation potentials. In addition, the VE-cadherin

promoter fused to green fluorescent protein was used to identify endothelialised ESCs and to screen for factors that promoted vascular commitment (James *et al* ., 2010). Using such techniques or by performing fluorescence activated cell sorting for DiI-ac-LDL uptake, it may be possible to isolate endothelialised MSCs from the total cellular population generating a more homogeneous source of EC-differentiated MSCs.

This chapter has suggested that high density culture may induce a proportion of MSCs to differentiate towards an EC lineage. The next chapter focuses on dissecting the mechanisms involved in regulating these differentiation events.

3.6. Summary

- MSCs cultured at high density adopted a cobble-stone like morphology
- VEGFR1 and VE-cadherin were induced in MSCs cultured at high density
- PECAM-1, vWF and VEGF-A were significantly enhanced in MSCs cultured at high density
- VEGFR1 was predominantly localised to the Golgi apparatus
- VWF showed punctate perinuclear localisation
- VE-cadherin and PECAM-1 showed punctate intracellular immunoreactivity
- MSCs cultured at high density exhibited ac-LDL uptake in a proportion of cells
- MSCs cultured at high density showed enhanced Matrigel network formation
- VCAM-1 could be induced by exogenous TNF-α in MSCs cultured at high density
- High density culture did not stimulate EC markers in HDFs
- The EC lineage was largely retained in low density culture at 7 days

CHAPTER 4

RESULTS

Mechanisms regulating the differentiation of MSC to ECs

CHAPTER 4: RESULTS

4.1. Mechanisms regulating the differentiation of MSC to ECs

It is becoming increasingly recognised that MSCs make an important contribution to promoting postnatal vascularisation during ischaemic myocardial tissue regeneration, wound healing and tumour vasculogenesis (Aghi *et al*., 2005; Al-Khaldi *et al*., 2003; Huang *et al* ., 2008; Reddy *et al* ., 2008; Roorda *et al* ., 2009; Silva *et al* ., 2005; Tang *et al* ., 2006; Wu *et al* ., 2005). To enable the therapeutic manipulation of MSCs during postnatal vasculogenesis, it is therefore crucial to determine the mechanisms which direct MSC differentiation towards an EC fate.

In Chapter 3 Results, high density culture induced MSCs to exhibit a range of EC characteristics, suggesting MSC differentiation towards ECs. To determine which molecular mechanisms may regulate this density-dependent differentiation to ECs, it was therefore necessary to consider the micro-environmental factors likely to influence cells in high density culture.

The level of secreted VEGF-A was significantly increased by MSCs that were cultured at high density (Chapter 3: Results, section 3.3.3). Previous studies have reported that MSCs can differentiate to ECs following exposure to exogenous VEGF for up to 14 days (Al-Khaldi *et al* ., 2003; Alviano *et al* ., 2007; Bai *et al* ., 2009; Chen *et al*., 2009; Chung *et al* ., 2009; Oswald *et al*., 2004; Wu *et al* ., 2005; Xu *et al* ., 2009; Zhang *et al* ., 2008). Furthermore, the addition of 50ng/ml VEGF-A to culture medium have been shown to up-regulate venous markers, whereas the addition of higher VEGF concentrations (100ng/ml) induced arterial marker genes (Zhang *et al*., 2008).

Since MSCs cultured at high density have a high degree of cell-cell contact, cell contact mechanisms, including Notch signalling, are expected to play an important role in regulating MSC density-dependent differentiation events. Notch signalling is critical in vascular development, regulating arterio-venous specification, vessel branching and

endothelial tip cell formation (Lawson *et al* ., 2001; Gridley *et al*, 2007; Boulton *et al* ., 2008a,b), and can direct MSCs to differentiate along chondrogenic, cardiomyocyte and osteogenic lineages (Hardingham *et al* ., 2006; Li *et al*., 2006; Oldershaw *et al* ., 2008; Scaffidi *et al* ., 2008). Its importance in blood vessel formation is highlighted by vascular abnormalities caused by mutations in the Notch receptors and ligands (Alva *et al* ., 2004; Bray *et al*, 2006; Opherk *et al* ; 2009). Furthermore, Notch signalling induced by cellular interactions has previously been implicated in MSC-endothelial differentiation (Zhang *et al* ., 2008; Siekmann *et al* ., 2008. Ohata *et al*., 2010). Notch signalling activated by cell-cell contact may, in part by modulating VEGF signalling, direct EC fate and coordinate the specification of arterial and venous ECs (Zhang *et al* ., 2008; Siekmann *et al* ., 2008). Notch activated experimentally over days in culture (Xu *et al* 2009), or during vascular development has been shown to enhance the differentiation of mesenchymal precursors to ECs (Ohata *et al* ., 2010).

In this section, the effects of VEGF-A and Notch signalling in regulating density-dependent differentiation of MSCs to an EC fate were investigated.

4.2. MSC density-dependent differentiation to ECs occurred in two phases

To identify mechanisms which regulate MSC differentiation towards ECs during high density culture, it was essential first to establish the timeframes which define initial MSC to EC commitment and subsequent differentiation events (Figure 4.1).

MSCs were cultured at low density for 14 days, or at high density from 24 hours up to 14 days (see Chapter 2:Materials and Methods, section 2.2.1 for definition of low and high density). Both PECAM-1 (Figure 4.1 (A)) and vWF (Figure 4.1 (B)) showed up-regulated expression after 24 hours at high density culture. While PECAM-1 expression remained constant up to 14 days, vWF expression significantly increased throughout the 14 day culture period. The expression of VEGFR1 (Figure 4.1 (C)) was induced after 24 hours culture at high density, which significantly increased during the 14 day culture period.

Figure 4.1

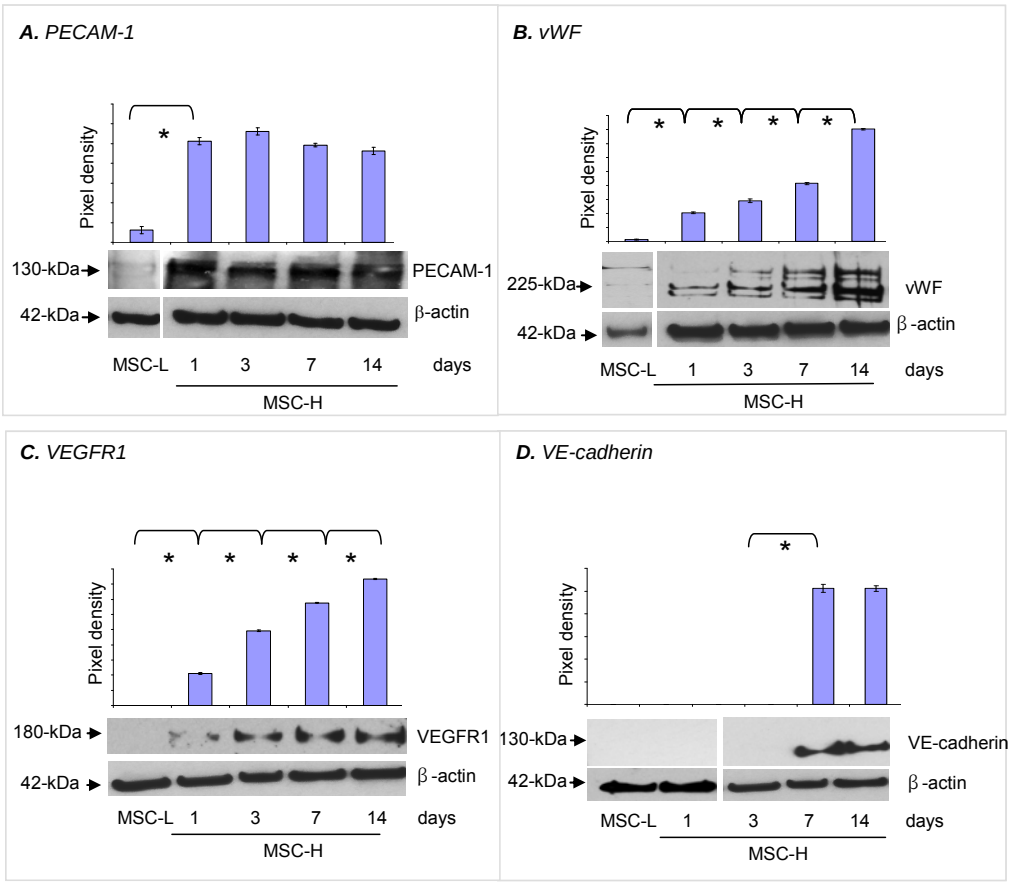

Figure 4.1. MSC density dependent differentiation to ECs occurred in two phases

Immunoblot analysis of **(A)** PECAM-1, **(B)** vWF, **(C)** VEGFR1 and **(D)** VE-cadherin in MSCs cultured at low density (MSC-L) for 14 days or at high density (MSC-H) up to 14 days, depicting initial MSC to EC commitment events and later differentiation events to consolidate the EC fate. For vWF, VEGFR1 and VE-cadherin, membranes were stripped and re-probed with β-actin to ensure equal loadings. For PECAM-1, equal volumes of lysate were immunoblotted for β-actin to determine equal loadings. Pixel density was normalised to β-actin and plotted as a bar graph. * represents $p<0.05$. Representatives of two independent experiments are shown for each analysis.

In contrast, the expression of VE-cadherin (Figure 4.1 (D) was only induced after 7 days of culture at high density, after which the expression remained constant up to 14 days. Thus, density-dependent differentiation of MSCs to ECs occurred in two phases, comprising an initial induction phase and a subsequent enhancement phase. Initial MSC commitment towards an EC fate, characterised by increased expression of PECAM-1 and vWF and induction of VEGFR1 expression, occurred during the first 24 hours of culture at high density, whilst later commitment characterised by VE-cadherin expression occurred after 7 days of culture at high density.

4.3. Involvement of VEGF-A in initiating MSC commitment to ECs

4.3.1. Exposure to VEGF-A did not induce MSCs to express EC markers

The angiogenic growth factor VEGF-A has been implicated in directing MSC differentiation towards ECs (Al-Khaldi *et al* ., 2003; Alviano *et al* ., 2007; Bai *et al* ., 2009; Chen *et al* ., 2009; Chung *et al* ., 2009; Oswald *et al*., 2004; Wu *et al* ., 2005; Xu *et al*., 2009; Zhang *et al* ., 2008) (see chapter 1: Introduction). However, these studies only analysed endothelial marker expression after 7-14 days in culture, by which time matrix deposition, autocrine growth factor secretion and cell density effects may also be critical mediators of this EC fate decision.

To establish whether MSCs could be induced to express EC markers by short term exposure to exogenous VEGF-A, MSCs in standard culture conditions (see Chapter 2: Materials and Methods, section 2.2.1 for definition) were exposed to 50ng/ml VEGF-A for 24 hours (Figure 4.2). Immunoblot analysis demonstrated that PECAM-1 (Figure 4.2 (A)), VEGFR1 (Figure 4.2 (B)) or VE-cadherin (Figure 4.2 (C)) were not expressed by MSCs in standard culture conditions in the presence of 50ng/ml VEGF-A suggesting that exposure to exogenous VEGF-A alone was not sufficient to induce MSCs to express endothelial markers.

Figure 4.2

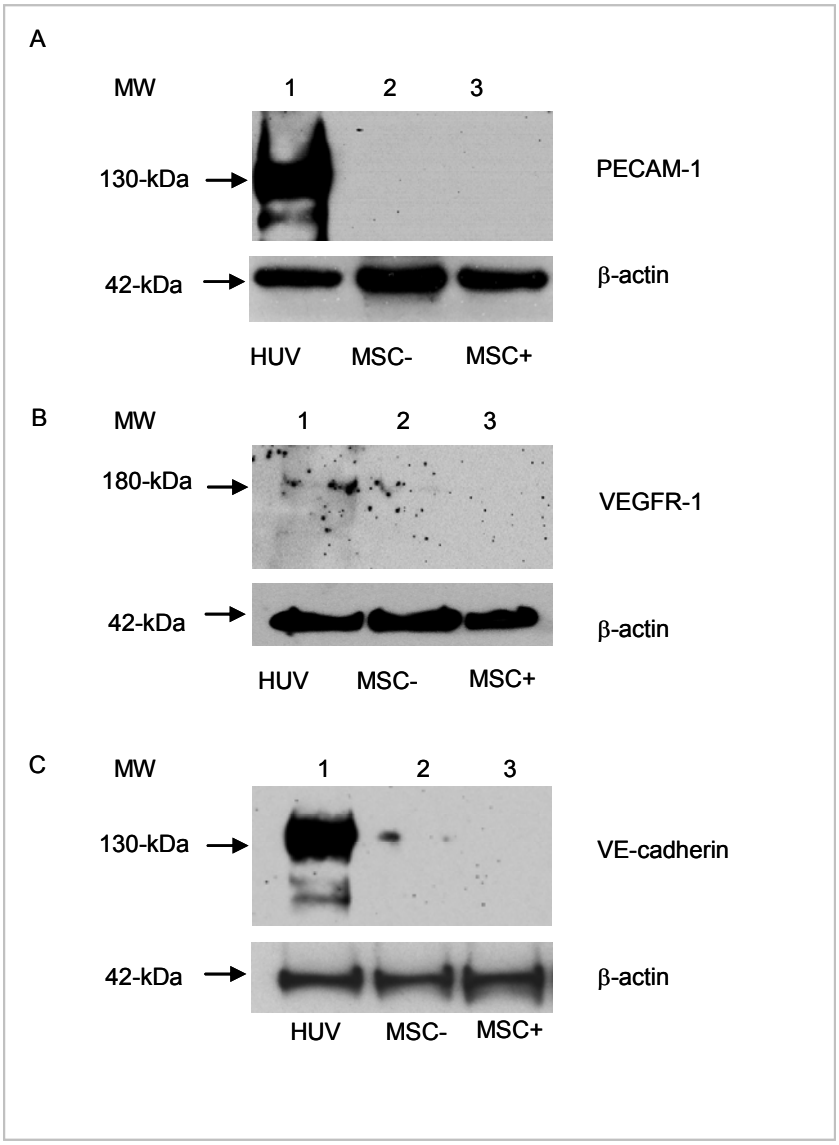

Figure 4.2 *Exposure to VEGF-A did not induce MSCs to express EC markers*

To determine whether exposure to exogenous VEGF-A alone could induce MSCs to express the EC markers **(A)** PECAM-1, **(B)** VEGFR1 or **(C)** VE-cadherin, MSCs cultured in standard conditions were stimulated with 50ng/ml VEGF-A for 24 hours (MSC+) or unstimulated (MSC-). HUVECs in standard culture conditions were used as a positive control. β-actin was used as loading controls. Representatives of two independent experiments are shown for each analysis.

4.3.2. VEGF-A neutralisation did not alter EC marker expression

As previously shown and discussed (Results chapter 3, section 3.3.3), MSCs cultured at high density displayed significantly enhanced VEGF-A secretion after 14 days. MSCs at high density also secreted increased VEGF-A after 24 hours (2466±48 pg/ml), compared with MSCs cultured at low density (910±51 pg/ml) (Figure 4.3 (A)). To determine whether up-regulated autocrine VEGF-A stimulated MSC towards EC commitment, MSCs were cultured at high density in the presence of a VEGF-A neutralising antibody (designated VEGF-I) for 24 hours (Figure 4.3 (B, C)). VEGF-I was subsequently confirmed to block VEGFR phosphorylation (see Antibody controls Figure 4.20). However, VEGF neutralisation over 24 hours had no detectable effect on either vWF (Figure 4.3 (B); lane 2) or VEGFR1 (Figure 4.3 (C); lane 2) compared to untreated controls (Figure 4.3 (B, C); lanes 1).

4.3.3. VEGF-A siRNA knockdown did not alter EC marker expression

To examine whether autocrine VEGF-A stimulation of MSCs at high cell density, contributed to inducing VEGFR1 or up-regulating vWF expression, VEGF-A siRNA knockdown was performed (Figure 4.4). Following VEGF-A siRNA knockdown for 24 hours, VEGF-A transcript level was markedly decreased (Figure 4.4 (A) and VEGF-A secretion significantly reduced by 79% (Figure 4.4 (B)), compared to MSCs transfected with scrambled siRNA. However, immunoblot analysis of MSCs transfected with VEGF-A siRNAs revealed no change in VEGFR1 or vWF protein levels after 24 hours (Figure 4.4 (C), 4.4 (D); lanes 2), compared to MSCs transfected with scrambled siRNAs (Figure 4.4 (C), 4.4 (D); lanes 1). Thus, exposure of MSCs to either high exogenous or low endogenous levels of VEGF-A for 24 hours did not contribute to inducing VEGFR1 or enhancing vWF expression during the first 24 hours of culture at high cell density. Therefore, exposure to VEGF-A was not sufficient to initiate density dependent differentiation of MSCs to an EC fate.

Figure 4.3

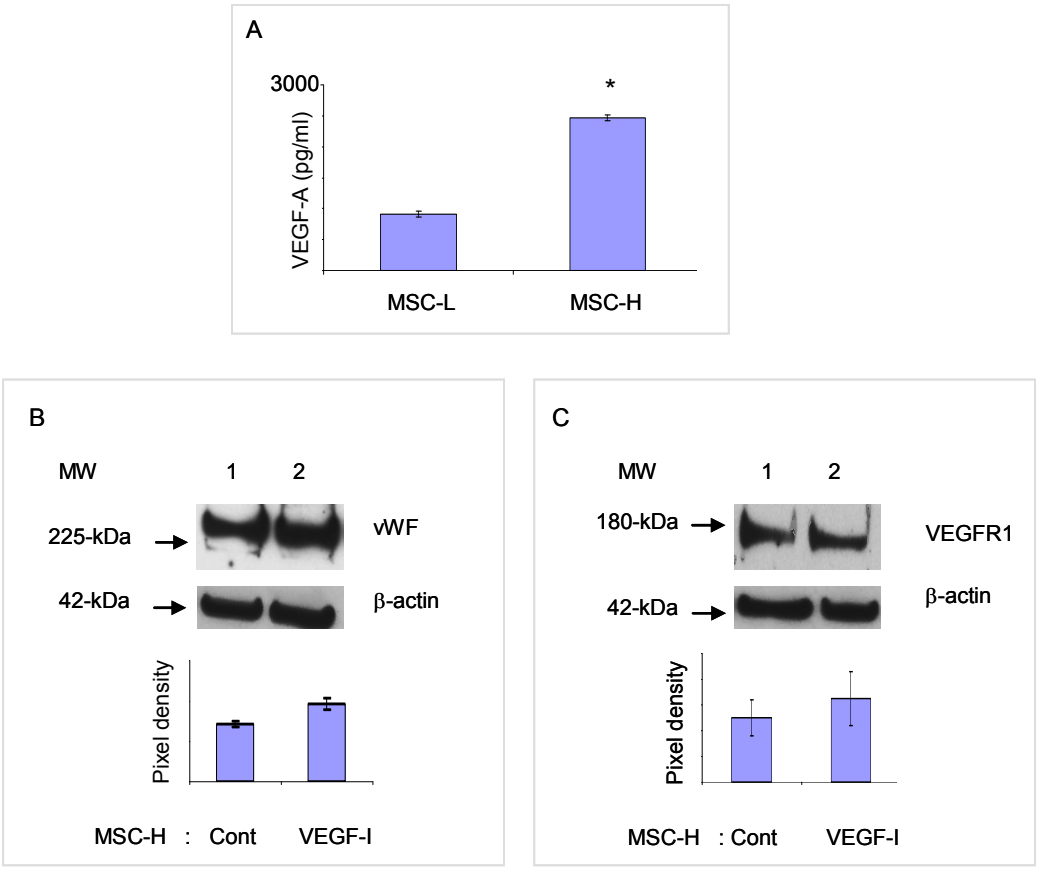

Figure 4.3. VEGF-A neutralisation did not alter EC marker expression

(A) ELISA assay of VEGF-A from the medium of MSCs cultured at low (MSC-L) or high density (MSC-H) for 24 hours. * represents $p<0.05$ compared to MSC-L. A representative of two independent experiments is shown for each analysis with each analysis performed in duplicate.

(B-C) To verify whether the VEGF-A secreted by MSCs altered at high cell density for 24 hours, induced MSCs to express VEGFR1 or up-regulate vWF, MSCs were treated with 1μg/ml VEGF neutralising antibody (VEGF-I) during the 24 hour culture period. Immunoblot analysis of **(B)** vWF or **(C)** VEGFR1 protein levels in untreated (cont) (lanes 1) or VEGF-I treated MSCs (lanes 2) is shown. β-actin was used as loading controls. Pixel density was normalised to β-actin and plotted as a bar graph. A representative of two independent experiments is shown.

Figure 4.4

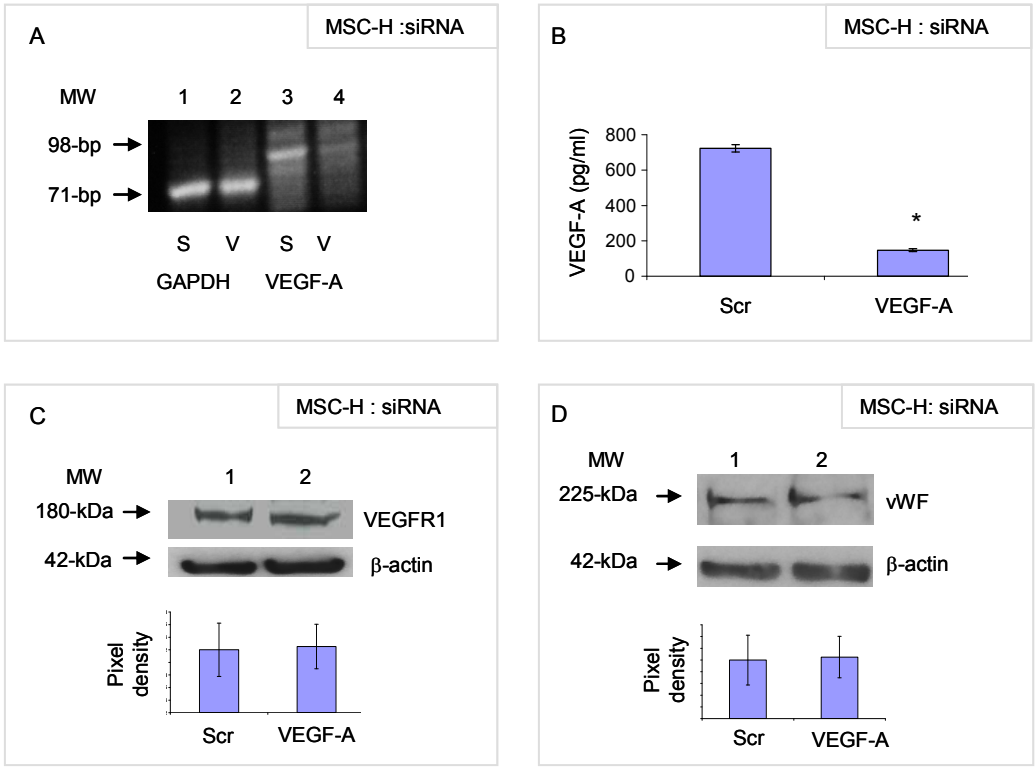

Figure 4.4. *VEGF-A siRNA knockdown did not alter EC marker expression*

To examine whether autocrine stimulation of MSCs at high cell density, contributed to inducing VEGFR1 or increasing vWF expression, VEGF-A siRNA knockdown was performed for 24 hours. **(A)** Semi-quantitative RT-PCR analysis using RNA isolated from MSCs cultured after plating at high cell density (MSC-H) for 24 hours after transfection with 3 μg scrambled siRNA as a control (S) or VEGF-A siRNAs (V). Lanes 1-2, GAPDH; lanes 3-4, VEGF-A transcripts.

(B) VEGF-A secreted by MSCs cultured at high density following transfection with 3 μg scrambled (Scr) control or VEGF-A siRNAs for 24 hours. * represents $p<0.05$ compared to Scr.

Following siRNA knockdown of VEGF-A, immunoblot analysis was performed to detect **(C)** VEGFR1 and **(D)** vWF protein levels. Lanes 1, scrambled (Scr) control transfected MSCs; lanes 2, VEGF-A siRNA transfected MSCs. Membranes were re-probed with β-actin as loading controls. A representative of two independent experiments is shown. Pixel density was normalised to β-actin and plotted as a bar graph.

4.4. Involvement of Notch signalling in initiating MSC commitment to ECs.

4.4.1. MSCs expressed Notch Receptors 1, 2 and 3

Having established that MSC exposure to VEGF-A did not initiate differentiation to an EC fate during the first 24 hour culture period at high cell density, other potential initiating mechanisms were examined. The possibility that Notch signalling was involved in directing the differentiation of high density MSCs towards an EC fate was therefore examined. MSCs were initially characterised for their expression of Notch receptors (Figure 4.5). Notch signalling, which requires receptor-ligand interactions between adjacent cells, is mediated by four transmembrane receptors (Notch 1-4) and five transmembrane ligands, Jagged 1 and 2 and Delta-like 1, 3 and 4 (Bray *et al*, 2006) (see Chapter 1: Introduction, section 1.6.5.1). Immunofluorescence analysis was performed to detect the Notch receptors 1-4 in MSCs cultured at low or high density for 24 hours. Immunofluorescence analysis identified cell surface localisation of Notch receptor 1, in both low and high density cultured MSCs (Figure 4.5 (A, B) respectively). Compared to low density cultures (Figure 4.5 (C)), interestingly, immunofluorescence analysis detected widespread prominent nuclear Notch receptor 2 expression in MSCs cultured at high density (Figure 4.5 (D)). In contrast, Notch receptor 3 predominantly localised to the Golgi apparatus in both low (Figure 4.5 (E)) and high density MSC cultures (Figure 4.5 (F)), while nuclear expression was also detected at high density.

4.4.2. High density MSC culture increased Notch signalling components

Having confirmed the expression of Notch receptors 1-3 in MSCs, RT-PCR analysis was performed to detect Notch signalling transcripts in MSCs during the first 24 hours at high density culture and up to 7 days (Figure 4.6). Compared to MSCs cultured at low density for 4 hours (Figure 4.6 (A)), culture at high density for 4 hours (Figure 4.6 (B); lane 1) increased the expression of all the Notch signalling transcripts examined; Notch receptor 1, 2, 3, Jagged-1, Delta-like 3 and the downstream Notch transcription factor HES-1.

Figure 4.5

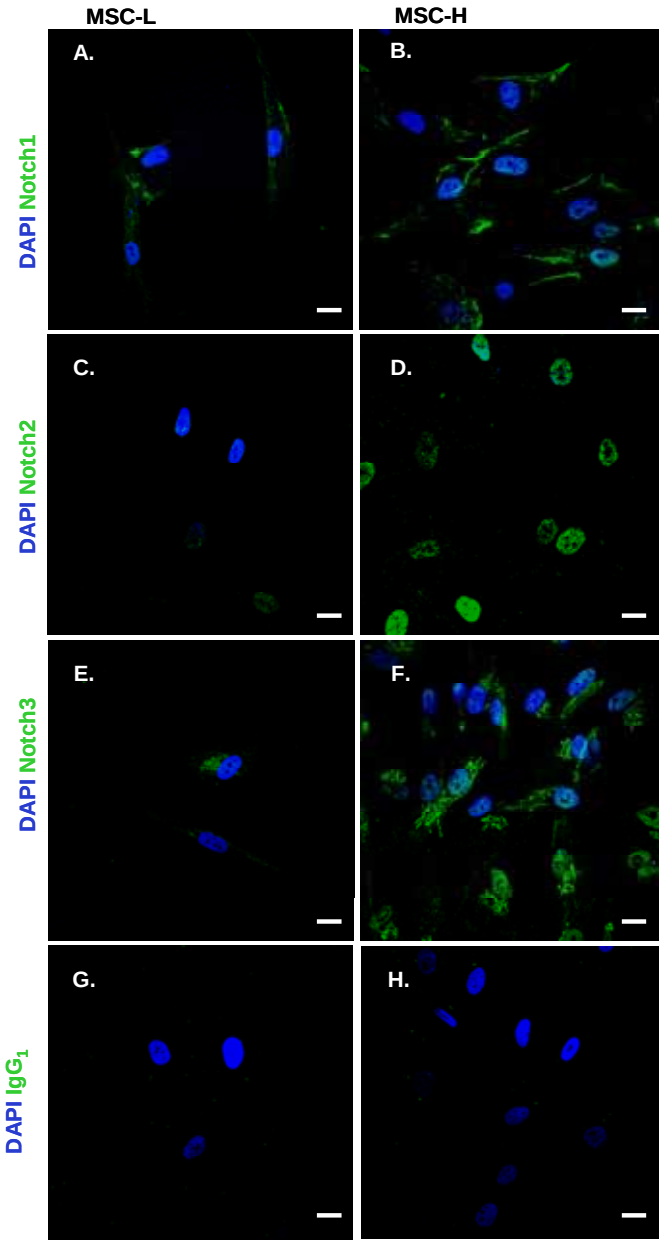

Figure 4.5. *MSCs expressed Notch receptors 1, 2 and 3*

(A-F) Immunofluorescence analysis of Notch receptors 1-3 in MSCs cultured at low (MSC-L) or high density (MSC-H) for 24 hours. Notch receptors = green, DAPI = blue. Primary antibodies used were Notch1 (C37C7) (recognises full length and transmembrane/intracellular region); Notch2 (8A1) (recognises full length and transmembrane/intracellular region); Notch3 (sc-5593) (recognises epitope corresponding to amino acids 2107-2240 mapping near the C-terminus of Notch 3) Ten representative images were taken using a Nikon C1 upright microscope (60× objective). Data are representative of two independent experiments. **(G, H)** IgG_1 is shown as a negative control. Scale bars = 7μm

After 10 hours, MSCs cultured at high density maintained their expression of Notch receptor 2, JAG-1, DLL3 and HES-1 transcripts (Figure 4.6 (B); lane 2), while the Notch receptor 1 transcript decreased, but the Notch receptor 3 transcript increased. At 24 hours, (Figure 4.6 (B); lane 3), the Notch receptor 3 transcript expression increased further, while the other Notch signalling transcripts decreased. At 7 days (Figure 4.6 (B); lane 4) the expression of Notch receptors 2 and 3 transcript levels were maintained, but the other Notch signalling transcripts decreased. Thus, RT-PCR analysis revealed that the highest levels of Notch 1 transcript expression occurred after 4 hours at high MSC density. The highest levels of Notch 2, JAG-1 and HES-1 occurred up to 10 hours. In contrast, the highest levels of DLL3 transcript occurred at 10 hours, while Notch 3 transcript expression increased up to 24 hours and was maintained after 7 days at high MSC density.

4.4.3. Notch signalling components fluctuated at high density

To further examine the levels of Notch signalling transcripts during the first 24 hours of MSC culture at high density, quantitative PCR was employed (Figure 4.7). While quantitative PCR demonstrated marked fluctuations in the levels of Notch signalling components during the 24 hour period examined, in general, the expression pattern coincided with those determined by RT-PCR analysis (Figure 4.6).

4.4.4. Notch signalling inhibition decreased EC markers and VEGF-A secretion

To investigate whether Notch signalling was involved in inducing MSC expression of VEGFR1, vWF and VEGF-A at high cell density, MSCs were treated with the Notch signalling inhibitor DAPT. DAPT is a chemical inhibitor of the enzyme gamma-secretase that cleaves Notch and allows the transcription of target genes, including HES, HEY and HES related repressor protein family members (Boulton *et al* ., 2008a) . Following MSC treatment with DAPT for 24 hours, down-regulation of the Notch transcription factor HES1 by DAPT was confirmed by RT-PCR analysis (*see* control

Figure 4.6

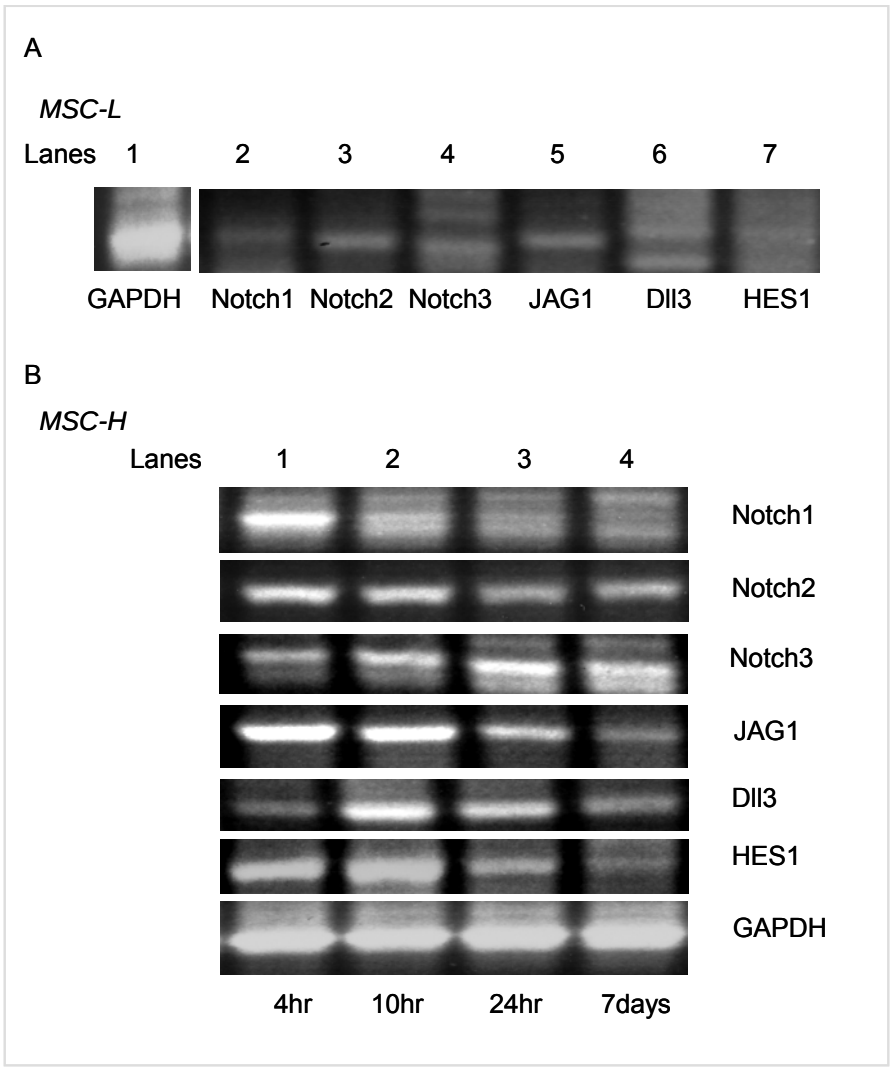

Figure 4.6. High density MSC culture increased Notch signalling components

The expression of Notch signalling transcripts; Notch receptors 1-3 (75-bp, 84-bp and 82-bp respectively), the Notch ligands Jagged-1 (JAG-1) (90-bp) and Delta-like 3 (Dll3) (72-bp) and the downstream Notch transcription factor (Hairy-Enhancer of Split-1 (HES-1) (91-bp) were examined by RT-PCR analysis (35 cycles), following culture of MSCs at **(A)** low density (MSC-L) for 4 hours, or **(B)** high density (MSC-H) for 4 (lane 1), 10 (lane 2), 24 hours (lane 3) and 7 days (lane 4). GAPDH expression of each time point was examined as a loading control. Two different primer pairs for each of the Notch transcripts gave similar results. Data are representative of two independent experiments.

Figure 4.7

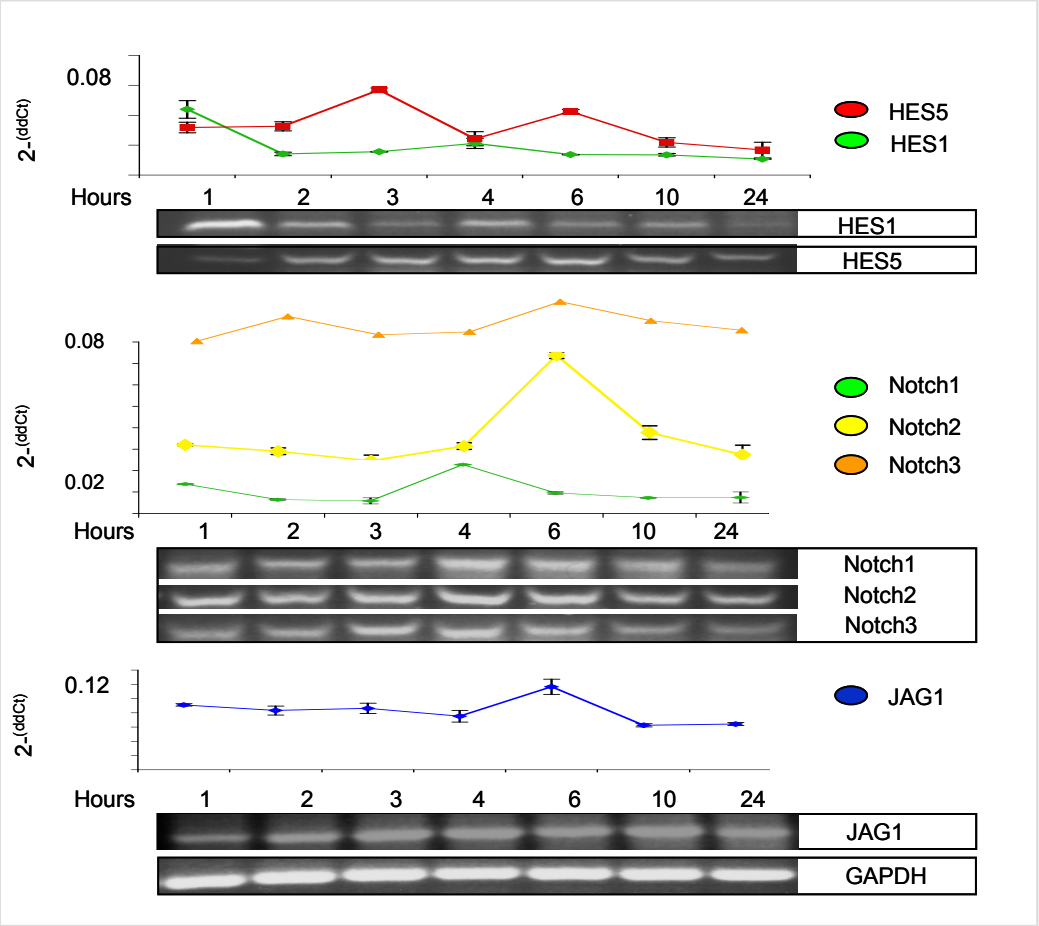

Figure 4.7. *Notch signalling components fluctuated at high density*

Quantitative PCR analysis of Notch signalling components, using RNA isolated from MSCs cultured at high density for 1-24 hours, with $2^{-(ddCt)}$ values plotted against time. Following quantitative PCR reactions, samples were run on a 2.5% agarose gel to verify that the correct product had been amplified. GAPDH was used to determine $2^{-(ddCt)}$ values. Data are representative of two independent experiments, with each sample run in triplicate

Figure 4.22). Immunoblot analysis of lysates derived from MSCs cultured at high density after DAPT treatment for 24 hours revealed a significant 66.9% decrease in VEGFR1 protein level, compared to DMSO-treated control MSCs (Figure 4.8 (A) lanes 1 and 2 respectively). Similarly, DAPT treatment resulted in a significant 60% decrease in vWF protein level compared to DMSO-treated control MSCs (Figure 4.8 (B) lanes 1 and 2 respectively). Furthermore, ELISA analysis of medium derived from MSCs cultured at high density for 24 hours also revealed that DAPT treatment inhibited endogenous VEGF-A expression (Figure 4.8 (C)). Thus, Notch signalling within the first 24 hours of culturing MSCs at high cell density, up-regulated the expression of VEGFR1, vWF and VEGF-A.

4.4.5. Notch receptor siRNA knockdown inhibited EC marker expression

To further confirm that Notch receptors induced MSC density-dependent expression of VEGFR1 and vWF, siRNA oligonucleotides (three target specific siRNAs in each case) were utilised to knockdown expression of Notch receptors 1, 2 and 3, respectively (Figure 4.9). The efficacy of each siRNA knockdown compared to scrambled siRNAs, was confirmed by immunoblot analysis (*see* control Figure 4.22). The specificity of each siRNA Notch receptor knockdown was confirmed by re-probing the blots for a non-target Notch receptor, which revealed unchanged protein levels in each case (see Figure 4.22).

Immunoblot analysis was used to determine which Notch receptors contributed to inducing MSCs to express VEGFR1 when cultured at high cell density for 24 hours (Figure 4.9). MSCs transfected with siRNA oligonucleotides for Notch receptor 1, Notch receptor 2 or Notch receptor 3 all demonstrated a significant decrease in VEGFR1 protein expression ($p<0.05$) (Figure 4.9 (A); lanes 2, 4, 6 respectively) compared to MSCs transfected with scrambled siRNAs (Figure 4.9 (A); lanes 1, 3, 5). Thus, Notch receptors 1, 2 and 3 all contributed to inducing MSCs to express VEGFR1.

Figure 4.8

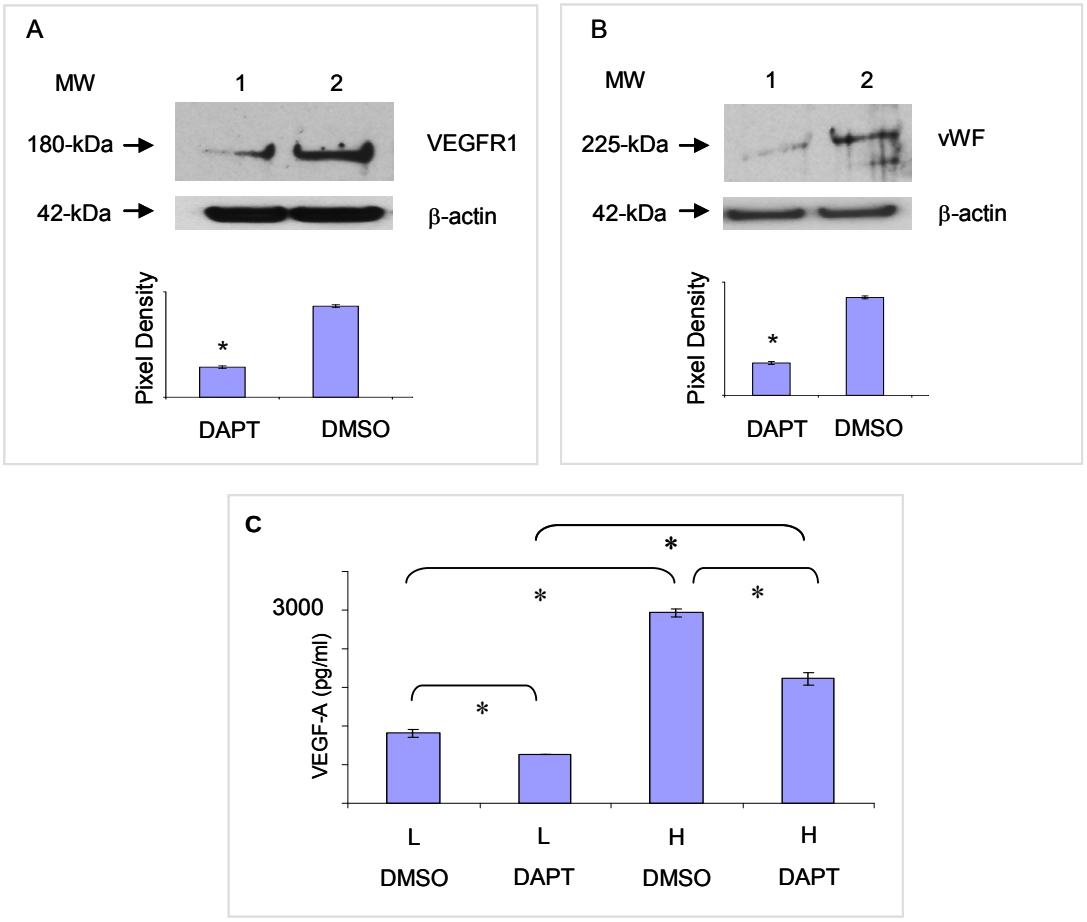

Figure 4.8. Notch signalling inhibition decreased EC markers and VEGF-A secretion

To determine whether Notch signalling regulated MSC density dependent expression of VEGFR1 and vWF, protein levels were determined following inhibition of Notch signalling by DAPT treatment (50 μM). DMSO was used as a diluent control**. (A)** immunoblot analysis of VEGFR1 protein or **(B)** vWF protein, derived from MSCs cultured for 24 hours at high cell density (MSCH) in the presence of DAPT (lanes 1) or DMSO (lanes 2). Pixel density was normalised to β-actin and plotted as a bar graph. * represents $p<0.05$ compared to MSCs cultured after plating at high cell density in the presence of DMSO only. **(C)** ELISA assay of VEGF-A from medium derived from MSCs at low cell density (L) or at high cell density (H) in the presence of DMSO with or without DAPT. * represents $p<0.05$. Membranes were reprobed with β-actin as loading controls. Data are representative of two independent experiments with each ELISA sample run in duplicate.

Figure 4.9

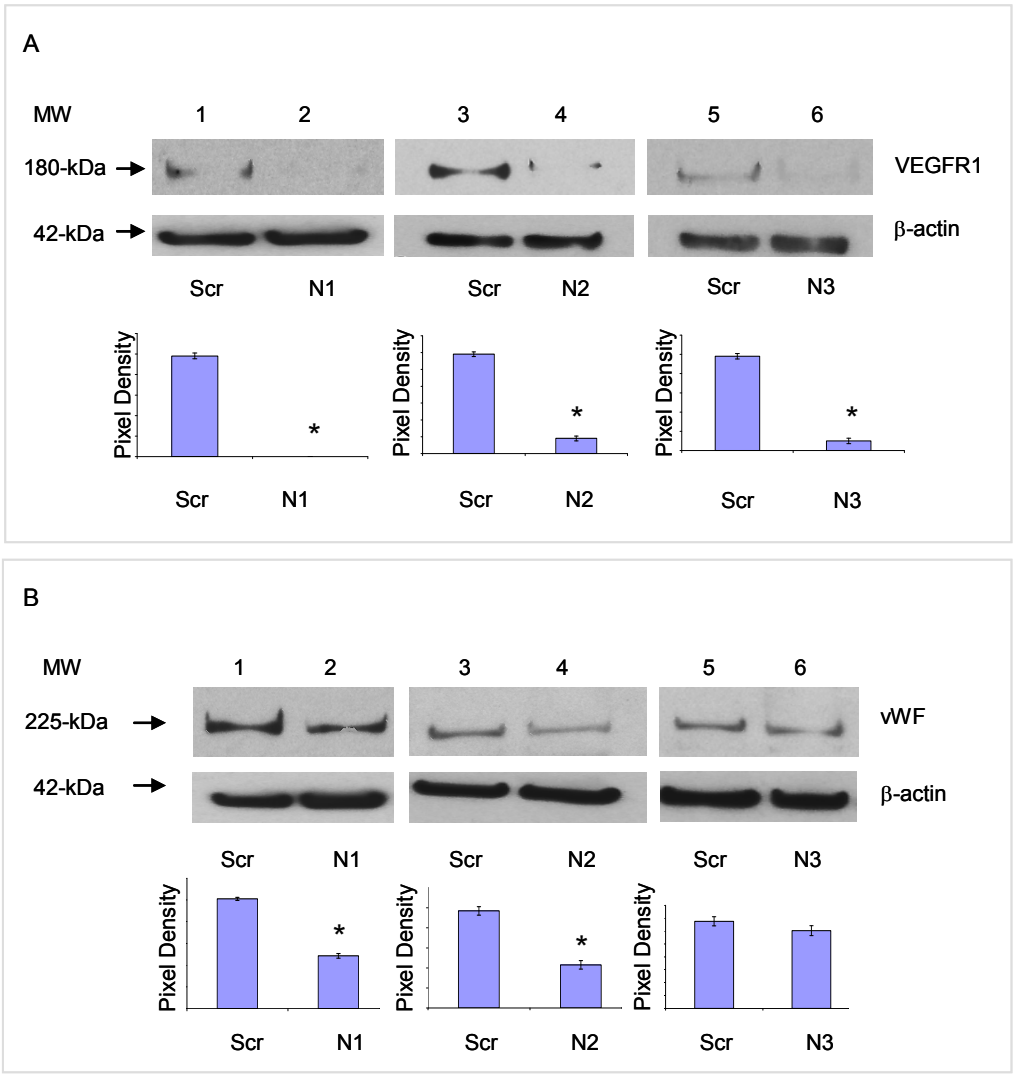

Figure 4.9. Notch receptor siRNA knockdown inhibited EC marker expression

To determine whether Notch signalling mediated MSC density dependent expression of VEGFR1 and vWF, siRNA knockdown of Notch receptors 1-3 was performed. Immunoblot analysis of **(A)** VEGFR1 and **(B)** vWF from MSCs cultured for 24 hours at high cell density, following transfection with scrambled (scr) controls (lanes 1, 3 and 5) or siRNAs for Notch receptors 1, 2 and 3 (lanes 2, 4 and 6). Membranes were reprobed with β-actin as loading controls. Pixel density was normalised to β-actin and plotted as a bar graph. * represents $p<0.05$ compared to scrambled control transfected MSCs. Data are representative of two independent experiments.

Similarly, following Notch 1 or 2 receptor siRNA knockdowns in MSCs cultured at high cell density for 24 hours (Figure 4.9 (B); lanes 2, 4), immunoblot analysis revealed that both knockdowns significantly decreased vWF protein expression ($p<0.05$), compared to MSCs transfected with scrambled siRNAs (Figure 4.9 (B), lanes 1 and 3). In contrast, however Notch 3 siRNA knockdown had no detectable effect on vWF protein expression (Figure 4.9 (B), lane 6), compared to scrambled siRNA control (Figure 4.9 (B), lane 5). Thus, Notch receptors 1, 2 and 3 are involved in inducing MSCs at high density to express VEGFR1, while Notch receptors 1 and 2 are involved in directing MSCs at high density to up-regulate vWF expression.

4.4.6. Notch activation stimulated MSCs at low density to express EC markers

Since inhibition of Notch signalling in MSCs cultured at high density for 24 hours significantly regulated the expression of VEGFR1 and vWF, experiments were conducted to establish whether activation of Notch signalling in MSCs cultured at low density would induce the expression of VEGFR1 and vWF (Figure 4.10). Notch signalling can be activated by treating cells with cation chelators, which cause the rapid shedding of the Notch extracellular domain, increasing Notch receptor 1 intranuclear staining and transcription of CBF1, a nuclear mediator of Notch signalling (Aster *et al*., 1999; Rand *et al* ., 1997, 2000). MSCs that had been cultured at high cell density in the presence of 5 mM EDTA displayed an increase in HES1 activation, demonstrating the effectiveness of EDTA treatment (*see* control Figure 4.22). Immunoblot analysis of MSCs cultured at low cell density for 24 hours in the presence of EDTA, demonstrated both VEGFR1 (Figure 4.10 (A); lane 2) and vWF expression (Figure 4.10 (B); lane 2). In comparison neither VEGFR1 nor the 225-kDa fragment of vWF could be detected after 24 hours in the absence of EDTA (Figure 4.10 (A, B); lanes 1). Thus, activation of Notch signalling in MSCs cultured at low density by EDTA exposure was sufficient to induce the expression of EC markers that would otherwise only be expressed by MSCs at high density.

Figure 4.10

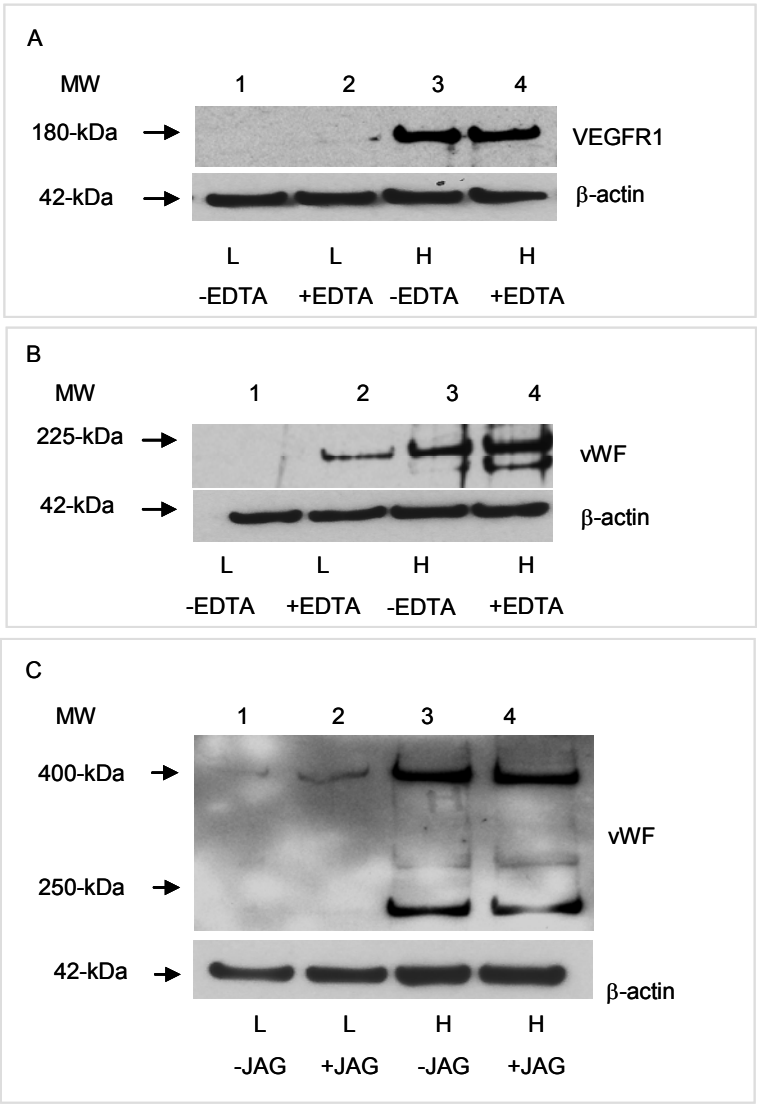

Figure 4.10. Notch activation stimulated MSCs at low density to express EC markers

To determine whether experimental activation of Notch could induce MSCs at low cell density for 24 hours to express vWF and VEGFR1 protein, MSCs were treated with Notch activators. **(A-C)**. Immunoblot analysis of **(A)** vWF or **(B)** VEGFR1 from MSCs cultured after plating at low cell density (L) (lanes 1 and 2) or high cell density (H) (lanes 3 and 4) in the absence (-) (lanes 1 and 3) or presence (+) (lanes 2 and 4) of 5 mM EDTA. **(C)** To further verify that MSCs cultured at low cell density could be induced to express vWF by Notch activation, Notch was activated using immobilised Jagged-1. Immunoblot analysis of vWF protein expression in MSCs cultured at low cell density (lanes 1 and 2) or high cell density (lanes 3 and 4) for 24 hours in the absence (-) (lanes 1 and 3) or presence (+) (lanes 2 and 4) of immobilised Jagged-1. Membranes were reprobed with β-actin as loading controls. Data are representative of two independent experiments.

To further demonstrate that MSCs cultured at low density for 24 hours could be induced to up-regulate their expression of vWF by Notch activation, MSCs at low density were exposed to the Notch ligand Jagged-1 (Figure 4.10 (C). Recombinant Jagged-1 was immobilised onto plates, the MSCs seeded at high or low cell density and cultured for 24 hours. Immunoblot analysis demonstrated that Jagged-1 enhanced the abundance of the high molecular weight (400 kDa) fragment of vWF in MSCs cultured in low density (Figure 4.10 (C); lane 2), compared to unstimulated MSCs, which only expressed low levels of this fragment (Figure 4.10 (C); lane 1). Thus, Jagged-1 activation of Notch signalling was sufficient to stimulate vWF expression in MSCs cultured at low cell density.

4.5. Involvement of VEGF-A in consolidating the EC fate.

4.5.1. Sustained exposure to VEGF-A enhanced VEGFR1 expression

Previous studies have analysed endothelial marker expression after 7-14 days in culture (see chapter introduction section 4.1)**.** The effects of MSC expression of endothelial markers following sustained exposure to VEGF-A for 14 days was therefore examined.

MSCs cultured at high cell density were exposed to exogenous 50 ng/ml VEGF-A for 14 days (Figure 4.11). RT-PCR analysis demonstrated that exposure to VEGF-A markedly increased VEGFR1 transcript expression after 14 days (Figure 4.11 (A); lane 3 and 6), but no detectable change in the level of vWF expression was detected (Figure 4.11 (A); lane 9 and 10). Subsequent immunoblot analysis confirmed that VEGF-A exposure for 14 days significantly increased the level of VEGFR1 protein expressed by MSCs cultured at high density (Figure 4.11 (B); lane 2) compared to unstimulated MSCs cultured at high density (Figure 4.11 (B); lane 1). In contrast, exposure to VEGF-A for 14 days produced no detectable change in the level of vWF expressed by MSCs cultured at high density (Figure 4.11 (C); lane 2) compared to unstimulated MSCs cultured at high density (Figure 4.11 (C); lane 1).

Figure 4.11

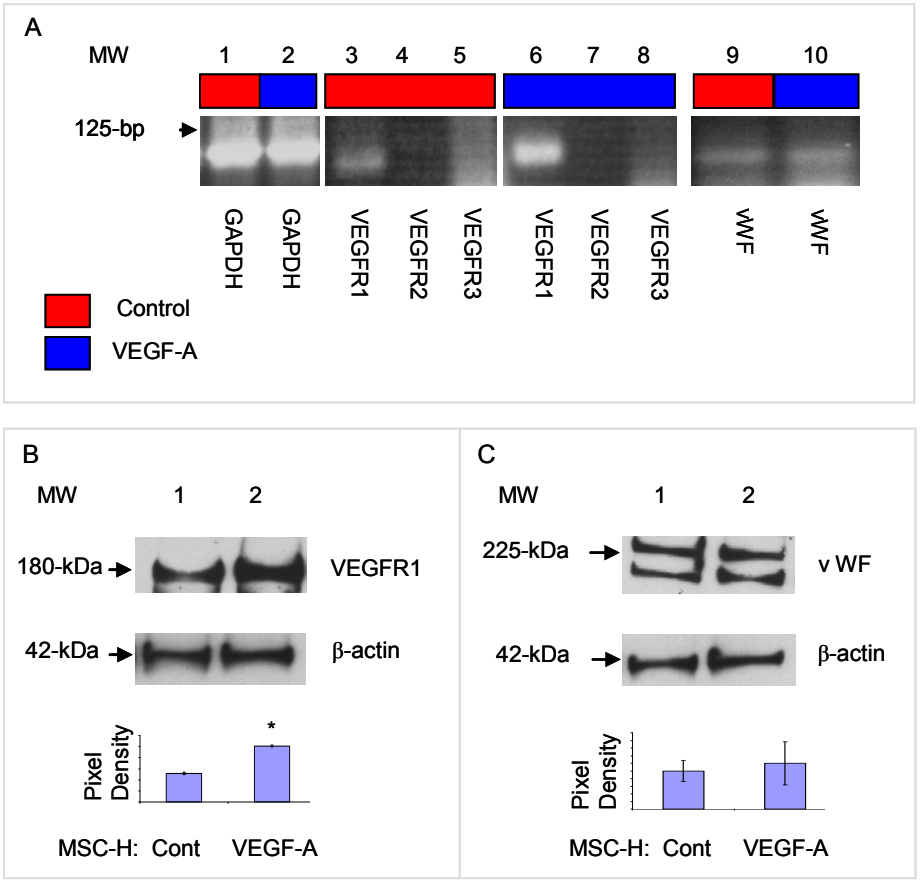

Figure 4.11. Sustained exposure to VEGF-A enhanced VEGFR1 expression

(A) MSCs cultured at high density were stimulated with 50ng/ml VEGF-A every other day for 14 days, then VEGFR1-3 (99-bp, 81-bp, 87-bp respectively) and vWF transcripts (95-bp) examined by semi-quantitative RT-PCR analysis. GAPDH (71-bp) was used to confirm equal RNA concentrations. Lanes 1-2, GAPDH in unstimulated (control) or VEGF-A treated MSCs respectively; lanes 3-5, VEGFR1-3 transcripts respectively in unstimulated MSCs; lanes 6-8, VEGFR1-3 transcripts respectively in VEGF-A treated MSCs; lanes 9-10, vWF transcripts in unstimulated or VEGF-A treated MSCs respectively. Two different primer pairs for VEGFR1-3 and vWF transcripts gave similar results. Red boxes = unstimulated cells; blue boxes = VEGF-A stimulated cells. Data are representative of two independent experiments. **(B, C)** Immunoblot analysis of **(B)** VEGFR1 or **(C)** vWF protein levels in MSCs cultured at high density for 14 days. Lanes 1, unstimulated MSCs, lanes 2, MSCs exposed to 50ng/ml VEGF-A. β-Actin was used as a loading control. Pixel density was normalised to β-actin and plotted as a bar graph. * represents $p<0.05$ compared to unstimulated MSCs cultured at high cell density. Data are representative of two independent experiments.

4.5.2. Sustained VEGF stimulation up-regulated EC markers

To determine whether endogenous levels of VEGF-A played a role in regulating the level of EC markers expressed by MSCs cultured at high density, MSCs were cultured in the presence of the VEGF-A neutralising antibody (VEGF-I) or a VEGFR signalling inhibitor (VEGFR-I) for 14 days (Figure 4.12). After 14 days in the presence of VEGF-I (Figure 4.12 (A); lane 2) or VEGFR-I (Figure 4.12 (A); lane 3), immunoblot analysis of MSCs cultured at high density revealed a significant decrease in VEGFR1 protein expression (the effectiveness of these inhibitors is shown in Figure 4.20), compared to untreated MSCs (Figure 4.12 (A); lane 1). In contrast, MSCs cultured at high density exposed to VEGF-I or VEGFR-I demonstrated no significant effect on vWF expression (Figure 4.12 (B) lanes 2 and 3 respectively), compared to the untreated cells (Figure 4.12 (B); lane 1). However, immunoblot analysis of VE-cadherin expressed by MSCs cultured at high density and exposed to VEGFR-I for 14 days (Figure 4.12 (C); lane 2) demonstrated a significant decrease in VE-cadherin expression, compared to the untreated cells (Fig 4.12 (C); lane 1). Thus, over a period of 14 days, autocrine VEGF-A stimulation of MSCs at high cell density specifically enhanced the expression of VEGFR1. In addition, inhibition of VEGFR1 signalling significantly reduced the induction of VE-cadherin expression by MSCs cultured at high cell density.

4.5.3. Notch and VEGF-A stimulated MSC differentiation to ECs over 14 days

Having established that sustained VEGF-A exposure significantly enhanced VEGFR1 expression over 14 days and that Notch signalling regulated both VEGFR1 and vWF expression after 24 hours, experiments were conducted to determine the effects of inhibiting both signalling pathways over 14 days.

When MSCs were cultured at high density in the presence of DAPT and VEGF-I for 14 days, immunoblot analysis demonstrated a significant decreased in VEGFR1 expression (Figure 4.13, lane 1), compared to MSCs treated with DAPT (Figure 4.13, lane 2) or

Figure 4.12

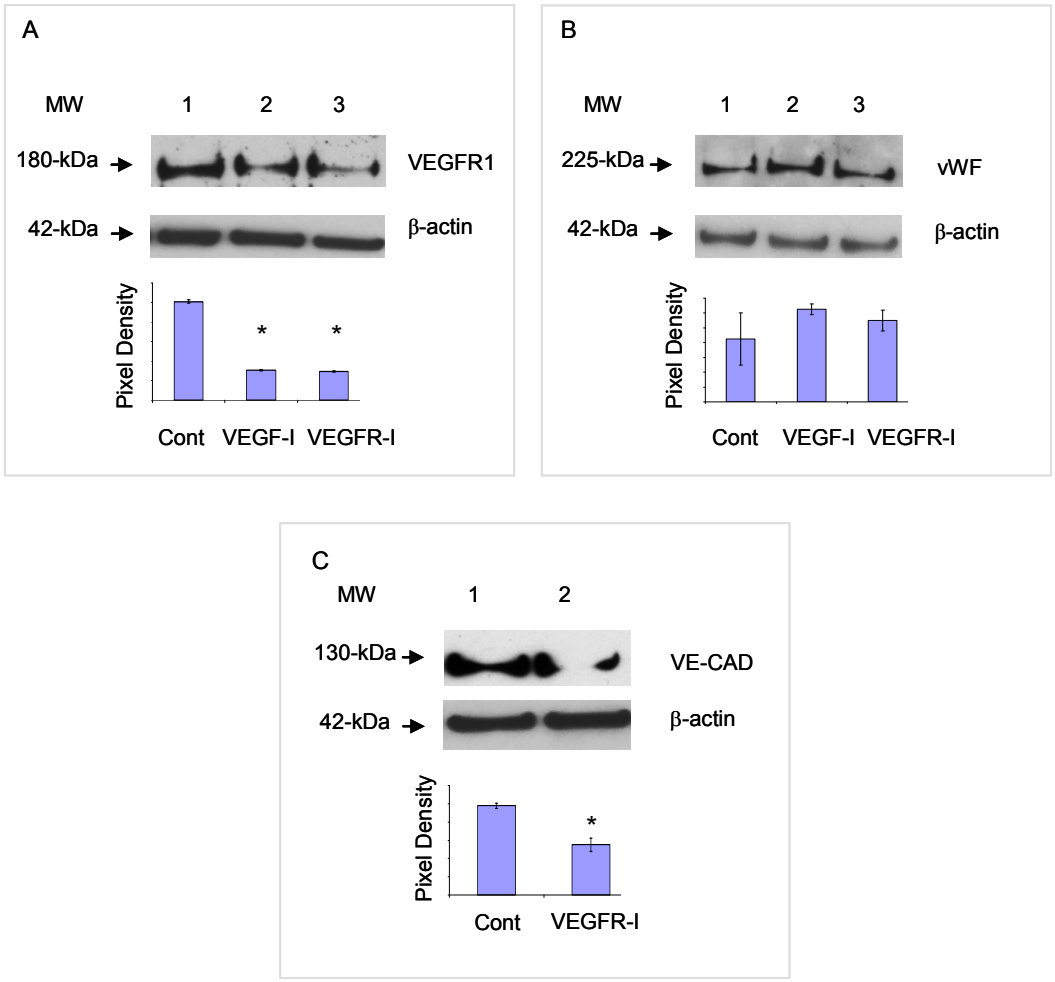

Figure 4.12. Sustained VEGF stimulation up-regulated EC markers

Immunoblot analysis of **(A)** VEGFR1, **(B)** vWF and **(C)** VE-cadherin expression by MSCs cultured at high density for 14 days, in the presence of 1 μg/ml VEGF neutralising antibody (VEGF-I) or 0.5 μM VEGFR tyrosine kinase inhibitor (VEGFR-I). Untreated MSCs were used as a control (cont). Membranes were re-probed with β-actin as loading controls. Pixel density was normalised to β-actin and plotted as a bar graph. * represent $p<0.05$ compared to untreated (cont) MSCs. A representative of two independent experiments is shown for each analysis.

VEGF-I alone (Figure 4.13, lane 3).Furthermore, when both inhibitors were removed and MSCs allowed to recover for 48 hours (Figure 4.13, lane 5) the level of VEGFR1 expressed by MSCs cultured a high density was restored to pre-inhibition levels (Figure 4.13, lane 4).

4.5.4. VEGF-A up-regulated PECAM-1 expression

As previously described, MSCs cultured at high density significantly upregulated PECAM-1 expression within 24 hours (see Results chapter 3, section 3.3.6). Experiments were therefore conducted to determine whether autocrine VEGF-A signalling regulated PECAM-1 expression by MSCs cultured at high density for 24 hours (Figure 4.14). When MSCs were cultured at high density for 24 hours in the presence of the VEGFR signalling inhibitor (VEGFR-I), immunoblot analysis revealed no change in PECAM-1 expression (Figure 4.14 (A); lane 2), compared to untreated MSCs. (Figure 4.14 (A); lane 1) However, when MSCs were cultured at high density for 24 hours in the presence of the VEGF neutralising antibody (VEGF-I), immunofluorescence analysis demonstrated a marked reduction in PECAM-1 immunopositivity (Figure 4.14 (D)) compared to control MSCs (Figure 4.14 (B)) or MSCs cultured in the presence of VEGFR-I (Figure 4.14 (C)). Thus, autocrine VEGF-A stimulated MSCs at high density to enhance PECAM-1 expression, but this stimulation was not mediated by VEGFR1.

4.5.5. MSCs at high density up-regulated PDGFR expression and signalling

Studies in this lab have previously shown that, in MSCs cultured in standard conditions which did not express VEGFRs, VEGF-A can signal through the PDGFRs (Ball *et al* ., 2007c). Immunoblot analysis of PDGFRα or PDGFRβ in MSCs cultured at either high or low density, in the presence of DAPT or DMSO, demonstrated that their expression (Figure 4.15 (A)) and phosphorylation status (Figure 4.15 (B)) increased at high density.

In these conditions, the level of PDGFRα expression was significantly up-regulated by

Figure 4.13

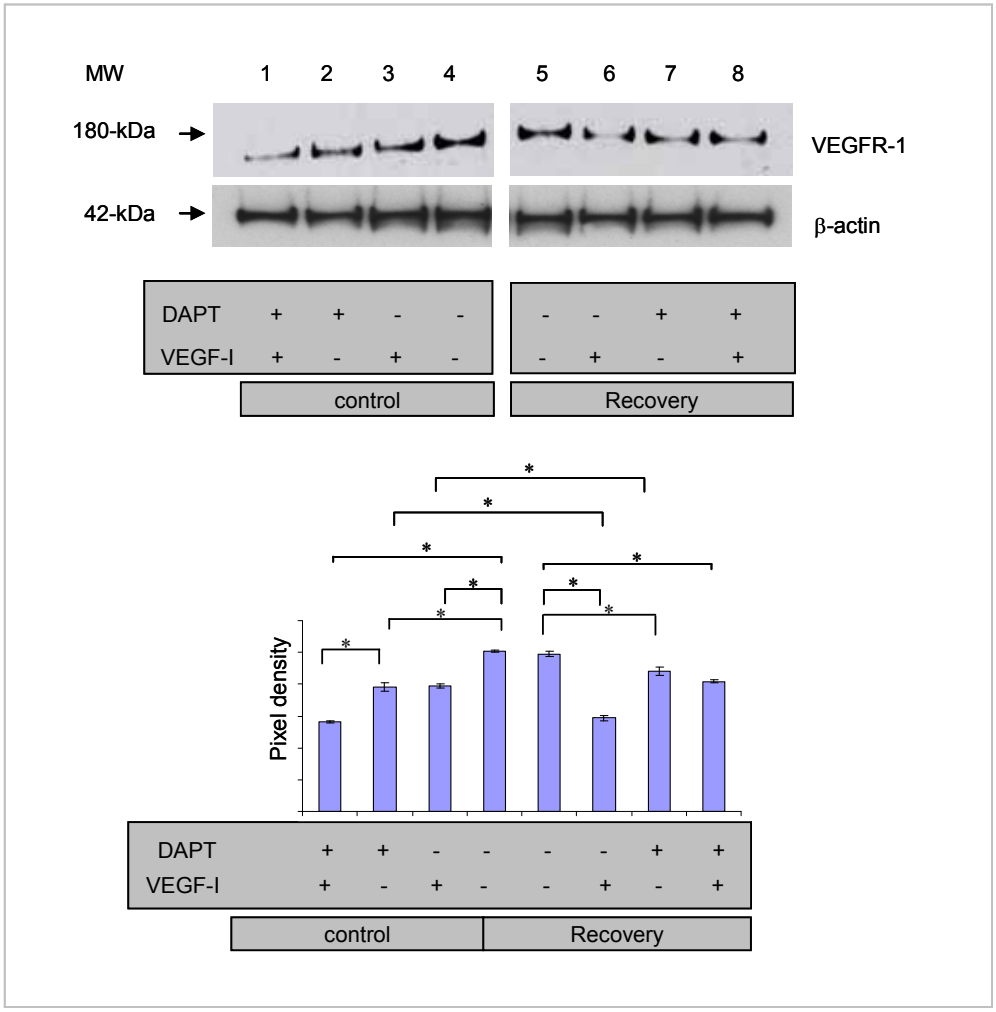

Figure 4.13. Notch and VEGF-A stimulated MSC differentiation to ECs over 14 days

To determine the effects of inhibiting both Notch and VEGF signalling pathways over 14 days, MSCs were cultured at high density for 14 days in the presence of both 50 μM DAPT and 1μg/ml VEGF neutralising antibody (VEGF-I). Lane 1, DAPT and VEGF-I; lane 2, DAPT alone; lane 3, VEGF-I alone; lane 4, without DAPT or VEGF-A. In addition, following culture of MSCs at high density for 14 days in the presence of inhibitors MSCs were washed twice then cultured for 48 hours in the presence of fresh inhibitors. Lane 5, MSCs cultured for 14 days with DAPT and VEGF-I then cultured for 48 hours with media alone; lane 6, MSCs cultured for 14 days with DAPT alone replaced with VEGF-I alone; lane 7, MSCs cultured for 14 days with VEGF-I alone replaced with DAPT alone; lane 8, MSCs cultured for 14 days in the absence of DAPT and VEGF-I replaced with DAPT and VEGF-I. Membranes were reprobed with β-actin as loading controls. Pixel density was normalised to β-actin and plotted as a bar graph. * represents $p<0.05$. Data are representative of two independent experiments.

Figure 4.14

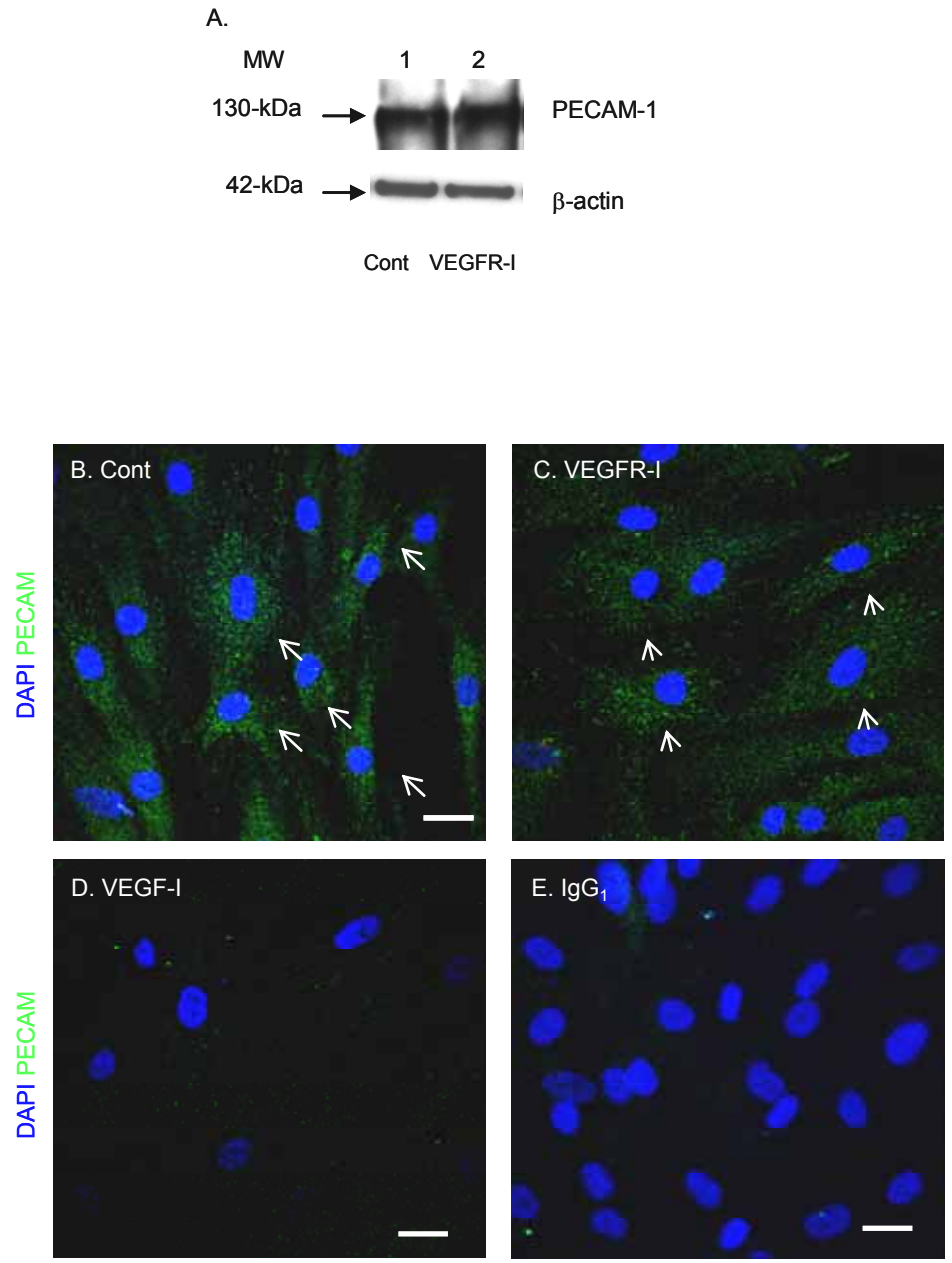

Figure 4.14. *VEGF-A up-regulated PECAM-1expression*

(A) Immunoprecipitation then immunoblot analysis of PECAM-1 expression in MSCs cultured at high density for 24 hours in the presence of 0.5μM VEGFR-I or untreated (Cont). Equal volumes of lysates were probed for β-actin and used as a loading control. **(B-E)** Immunofluorescence analysis of PECAM-1 in MSCs cultured at high density for 24 hours in the presence of 0.5μM VEGFR-I or 1μg/ml VEGF-I or untreated (cont). Twenty representative images of each analysis were taken using a Nikon upright C1 microscope (60× objective). DAPI = blue, PECAM-1 = green. Data represent two independent experiments. Arrows depict PECAM-1 immunopositivity. Scale bars = 7μm

Notch signalling inhibition, whilst the expression of PDGFRβ did not alter following DAPT treatment (Figure 4.15 (A)). Notch inhibition did not appear to decrease the level of PDGFR phosphorylation (Figure 4.15 (B)).

4.5.6. VEGF-A-PDGFR signalling up-regulated PECAM-1 expression

To determine whether VEGF-A mediated PDGFR signalling regulated PECAM-1 expression in MSCs cultured for 24 hours at high density, MSCs were cultured in the presence of a PDGFR receptor inhibitor (designated PDGFR-I) or VEGF-I for 24 hours (Figure 4.16). Control experiments were performed to demonstrate that PDGFR-I inhibited PDGFRβ phosphorylation in MSCs (Figure 4.21). Immunoblot analysis of MSCs cultured at high density in the presence of either PDGFR-I or VEGF-I, showed a decrease in PECAM-1 expression compared to control untreated MSCs (Figure 4.16 (A)). To determine whether VEGF-A mediated PDGFR signalling regulated PECAM-1 expression, immunofluorescence analysis of PECAM-1 expression was performed. MSCs cultured at high density for 24 hours in the presence of PDGFR-I (Figure 4.16 (C)), demonstrated loss of PECAM-1 immunostaining compared to untreated MSCs (Figure 4.16 (B)). The isotype IgG_1 control did not bind (Figure 4.16 (D)).

4.5.7. PDGFRα mediated PECAM-1 expression

To verify whether VEGF-A signalling through the PDGFRs regulated PECAM-1 expression, MSCs were cultured at high density in the presence of 10μg/ml PDGFR-α or PDGFRβ neutralisation antibodies (Figure 4.17). Control experiments were performed to demonstrate that the neutralisation antibodies blocked their target PDGFR phosphorylation in MSCs (Figure 4.21). Compared to untreated control MSCs (Figure 4.17 (A)), treatment with PDGFRα neutralisation antibody (Figure 4.17 (B)) resulted in loss of PECAM-1 immunoreactivity. In contrast however, PDGFRβ neutralisation had no effect on PECAM-1 immunoreactivity (Figure 4.17 (C)). Thus, PDGFRα mediated PECAM-1 expression during the first 24 hours of culturing MSCs at high density.

Figure 4.15

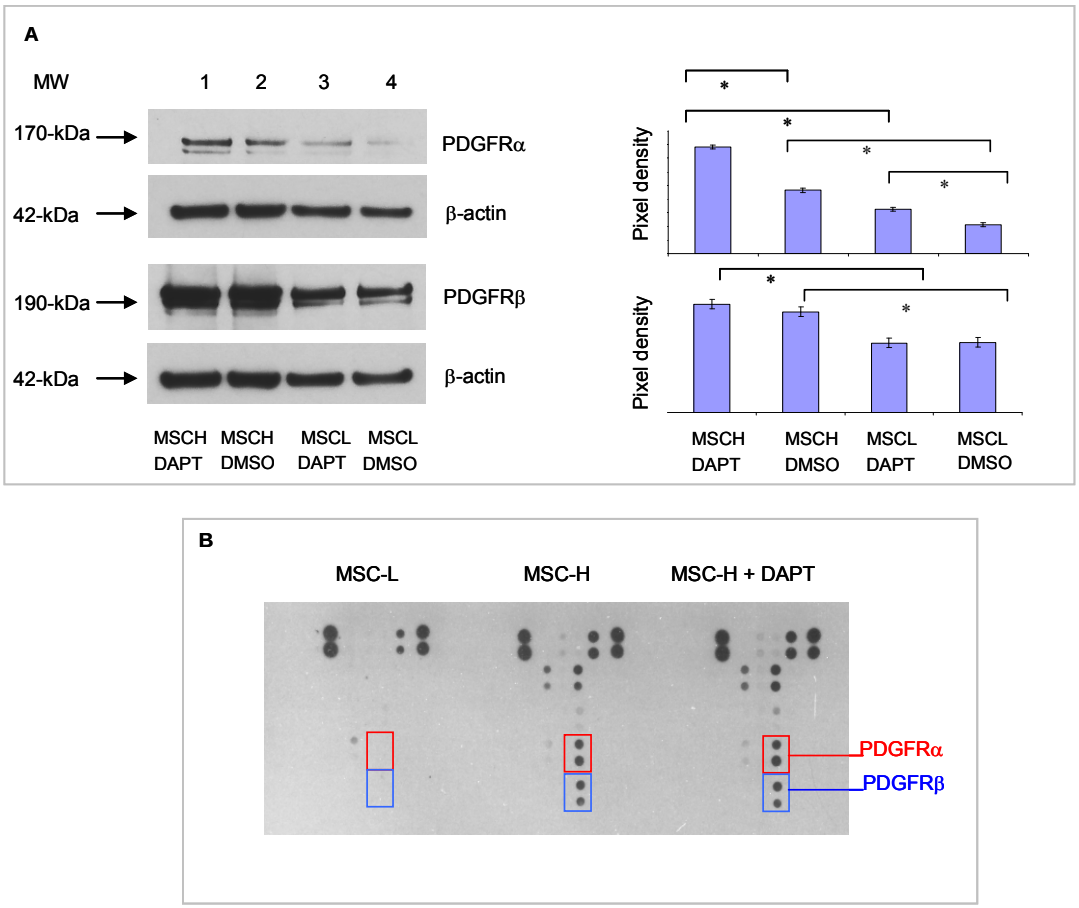

Figure 4.15. MSC at high density up-regulated PDGFR expression and signalling

(A) Immunoblot analysis of PDGFRα and β expression in MSCs cultured at high (MSC-H) or low (MSC-L) density in the presence of 50μM DAPT or DMSO. β-actin was used as a loading control. Pixel density was normalised to β-actin and plotted as a bar graph. * represents $p<0.05$.

(B) Receptor tyrosine kinase phosphorylation array (RTK) analysis using lysates derived from MSC-L or MSC-H cultured for 24 hours in the presence of DMSO or DAPT (MSC-H + DAPT). Data are representative of two independent experiments.

Figure 4.16

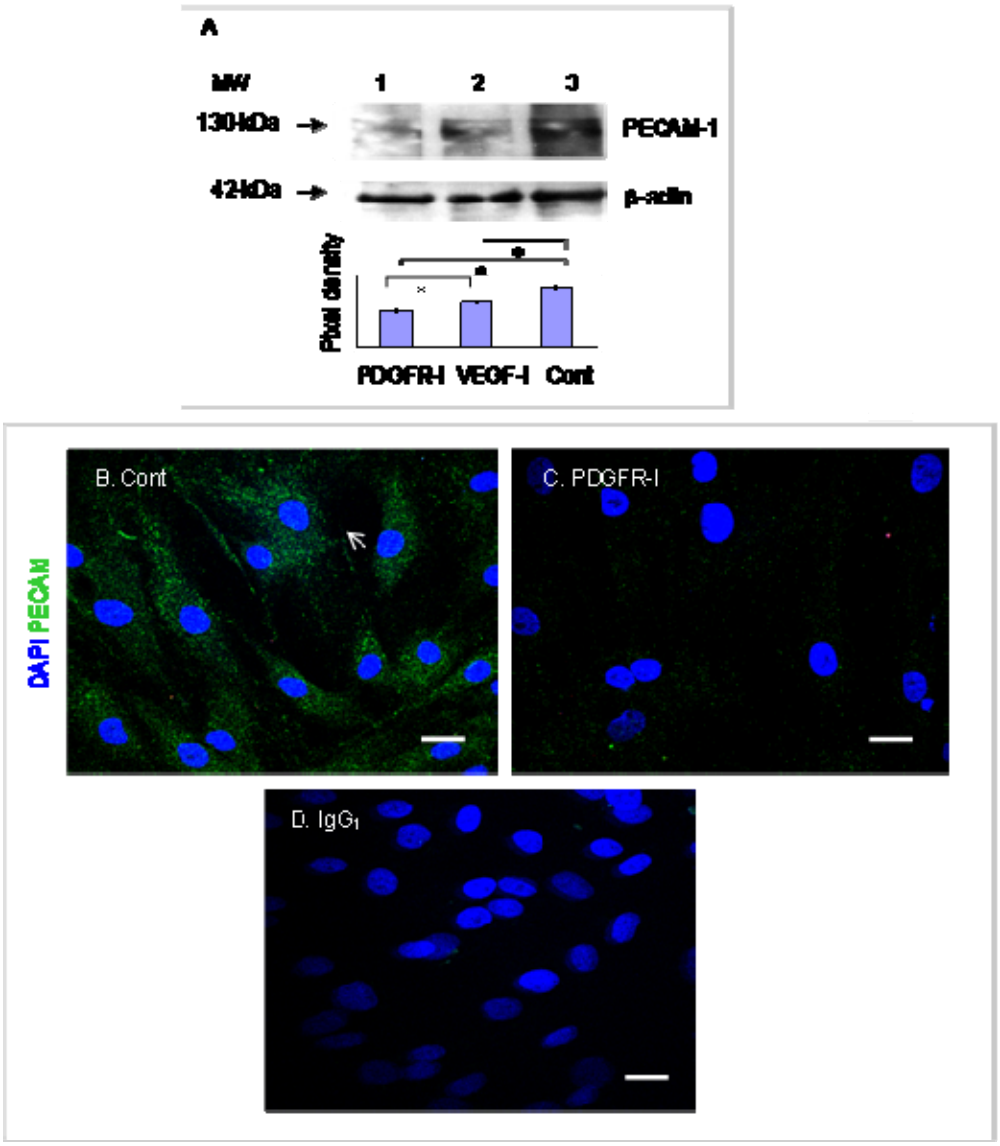

Figure 4.16. VEGF-A- PDGFR signalling up-regulated PECAM-1 expression

(A) Immunoprecipitation and Immunoblot analysis of PECAM-1 expression in MSCs cultured at high density for 24 hours in the presence of 1 µg/ml VEGF-I or 0.1 µM PDGFR-inhibitor (PDGFR-I) or untreated (Cont). Equal volumes of protein lysate was blotted for β-actin and used as loading controls for each analysis.

(B-D) Immunofluorescence analysis of PECAM-1 in MSCs cultured at high density for 24 hours in the presence of 0.1 µM PDGFR-I or untreated (cont). Twenty representative images of each analysis were taken using a Nikon upright C1 microscope 60× objective. DAPI = blue, PECAM-1 = green. Data are representative of two independent experiments. Arrows depict PECAM-1 immunopositivity. Scale bars = 7 µm

4.5.8. VEGF-A did not regulate Notch signalling

The close relationship between the Notch signalling pathway and the VEGF signalling pathway has been shown in a number of studies (Kearney *et al* ., 2002; Cameliet *et al*., 2009; Phng *et al* ., 2009; Boulton *et al* ., 2008b). As shown previously (Figure 4.8), Notch signalling inhibition with DAPT significantly inhibited VEGF-A autocrine secretion. In addition, previous studies have demonstrated that VEGF can regulate the expression of Notch signalling components (Kearney *et al* ., 2002; Cameliet *et al* ., 2009; Phng *et al* ., 2009; Boulton *et al* ., 2008b) (Chapter 4: Results; section 4.1).

To determine whether autocrine VEGF-A can regulate Notch signalling components in MSCs cultured at high density, MSCs were treated with VEGF-I for 48 hours and the expression of HES-1, Notch receptor 2, Notch receptor 3 and Jagged-1 determined by immunoblot analysis (Figure 4.18). However, treatment with VEGF-I (Figure 4.18; lane 2), had no significant difference in the expression of the Notch components, compared to MSCs cultured in the absence of VEGF-I (Figure 4.18; lane 1), Thus, autocrine VEGF-A stimulation was not a major mechanism regulating Notch signalling in MSCs cultured at high density.

4.6. Other possible mechanisms involved in density-dependent differentiation

This study has demonstrated how Notch signalling is a major determinant in initiating MSC commitment to ECs, whilst VEGF-A is essential to consolidate the EC fate. However other signalling mechanisms are also likely to play a role in regulating density-dependent MSC differentiation. RTK analysis which determines phosphorylation status of forty-two different RTKs, identified several RTKs which were significantly activated in cell lysates derived from MSCs cultured at high density (Figure 4.19). These RTKs which included hepatocyte growth factor receptor (HGFR), epidermal growth factor receptor (EGFR/ErbB-1/HER1)), EphA7, Insulin receptor, IGF receptor and Axl may also play a critical role in regulating cell density dependent differentiation towards ECs.

Figure 4.17

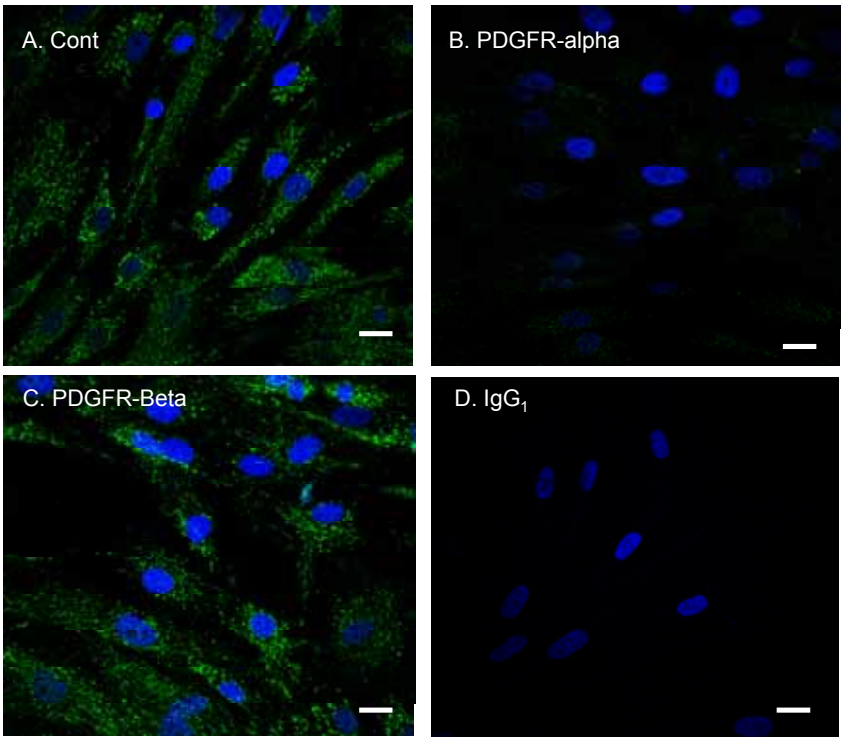

Figure 4.17. PDGFRα mediated PECAM-1 expression.

MSCs were incubated with **(B)** 10μg/ml anti PDGFRα or **(C)** anti-PDGFRβ neutralisation antibodies for 24 hours at 37^{o}C. **(A)** Untreated MSCs were used as a control (Cont). IgG_1 is shown as a control. Cells were immunostained for PECAM-1 = green, nuclei stained with DAPI = blue. Twenty representative images of each analysis were taken using a Nikon upright C1 microscope (60$\times$ objective). Scale bars = 7μm.

Figure 4.18

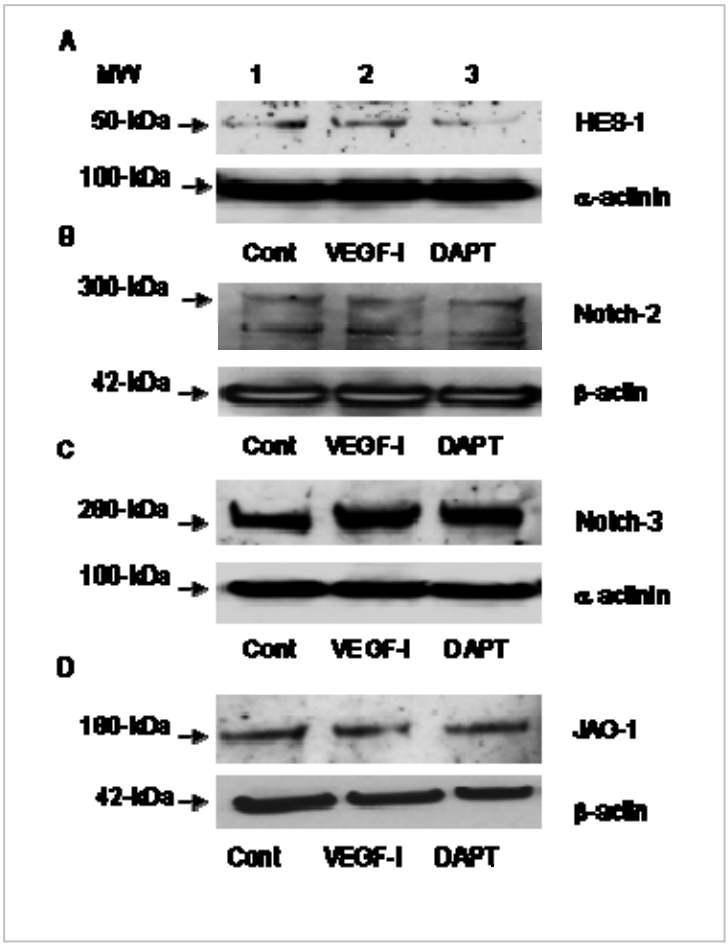

Figure 4.18. VEGF-A did not regulate Notch signalling

To determine whether VEGF-A regulates Notch signalling, immunoblot analysis was performed for the Notch components **(A)** HES-1, **(B)** Notch receptor 2 and **(C)** Notch receptor 3 and **(D)** the Notch ligand Jagged 1 (JAG-1) in MSCs cultured at high density for 24 hours in the presence of 1 μg/ml VEGF-I or 50 μM DAPT. Untreated MSCs at high density for 24 hours were used as controls (Cont). Membranes were reprobed with β-actin as loading controls. Data are representative of two independent experiments.

Figure 4.19

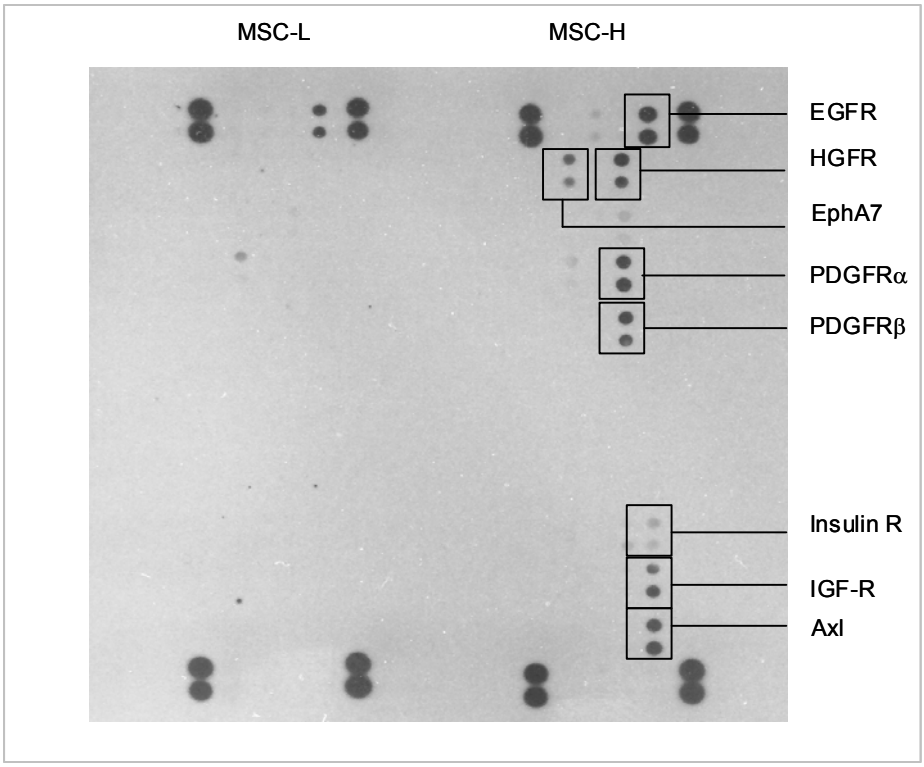

Figure 4.19. Involvement of other signalling mechanisms in density dependent differentiation

RTK phosphorylation array using lysates taken from MSCs cultured at low density (MSC-L) or high density (MSC-H) for 24 hours showing phosphorylation status of 42 different RTKs. Receptors showing a significant increase in phosphorylation during MSC culture at high density are highlighted, these include epidermal growth factor receptor (EGFR/ErbB-1/HER1)), hepatocyte growth factor receptor (HFGR) and insulin growth factor receptor (IGF-R). Data are representative of two independent experiments.

Figure 4.20

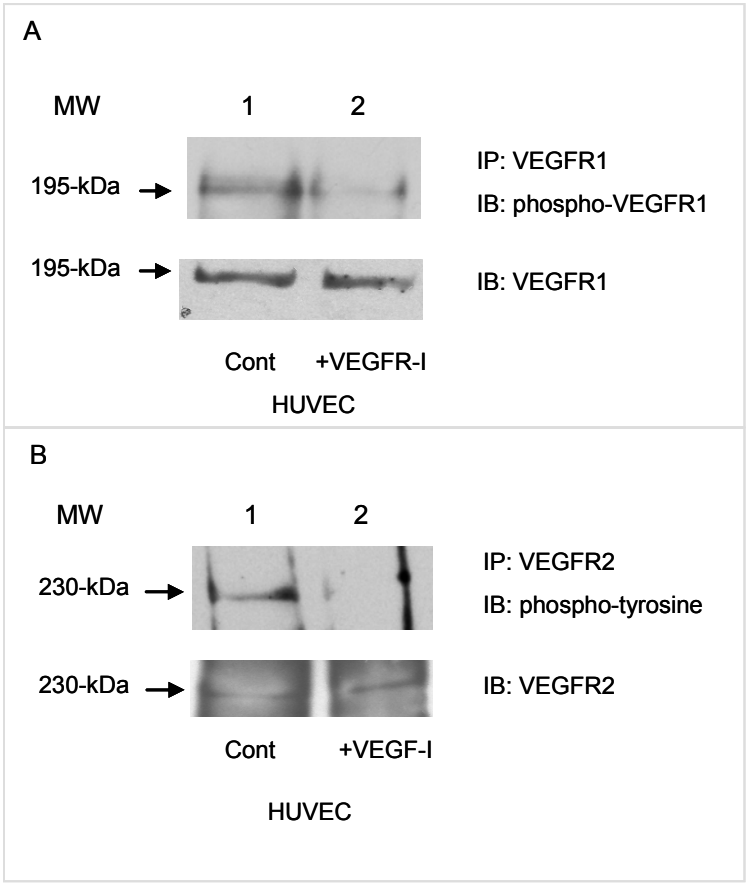

Figure 4.20. VEGFR signalling controls

(A) HUVECs were treated with 0.5 μM VEGF receptor tyrosine kinase inhibitor (KRN633) or were left untreated (Cont). VEGFR1 was isolated by immunoprecipitation using an anti-VEGFR1 antibody, and tyrosine phosphorylation was detected by immunoblot analysis using an anti-phosphoVEGFR1 antibody. Membranes were re-probed with an antibody to total VEGFR1 as a loading control. **(B)** HUVECs were treated with 1 μg/ml anti-VEGF neutralising antibody (+VEGF-I), or were left untreated (Cont), for 15 minutes in 0.5% serum DMEM, then cells stimulated with 50 ng/ml VEGF-A. VEGFR2 was isolated by immunoprecipitation using an anti-VEGFR2 antibody, and tyrosine phosphorylation detected by immunoblot analysis using an anti phosphotyrosine antibody. Membranes were re-probed with an antibody to total VEGFR2 for loading controls.

Figure 4.21

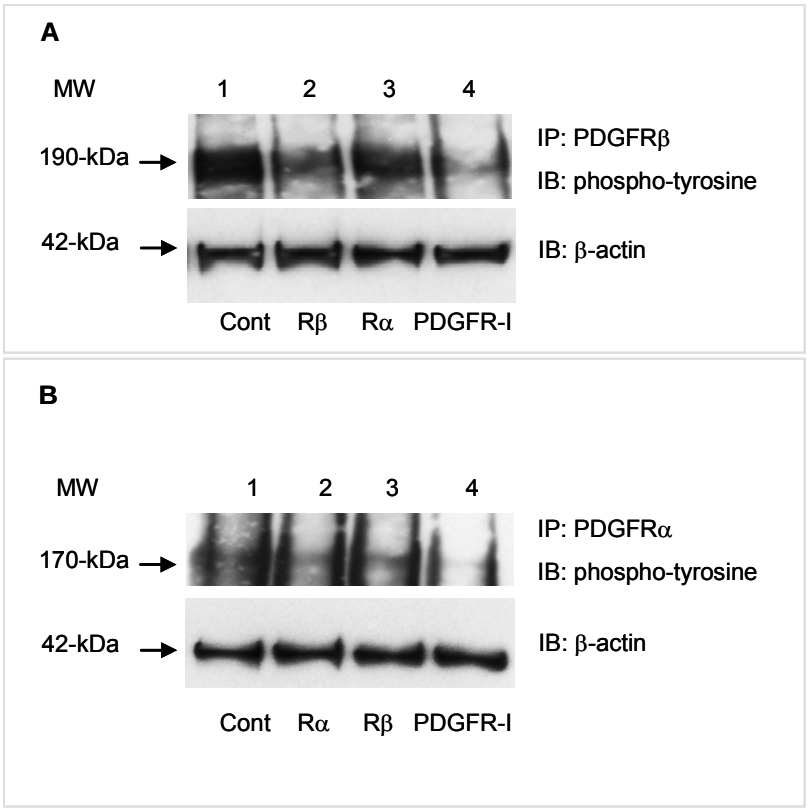

Figure 4.21. PDGFR signalling controls

MSCs cultured at high density were treated with 10μg/ml PDGFRα or PDGFRβ neutralisation antibodies or 0.1μM PDGFR-I for 48 hours, or were left untreated (cont). **(A)** PDGFRβ or **(B)** PDGFRα were isolated by immunoprecipitation using anti-PDGFRβ antibody or anti-PDGFRα antibodies, then tyrosine phosphorylation detected by immunoblot analysis using an anti phosphotyrosine antibody. Membranes were re-probed with β-actin for loading controls.

Figure 4.22

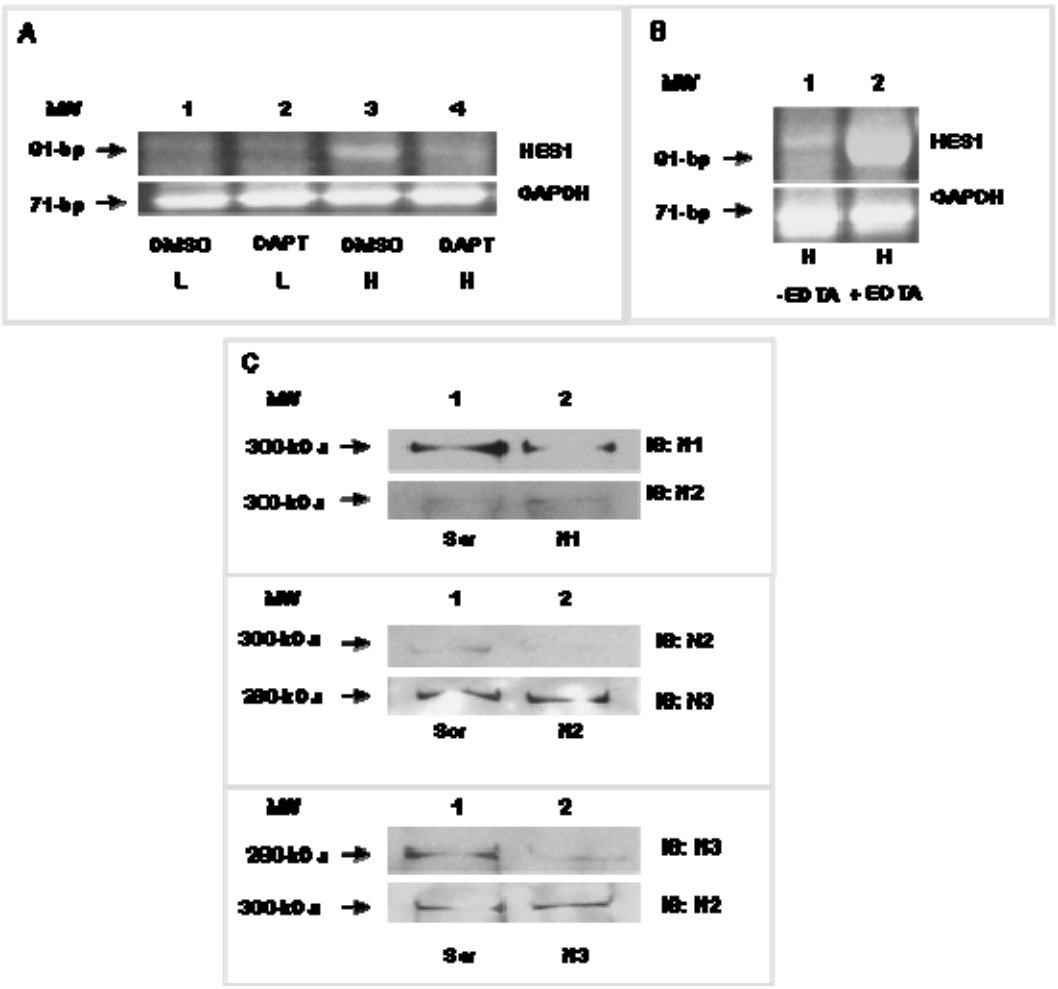

Figure 4.22. Notch signalling controls.

(A) As a control for DAPT treatment, HES1 transcript levels were determined by RT-PCR, following 50 μM DAPT treatment in MSCs cultured at low (L) or high density (H) for 24 hours. GAPDH was used as loading controls.

(B) As a control for EDTA treatment, HES1 transcript levels were determined by RT-PCR, following 5 mM EDTA treatment in MSCs cultured at high density (H) for 24 hours. GAPDH was used as loading controls.

(C) siRNA knockdown of Notch receptors. Immunoblot analysis of Notch1 (N1), Notch2 (N2) and Notch3 (N3) protein expression in MSCs which were cultured for 24 hours at high cell density, following transfection with 3 μg scrambled (scr) siRNA as controls (lanes 1, 3 and 5) or target siRNAs for Notch receptors 1, 2 or 3 (lanes 2, 4 and 6 respectively). Membranes were re-probed with an alternative Notch receptor as loading controls and to validate the specificity of each Notch receptor siRNA.

4.7. Discussion

Identifying the initial regulating mechanisms which direct MSC differentiation towards ECs, is fundamental to utilising MSCs in future therapeutic applications. In this study, the Notch signalling pathway was shown to be a primary mechanism in controlling the initial stages of directing MSCs to differentiate towards an EC fate.

Previous studies have reported that MSCs exposed to VEGF-A over 14 days, differentiate towards ECs (Chapter 4: Results; section 4.1). Consequently, exposure to VEGF-A was presumed to be the primary stimulus driving differentiation, even though in some cases the MSCs were shown to express no VEGFRs. (Oswald *et al* ., 2004; Chen *et al* ., 2009). In these studies, the MSCs were cultured at low cell density in the presence of VEGF-A, which resulted in EC markers only being detected after 7 days. As MSCs cultured for 7 days would be at high density by this time, VEGF exposure alone is therefore not the only mechanism involved in directing MSCs to differentiate towards ECs.

In this study, MSCs cultured at low density in the presence of VEGF-A for 24 hours did not express EC markers, whilst culture of MSCs at high density for 24 hours was sufficient to induce the expression of EC markers. Furthermore, analysis of MSCs cultured at high density for 24 hours following VEGF-A siRNA knockdown or neutralisation, revealed that VEGF-A did not control the initiation of VEGFR1 expression or up-regulation of vWF expression. Thus, VEGF-A was not sufficient to initiate the differentiation of MSCs to ECs. However, since VEGF-A has been shown to stimulate proliferation, VEGF-A may well play an important role in accelerating density-dependent differentiation.

Notch signalling was found to induce MSC cultured at high density to express VEGFR1. Previous studies have suggested that Notch signalling can alter expression levels of all three VEGF receptors (Suchting *et al ,* 2007; Harrington *et al ,* 2008). Two recent reports suggest that VEGFR1 expression may be increased by Notch signalling.

(Suchting *et al ,* 2007; Harrington *et al ,* 2008). The Notch target gene Hey1 has been shown to downregulate VEGFR2 (Holderfield *et al* ., 2006; Taylor *et al ,* 2002) suggesting that Notch can provide negative feedback to reduce the activity of the VEGF/VEGFR system. In addition, studies in several systems, established that VEGF regulates the expression of Notch signalling components (Thurston *et al* ., 2008; Patel *et al* ., 2005; Hainaud *et al* ., 2006; Ridgway *et al* ., 2006). Here, Notch-dependent VEGF-A secretion was found to induce VE-cadherin expression through VEGFR1 signalling and stimulated PECAM-1 expression through PDGFR-α signalling. Thus, whilst VEGF-A is not sufficient to induce MSC differentiation to ECs, VEGF-A is essential to consolidate the EC fate. VEGF-A has previously been demonstrated to induce VE-cadherin expression, which is considered to be a late EC differentiation marker, in rat placental trophoblasts (Nikolova-Krstevski *et al* ., 2008; Chang *et al* ., 2005), however it is unreported whether VEGF acting through VEGFR1 mediated the induction in this system. Thus, a complex relationship exists between the signalling mediated by Notch, VEGFR1, PDGFRα and VEGF-A which control EC specification (Jakobsson *et al* ., 2009; Kearney *et al* ., 2002; Carmeliet *et al* ., 2009; Phng *et al* ., 2009; Boulton *et al* ., 2008b).

As previously mentioned, the results indicated that VEGF-A signalling through PDGFRα in MSCs cultured at high density stimulated PECAM-1 expression. In MSCs which expressed no VEGFRs, VEGF-A has been shown to signal through both PDGFRs (Ball *et al* ., 2007c). In MSCs at high density which express low levels of surface VEGFR1, VEGF-A may thus signal through both VEGFR and PDGFR systems. PDGFR signalling plays a predominant role in regulating the vSMC phenotype and function (Owens 1995) and regulating the SMC characteristics of MSCs (Ball *et al*., 2007a; 2010b; Kinner *et al*., 2002). Furthermore, studies have shown that PDGFRα signalling mediated by a RhoA and Rho-associated kinase dependent mechanism, enhanced αSMA filament polymerisation (Ball *et al* ., 2007b). In addition, mechanical stress shown to increase PDGFRα signalling in SMCs, induced MSCs to express enhanced SMC markers, suggesting a differentiation to a SMC phenotype (Hu *et al* ., 1998). Interestingly Notch

signalling has been shown to regulate PDGFR signalling in vSMCs, with activation of either Notch 1 or Notch 3 up-regulating PDGFRβ, but down-regulating PDGFRα expression (Jin ., 2008) In this study, whilst the expression of PDGFRα was down-regulated in response to Notch activation, signalling of both PDGFRs on MSCs increased with high density culture and were not affected by DAPT treatment. It is probable that whilst PDGFRα signalling mediates SMC differentiation in MSCs which lack VEGFRs, PDGFRα signalling acting in concert with VEGFR1 signalling, may contribute to determining an EC fate, by decreasing the SMC signalling pathways. Thus, these two crucial signalling systems are intricately linked in MSC fate determination.

The localisation of Notch receptors in MSCs cultured at high density during the first 24 hours showed that Notch receptor 2 was predominantly localised to the nucleus, reflecting active Notch signalling. In comparison, Notch receptor 1 was largely localised to the cell periphery while Notch receptor 3 was mainly localised to the Golgi apparatus with only a small proportion detected in the nucleus indicating a low level of active Notch signalling. This result may be explored further by confirming the distribution by western blot of cellular fractions (nuclear, cytoplasms and membrane bound). Previous studies have shown that Notch receptor proteins display a selective cellular and tissue distribution. In the vasculature, ECs express all four Notch receptors but Notch receptor 4 displays an almost exclusively endothelial expression pattern, whereas Notch receptors 1-3 are expressed more ubiquitously (Uyttendaela *et al* ., 1996; Quillard *et al* ., 2009). While Notch receptor is predominantly expressed by vascular ECs, prominent in both arteries and veins, the expression of Notch receptor 2 has also been reported in pulmonary endothelium (Villa *et al* ., 2001). Notch receptor 3 is primarily expressed in adult arterial vSMCs (Mumm *et al* ., 2000).The localisation of Notch receptors correlates with siRNA knockdown of the individual receptors showing Notch receptors 1 and 2 to be key in regulating both VEGFR1 and vWF expression, whilst Notch receptor 3 did not have any detectable effect on vWF protein expression. All three Notch receptors regulated VEGFR1 expression which may suggest that each Notch receptor has an essential non-redundant function in regulating MSC commitment towards ECs. The

ability of more than one Notch receptor to regulate the same event has previously been documented in vascular smooth muscle cells where both Notch 1 and 3 regulate cell growth, apoptosis and migration (Sweeney et al., 2004). However, the thresholds of detection may be misleading in this case as the Notch receptor expression is low in the scrambled control, thus each knockdown may only have a partial effect on VEGFR1 levels.

Recently, Notch signalling has been shown to be important in regulating chondrogenesis in human BM stromal cells during 3D cell aggregate culture (Oldershaw *et al* ., 2008). Expression analysis of Notch signalling components demonstrated a sharp increase in Jagged-1 and HEY-1 expression during the initial stages of aggregate culture, followed by a decline in expression with time. Attenuation of Notch signalling was critical for the MSCs to complete chondrogenesis, since continuous elevated expression of Jagged-1, by adenoviral transduction, completely blocked chondrogenesis. There are interesting parallels between culturing BM-derived stromal cells in 3D aggregates and density dependent differentiation of MSCs to ECs, however, there are also distinct differences. One such difference is the use of defined chemicals to induce chondrogenesis in aggregate culture and subsequent suspension culture of aggregates. Moreover, the surface area in contact and the degree of hypoxia elicited in aggregate culture all reflect important differences from density-dependent differentiation of MSCs to ECs.

This study demonstrated that Notch signalling in MSCs cultured at high density was most critical during the first 24 hours, when VEGFR1 was induced and vWF and PECAM-1 expression were significantly enhanced. This up-regulation in EC markers correlated with high expression levels of Notch receptors and Jagged-1 and HES-1 transcripts. These Notch signalling components decreased with time, similar to their expression pattern in 3D aggregate cultures during chondrogenesis. However, VE-cadherin expression was only induced after 7 days of high density culture. Furthermore, when MSCs cultured at high density were sub-cultured at low density, the expression of both vWF and VEGFR1 was retained (see Results chapter 3, section 3.4.1) suggesting

that sustained Notch signalling was not necessary for maintaining differentiation and consolidating the EC phenotype. Interestingly, Notch signalling inhibition by DAPT in MSCs cultured at high density for 14 days resulted in a significant decrease in both VEGFR1 and VE-cadherin expression, but this may well be an indirect effect resulting from the decrease in Notch regulated VEGF-A secretion and autocrine stimulation. This was further reflected when DAPT inhibition was removed, resulting in restoration of VEGFR1 expression. It would be interesting to determine whether sustained Notch activation could prevent differentiation of MSCs to ECs, similar to that determined in 3D aggregate cultures of BM-derived stromal cells during differentiation to chondrocytes.

Due to their pluripotency, numerous studies have shown that ESCs can readily be induced to differentiate to ECs (Levenberg *et al* ., 2002; McCloskey *et al* ., 2006; Nikolova-Krstevski *et al* ., 2008; Yamamoto *et al*., 2005; Zeng *et al* ., 2006). Mechanisms which have been identified to control ESC differentiation to ECs, may also be involved in regulating MSC differentiation to ECs. In this respect, laminar flow was shown to enhance ESC proliferation and differentiation towards ECs by stabilising and activating histone deacetylase 3 (Zeng *et al* ., 2006). Interestingly, a similar signalling pathway was also detected during VEGF–induced ESC differentiation to ECs (Zeng *et al* ., 2006). histone deacetylase 3 is also involved in epigenetic modification of the chromatin to regulate gene transcription, which is essential for modulation of EC marker gene expression and has been shown to modulate EC marker gene expression (Zeng *et al* ., 2006; Yamamoto *et al* ., 2005), however whether histone deacetylase 3 is activated in MSCs following VEGF-A stimulation remains to be determined.

MSCs cultured at high density activated a number of different RTKs. Notably, high density MSC culture significantly increased the phosphorylation status of both PDGFRα and PDGFRβ, EGFR, EphA7, Axl and the insulin receptor. VEGF-A_{165} stimulation of MSCs has previously been shown to induce a similar complement of RTKs including tyrosine PDGFRs, EGFR, EphA7, and Axl, (Ball *et al* ., 2007c) and these receptors are therefore likely to have key roles in density dependent differentiation of MSCs to ECs. Density dependent differentiation phosphorylation of EGF receptor may also be a

secondary consequence of VEGF or Notch stimulation and may play an important role during MSC differentiation since EGF receptor signalling has recently been documented to reversibly prevent multilineage differentiation in BM-derived MSCs, indicating that the EGF receptor may control lineage commitment (Bobis *et al* ., 2006; Krampera *et al*., 2005). The insulin receptor has been reported to play an important function during chondrogenesis aggregate culture, with insulin-like growth factor-1 modulating MSC chondrogenesis by stimulating proliferation, regulating cell apoptosis and inducing expression of chondrocyte markers (Longobardi *et al*., 2006). Since there are clear parallels between MSCs cultured in 3D aggregate culture to induce chondrogenesis and MSCs cultured at high density to induce differentiation to ECs, it would be interesting to determine whether the insulin receptors play a key role in this study.

Here, Notch signalling activated in MSCs cultured at high cell density was a critical step in initiating differentiation to ECs. These mechanistic insights further our understanding of how MSCs differentiation is regulated and provide the basis for therapeutic manipulation during postnatal vasculogenesis events and in tissue engineering applications. The next chapter therefore focuses on the response of MSCs cultured at high density to pro-angiogenic environments.

4.8. Summary.

- MSCs cultured at high density for 24 hours expressed VEGFR1, vWF and PECAM
- MSCs expressed Notch receptors 1, 2 and 3
- Notch signalling up-regulated VEGFR1, vWF and VEGF-A expression within 24 hours.
- VEGF-A stimulation did not modulate VEGFR1 or vWF expression within 24 hours.
- Notch receptors 1, 2 and 3 regulated VEGFR1 and vWF expression
- Activation of Notch signalling alone was sufficient to induce EC markers in MSCs at low density.
- Notch dependent VEGF-A signalling mediated by PDGFRα, regulated PECAM-1 expression.
- Notch dependent VEGF-A signalling regulated the expression of VEGFR1 over 14 days.
- Notch dependent VEGF-A signalling mediated by VEGFR1 induced VE-cadherin expression.

CHAPTER 5

RESULTS

Behaviour of endothelialised MSCs in pro-angiogenic environments

CHAPTER 5: RESULTS

5.1. Behaviour of Endothelialised MSCs in angiogenic environments.

To understand the mechanisms regulating the differentiation of stem cells, it is critical to consider the surrounding environment. Most of our knowledge of MSC biology is derived from *in vitro* culture studies that are often highly contrived to favour MSC culture expansion or differentiation events. It has been suggested that ECs derived from *in vitro* differentiated stem cells may lack complete functional maturation (McCloskey *et al* ., 2006). In comparison to normal mature adult ECs, ESC derived ECs expressed lower levels of PECAM-1 and VE-cadherin and significantly lower levels of ac-LDL uptake and vWF expression. In addition, although ESC derived ECs expressed VE-cadherin, it did not localise to the cell-cell junctions, similar to the findings in this study (see Chapter 3 Results, section 3.3.52).

Thus, any conclusions drawn from *in vitro* studies regarding MSC differentiation capacity or therapeutic potential for cell transplantation therapy must therefore be validated by *in vivo* studies; which requires model systems for MSC transplantation that are permissive for both engraftment and differentiation.

As previously discussed, the MSC microenvironment has a critical role in modulating MSC behaviour and function. Within a specific MSC niche, a dynamic complement of microenvironmental factors such as mechanical cues, soluble factors and cell-matrix and cell-cell interactions will contribute to regulating MSC differentiation, and will also modulate MSC signalling to the surrounding environment (Butler *et al* ., 2010; Edelberg *et al*., 2008; Kuhn *et al* ., 2009; Moore *et al* ., 2006; Scadden *et al*, 2006). In this respect, the vascular niche of small calibre arteries and veins not only permits the delivery of essential nutrients and oxygen, but also functions to provide angiogenic factors, or direct EC-MSC interactions which may instructively regulate MSC differentiation, initiate MSC mobilisation and facilitate tissue regeneration (Abedin *et al* ., 2004; Huang *et al* ., 2008; Jakobsson *et al* ., 2007; Sales *et al* ., 2005; Riha *et al* ., 2005). Furthermore, MSCs can

secrete paracrine factors such as VEGF-A, which can act to regulate EC growth and sprouting (Sorrell *et al*., 2009).

Previous studies have shown that MSCs can be differentiated into ECs *in vitro* (see Introduction). This study has shown that MSC-to-EC *in vitro* differentiation is strongly regulated by cell density and initiated and consolidated by Notch and VEGF-A, respectively (see Chapter 3:Results; Chapter 4:Results). In addition, MSCs cultured at high density in three dimensional Matrigel culture, a basement membrane extract derived from the Engelbreth-Holm-Swarm mouse tumour on which MSCs spontaneously form networks, were shown to exhibit significantly enhanced networks and branch points (see Chapter 3: Results; Chapter 4: Results). While a range of two-dimensional and three-dimensional environments have been investigated for the manipulation of MSC differentiation pathways *in vitro,* three-dimensional environments have been shown to profoundly influence EC growth and differentiation (Baatout *et al*, 1997; Kleinman *et al* ., 2005; O'Cearbhaill *et al*., 2010).

In this chapter, MSCs that had been pre-cultured at high density for 28 days (endothelialised MSCs) were cultured within three-dimensional Matrigel and the effects on MSC differentiation and maturation to ECs determined. In addition, the response of endothelialised MSCs within the chick chorioallantoic membrane (CAM), a highly vascularised membrane produced by fusion of the allantois and the chorion, a commonly used angiogenesis assay (Ribatti *et al* ., 2006; Storgard *et al* ., 2005) was evaluated. Furthermore, endothelialised MSCs were monitored for integration into the functional host vasculature, as well as determining potential effects on blood vessel growth.

5.2. Effects of *in vitro* Matrigel culture on MSC differentiation to ECs.

5.2.1. Endothelialised MSCs enhanced VE-cadherin in Matrigel

This study has previously shown that MSCs cultured at high density form enhanced networks in Matrigel (Chapter 3: Results section 3.3.7.2). Since three dimensional

culture has been reported to promote EC differentiation (Baatout *et al* ., 1996), MSCs that had been pre-cultured at high density for 28 days (endothelialised MSCs) were cultured in three dimensions using Matrigel, and the effects on differentiation towards ECs evaluated by determining VE-cadherin expression.

Immunofluorescence analysis revealed endothelialised MSCs in Matrigel exhibited enhanced VE-cadherin expression compared with MSCs pre-cultured in standard conditions (Figure 5.1 (A)). Furthermore, immunoblot analysis of endothelialised MSCs cultured in Matrigel demonstrated a significant increase in VE-cadherin expression (Figure 5.1 (B)) compared to the same endothelialised MSCs cultured on tissue culture plastic.

5.2.2. Endothelialised MSCs potentially expressed VEGFR2 in Matrigel

VE-cadherin is known to form a complex with β-catenin, phosphoinositide-3-OH kinase and VEGFR2 in response to VEGF-A induced survival signals (Carmeliet *et al* ., 1999). In addition, VE-cadherin has been shown to regulate VEGFR2 internalisation and signaling from intracellular compartments (Lampugnani *et al*., 2006). Conversely, VEGF-A stimulated VEGFR2 signalling has been shown to regulate VE-cadherin internalisation (Gavard *et al*., 2006; Wallez *et al*., 2007; Lampugnani *et al* ., 2006). Thus the signalling pathways mediated by VE-cadherin and VEGFR2 are intricately linked in ECs. Since three dimensional Matrigel culture of endothelialised MSCs increased their expression of VE-cadherin, the effects of Matrigel culture on VEGFR2 expression was also examined.

Immunofluorescence analysis demonstrated that endothelialised MSCs in Matrigel displayed potential positive VEGFR2 immunoreactivity, whereas MSCs pre-cultured in standard conditions exhibited no detectable VEGFR2 immunoreactivity (Figure 5.2 (A)). To confirm that Matrigel induced endothelialised MSCs to express VEGFR2, immunoblot analysis was performed. Using HUVECs cultured on tissue culture plastic as a positive control, a double band was detected at 220-kDa which correlated to the anticipated size

Figure 5.1

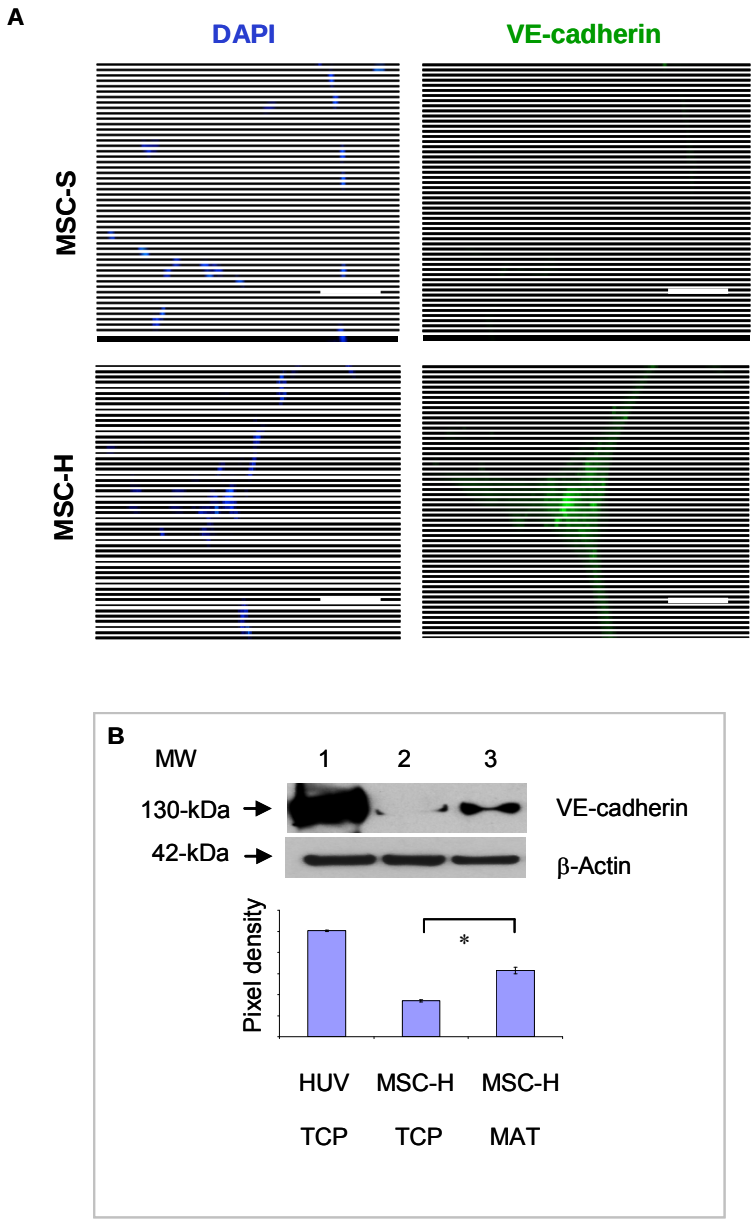

Figure 5.1. *Endotheliallised MSCs enhanced VE-cadherin in Matrigel*

To determine whether an *in vitro* three-dimensional culture environment influenced MSC differentiation to ECs, either 20,000 HUVECs as a control, standard cultured MSCs (MSC-S) or endothelialised MSCs (MSC-H) were seeded onto growth factor reduced Matrigel (MAT), or on tissue culture plastic (TCP), in 0.5% serum DMEM for 48 hours. **(A)** Immunofluorescence analysis of VE-cadherin expression in Matrigel. Widefield images using 20× objective. Scale bars= 200μm. DAPI (blue), VE-cadherin (green) **(B)** Immunoblot analysis of VE-cadherin protein levels in lane 1, HUVECs; lane 2, MSC-H cultured on TCP; lane 3, MSC-H cultured on Matrigel. * represents $p<0.05$ compared to endothelialised MSCs cultured on TCP.

of VEGFR2 (Figure 5.2 (B); lane 1). In comparison, this double band was not detected in endothelialised MSCs cultured on tissue culture plastic (Figure 5.2 (B); lane 2), demonstrating that Matrigel induced endothelialised MSCs to potentially express VEGFR2.

5.2.3. Endothelialised MSCs decreased PECAM-1 in Matrigel

To further examine the effects of Matrigel on influencing endothelial MSC differentiation, the expression of PECAM-1 was also evaluated. Immunofluorescence analysis of endothelialised MSCs in Matrigel displayed increased PECAM-1 immunoreactivity, compared to MSCs pre-cultured in standard conditions (Figure 5.3 (A)). Interestingly, immunoblot analysis of endothelialised MSCs cultured in Matrigel demonstrated a significant decrease in PECAM-1 expression (Figure 5.3 (B)), compared to when the same endothelialised MSCs were cultured on tissue culture plastic. RTK phosphorylation array analysis of endothelialised MSCs cultured of tissue culture plastic or Matrigel, demonstrated a significant decrease in PDGFRα and PDGFRβ phosphorylation levels as well as the epidermal growth factor receptor (EGFR/ErbB-1/HER1) and EphA7 (Figure 5.3 (C)). In this respect, previous studies have demonstrated that PECAM-1 can be downregulated during angiogenesis (Romero *et al*., 1997; Berger *et al* ., 1993; Delisser *et al* ., 1997).

Having established that an *in vitro* three-dimensional Matrigel environment promoted endothelialised MSCs to form increased network assemblies, enhanced VE-cadherin expression and induced VEGFR2 expression, the effects of an *in ovo* environment was next evaluated.

5.3. Effect of *in ovo* Matrigel culture on MSC differentiation to ECs

Figure 5.2

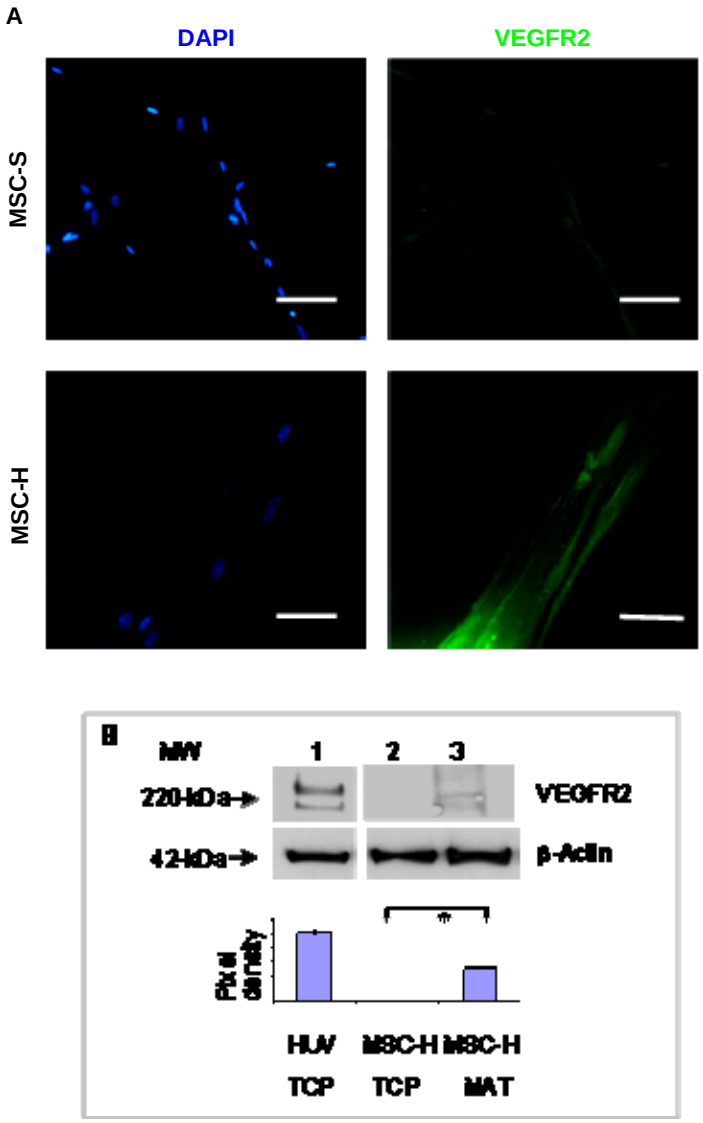

Figure 5.2. *Endothelialised MSCs potentially expressed VEGFR2 in Matrigel*

MSCs pre-cultured in standard conditions (MSC-S) or endothelialised MSCs (MSC-H) were seeded onto growth factor reduced Matrigel for 48 hours. **(A)** Immunofluorescence analysis of VEGFR2 expression taken using an Olympus BX51 widefield microscope 20× objective. Scale bars represent 200 μm. **(B)** Immunoprecipitation then immunoblot analysis of VEGFR2 protein levels in MSC-H cultured in HUVECs (HUV) as controls (lane 1); MSC-H cultured on tissue culture plastic (TCP) (lane 2); MSC-H cultured on Matrigel (MAT) (lane 3). * represents $p<0.05$ compared to endothelialised MSCs cultured on TCP. For VEGFR2, equal volumes of protein lysate was blotted for β-actin and used as loading controls for each analysis. A representative of two independent experiments is shown in each case.

Figure 5.3

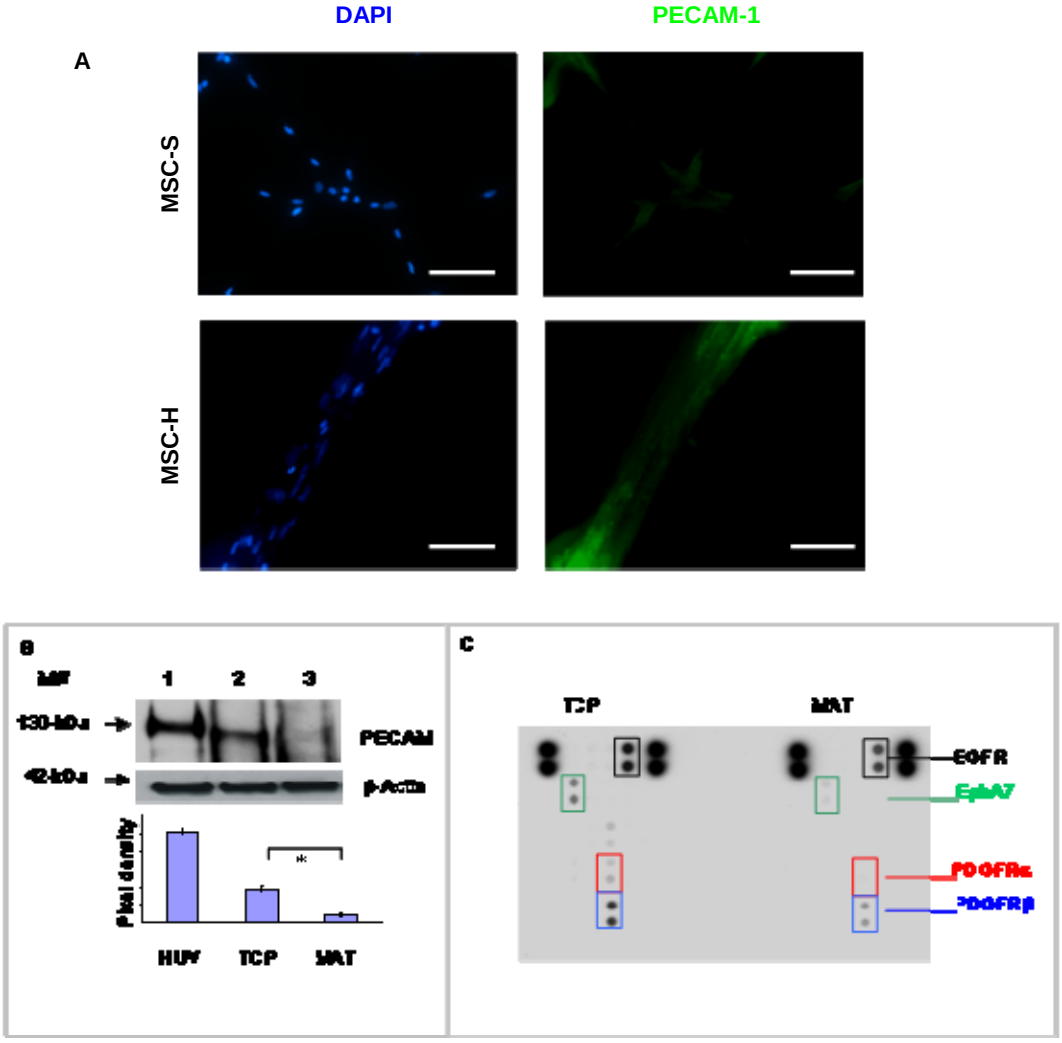

Figure 5.3. *Endothelialised MSCs decreased PECAM-1 expression in Matrigel*

MSCs pre-cultured in standard conditions (MSC-S) or endothelialised MSCs (MSC-H) were seeded onto growth factor reduced Matrigel for 48 hours. **(A)** Immunofluorescence analysis of PECAM-1. Widefield images using 20× objective. Scale bars represent 200μm. **(B)** Immunoprecipitation then Immunoblot analysis of PECAM-1 protein levels in HUVECs as controls (lane 1); endothelialised MSCs (MSC-H) cultured on tissue culture plastic, TCP (lane 2); endothelialised MSCs cultured on Matrigel, MAT (lane 3). * represents $p<0.05$ compared to endothelialised MSCs cultured on TCP. For PECAM-1, equal volumes of protein lysate was blotted for β-actin and used as loading controls for each analysis **(C)** RTK phosphorylation array analysis using lysates derived from endothelialised MSCs cultured on TCP or on Matrigel. Coloured boxes indicate RTK receptor displaying a difference between conditions. EGFR=epidermal growth factor receptor. A representative of two independent experiments is shown in each case.

5.3.1. Endothelialised MSCs formed enhanced networks within the CAM

Immunofluorescence analysis of coverslips that had been removed from the chick CAM revealed that endothelialised MSCs formed enhanced networks on Matrigel, compared to MSCs pre-cultured in standard conditions (Figures 5.4, 5.5). In these analyses, MSC were labelled with DiI to distinguish implanted MSCs from endogenous chick cells. These enhanced networks displayed a marked increase in immunoreactivity for the EC markers vWF (Figure 5.4), VE-cadherin (Figure 5.5), PECAM-1 (Figure 5.7) and VEGFR2 (Figure 5.8) which were all widely distributed throughout the networks. In addition VE-cadherin became localised at the cell surface (Figure 5.6).

5.3.2. Endothelialised MSCs promoted CAM vascularisation

It is widely acknowledged that MSCs release a number of angiogenic ligands and cytokines (Chen *et al* ., 2008; Beckermann *et al* ., 2008; Burchfield *et al* ., 2008). Increasing evidence suggests that an important mechanism of action by which MSCs provide tissue protection and repair, is the release of paracrine factors which have the potential to stimulate neovascularisation and blood vessel growth (Beckermann *et al* ., 2008; Chen *et al* ., 2008; Greenberg *et al* ., 2008). Furthermore, in this study (Chapter 3: Results, section 3.3.3), it was established that high density culture stimulated the secretion of the angiogenic growth factor VEGF-A in MSCs.

To determine whether endothelialised MSCs induced a pro-angiogenic effect of the chick CAM vasculature, the size and length of the underlying CAM blood vessels were examined (Figure 5.9). CAMs which had not been exposed to implanted cells or exposed to implanted HUVECs or MSCs pre-cultured in standard conditions exhibited no significant difference in length or size of vessels or number of junctions, as quantified by angioquant software. In contrast however, endothelialised MSCs implanted onto the chick CAM for 48 hours, promoted extensive blood vessel growth in the underlying CAM, significantly enhanced the total number of junctions and diameters and lengths of

Figure 5.4

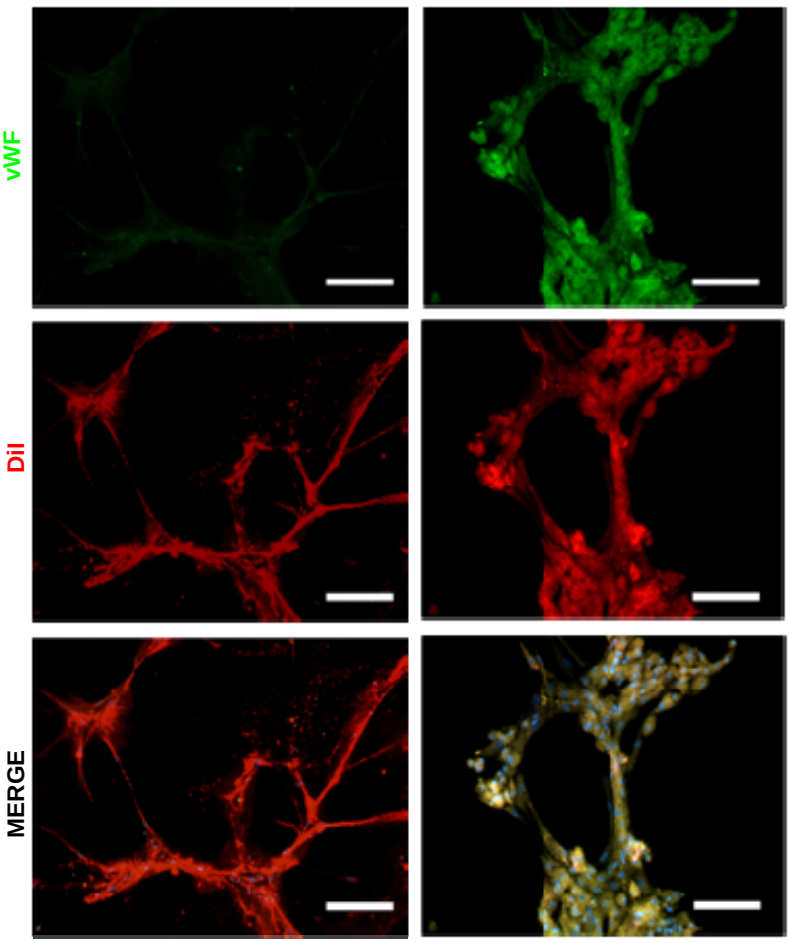

Figure 5.4. *Endothelialised MSCs formed enhanced networks within the CAM*

To determine whether an *in vivo* three-dimensional environment influenced MSC differentiation towards ECs, either 20,000 DiI labelled control standard MSCs (MSC-S) (left panels) or endothelialised MSCs (MSC-H) (right panels) were seeded onto growth factor reduced Matrigel-treated coverslips in 0.5% serum DMEM. Cells were left to adhere for one hour, then placed upon the chick CAM of a day five chick embryo for 48 hours. Immunofluorescence analysis of vWF using Olympus BX51 widefield microscope and 20× objective. vWF = green; DiI = red. Scale bars represent 200μm. A representative of two independent experiments are shown in each case.

Figure 5.5

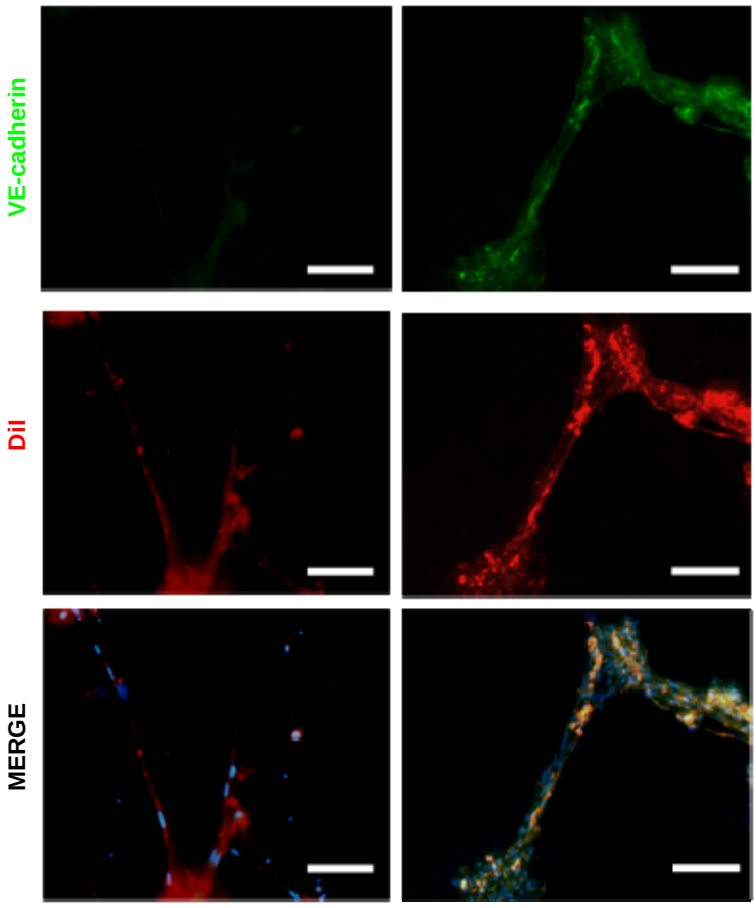

Figure 5.5. *VE-cadherin expression in endothelialised MSC networks within the CAM.*

Either 20,000 DiI labelled control standard cultured MSCs (MSC-S) (left panels), or endothelialised MSCs (MSC-H) (right panels) were seeded on Matrigel, then placed into the chick CAM for 48 hours. Immunofluorescence analysis of VE-cadherin expression. Images were obtained using an Olympus BX51 widefield microscope and 20× objective. Scale bars represent 200µm. VE-cadherin = green; DiI = red. A representative of two independent experiments is shown in each case.

Figure 5.6

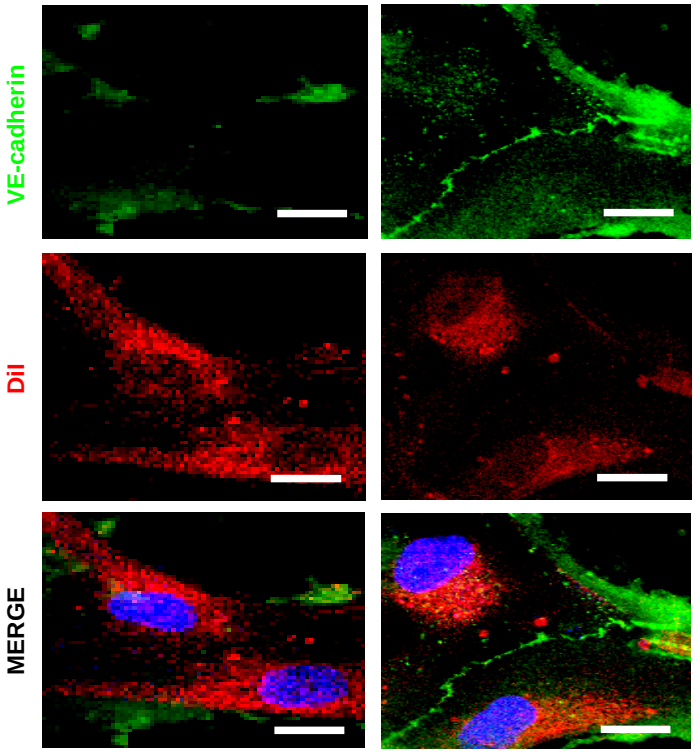

Figure 5.6. *VE-cadherin localised to the cell surface in endothelialised MSCs within the CAM*

Either 20,000 DiI labelled control standard cultured MSCs (MSC-S) (left panels), or endothelialised MSCs (MSC-H) (right panels) were seeded on Matrigel, then placed into the chick CAM for 48 hours. Immunofluorescence analysis of VE-cadherin expression. Images were obtained using a Nikon C1 upright confocal microscope with 60× objective. Scale bars represent 7µm. VE-cadherin= green; DiI=red. A representative of two independent experiments is shown in each case.

Figure 5.7

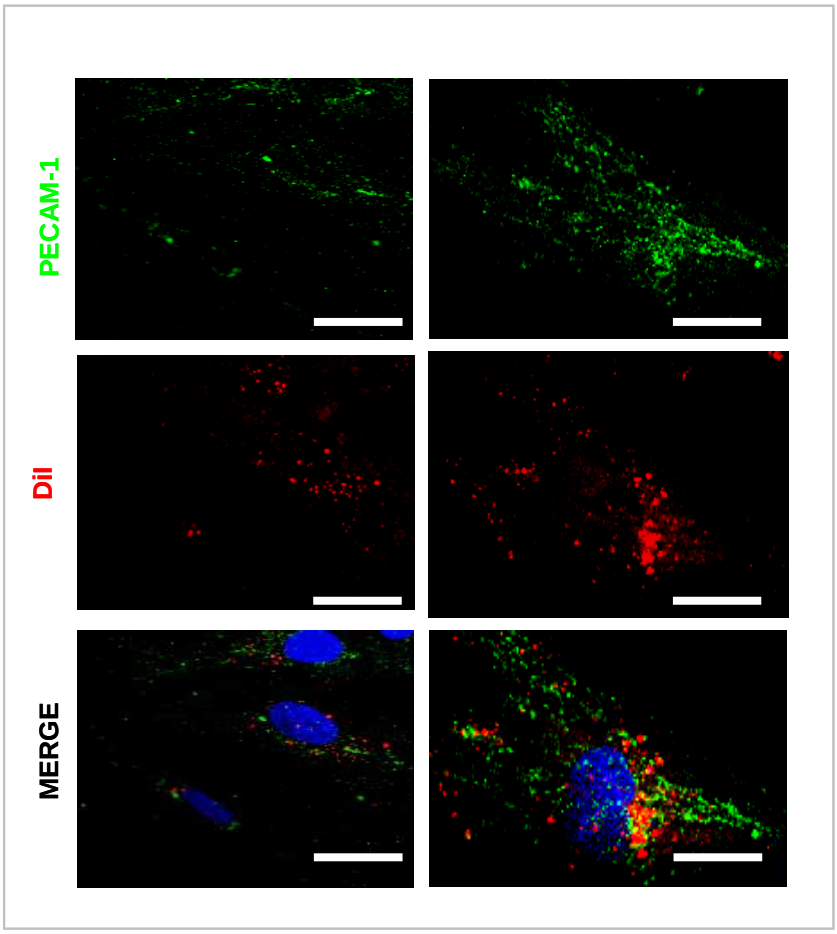

Figure 5.7. PECAM-expression *in endothelialised MSCs within the chick CAM*

Either 20,000 DiI labelled control standard cultured MSCs (MSC-S) (left panels), or endothelialised MSCs (MSC-H) (right panels) were seeded on Matrigel, then placed into the chick CAM for 48 hours. Immunofluorescence analysis of PECAM-1 expression. Images were obtained using a Nikon C1 upright confocal microscope with 60× objective. Scale bars represent 7µm. PECAM-1= green; DiI=red. A representative of two independent experiments is shown in each case.

Figure 5.8

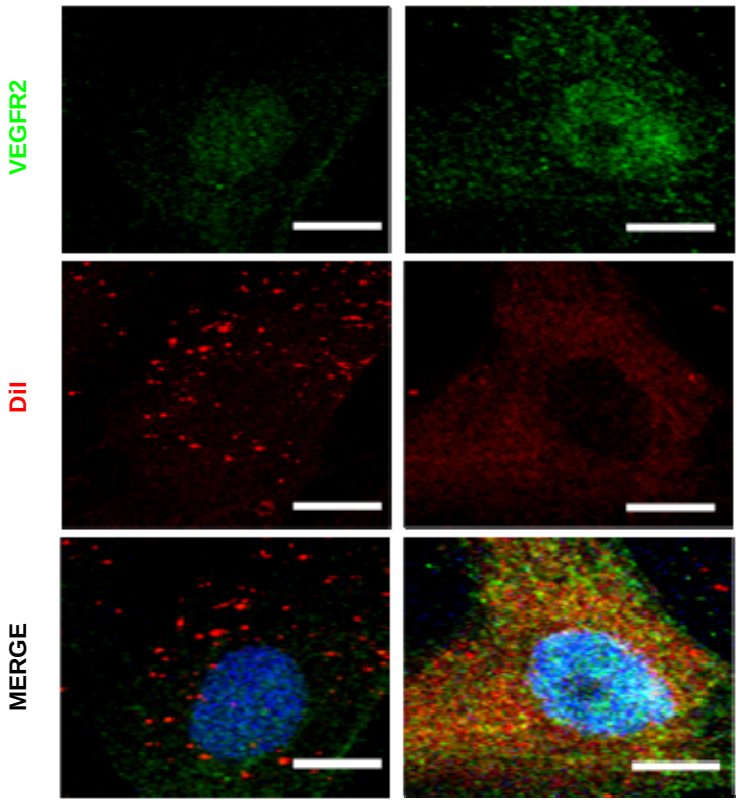

Figure 5.8. VEGFR2 expression *in endothelialised MSCs within the chick CAM*

Either 20,000 DiI labelled control standard cultured MSCs (MSC-S) (left panels), or endothelialised MSCs (MSC-H) (right panels) were seeded on Matrigel, then placed into the chick CAM for 48 hours. Immunofluorescence analysis of VEGFR2. Images were obtained using a Nikon C1 upright confocal microscope with 60× objective. Scale bars represent 7μm. VEGFR2= green; DiI=red. A representative of two independent experiments is shown in each case.

Figure 5.9

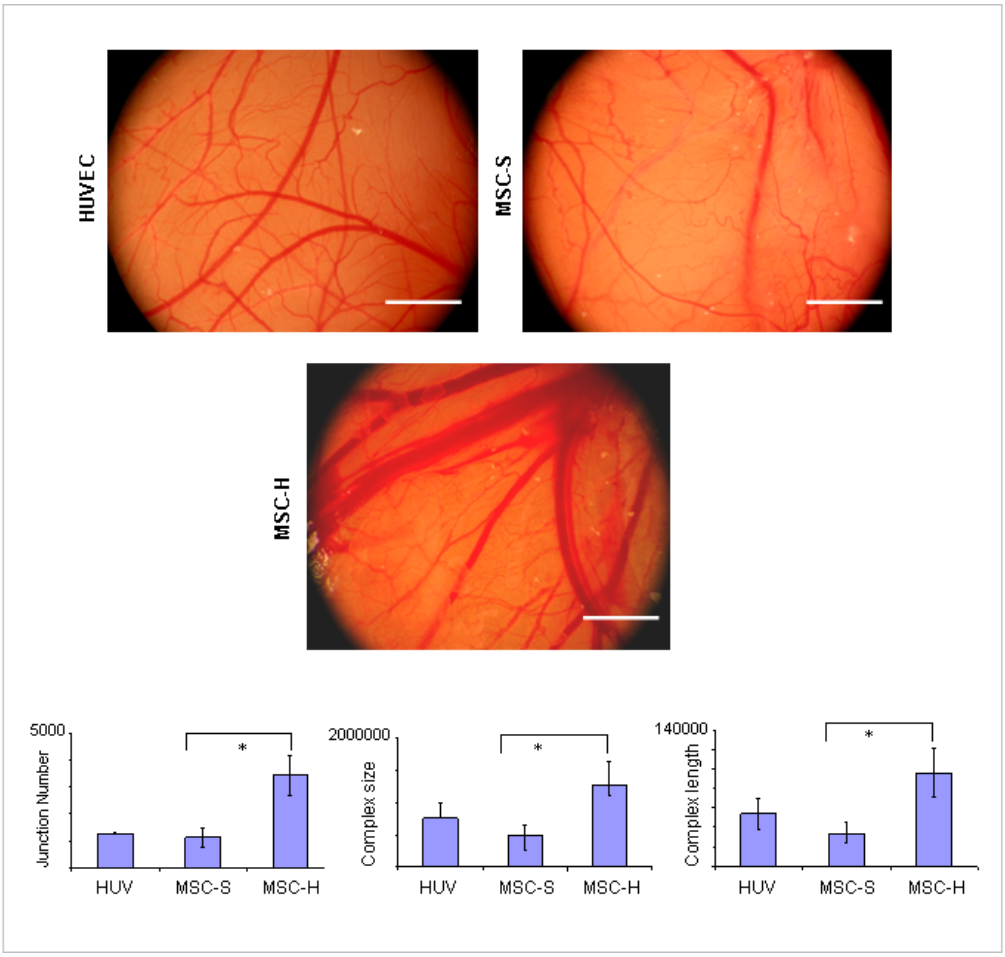

Figure 5.9. *Endothelialised MSCs promoted CAM vascularisation*

Either 20,000 HUVECs, MSCs pre-cultured in standard conditions (MSC-S) or endothelialised MSCs (MSC-H) were seeded onto Matrigel coated coverslips, then placed onto a chick CAM for 48 hours. Following removal of the coverslips, the degree of vascularisation was quantified with Angioquant software measuring total number of junctions, total size of complexes and total lengths of complexes. * represent $p<0.05$ compared to MSC-S. Ten representative images were taken for each treatment, using a Nikon stereo microscope with each analysis performed in triplicate. Scale bars represent 6 mm. A representative of two independent experiments is shown in each case.

vessels, compared to the same number of implanted HUVECs or MSCs pre-cultured in standard conditions (Figure 5.9).

5.3.3. MSCs integrated into preformed endothelial networks

Having established that endothelialised MSCs significantly enhanced the underlying CAM vascularisation, it was necessary to determine whether increased blood vessel growth resulted from MSC paracrine effects and/or from direct integration of MSCs into the pre-existing vasculature. Experiments were initially conducted *in vitro* to determine whether endothelialised MSCs could integrate into preformed HUVEC networks on matrigel. HUVECs were labelled with DiI, to distinguish HUVECs from unlabelled MSCs, then seeded onto Matrigel for 24 hours. Once HUVEC networks were established, unlabelled MSCs in standard culture conditions or endothelialised MSCs were seeded onto the preformed EC networks. Both MSCs pre-cultured in standard conditions or endothelialised MSCs were found to integrate into preformed HUVEC networks (Figure 5.10), suggesting that direct integration may occur to enhance vascularisation in the chick CAM.

To further validate this hypothesis, preliminary studies were carried out *in vivo* to determine whether endothelialised MSCs could integrate into the chick vasculature (Figure 5.11). Interestingly, MSCs pre-cultured in standard conditions could not be detected within the CAM vasculature. In contrast however, endothelialised MSCs were detected within the CAM blood vessels, suggesting that endothelialised MSCs may integrate directly into the pre-existing CAM vasculature resulting in enhanced vessel growth.

5.4. Discussion

BM–derived MSC have demonstrated considerable potential for regenerative medicine strategies (Adams *et al* ., 2007; Bobis *et al* ., 2006; Dai *et al* ., 2009; Granero-

Figure 5.10

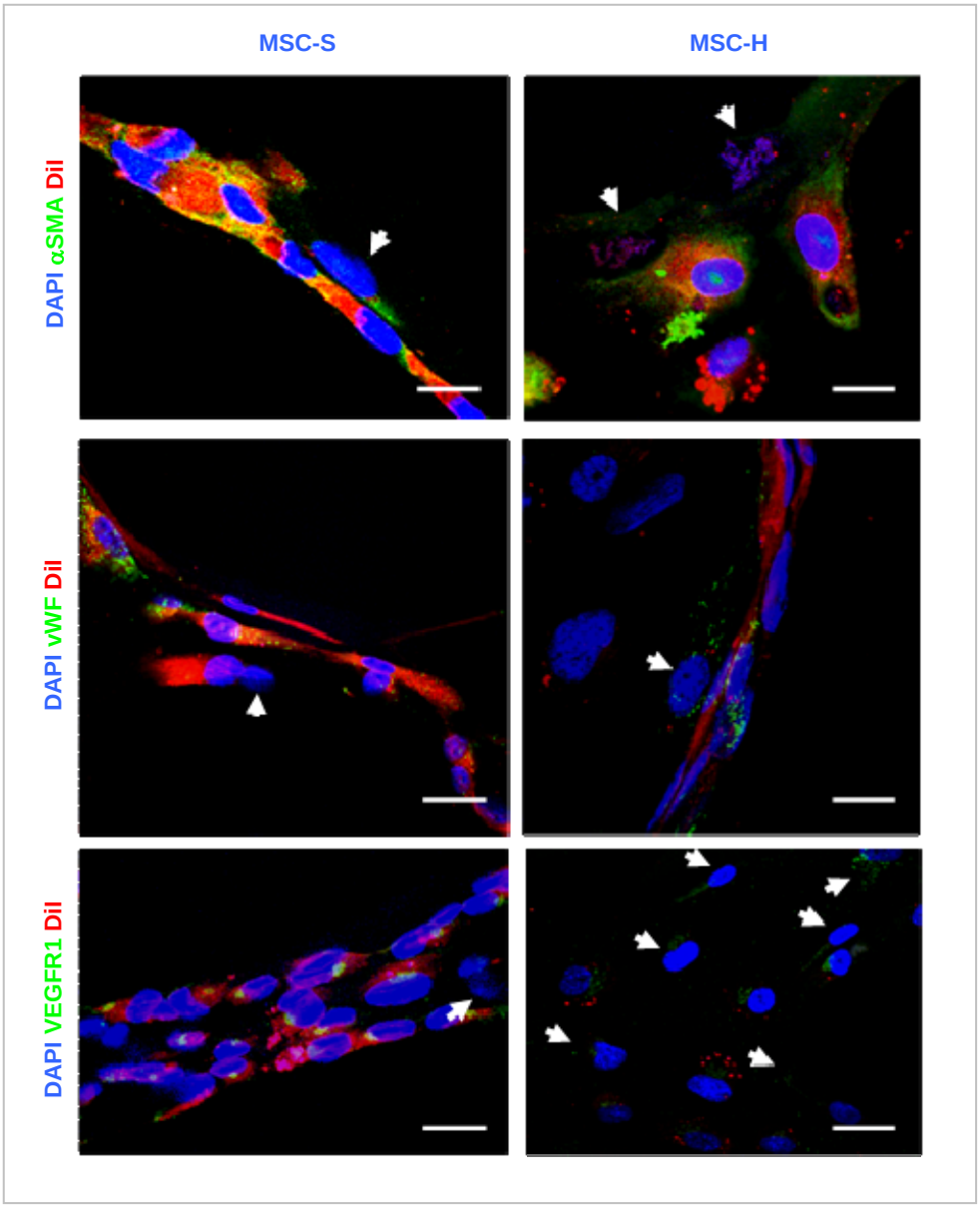

Figure 5.10. MSCs integrated into preformed endothelial networks

HUVECs were labelled with 10μg/ml DiI and seeded onto growth factor reduced matrigel for 24 hours to enable network formation to occur. Unlabelled MSCs (arrows) were then seeded onto preformed HUVEC networks and cultured for 24 hours, then immunofluorescence analysis was performed. Images were obtained using a Nikon C1 upright confocal microscope with 60× objective. Scale bars represent 7μm. αSMA/vWF/VEGFR1 = green; DiI = red. A representative of two independent experiments is shown in each case.

Figure 5.11

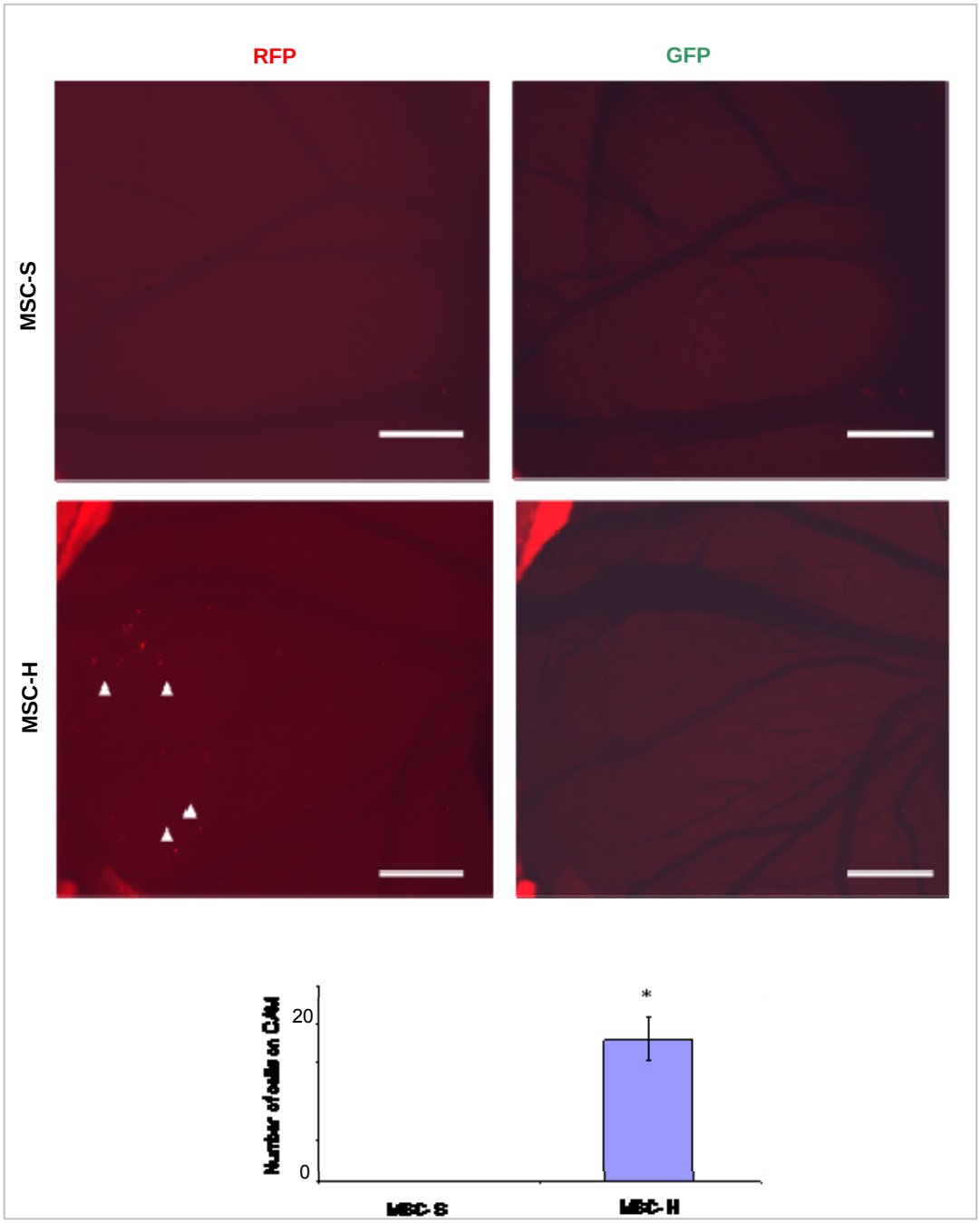

Figure 5.11. Endothelialised MSCs were detected on the CAM surface

Either 20,000 DiI labelled MSCs pre-cultured in standard conditions (MSC-S) or endothelialised MSCs (MSC-H) were seeded onto Matrigel coated coverslips, then placed onto a chick CAM for 48 hours. Following removal of the coverslips the number of DiI labelled MSCs localising on the surface of the chick CAM was evaluated (arrows) and quantified as a bar graph. DiI=red (arrows). Scale bars represent 6 mm. A representative of two independent experiments is shown, in each case 10 representative images were taken for each analysis using the RFP channel or the GFP channel to eliminate autofluorescence. *=$p<0.05$ compared to MSC-S.

Molto *et al*., 2008; Hanson *et al* ., 2009; Miura *et al* ., 2006; Riha *et al* ., 2005; Slater *et al* 2008). Understanding how different microenvironmental factors can regulate the fate of MSCs during *in vitro* culture and after implantation *in vivo,* is crucial for successful tissue regeneration therapies. In this chapter, three dimensional culture *in vitro* using Matrigel was shown to promote further MSC differentiation towards an EC fate by inducing VEGFR2 expression and significantly enhancing VE-cadherin expression throughout the network assemblies. It must however be noted that the high density MSCs in the middle of the network may be undergoing apoptosis so in this case the western blot is more convincing. Furthermore, implanted endothelialised MSCs in the pro-angiogenic environment of the chick CAM, expressed cell surface VE-cadherin, formed enhanced network assemblies and stimulated growth of the underlying chick vasculature.

Matrigel promotes many cell types to adopt a more mature phenotype, as well as the outgrowth of differentiated cells from tissue explants (Bradham *et al* ., 1995; Hadley *et al* ., 1995; Hoffman *et al* ., 1986; Kibbey *et al* ., 1992; Kleinman *et al* ., 1987; Li *et al*., 1987 2005; Oliver *et al* ., 1987; Sawada *et al* ., 1987; Schuetz *et al* ., 1988; Vukicevic *et al* ., 1990). Matrigel significantly reduces the proliferative capacity of many cell lines, which in many cases results in the morphology and gene expression profile reflecting a more differentiated phenotype. Epithelial cells, become more columnar when cultured on top of Matrigel, but form ducts, ductules and large glandular-like structures with a lumen when cultured in three-dimension within the matrix (Li *et al* ., 1987) In contrast, chondrocytes form cartilaginous nodules when cultured on the surface of the Matrigel (Bradham *et al* ., 1995). ECs cultured within Matrigel rapidly attach and align then form capillary-like structures with a lumen (Kubota *et al* ., 1988), whilst salivary gland cells form acinar-like structures and produce amylase when cultured on Matrigel (Hoffman *et al* ., 1996).

Basement membrane components are the first ECMs synthesised in the developing embryo, with laminin expressed at the two-cell stage and a basement membrane apparent at gastrulation (Kleinman *et al* ., 2005). Since basement membranes are the

first ECMs that stem cells contact, it would be expected that such matrices would have a profound effect on regulating their differentiation.

The multiple responses observed when cells are cultured in Matrigel are not well understood but undoubtedly involve a variety of mechanisms. Cells cultured within the three dimensional environment of Matrigel rapidly associate and become polarised. Thus, MSCs within Matrigel will have cell-cell contacts which are more representative of *in vivo* tissues. Matrigel, as well as being composed of basement membrane components, contains a rich store of angiogenic growth factors. In addition, fragments of laminin-1, collagen IV, and other matrix proteins have been shown to contribute angiogenic- and growth-promoting signals (Engbring *et al* ., 2003). For example, certain peptide sequences in laminin-1 have been shown to increase angiogenesis, protease activity, and/or tumor growth and metastasis via integrin receptors αvβ3 and α5β1. (Enbring *et al* ., 2003; Markwald *et al*, 1987; Ponce *et al* ., 1999; Stack *et al* ., 1993; Frisch *et al* ., 1996).

As previously discussed, VEGFR2 plays a key role in regulating angiogenesis, therefore an environment such as Matrigel that is conducive to network formation or blood vessel development may well be expected to induce VEGFR2 expression (Smadja et al., 2007).However, it must be noted that VEGFR2 only shows weak localisation by immunofluorescence analysis and low expression levels by western analysis. Regulation of VEGFR2 is an important mechanism during blood vessel formation, therefore it would be interesting to determine the components in Matrigel that are responsible for inducing this critical gene. RT-PCR analysis (Figure 4.11) showed that exogenous VEGF-A is not capable of inducing VEGFR2 in MSCs cultured at high density on tissue culture plastic. Previous studies have implicated BMP4, fibroblast growth factor 8 and Wnt-signalling pathways (Nimmagadda *et al* ., 2007) In addition, TNF-α known to be involved in inducing VCAM-1 expression, has also been shown to up-regulate VEGFR2 expression and function in a dose- and time-dependent manner, as well as the expression of its co-receptor neuropilin-1 in human endothelium (Giraudo *et al* ., 1998).

The aforementioned potential induction of VEGFR2 may contribute to the enhanced networks formed by endothelialised MSCs (Smadja et al., 2007). In addition, it may explain why endothelialised MSCs were detected within the CAM blood vessels, whilst MSCs pre-cultured in standard culture conditions could not be detected in these vessels. VEGFR2-positive endothelialised MSCs may have adopted a more migratory phenotype in response to paracrine stimulation. Molecular blockade of VEGFR2 has been shown to inhibit several critical steps involved in angiogenesis. VEGFR2 blockade attenuated EC proliferation, reduced migration, and disrupted differentiation and formation of capillary-like networks (Li *et al*., 2005; Koolwijk *et al*., 2001). Interestingly, both PECAM-1 and PDGFR signalling was shown to decrease in endothelialised MSCs cultured on Matrigel. A number of previous studies have demonstrated that PECAM-1 can be downregulated during angiogenesis in HUVECs (Romero *et al*., 1997; Berger *et al* ., 1993; Delisser *et al* ., 1997). In this study, PDGFRα signalling has been shown to regulate PECAM-1 (Chapter 4 Results; section 4.56) and may explain the observed decrease in PECAM-1 expression.

The implanted endothelialised MSCs resulted in enhanced CAM blood vessel growth. This enhanced growth may be attributed to the MSCs providing increased paracrine angiogenic stimulation and/or to direct integration of the endothelialised MSCs within the CAM vasculature. Endothelialised MSCs were found to incorporate *in vitro* into preformed endothelial networks and were distributed *in vivo* around CAM blood vessels suggesting endothelialised MSCs may incorporate into the pre-existing CAM vasculature, although longer time periods would be needed to fully assess functional incorporation as well as improved confocal microscopy techniques. The endothelialised MSCs may also result in enhanced blood vessel growth by providing an increased source of angiogenic factors. Bone marrow MSCs have been shown in a number of studies to secrete differential levels of numerous cytokines including EGF, keratinocyte growth factor, insulin like growth factor 1, VEGF-A and PDGF-BB (Burchfield *et al* ., 2008; Tang *et al*., 2005b). Indeed, this study has shown that VEGF-A is significantly enhanced in endothelialised MSCs. It would therefore be interesting to determine if

knockdown of VEGF-A in endothelialised MSCs, reduced the pronounced blood vessel growth.

5.5. Summary

- *In vitro* Matrigel culture induced endothelialised MSCs to express low levels of VEGFR2, enhanced VE-cadherin but decreased PECAM-1 expression
- Endothelialised MSCs formed enhanced network assemblies *in vitro* expressing vWF, PECAM-1, VE-cadherin and possible VEGFR2
- Endothelialised MSCs formed enhanced networks *in ovo*
- Endothelialised MSCs *in ovo* increased expression of vWF, PECAM1 and VEGFR2 and VE-cadherin was promoted to the cell surface
- Endothelialised MSCs enhanced CAM blood vessel growth and localised to the surface of blood vessels

CHAPTER 6

FINAL DISCUSSION

CHAPTER 6. FINAL DISCUSSION

6.1. Potential therapeutic strategies

Therapeutic angiogenesis/vasculogenesis is a promising option for treating peripheral artery diseases, ischaemic heart diseases, and cerebral ischaemia. Clinical trials have confirmed that autologous cell therapies using BM-derived or circulating blood-derived progenitor cells are safe and provide beneficial effects (Li *et al*., 2009a; Iba *et al*., 2002; Tateishi-Yuyama *et al*., 2002; Huang *et al* ., 2004; Riha *et al*., 2005). Interestingly, it has been shown that highly differentiated cells may lose their therapeutic potential, as adult ECs provide no benefits to postnatal neovascularisation (Yang *et al*., 2004; Sone *et al*., 2007). The vascular regenerative potential of EPCs is limited, due to their sparse numbers in the bone marrow and peripheral circulation, low *ex vivo* expansion potential, as well as a number of coronary artery disease risk factors, including age, smoking, diabetes and hypercholesterolemia which all reduce EPC number, migration and function (Ball *et al* ., 2010b; Rodriguez *et al* .,2009).

6.2. Stem cell therapy

The majority of studies documenting stem cell therapy for vascular disorders have utilised undifferentiated stem cells, particularly ESCs. However major risks associated with the use of ESCs are the possibility of teratoma formation following transplantation, immune rejection and uncontrolled neovascularisation, which contributes to tumorigenesis and diabetic and age-related retinopathies (Blum *et al* ., 2008; Li *et al* ., 2009b; Nussbaum *et al* ., 2007; Swijnenburg *et al* ., 2005; Xu *et al* ., 2001). It is vital therefore to identify, characterise, and isolate progenitor populations that will not form teratomas, but yet are capable of proliferation and continual differentiation into functional ECs for cell therapy and the development of functional vascular grafts.

MSCs can be readily isolated from a variety of different tissue locations, are easily expanded *ex vivo,* are largely non-immunogenic and can differentiate towards ECs

during neovascularisation (Caplan *et al*, 2009; Devine *et al* ., 2003; Phinney *et al* ., 2007a; Silva *et al* ., 2005; Tomita *et al* ., 2002). In addition, a number of studies have shown how MSCs transplanted directly into tissues, by local intravascular administration or by systemic delivery, can enhance neovascularisation by direct integration into blood vessel walls or by acting as a source of angiogenic factors, such as VEGF-A (Li *et al* ., 2009a; Sasaki *et al* ., 2008; Shoji *et al* ., 2010; Xu *et al* ., 2010; Wakabayashi *et al*., 2010; Zhang *et al*., 2010). These properties make MSCs remarkably appealing for vascular regenerative or vascular graft applications. Furthermore, *ex vivo* expansion and manipulation of MSCs prior to transplantation may increase the opportunities to improve vascular regenerative therapy.

A major challenge of stem cell based vascular regeneration has been the production of sufficient numbers of differentiated ECs. The efficiency of endothelial differentiation from ESCs is typically low, ranging from 1% to 3% (Levenberg *et al* ., 2002; Li *et al* ., 2009b). However, one study demonstrated that 10% CD34+ progenitor cells were present by monolayer culturing of hESCs on murine embryonic fibroblast feeder layer for 10 days (Wang *et al*., 2007b). In addition, a further study introduced a different two-step method by attaching day 9 embryoid bodies to dishes, culturing them for 7–9 days, then mechanically isolating the center region, eventually yielding 40% cells that were positive for vWF (Cho *et al* ., 2007). Compared to ESCs, work presented in this thesis has demonstrated that MSC differentiation to ECs yields much higher numbers of differentiated ECs, with 100% of differentiated cells expressing vWF and 50% positive for ac-LDL uptake. Furthermore, differentiated MSCs exhibited moderately stable commitment to an EC lineage, limiting the possibility of dysregulated stem cell differentiation.

Moreover, recent research on hESC-based therapy showed poor long-term engraftment of human ESC-derived ECs and poor cell survival by serial bioluminescence imaging (Li *et al*., 2008b). However, preliminary investigations in this study revealed that endothelialised MSCs are present on the surface of the CAM suggesting that they may

integrate into preformed endothelial networks over longer periods of time. However to understand more fully the beneficial effects of MSC therapy using endothelialised MSCs, it will be necessary to either perform histological analysis to determine viable engraftment of the transplanted MSCs, or track transplanted MSCs in animal models over time to monitor functional engraftment.

6.3. Therapeutic manipulation

Defining the critical mechanisms which regulate the initiation of MSC differentiation towards an EC fate is crucial for the effective therapeutic manipulation of MSCs within *in vivo* environments, potentially enabling targeted modulation of neovascularisation during ischemia, wound healing and tumourigenesis. This study has identified Notch signalling as a primary mechanism regulating density dependent differentiation to ECs. Notch signalling is sufficient to initiate MSC commitment to ECs, by stimulating VEGFR1 and vWF expression and VEGF-A secretion. In addition, to consolidate further the EC fate, Notch-activated VEGF-A stimulated the adhesion molecules VE-cadherin and PECAM-1, mediated through differential VEGFR1 and PDGFRα signalling respectively. Targeted regulation of Notch signalling could therapeutically be used to modulate MSC differentiation towards ECs during postnatal neovascularisation events. MicroRNAs are a family of small, non-coding single stranded RNAs of 19-25 nucleotides in length that base pair with target mRNAs invoking post-transcriptional gene silencing through mRNA cleavage or translational repression (He et al., 2004; Kim et al., 2005c). In this respect, microRNAs mimetics could be applied to potentially stimulate gene translation and enhance MSC endothelialisation at sites of ischemic injury or vascular injury. In contrast, miRNAs could be identified to repress Notch receptor translation and prevent MSC differentiation events and subsequent neovascularisation in pathological situation such as in tumorigenesis. However a single miRNA can have multiple targets, each target can be regulated by several miRNAs, and the effects of a specific miRNA are variable depending a cell context, therefore this approach is likely to be challenging.

An alternative approach is to modify genetically MSCs overexpressing a particular Notch receptor or ligand to stimulate Notch signalling, to enable controlled recruitment, differentiation and functional incorporation into blood vessel walls. Similarly, MSCs engineered to overexpress truncated Notch receptors or ligands may also enable repression of MSC differentiation. Recent studies have investigated the use of MSCs for gene therapy, including transplantation of MSCs transiently expressing VEGF for the improvement of heart function in myocardial rat infarction models (Kumar *et al* ., 2008; Tang *et al* ., 2006) MSCs expressing BMP2 to promote bone formation and MSCs as a vehicle for interferon-β delivery into tumors in mice have also been reported (Studeny *et al* ., 2002). In addition, genetically modified MSCs have been used in several therapeutic applications in pre-clinical models of human diseases (Kumar *et al* ., 2008). However concerns regarding the exposure to viral vectors and foreign genetic material have to be considered.

6.4. Notch regulation of stem cell differentiation

It should be noted that a number of previous studies have demonstrated that Notch signalling is an important mechanism involved in regulating stem cell differentiation to chondrocytes (Oldershaw *et al* ., 2008) cardiomyocytes (Li *et al* ., 2006) and neurons (Dezawa *et al* ., 2004). In studies inducing chondrogenic differentiation, aggregates were cultured in serum free medium containing a chondrogenic differentiation supplement for up to 14 days. Notch signalling was shown to be necessary to initiate chondrogenesis, but had to be switched off for chondrogenesis to proceed to completion (Oldershaw *et al* ., 2008). In addition, MSCs transfected with the intracellular domain of the Notch receptor (NICD) stimulated with neural differentiation factors, efficiently induced MSCs with neuronal characteristics (Dezawa *et al* ., 2004). However in both these studies, it is unclear whether Notch signalling in MSCs cultured without differentiation supplements would be sufficient to induce differentiation. In this thesis, high MSC density and subsequent Notch signalling did not result in the induction of the chondrogenic gene Col2A1 or Col9A2, suggesting that Notch signalling alone in two dimensional culture is not sufficient to initiate chondrogenesis. However, Notch signalling alone has been

shown to be sufficient to stimulate the differentiation of MSCs to cardiomyocytes when MSCs and cardiomyocytes were co-cultured together (Li *et al* ., 2006). The overall effects of Notch signalling activation are therefore likely to be dependent on the specific Notch ligands and receptors involved, the cell type being stimulated and the timing of the activation.

6.5. MSCs as a vascular progenitor cell

Recently it has been shown that Notch signalling alone, stimulated by using immobilised Jagged-1, transfected with the intracellular domain of the Notch receptor or following co-culture with fibroblasts overexpressing the Notch ligand DLL1, was sufficient to induce the vSMC markers SM-MHC-1 and myocardin in MSCs (Kurpinski *et al* ., 2010). Our preliminary studies have also detected a significant up-regulation of vSMC markers, including SM-MHC-1 after MSCs were cultured at high density for 24 hours, suggesting that at this early time point MSCs are forming a vascular progenitor cell with the capability of differentiating towards an EC or vSMC fate. Moreover, the vSMC markers were markedly decreased with time as the EC fate was consolidated. Thus, understanding the mechanisms driving density differentiation to ECs may enable manipulation of this differentiation pathway to generate vSMCs. However, it must be noted that the appearance of vSMC markers alone is not sufficient to identify MSC to vSMC differentiation. Functional responses of differentiated MSCs must be assessed, including intracellular responses to calcium signalling agonists (Hill *et al* ., 2010) and contractility (Davis *et al* ., 1992). Interestingly, recently studies have suggested that MSCs can adopt both a vSMC-like and an EC-like state simultaneously (Lozito *et al* ., 2009 a, b). Direct co-culture of MSCs with HUVECs increased mRNA expression of both αSMA and PECAM-1. However, since MSCs express high levels of αSMA endogenously, differentiation to vSMCs can only be suggested by the expression of late vSMC markers including SM-MHC-1 and desmin.

6.6. Density dependent differentiation of MSCs to ECs *in vivo*

It is important to consider whether high MSC density is potentially representative of an *in vivo* situation, such that the *in vitro* Notch signalling identified in this study would also occur *in vivo*, either at a wound site, during neovascularisation of a tumour or in ischaemia. As previously discussed, BM-derived MSCs have the capacity to leave the BM, circulate in the blood and home to injured tissues. Studies have shown that when, $1x10^6$ MSCs were administered, $7.4x10^2$ MSCs were detected in wounded murine dermis (Sasaki *et al* ., 2008). In addition, another study documented that when mice were injected with $1x10^6$ MSCs, approximately $9x10^2$ MSCs were detected in $1cm^2$ of wounded murine skin (Wu *et al* ., 2007). Thus, using these murine models only a limited proportion of injected MSCs reached sites of neovascularisation. However, studies determining the number of detected MSCs reaching sites of active vascular remodelling or neovascularisation, such as during ischaemia or tumourigenesis are limited. To increase the abundance of MSCs reaching sites of neovascularisation and reaching a critical density to initiate Notch signalling, more specific targeting of MSCs to sites of repair and regeneration is required. It is likely that MSCs residing in blood vessel walls will rapidly respond to minor vascular injuries, however it is not known whether their numbers will be sufficient to reach high density. Major vascular damage or pathological neovascularisation will require a greater number of MSCs, however the chemotactic stimulus mediated in part by hypoxia will induce a greater number of MSCs to be recruited to these sites.

This study demonstrates that a high density of MSCs *in vitro* is required to initiate Notch signalling and induce EC differentiation events (Figure 6.1). However, a significantly lower number of MSCs might be sufficient *in vivo* to promote EC differentiation due to the three dimensional environment: Irrespective of whether the high MSC density is attained *in vivo,* this study has shown that MSCs can be induced to differentiate towards an EC lineage *in vitro* and has identified an important *in vitro* culture method to pre-condition MSCs towards an EC fate prior to therapeutic utilisation *in vivo*. Thus optimised culture methods could be developed to accelerate the MSC-to-EC

differentiation event, enabling the endothelialised MSCs to be rapidly administered *in vivo* for vascular repair or regeneration therapies.

The work presented in this thesis demonstrates not only a novel density dependent mechanism for differentiation of MSCs to ECs, which advances our current understanding of this crucial differentiation event during vascular wall regeneration, but also provides a potentially unrecognised opportunity to regulate MSCs contribution to postnatal neovascularisation.

Figure 6.1

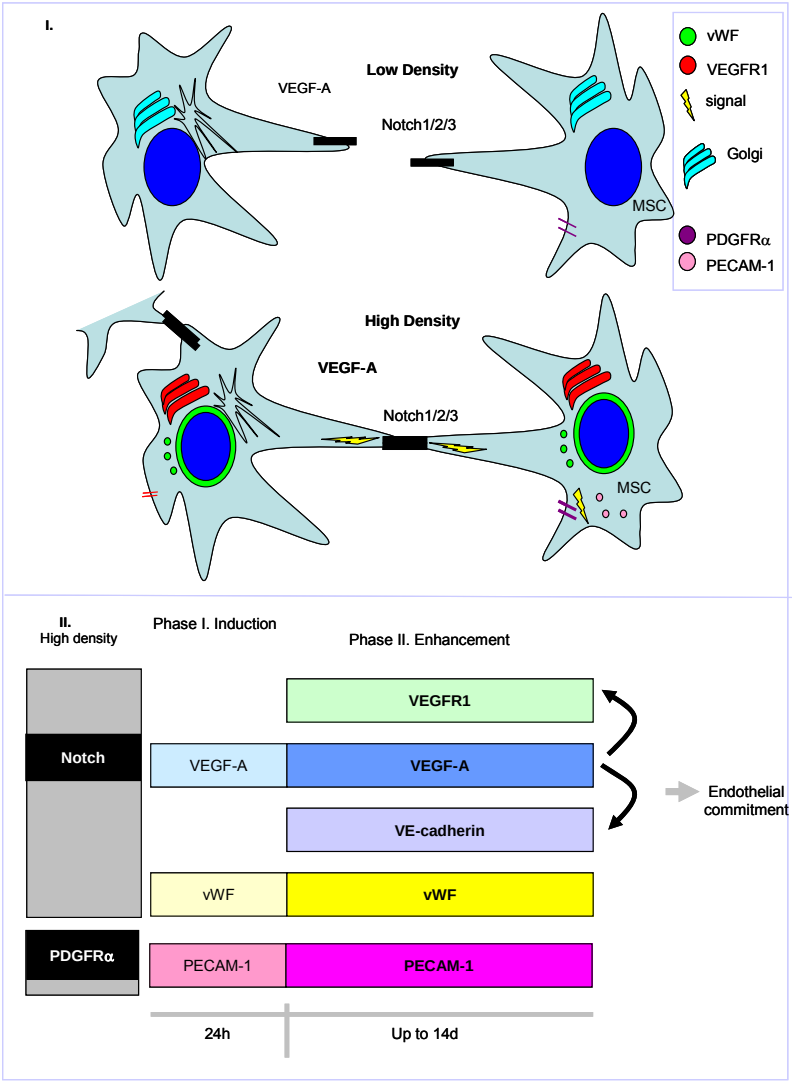

Figure 6.1. Model of how Notch signalling initiates MSCs to EC commitment

(I) Schematic model of cell density dependent regulation of VEGFR1 and vWF expression by MSCs. In MSC-L, Notch signalling is low and VEGFR1 is not expressed. In MSC-H, cell-cell contact enhances Notch receptor activation which induces expression of VEGFR1, enhances autocrine VEGF-A expression, and induces punctuate perinuclear vWF immunostaining. By 24 hours, newly synthesized VEGFR1 is mainly in the Golgi, with low levels of VEGFR1signalling at the cell surface. VEGF-A, through PDGFRs, induces PECAM-1. Subsequently, Notch and VEGF-A signalling induce VE-cadherin cell-cell contacts (not shown). **(II)** Co-ordinated pathways of MSC differentiation to ECs. Notch signals stimulate expression of VEGFR1, VEGF-A, VE-cadherin and vWF, and induce EC morphology. Upregulated VEGF-A further activates Notch, and stimulates PECAM-1 and VE-cadherin expression and EC commitment

6.7. Summary

This study provides evidence that MSC density is an important microenvironmental factor in regulating the *in vitro* differentiation of MSCs to ECs and also demonstrates that a proportion of MSCs can be differentiated to a functional EC under these conditions. Notch signalling was the primary stimulus initiating MSC commitment to an EC lineage, whilst VEGF-A stimulation was required to consolidate the EC fate. This study has identified a novel approach for generating ECs from MSCs and isolating and expanding these endothelialised MSCs may provide new opportunities for *in vitro* engineering of artificial vascularised tissues based on endothelialised MSCs. The mechanisms identified could be utilised to pre-condition MSCs prior to *in vivo* implantation, to improve vascular repair or regeneration events such as in ischaemia or wound healing. Conversely, they could provide therapeutic targets to inhibit *in vivo* neovascularisation events, such as during tumourigenesis. Taken together, this study demonstrates the potential of MSCs to differentiate to a functional EC, their prospective therapeutic role during postnatal neovascularisation, and conveys potential pharmacologic targeting to regulate MSC derived vascularisation.

7.0 References

Abedin, M., Tintut, Y., and Demer, L.L. (2004). Mesenchymal stem cells and the artery wall. Circ Res *95*, 671-676.

Adams, B., Xiao, Q., and Xu, Q. (2007). Stem cell therapy for vascular disease. Trends Cardiovasc Med *17*, 246-251.

Aghi, M., and Chiocca, E.A. (2005). Contribution of bone marrow-derived cells to blood vessels in ischemic tissues and tumors. Mol Ther *12*, 994-1005.

Aird, W.C. (2003). Endothelial cell heterogeneity. Crit Care Med *31*, S221-230.

Al-Khaldi, A., Eliopoulos, N., Martineau, D., Lejeune, L., Lachapelle, K., and Galipeau, J. (2003). Postnatal bone marrow stromal cells elicit a potent VEGF-dependent neoangiogenic response in vivo. Gene Ther *10*, 621-629.

Altman, G.H., Horan, R.L., Martin, I., Farhadi, J., Stark, P.R., Volloch, V., Richmond, J.C., Vunjak-Novakovic, G., and Kaplan, D.L. (2002). Cell differentiation by mechanical stress. FASEB J *16*, 270-272.

Alva, J.A., and Iruela-Arispe, M.L. (2004). Notch signaling in vascular morphogenesis. Curr Opin Hematol *11*, 278-283.

Alviano, F., Fossati, V., Marchionni, C., Arpinati, M., Bonsi, L., Franchina, M., Lanzoni, G., Cantoni, S., Cavallini, C., Bianchi, F.*,* . (2007). Term Amniotic membrane is a high throughput source for multipotent Mesenchymal Stem Cells with the ability to differentiate into endothelial cells in vitro. BMC Dev Biol *7*, 11.

Annabi, B., Naud, E., Lee, Y.T., Eliopoulos, N., and Galipeau, J. (2004). Vascular progenitors derived from murine bone marrow stromal cells are regulated by fibroblast growth factor and are avidly recruited by vascularizing tumors. J Cell Biochem *91*, 1146-1158.

Asahara, T., Takahashi, T., Masuda, H., Kalka, C., Chen, D., Iwaguro, H., Inai, Y., Silver, M., and Isner, J.M. (1999). VEGF contributes to postnatal neovascularization by mobilizing bone marrow-derived endothelial progenitor cells. EMBO J *18*, 3964-3972.

Asakura, A., Komaki, M., and Rudnicki, M. (2001). Muscle satellite cells are multipotential stem cells that exhibit myogenic, osteogenic, and adipogenic differentiation. Differentiation *68*, 245-253.

Aster, J.C., Simms, W.B., Zavala-Ruiz, Z., Patriub, V., North, C.L., and Blacklow, S.C. (1999). The folding and structural integrity of the first LIN-12 module of human Notch1 are calcium-dependent. Biochemistry *38*, 4736-4742.

Baatout, S., and Cheta, N. (1996). Matrigel: a useful tool to study endothelial differentiation. Rom J Intern Med *34*, 263-269.

Baatout, S. (1997). Endothelial differentiation using Matrigel (review). Anticancer Res *17*, 451-455.

Bai, K., Huang, Y., Jia, X., Fan, Y., and Wang, W. (2009). Endothelium oriented differentiation of bone marrow mesenchymal stem cells under chemical and mechanical stimulations. J Biomech *43*, 1176-1181.

Bailey, A.S., and Fleming, W.H. (2003). Converging roads: evidence for an adult hemangioblast. Exp Hematol *31*, 987-993.

Bailey, A.S., Willenbring, H., Jiang, S., Anderson, D.A., Schroeder, D.A., Wong, M.H., Grompe, M., and Fleming, W.H. (2006). Myeloid lineage progenitors give rise to vascular endothelium. Proc Natl Acad Sci U S A *103*, 13156-13161.

Baksh, D., Song, L., and Tuan, R.S. (2004). Adult mesenchymal stem cells: characterization, differentiation, and application in cell and gene therapy. J Cell Mol Med *8*, 301-316.

Ball, S.G., Shuttleworth, A.C., and Kielty, C.M. (2004). Direct cell contact influences bone marrow mesenchymal stem cell fate. Int J Biochem Cell Biol *36*, 714-727.

Ball, S.G., Shuttleworth, C.A., and Kielty, C.M. (2007a). Mesenchymal stem cells and neovascularization: role of platelet-derived growth factor receptors. J Cell Mol Med *11*, 1012-1030.

Ball, S.G., Shuttleworth, C.A., and Kielty, C.M. (2007b). Platelet-derived growth factor receptor-alpha is a key determinant of smooth muscle alpha-actin filaments in bone marrow-derived mesenchymal stem cells. Int J Biochem Cell Biol *39*, 379-391.

Ball, S.G., Shuttleworth, C.A., and Kielty, C.M. (2007c). Vascular endothelial growth factor can signal through platelet-derived growth factor receptors. J Cell Biol *177*, 489-500.

Ball, S.G., Bayley, C., Shuttleworth, C.A., and Kielty, C.M. (2010a) Neuropilin-1 regulates platelet-derived growth factor receptor signalling in mesenchymal stem cells. Biochem J *427*, 29-40.

Ball, S.G., Shuttleworth, C.A., and Kielty, C.M. (2010b) Platelet-derived growth factor receptors regulate mesenchymal stem cell fate: implications for neovascularization. Expert Opin Biol Ther *10*, 57-71.

Banerjee, S., Mehta, S., Haque, I., Sengupta, K., Dhar, K., Kambhampati, S., Van Veldhuizen, P.J., and Banerjee, S.K. (2008). VEGF-A165 induces human aortic smooth muscle cell migration by activating neuropilin-1-VEGFR1-PI3K axis. Biochemistry *47*, 3345-3351.

Baron, W., Shattil, S.J., and French-Constant, C. (2002). The oligodendrocyte precursor mitogen PDGF stimulates proliferation by activation of alpha(v)beta3 integrins. EMBO J *21*, 1957-1966.

Barry, F.P. (2003). Biology and clinical applications of mesenchymal stem cells. Birth Defects Res C Embryo Today *69*, 250-256.

Bazzoni, G., and Dejana, E. (2004). Endothelial cell-to-cell junctions: molecular organization and role in vascular homeostasis. Physiol Rev *84*, 869-901.

Beckermann, B.M., Kallifatidis, G., Groth, A., Frommhold, D., Apel, A., Mattern, J., Salnikov, A.V., Moldenhauer, G., Wagner, W., Diehlmann, A*., .* (2008). VEGF expression by mesenchymal stem cells contributes to angiogenesis in pancreatic carcinoma. Br J Cancer *99*, 622-631.

Beltrami, A.P., Barlucchi, L., Torella, D., Baker, M., Limana, F., Chimenti, S., Kasahara, H., Rota, M., Musso, E., Urbanek, K*., .* (2003). Adult cardiac stem cells are multipotent and support myocardial regeneration. Cell *114*, 763-776.

Berger, R., Albelda, S.M., Berd, D., Ioffreda, M., Whitaker, D., and Murphy, G.F. (1993). Expression of platelet-endothelial cell adhesion molecule-1 (PECAM-1) during melanoma-induced angiogenesis in vivo. J Cutan Pathol *20*, 399-406.

Betsholtz, C., Karlsson, L., and Lindahl, P. (2001). Developmental roles of platelet-derived growth factors. Bioessays *23*, 494-507.

Betsholtz, C. (2004). Insight into the physiological functions of PDGF through genetic studies in mice. Cytokine Growth Factor Rev *15*, 215-228.

Blum, B., and Benvenisty, N. (2008). The tumorigenicity of human embryonic stem cells. Adv Cancer Res *100*, 133-158.

Bobis, S., Jarocha, D., and Majka, M. (2006). Mesenchymal stem cells: characteristics and clinical applications. Folia Histochem Cytobiol *44*, 215-230.

Bouis, D., Hospers, G.A., Meijer, C., Molema, G., and Mulder, N.H. (2001). Endothelium in vitro: a review of human vascular endothelial cell lines for blood vessel-related research. Angiogenesis *4*, 91-102.

Boulton, M.E., Cai, J., and Grant, M.B. (2008a). gamma-Secretase: a multifaceted regulator of angiogenesis. J Cell Mol Med *12*, 781-795.

Boulton, M.E., Cai, J., Grant, M.B., and Zhang, Y. (2008b). Gamma-secretase regulates VEGFR1 signalling in vascular endothelium and RPE. Adv Exp Med Biol *613*, 313-319.

Bradham, D.M., Passaniti, A., and Horton, W.E., Jr. (1995). Mesenchymal cell chondrogenesis is stimulated by basement membrane matrix and inhibited by age-associated factors. Matrix Biol *14*, 561-571.

Bray, S.J. (2006). Notch signalling: a simple pathway becomes complex. Nat Rev Mol Cell Biol *7*, 678-689.

Brittan, M., and Wright, N.A. (2002). Gastrointestinal stem cells. J Pathol *197*, 492-509.

Burchfield, J.S., and Dimmeler, S. (2008). Role of paracrine factors in stem and progenitor cell mediated cardiac repair and tissue fibrosis. Fibrogenesis Tissue Repair *1*, 4.

Bussolati, B., Bruno, S., Grange, C., Buttiglieri, S., Deregibus, M.C., Cantino, D., and Camussi, G. (2005). Isolation of renal progenitor cells from adult human kidney. Am J Pathol *166*, 545-555.

Butler, J.M., Kobayashi, H., and Rafii, S. (2010) Instructive role of the vascular niche in promoting tumour growth and tissue repair by angiocrine factors. Nat Rev Cancer *10*, 138-146.

Buxboim, A., Ivanovska, I.L., and Discher, D.E. (2010) Matrix elasticity, cytoskeletal forces and physics of the nucleus: how deeply do cells 'feel' outside and in? J Cell Sci *123*, 297-308.

Cao, R., Brakenhielm, E., Li, X., Pietras, K., Widenfalk, J., Ostman, A., Eriksson, U., and Cao, Y. (2002). Angiogenesis stimulated by PDGF-CC, a novel member in the PDGF family, involves activation of PDGFR-alphaalpha and -alphabeta receptors. FASEB J *16*, 1575-1583.

Caplan, A.I. (1991). Mesenchymal stem cells. J Orthop Res *9*, 641-650.

Caplan, A.I., and Bruder, S.P. (2001). Mesenchymal stem cells: building blocks for molecular medicine in the 21st century. Trends Mol Med *7*, 259-264.

Caplan, A.I. (2009). Why are MSCs therapeutic? New data: new insight. J Pathol *217*, 318-324.

Carmeliet, P., Lampugnani, M.G., Moons, L., Breviario, F., Compernolle, V., Bono, F., Balconi, G., Spagnuolo, R., Oosthuyse, B., Dewerchin, M., . (1999). Targeted deficiency or cytosolic truncation of the VE-cadherin gene in mice impairs VEGF-mediated endothelial survival and angiogenesis. Cell *98*, 147-157.

Carmeliet, P., De Smet, F., Loges, S., and Mazzone, M. (2009). Branching morphogenesis and antiangiogenesis candidates: tip cells lead the way. Nat Rev Clin Oncol *6*, 315-326.

Cevallos, M., Riha, G.M., Wang, X., Yang, H., Yan, S., Li, M., Chai, H., Yao, Q., and Chen, C. (2006). Cyclic strain induces expression of specific smooth muscle cell markers in human endothelial cells. Differentiation *74*, 552-561.

Chang, C.C., Chang, T.Y., Yu, C.H., and Tsai, M.L. (2005). Induction of VE-cadherin in rat placental trophoblasts by VEGF through a NO-dependent pathway. Placenta *26*, 234-241.

Charbord, P. Bone Marrow Mesenchymal Stem Cells: Historical Overview and Concepts. (2010) Hum Gene Ther.Epub ahead of print.

Chen, L., Tredget, E.E., Wu, P.Y., and Wu, Y. (2008). Paracrine factors of mesenchymal stem cells recruit macrophages and endothelial lineage cells and enhance wound healing. PLoS One *3*, e1886.

Chen, M.Y., Lie, P.C., Li, Z.L., and Wei, X. (2009). Endothelial differentiation of Wharton's jelly-derived mesenchymal stem cells in comparison with bone marrow-derived mesenchymal stem cells. Exp Hematol *37*, 629-640.

Chen, T.T., Luque, A., Lee, S., Anderson, S.M., Segura, T., and Iruela-Arispe, M.L. (2010) Anchorage of VEGF to the extracellular matrix conveys differential signaling responses to endothelial cells. J Cell Biol *188*, 595-609.

Chiba, S. (2006). Notch signaling in stem cell systems. Stem Cells *24*, 2437-2447.

Cho, S.W., Moon, S.H., Lee, S.H., Kang, S.W., Kim, J., Lim, J.M., Kim, H.S., Kim, B.S., and Chung, H.M. (2007). Improvement of postnatal neovascularization by human embryonic stem cell derived endothelial-like cell transplantation in a mouse model of hindlimb ischemia. Circulation *116*, 2409-2419.

Choong, P.F., Mok, P.L., Cheong, S.K., Leong, C.F., and Then, K.Y. (2007). Generating neuron-like cells from BM-derived mesenchymal stromal cells in vitro. Cytotherapy *9*, 170-183.

Chung, N., Jee, B.K., Chae, S.W., Jeon, Y.W., Lee, K.H., and Rha, H.K. (2009). HOX gene analysis of endothelial cell differentiation in human bone marrow-derived mesenchymal stem cells. Mol Biol Rep *36*, 227-235.

Cines, D.B., Pollak, E.S., Buck, C.A., Loscalzo, J., Zimmerman, G.A., McEver, R.P., Pober, J.S., Wick, T.M., Konkle, B.A., Schwartz, B.S., . (1998). Endothelial cells in physiology and in the pathophysiology of vascular disorders. Blood *91*, 3527-3561.

Claesson-Welsh, L. (1994). Platelet-derived growth factor receptor signals. J Biol Chem *269*, 32023-32026.

Claesson-Welsh, L. (1996). Mechanism of action of platelet-derived growth factor. Int J Biochem Cell Biol *28*, 373-385.

Claesson-Welsh, L. (2003). Signal transduction by vascular endothelial growth factor receptors. Biochem Soc Trans *31*, 20-24.

Conway, E.M., Collen, D., and Carmeliet, P. (2001). Molecular mechanisms of blood vessel growth. Cardiovasc Res *49*, 507-521.
Crisan, M., Yap, S., Casteilla, L., Chen, C.W., Corselli, M., Park, T.S., Andriolo, G., Sun, B., Zheng, B., Zhang, L., . (2008). A perivascular origin for mesenchymal stem cells in multiple human organs. Cell Stem Cell *3*, 301-313.

Cross, M.J., Dixelius, J., Matsumoto, T., and Claesson-Welsh, L. (2003). VEGF-receptor signal transduction. Trends Biochem Sci *28*, 488-494.

Dai, L.J., Li, H.Y., Guan, L.X., Ritchie, G., and Zhou, J.X. (2009). The therapeutic potential of bone marrow-derived mesenchymal stem cells on hepatic cirrhosis. Stem Cell Res *2*, 16-25.

Davis, M.J., Meininger, G.A., and Zawieja, D.C. (1992). Stretch-induced increases in intracellular calcium of isolated vascular smooth muscle cells. Am J Physiol *263*, H1292-1299.

Dejana, E. (2004). Endothelial cell-cell junctions: happy together. Nat Rev Mol Cell Biol *5*, 261-270.

DeLisser, H.M., Christofidou-Solomidou, M., Strieter, R.M., Burdick, M.D., Robinson, C.S., Wexler, R.S., Kerr, J.S., Garlanda, C., Merwin, J.R., Madri, J.A., . (1997). Involvement of endothelial PECAM-1/CD31 in angiogenesis. Am J Pathol *151*, 671-677.

Delorme, B., Ringe, J., Gallay, N., Le Vern, Y., Kerboeuf, D., Jorgensen, C., Rosset, P., Sensebe, L., Layrolle, P., Haupl, T., . (2008). Specific plasma membrane protein phenotype of culture-amplified and native human bone marrow mesenchymal stem cells. Blood *111*, 2631-2635.

Delorme, B., Ringe, J., Pontikoglou, C., Gaillard, J., Langonne, A., Sensebe, L., Noel, D., Jorgensen, C., Haupl, T., and Charbord, P. (2009). Specific lineage-priming of bone marrow mesenchymal stem cells provides the molecular framework for their plasticity. Stem Cells *27*, 1142-1151.

Devine, S.M., Cobbs, C., Jennings, M., Bartholomew, A., and Hoffman, R. (2003). Mesenchymal stem cells distribute to a wide range of tissues following systemic infusion into nonhuman primates. Blood *101*, 2999-3001.

Dezawa, M., Kanno, H., Hoshino, M., Cho, H., Matsumoto, N., Itokazu, Y., Tajima, N., Yamada, H., Sawada, H., Ishikawa, H., . (2004). Specific induction of neuronal cells from bone marrow stromal cells and application for autologous transplantation. J Clin Invest *113*, 1701-1710.

Dezawa, M., Ishikawa, H., Itokazu, Y., Yoshihara, T., Hoshino, M., Takeda, S., Ide, C., and Nabeshima, Y. (2005). Bone marrow stromal cells generate muscle cells and repair muscle degeneration. Science *309*, 314-317.

Dhawan, J., and Rando, T.A. (2005). Stem cells in postnatal myogenesis: molecular mechanisms of satellite cell quiescence, activation and replenishment. Trends Cell Biol *15*, 666-673.

Dominici, M., Le Blanc, K., Mueller, I., Slaper-Cortenbach, I., Marini, F., Krause, D., Deans, R., Keating, A., Prockop, D., and Horwitz, E. (2006). Minimal criteria for defining multipotent mesenchymal stromal cells. The International Society for Cellular Therapy position statement. Cytotherapy *8*, 315-317.

Du, K.L., Ip, H.S., Li, J., Chen, M., Dandre, F., Yu, W., Lu, M.M., Owens, G.K., and Parmacek, M.S. (2003). Myocardin is a critical serum response factor cofactor in the

transcriptional program regulating smooth muscle cell differentiation. Mol Cell Biol *23*, 2425-2437.

Edelberg, J.M., and Ballard, V.L. (2008). Stem cell review series: regulating highly potent stem cells in aging: environmental influences on plasticity. Aging Cell *7*, 599-604.

Edgell, C.J., McDonald, C.C., and Graham, J.B. (1983). Permanent cell line expressing human factor VIII-related antigen established by hybridization. Proc Natl Acad Sci U S A *80*, 3734-3737.

Eichmann, A., Yuan, L., Moyon, D., Lenoble, F., Pardanaud, L., and Breant, C. (2005). Vascular development: from precursor cells to branched arterial and venous networks. Int J Dev Biol *49*, 259-267.

Eilken, H.M., Nishikawa, S., and Schroeder, T. (2009). Continuous single-cell imaging of blood generation from haemogenic endothelium. Nature *457*, 896-900.

Engbring, J.A., and Kleinman, H.K. (2003). The basement membrane matrix in malignancy. J Pathol *200*, 465-470.

Engler, A.J., Sen, S., Sweeney, H.L., and Discher, D.E. (2006). Matrix elasticity directs stem cell lineage specification. Cell *126*, 677-689.

Erices, A., Conget, P., and Minguell, J.J. (2000). Mesenchymal progenitor cells in human umbilical cord blood. Br J Haematol *109*, 235-242.

Ewenstein, B.M., Warhol, M.J., Handin, R.I., and Pober, J.S. (1987). Composition of the von Willebrand factor storage organelle (Weibel-Palade body) isolated from cultured human umbilical vein endothelial cells. J Cell Biol *104*, 1423-1433.

Ferrara, N. (2005). The role of VEGF in the regulation of physiological and pathological angiogenesis. EXS, 209-231.

Friedman, M.S., Long, M.W., and Hankenson, K.D. (2006). Osteogenic differentiation of human mesenchymal stem cells is regulated by bone morphogenetic protein-6. J Cell Biochem *98*, 538-554.

Frisch, S.M., Vuori, K., Ruoslahti, E., and Chan-Hui, P.Y. (1996). Control of adhesion-dependent cell survival by focal adhesion kinase. J Cell Biol *134*, 793-799.

Garlanda, C., and Dejana, E. (1997). Heterogeneity of endothelial cells. Specific markers. Arterioscler Thromb Vasc Biol *17*, 1193-1202.

Gavard, J., and Gutkind, J.S. (2006). VEGF controls endothelial-cell permeability by promoting the beta-arrestin-dependent endocytosis of VE-cadherin. Nat Cell Biol *8*, 1223-1234.

Gavard, J., and Gutkind, J.S. (2008). VE-cadherin and claudin-5: it takes two to tango. Nat Cell Biol *10*, 883-885.

Gerstenfeld, L.C., Cruceta, J., Shea, C.M., Sampath, K., Barnes, G.L., and Einhorn, T.A. (2002). Chondrocytes provide morphogenic signals that selectively induce osteogenic differentiation of mesenchymal stem cells. J Bone Miner Res *17*, 221-230.

Gerstenfeld, L.C., Barnes, G.L., Shea, C.M., and Einhorn, T.A. (2003). Osteogenic differentiation is selectively promoted by morphogenetic signals from chondrocytes and synergized by a nutrient rich growth environment. Connect Tissue Res *44 Suppl 1*, 85-91.

Gerwins, P., Skoldenberg, E., and Claesson-Welsh, L. (2000). Function of fibroblast growth factors and vascular endothelial growth factors and their receptors in angiogenesis. Crit Rev Oncol Hematol *34*, 185-194.

Giraudo, E., Primo, L., Audero, E., Gerber, H.P., Koolwijk, P., Soker, S., Klagsbrun, M., Ferrara, N., and Bussolino, F. (1998). Tumor necrosis factor-alpha regulates expression of vascular endothelial growth factor receptor-2 and of its co-receptor neuropilin-1 in human vascular endothelial cells. J Biol Chem *273*, 22128-22135.

Goessler, U.R., Bugert, P., Bieback, K., Deml, M., Sadick, H., Hormann, K., and Riedel, F. (2005). In-vitro analysis of the expression of TGFbeta -superfamily-members during chondrogenic differentiation of mesenchymal stem cells and chondrocytes during dedifferentiation in cell culture. Cell Mol Biol Lett *10*, 345-362.

Goldberger, A., Middleton, K.A., Oliver, J.A., Paddock, C., Yan, H.C., DeLisser, H.M., Albelda, S.M., and Newman, P.J. (1994). Biosynthesis and processing of the cell adhesion molecule PECAM-1 includes production of a soluble form. J Biol Chem *269*, 17183-17191.

Goldring, M.B., Tsuchimochi, K., and Ijiri, K. (2006). The control of chondrogenesis. J Cell Biochem *97*, 33-44.

Granero-Molto, F., Weis, J.A., Longobardi, L., and Spagnoli, A. (2008). Role of mesenchymal stem cells in regenerative medicine: application to bone and cartilage repair. Expert Opin Biol Ther *8*, 255-268.

Greenberg, J.I., Shields, D.J., Barillas, S.G., Acevedo, L.M., Murphy, E., Huang, J., Scheppke, L., Stockmann, C., Johnson, R.S., Angle, N., . (2008). A role for VEGF as a negative regulator of pericyte function and vessel maturation. Nature *456*, 809-813.

Gridley, T. (2007). Notch signaling in vascular development and physiology. Development *134*, 2709-2718.

Griffiths, M.J., Bonnet, D., and Janes, S.M. (2005). Stem cells of the alveolar epithelium. Lancet *366*, 249-260.

Grigolo, B., Lisignoli, G., Piacentini, A., Fiorini, M., Roseti, L., De Franceschi, L., Tognana, E., Pavesio, A., and Facchini, A. (2003). Tissue engineering for cartilage repair: in vitro properties of a hyaluronan-derivative. Chir Organi Mov *88*, 351-355.

Gustafsson, M.V., Zheng, X., Pereira, T., Gradin, K., Jin, S., Lundkvist, J., Ruas, J.L., Poellinger, L., Lendahl, U., and Bondesson, M. (2005). Hypoxia requires notch signaling to maintain the undifferentiated cell state. Dev Cell *9*, 617-628.

Guo, Y., Lubbert, M., and Engelhardt, M. (2003). CD34- hematopoietic stem cells: current concepts and controversies. Stem Cells *21*, 15-20.

Hadley, M.A., Byers, S.W., Suarez-Quian, C.A., Kleinman, H.K., and Dym, M. (1985). Extracellular matrix regulates Sertoli cell differentiation, testicular cord formation, and germ cell development in vitro. J Cell Biol *101*, 1511-1522.

Hainaud, P., Contreres, J.O., Villemain, A., Liu, L.X., Plouet, J., Tobelem, G., and Dupuy, E. (2006). The role of the vascular endothelial growth factor-Delta-like 4 ligand/Notch4-ephrin B2 cascade in tumor vessel remodeling and endothelial cell functions. Cancer Res *66*, 8501-8510.

Hanson, S., Thibeault, S.L., and Hematti, P. (2009). Clinical Applications of Mesenchymal Stem Cells in Laryngotracheal Reconstruction. Curr Stem Cell Res Ther.

Hardingham, T.E., Oldershaw, R.A., and Tew, S.R. (2006). Cartilage, SOX9 and Notch signals in chondrogenesis. J Anat *209*, 469-480.

Harrington, L.S., Sainson, R.C., Williams, C.K., Taylor, J.M., Shi, W., Li, J.L., and Harris, A.L. (2008). Regulation of multiple angiogenic pathways by Dll4 and Notch in human umbilical vein endothelial cells. Microvasc Res *75*, 144-154.

Hayden, M.R., Sowers, J.R., and Tyagi, S.C. (2005). The central role of vascular extracellular matrix and basement membrane remodeling in metabolic syndrome and type 2 diabetes: the matrix preloaded. Cardiovasc Diabetol *4*, 9.

He, L., and Hannon, G.J. (2004). MicroRNAs: small RNAs with a big role in gene regulation. Nat Rev Genet *5*, 522-531.

Hellstrom, M., Kalen, M., Lindahl, P., Abramsson, A., and Betsholtz, C. (1999). Role of PDGF-B and PDGFR-beta in recruitment of vascular smooth muscle cells and pericytes during embryonic blood vessel formation in the mouse. Development *126*, 3047-3055.

Herrera, M.B., Bruno, S., Buttiglieri, S., Tetta, C., Gatti, S., Deregibus, M.C., Bussolati, B., and Camussi, G. (2006). Isolation and characterization of a stem cell population from adult human liver. Stem Cells *24*, 2840-2850.

Hickey, M.M., and Simon, M.C. (2006). Regulation of angiogenesis by hypoxia and hypoxia-inducible factors. Curr Top Dev Biol *76*, 217-257.

Hill, K.L., Obrtlikova, P., Alvarez, D.F., King, J.A., Keirstead, S.A., Allred, J.R., and Kaufman, D.S. (2010) Human embryonic stem cell-derived vascular progenitor cells capable of endothelial and smooth muscle cell function. Exp Hematol *38*, 246-257 e241.

Ho, A.D., Wagner, W., and Franke, W. (2008). Heterogeneity of mesenchymal stromal cell preparations. Cytotherapy *10*, 320-330.

Hoffman, M.P., Kibbey, M.C., Letterio, J.J., and Kleinman, H.K. (1996). Role of laminin-1 and TGF-beta 3 in acinar differentiation of a human submandibular gland cell line (HSG). J Cell Sci *109 (Pt 8)*, 2013-2021.

Holderfield, M.T., Henderson Anderson, A.M., Kokubo, H., Chin, M.T., Johnson, R.L., and Hughes, C.C. (2006). HESR1/CHF2 suppresses VEGFR2 transcription independent of binding to E-boxes. Biochem Biophys Res Commun *346*, 637-648.

Hollenbeck, S.T., Itoh, H., Louie, O., Faries, P.L., Liu, B., and Kent, K.C. (2004). Type I collagen synergistically enhances PDGF-induced smooth muscle cell proliferation through pp60src-dependent crosstalk between the alpha2beta1 integrin and PDGFbeta receptor. Biochem Biophys Res Commun *325*, 328-337.

Holthofer, H., Virtanen, I., Kariniemi, A.L., Hormia, M., Linder, E., and Miettinen, A. (1982). Ulex europaeus I lectin as a marker for vascular endothelium in human tissues. Lab Invest *47*, 60-66.

Hong, J.H., Hwang, E.S., McManus, M.T., Amsterdam, A., Tian, Y., Kalmukova, R., Mueller, E., Benjamin, T., Spiegelman, B.M., Sharp, P.A., . (2005). TAZ, a transcriptional modulator of mesenchymal stem cell differentiation. Science *309*, 1074-1078.

Hordijk, P.L., Anthony, E., Mul, F.P., Rientsma, R., Oomen, L.C., and Roos, D. (1999). Vascular-endothelial-cadherin modulates endothelial monolayer permeability. J Cell Sci *112 (Pt 12)*, 1915-1923.

Horwitz, E.M., Le Blanc, K., Dominici, M., Mueller, I., Slaper-Cortenbach, I., Marini, F.C., Deans, R.J., Krause, D.S., and Keating, A. (2005). Clarification of the nomenclature for

MSC: The International Society for Cellular Therapy position statement. Cytotherapy *7*, 393-395.

Hu, Y., Bock, G., Wick, G., and Xu, Q. (1998). Activation of PDGF receptor alpha in vascular smooth muscle cells by mechanical stress. FASEB J *12*, 1135-1142.

Huang, P.P., Li, S.Z., Han, M.Z., Xiao, Z.J., Yang, R.C., Qiu, L.G., and Han, Z.C. (2004). Autologous transplantation of peripheral blood stem cells as an effective therapeutic approach for severe arteriosclerosis obliterans of lower extremities. Thromb Haemost *91*, 606-609.

Huang, N.F., and Li, S. (2008). Mesenchymal stem cells for vascular regeneration. Regen Med *3*, 877-892.

Huang, G.T., Gronthos, S., and Shi, S. (2009). Mesenchymal stem cells derived from dental tissues vs. those from other sources: their biology and role in regenerative medicine. J Dent Res *88*, 792-806.

Hung, S.C., Deng, W.P., Yang, W.K., Liu, R.S., Lee, C.C., Su, T.C., Lin, R.J., Yang, D.M., Chang, C.W., Chen, W.H., . (2005). Mesenchymal stem cell targeting of microscopic tumors and tumor stroma development monitored by noninvasive in vivo positron emission tomography imaging. Clin Cancer Res *11*, 7749-7756.

Hunziker, E.B. (2000). Articular cartilage repair: problems and perspectives. Biorheology *37*, 163-164.

Hutley, L.J., Herington, A.C., Shurety, W., Cheung, C., Vesey, D.A., Cameron, D.P., and Prins, J.B. (2001). Human adipose tissue endothelial cells promote preadipocyte proliferation. Am J Physiol Endocrinol Metab *281*, E1037-1044.

Huusko, J., Merentie, M., Dijkstra, M.H., Ryhanen, M.M., Karvinen, H., Rissanen, T.T., Vanwildemeersch, M., Hedman, M., Lipponen, J., Heinonen, S.E., Eriksson, U., Shibuya, M., Yla-Herttuala, S. (2009). The effects of VEGF-R1 and VEGF-R2 ligands on angiogenic responses and left ventricular function in mice. Cardiovasc Res *86*, 122-130.

Hwang, N.S., Varghese, S., Puleo, C., Zhang, Z., and Elisseeff, J. (2007). Morphogenetic signals from chondrocytes promote chondrogenic and osteogenic differentiation of mesenchymal stem cells. J Cell Physiol *212*, 281-284.

Iba, O., Matsubara, H., Nozawa, Y., Fujiyama, S., Amano, K., Mori, Y., Kojima, H., and Iwasaka, T. (2002). Angiogenesis by implantation of peripheral blood mononuclear cells and platelets into ischemic limbs. Circulation *106*, 2019-2025.

Ishida, A., Murray, J., Saito, Y., Kanthou, C., Benzakour, O., Shibuya, M., and Wijelath, E.S. (2001). Expression of vascular endothelial growth factor receptors in smooth muscle cells. J Cell Physiol *188*, 359-368.

Jackson, L., Jones, D.R., Scotting, P., and Sottile, V. (2007). Adult mesenchymal stem cells: differentiation potential and therapeutic applications. J Postgrad Med *53*, 121-127.

Jager, M., Feser, T., Denck, H., and Krauspe, R. (2005). Proliferation and osteogenic differentiation of mesenchymal stem cells cultured onto three different polymers in vitro. Ann Biomed Eng *33*, 1319-1332.

Jakkaraju, S., Zhe, X., Pan, D., Choudhury, R., and Schuger, L. (2005). TIPs are tension-responsive proteins involved in myogenic versus adipogenic differentiation. Dev Cell *9*, 39-49.

Jakobsson, L., Kreuger, J., and Claesson-Welsh, L. (2007). Building blood vessels--stem cell models in vascular biology. J Cell Biol *177*, 751-755.

Jakobsson, L., Bentley, K., and Gerhardt, H. (2009). VEGFRs and Notch: a dynamic collaboration in vascular patterning. Biochem Soc Trans *37*, 1233-1236.

James, D., Nam, H.S., Seandel, M., Nolan, D., Janovitz, T., Tomishima, M., Studer, L., Lee, G., Lyden, D., Benezra, R., . Expansion and maintenance of human embryonic stem cell-derived endothelial cells by TGFbeta inhibition is Id1 dependent. Nat Biotechnol *28*, 161-166.

Jin, S., Hansson, E.M., Tikka, S., Lanner, F., Sahlgren, C., Farnebo, F., Baumann, M., Kalimo, H., and Lendahl, U. (2008). Notch signaling regulates platelet-derived growth factor receptor-beta expression in vascular smooth muscle cells. Circ Res *102*, 1483-1491.

Johnson, A.R., and Erdos, E.G. (1977). Metabolism of vasoactive peptides by human endothelial cells in culture. Angiotensin I converting enzyme (kininase II) and angiotensinase. J Clin Invest *59*, 684-695.

Kaltz, N., Ringe, J., Holzwarth, C., Charbord, P., Niemeyer, M., Jacobs, V.R., Peschel, C., Haupl, T., and Oostendorp, R.A. (2010). Novel markers of mesenchymal stem cells defined by genome-wide gene expression analysis of stromal cells from different sources. Exp Cell Res *316*, 2609-2617.

Kearney, J.B., Ambler, C.A., Monaco, K.A., Johnson, N., Rapoport, R.G., and Bautch, V.L. (2002). Vascular endothelial growth factor receptor Flt-1 negatively regulates developmental blood vessel formation by modulating endothelial cell division. Blood *99*, 2397-2407.

Khakoo, A.Y., and Finkel, T. (2005). Endothelial progenitor cells. Annual Rev Med *56*, 79-101.

Kibbey, M.C., Royce, L.S., Dym, M., Baum, B.J., and Kleinman, H.K. (1992). Glandular-like morphogenesis of the human submandibular tumor cell line A253 on basement membrane components. Exp Cell Res *198*, 343-351.

Kim, C.F., Jackson, E.L., Woolfenden, A.E., Lawrence, S., Babar, I., Vogel, S., Crowley, D., Bronson, R.T., and Jacks, T. (2005a). Identification of bronchioalveolar stem cells in normal lung and lung cancer. Cell *121*, 823-835.

Kim, I., Yilmaz, O.H., and Morrison, S.J. (2005b). CD144 (VE-cadherin) is transiently expressed by fetal liver hematopoietic stem cells. Blood *106*, 903-905.

Kim, V.N. (2005c). MicroRNA biogenesis: coordinated cropping and dicing. Nat Rev Mol Cell Biol *6*, 376-385.

Kim, H.K., Lee, Y.S., Sivaprasad, U., Malhotra, A., and Dutta, A. (2006). Muscle-specific microRNA miR-206 promotes muscle differentiation. J Cell Biol *174*, 677-687.

Kinnaird, T., Stabile, E., Burnett, M.S., Shou, M., Lee, C.W., Barr, S., Fuchs, S., and Epstein, S.E. (2004). Local delivery of marrow-derived stromal cells augments collateral perfusion through paracrine mechanisms. Circulation *109*, 1543-1549.

Kinner, B., Zaleskas, J.M., and Spector, M. (2002). Regulation of smooth muscle actin expression and contraction in adult human mesenchymal stem cells. Exp Cell Res *278*, 72-83.

Kleinman, H.K., Graf, J., Iwamoto, Y., Kitten, G.T., Ogle, R.C., Sasaki, M., Yamada, Y., Martin, G.R., and Luckenbill-Edds, L. (1987). Role of basement membranes in cell differentiation. Ann N Y Acad Sci *513*, 134-145.

Kleinman, H.K., and Martin, G.R. (2005). Matrigel: basement membrane matrix with biological activity. Semin Cancer Biol *15*, 378-386.

Kliche, S., and Waltenberger, J. (2001). VEGF receptor signaling and endothelial function. IUBMB Life *52*, 61-66.

Klinghoffer, R.A., Mueting-Nelsen, P.F., Faerman, A., Shani, M., and Soriano, P. (2001). The two PDGF receptors maintain conserved signaling in vivo despite divergent embryological functions. Mol Cell *7*, 343-354.

Kobayashi, N., Yasu, T., Ueba, H., Sata, M., Hashimoto, S., Kuroki, M., Saito, M., and Kawakami, M. (2004). Mechanical stress promotes the expression of smooth muscle-like properties in marrow stromal cells. Exp Hematol *32*, 1238-1245.

Koblas, T., Zacharovova, K., Berkova, Z., Mindlova, M., Girman, P., Dovolilova, E., Karasova, L., and Saudek, F. (2007). Isolation and characterization of human CXCR4-positive pancreatic cells. Folia Biol (Praha) *53*, 13-22.

Kolf, C.M., Cho, E., and Tuan, R.S. (2007). Mesenchymal stromal cells. Biology of adult mesenchymal stem cells: regulation of niche, self-renewal and differentiation. Arthritis Res Ther *9*, 204.

Koolwijk, P., Peters, E., van der Vecht, B., Hornig, C., Weich, H.A., Alitalo, K., Hicklin, D.J., Wu, Y., Witte, L., and van Hinsbergh, V.W. (2001). Involvement of VEGFR2 (kdr/flk-1) but not VEGFR1 (flt-1) in VEGF-A and VEGF-C-induced tube formation by human microvascular endothelial cells in fibrin matrices in vitro. Angiogenesis *4*, 53-60.

Krampera, M., Pasini, A., Rigo, A., Scupoli, M.T., Tecchio, C., Malpeli, G., Scarpa, A., Dazzi, F., Pizzolo, G., and Vinante, F. (2005). HB-EGF/HER-1 signaling in bone marrow mesenchymal stem cells: inducing cell expansion and reversibly preventing multilineage differentiation. Blood *106*, 59-66.

Kubota, Y., Kleinman, H.K., Martin, G.R., and Lawley, T.J. (1988). Role of laminin and basement membrane in the morphological differentiation of human endothelial cells into capillary-like structures. J Cell Biol *107*, 1589-1598.

Kuhn, N.Z., and Tuan, R.S. Regulation of stemness and stem cell niche of mesenchymal stem cells: implications in tumorigenesis and metastasis. J Cell Physiol *222*, 268-277.

Kumar, S., Chanda, D., and Ponnazhagan, S. (2008). Therapeutic potential of genetically modified mesenchymal stem cells. Gene Ther *15*, 711-715.

Kundu, A.K., and Putnam, A.J. (2006). Vitronectin and collagen I differentially regulate osteogenesis in mesenchymal stem cells. Biochem Biophys Res Commun *347*, 347-357.

Kurpinski, K., Lam, H., Chu, J., Wang, A., Kim, A., Tsay, E., Agrawal, S., Schaffer, D.V., and Li, S. (2010). Transforming growth factor-beta and notch signaling mediate stem cell differentiation into smooth muscle cells. Stem Cells *28*, 734-742.

Lampugnani, M.G., Corada, M., Andriopoulou, P., Esser, S., Risau, W., and Dejana, E. (1997). Cell confluence regulates tyrosine phosphorylation of adherens junction components in endothelial cells. J Cell Sci *110 (Pt 17)*, 2065-2077.

Lampugnani, M.G., Orsenigo, F., Gagliani, M.C., Tacchetti, C., and Dejana, E. (2006). Vascular endothelial cadherin controls VEGFR2 internalization and signaling from intracellular compartments. J Cell Biol *174*, 593-604.

Lancrin, C., Sroczynska, P., Stephenson, C., Allen, T., Kouskoff, V., and

Lacaud, G. (2009). The haemangioblast generates haematopoietic cells through a haemogenic endothelium stage. Nature *457*, 892-895.

Lawson, N.D., Scheer, N., Pham, V.N., Kim, C.H., Chitnis, A.B., Campos-Ortega, J.A., and Weinstein, B.M. (2001). Notch signaling is required for arterial-venous differentiation during embryonic vascular development. Development *128*, 3675-3683.

Lehti, K., Allen, E., Birkedal-Hansen, H., Holmbeck, K., Miyake, Y., Chun, T.H., and Weiss, S.J. (2005). An MT1-MMP-PDGF receptor-beta axis regulates mural cell investment of the microvasculature. Genes Dev *19*, 979-991.

Leri, A., Kajstura, J., and Anversa, P. (2005). Cardiac stem cells and mechanisms of myocardial regeneration. Physiol Rev *85*, 1373-1416.

Leveen, P., Pekny, M., Gebre-Medhin, S., Swolin, B., Larsson, E., and Betsholtz, C. (1994). Mice deficient for PDGF B show renal, cardiovascular, and hematological abnormalities. Genes Dev *8*, 1875-1887.

Levenberg, S., Golub, J.S., Amit, M., Itskovitz-Eldor, J., and Langer, R. (2002). Endothelial cells derived from human embryonic stem cells. Proc Natl Acad Sci U S A *99*, 4391-4396.

Li, M.L., Aggeler, J., Farson, D.A., Hatier, C., Hassell, J., and Bissell, M.J. (1987). Influence of a reconstituted basement membrane and its components on casein gene expression and secretion in mouse mammary epithelial cells. Proc Natl Acad Sci U S A *84*, 136-140.

Li, J., Huang, S., Armstrong, E.A., Fowler, J.F., and Harari, P.M. (2005). Angiogenesis and radiation response modulation after vascular endothelial growth factor receptor-2 (VEGFR2) blockade. Int J Radiat Oncol Biol Phys *62*, 1477-1485.

Li, H., Yu, B., Zhang, Y., Pan, Z., and Xu, W. (2006). Jagged1 protein enhances the differentiation of mesenchymal stem cells into cardiomyocytes. Biochem Biophys Res Commun *341*, 320-325.

Li, X., Claesson-Welsh, L., and Shibuya, M. (2008a). VEGF receptor signal transduction. Methods Enzymol *443*, 261-284.

Li, Z., Suzuki, Y., Huang, M., Cao, F., Xie, X., Connolly, A.J., Yang, P.C., and Wu, J.C. (2008b). Comparison of reporter gene and iron particle labeling for tracking fate of human embryonic stem cells and differentiated endothelial cells in living subjects. Stem Cells *26*, 864-873.

Li, Q., Yao, D., Ma, J., Zhu, J., Xu, X., Ren, Y., Ding, X., and Mao, X. (2009a). Transplantation of MSCs in Combination with Netrin-1 Improves Neoangiogenesis in a Rat Model of Hind Limb Ischemia. J Surg Res. Epub ahead of print.

Li, Z., Han, Z., and Wu, J.C. (2009b). Transplantation of human embryonic stem cell-derived endothelial cells for vascular diseases. J Cell Biochem *106*, 194-199.

Liechty, K.W., MacKenzie, T.C., Shaaban, A.F., Radu, A., Moseley, A.M., Deans, R., Marshak, D.R., and Flake, A.W. (2000). Human mesenchymal stem cells engraft and demonstrate site-specific differentiation after in utero transplantation in sheep. Nat Med *6*, 1282-1286.

Longobardi, L., Torello, M., Buckway, C., O'Rear, L., Horton, W.A., Hwa, V., Roberts, C.T., Jr., Chiarelli, F., Rosenfeld, R.G., and Spagnoli, A. (2003). A novel insulin-like growth factor (IGF)-independent role for IGF binding protein-3 in mesenchymal chondroprogenitor cell apoptosis. Endocrinology *144*, 1695-1702.

Longobardi, L., O'Rear, L., Aakula, S., Johnstone, B., Shimer, K., Chytil, A., Horton, W.A., Moses, H.L., and Spagnoli, A. (2006). Effect of IGF-I in the chondrogenesis of bone marrow mesenchymal stem cells in the presence or absence of TGF-beta signaling. J Bone Miner Res *21*, 626-636.

Lozito, T.P., Kuo, C.K., Taboas, J.M., and Tuan, R.S. (2009a). Human mesenchymal stem cells express vascular cell phenotypes upon interaction with endothelial cell matrix. J Cell Biochem *107*, 714-722.

Lozito, T.P., Taboas, J.M., Kuo, C.K., and Tuan, R.S. (2009b). Mesenchymal stem cell modification of endothelial matrix regulates their vascular differentiation. J Cell Biochem *107*, 706-713.

Mace, K.A., Restivo, T.E., Rinn, J.L., Paquet, A.C., Chang, H.Y., Young, D.M., and Boudreau, N.J. (2009). HOXA3 modulates injury-induced mobilization and recruitment of bone marrow-derived cells. Stem Cells *27*, 1654-1665.

Mamdouh, Z., Chen, X., Pierini, L.M., Maxfield, F.R., and Muller, W.A. (2003). Targeted recycling of PECAM from endothelial surface-connected compartments during diapedesis. Nature *421*, 748-753.

Markwald, R.R. (1987). Role of extracellular matrix in morphogenesis. Mead Johnson Symp Perinat Dev Med, 7-13.

Matsumoto, T., and Claesson-Welsh, L. (2001). VEGF receptor signal transduction. Sci STKE *2001*, re21.

Matsumoto, T., and Mugishima, H. (2006). Signal transduction via vascular endothelial growth factor (VEGF) receptors and their roles in atherogenesis. J Atheroscler Thromb *13*, 130-135.

Mauck, R.L., Yuan, X., and Tuan, R.S. (2006). Chondrogenic differentiation and functional maturation of bovine mesenchymal stem cells in long-term agarose culture. Osteoarthritis Cartilage *14*, 179-189.

McBeath, R., Pirone, D.M., Nelson, C.M., Bhadriraju, K., and Chen, C.S. (2004). Cell shape, cytoskeletal tension, and RhoA regulate stem cell lineage commitment. Dev Cell *6*, 483-495.

McCloskey, K.E., Smith, D.A., Jo, H., and Nerem, R.M. (2006). Embryonic stem cell-derived endothelial cells may lack complete functional maturation in vitro. J Vasc Res *43*, 411-421.

McHale, J.F., Harari, O.A., Marshall, D., and Haskard, D.O. (1999). TNF-alpha and IL-1 sequentially induce endothelial ICAM-1 and VCAM-1 expression in MRL/lpr lupus-prone mice. J Immunol *163*, 3993-4000.

Mimeault, M., and Batra, S.K. (2006). Concise review: recent advances on the significance of stem cells in tissue regeneration and cancer therapies. Stem Cells *24*, 2319-2345.

Mimeault, M., Hauke, R., and Batra, S.K. (2007). Stem cells: a revolution in therapeutics-recent advances in stem cell biology and their therapeutic applications in regenerative medicine and cancer therapies. Clin Pharmacol Ther *82*, 252-264.

Mittar, S., Ulyatt, C., Howell, G.J., Bruns, A.F., Zachary, I., Walker, J.H., and Ponnambalam, S. (2009). VEGFR1 receptor tyrosine kinase localization to the Golgi apparatus is calcium-dependent. Exp Cell Res *315*, 877-889.

Miura, M., Miura, Y., Sonoyama, W., Yamaza, T., Gronthos, S., and Shi, S. (2006). Bone marrow-derived mesenchymal stem cells for regenerative medicine in craniofacial region. Oral Dis *12*, 514-522.

Moore, M.A., Hattori, K., Heissig, B., Shieh, J.H., Dias, S., Crystal, R.G., and Rafii, S. (2001). Mobilization of endothelial and hematopoietic stem and progenitor cells by adenovector-mediated elevation of serum levels of SDF-1, VEGF, and angiopoietin-1. Ann N Y Acad Sci *938*, 36-45; discussion 45-37.

Moore, M.A. (2002). Putting the neo into neoangiogenesis. J Clin Invest *109*, 313-315.

Moore, K.A., and Lemischka, I.R. (2006). Stem cells and their niches. Science *311*, 1880-1885.

Mukherjee, S., Tessema, M., and Wandinger-Ness, A. (2006). Vesicular trafficking of tyrosine kinase receptors and associated proteins in the regulation of signaling and vascular function. Circ Res *98*, 743-756.

Mumm, J.S., and Kopan, R. (2000). Notch signaling: from the outside in. Dev Biol *228*, 151-165.

Munoz-Chapuli, R., Quesada, A.R., and Angel Medina, M. (2004). Angiogenesis and signal transduction in endothelial cells. Cell Mol Life Sci *61*, 2224-2243.

Nagaya, N., Fujii, T., Iwase, T., Ohgushi, H., Itoh, T., Uematsu, M., Yamagishi, M., Mori, H., Kangawa, K., and Kitamura, S. (2004). Intravenous administration of mesenchymal stem cells improves cardiac function in rats with acute myocardial infarction through angiogenesis and myogenesis. Am J Physiol Heart Circ Physiol *287*, H2670-2676.

Neumann, K., Endres, M., Ringe, J., Flath, B., Manz, R., Haupl, T., Sittinger, M., and Kaps, C. (2007). BMP7 promotes adipogenic but not osteo-/chondrogenic differentiation of adult human bone marrow-derived stem cells in high-density micro-mass culture. J Cell Biochem *102*, 626-637.

Newman, P.J., and Newman, D.K. (2003). Signal transduction pathways mediated by PECAM-1: new roles for an old molecule in platelet and vascular cell biology. Arterioscler Thromb Vasc Biol *23*, 953-964.

Nerem, R.M., and Seliktar, D. (2001). Vascular tissue engineering. Annu Rev Biomed Eng *3*, 225-243.

Nikolova-Krstevski, V., Bhasin, M., Otu, H.H., Libermann, T., and Oettgen, P. (2008). Gene expression analysis of embryonic stem cells expressing VE-cadherin (CD144) during endothelial differentiation. BMC Genomics *9*, 240.

Nimmagadda, S., Geetha-Loganathan, P., Scaal, M., Christ, B., and Huang, R. (2007). FGFs, Wnts and BMPs mediate induction of VEGFR2 (Quek-1) expression during avian somite development. Dev Biol *305*, 421-429.

Nussbaum, J., Minami, E., Laflamme, M.A., Virag, J.A., Ware, C.B., Masino, A., Muskheli, V., Pabon, L., Reinecke, H., and Murry, C.E. (2007). Transplantation of undifferentiated murine embryonic stem cells in the heart: teratoma formation and immune response. FASEB J *21*, 1345-1357.

O'Cearbhaill, E.D., Murphy, M., Barry, F., McHugh, P.E., and Barron, V. (2010) Behavior of human mesenchymal stem cells in fibrin-based vascular tissue engineering constructs. Ann Biomed Eng *38*, 649-657.

Ohata, E., Tadokoro, R., Sato, Y., Saito, D., and Takahashi, Y. (2009). Notch signal is sufficient to direct an endothelial conversion from non-endothelial somitic cells conveyed to the aortic region by CXCR4. Dev Biol *335*, 33-42.

Oldershaw, R.A., Tew, S.R., Russell, A.M., Meade, K., Hawkins, R., McKay, T.R., Brennan, K.R., and Hardingham, T.E. (2008). Notch signaling through Jagged-1 is necessary to initiate chondrogenesis in human bone marrow stromal cells but must be switched off to complete chondrogenesis. Stem Cells *26*, 666-674.

Oliver, C., Waters, J.F., Tolbert, C.L., and Kleinman, H.K. (1987). Culture of parotid acinar cells on a reconstituted basement membrane substratum. J Dent Res *66*, 594-595.

Olsson, A.K., Dimberg, A., Kreuger, J., and Claesson-Welsh, L. (2006). VEGF receptor signalling - in control of vascular function. Nat Rev Mol Cell Biol *7*, 359-371.

Opherk, C., Duering, M., Peters, N., Karpinska, A., Rosner, S., Schneider, E., Bader, B., Giese, A., and Dichgans, M. (2009). CADASIL mutations enhance spontaneous multimerization of NOTCH3. Hum Mol Genet *18*, 2761-2767.

Oswald, J., Boxberger, S., Jorgensen, B., Feldmann, S., Ehninger, G., Bornhauser, M., and Werner, C. (2004). Mesenchymal stem cells can be differentiated into endothelial cells in vitro. Stem Cells *22*, 377-384.

Owens, G.K. (1995). Regulation of differentiation of vascular smooth muscle cells. Physiol Rev *75*, 487-517.

Park, J.S., Chu, J.S., Cheng, C., Chen, F., Chen, D., and Li, S. (2004). Differential effects of equiaxial and uniaxial strain on mesenchymal stem cells. Biotechnol Bioeng *88*, 359-368.

Patel, N.S., Li, J.L., Generali, D., Poulsom, R., Cranston, D.W., and Harris, A.L. (2005). Up-regulation of delta-like 4 ligand in human tumor vasculature and the role of basal expression in endothelial cell function. Cancer Res *65*, 8690-8697.

Peault, B., Rudnicki, M., Torrente, Y., Cossu, G., Tremblay, J.P., Partridge, T., Gussoni, E., Kunkel, L.M., and Huard, J. (2007). Stem and progenitor cells in skeletal muscle development, maintenance, and therapy. Mol Ther *15*, 867-877.

Phinney, D.G., and Prockop, D.J. (2007a). Concise review: mesenchymal stem/multipotent stromal cells: the state of transdifferentiation and modes of tissue repair--current views. Stem Cells *25*, 2896-2902.

Phinney, D.G. (2007b). Biochemical heterogeneity of mesenchymal stem cell populations: clues to their therapeutic efficacy. Cell Cycle *6*, 2884-2889.

Phng, L.K., Potente, M., Leslie, J.D., Babbage, J., Nyqvist, D., Lobov, I., Ondr, J.K., Rao, S., Lang, R.A., Thurston, G.*,* . (2009). Nrarp coordinates endothelial Notch and Wnt signaling to control vessel density in angiogenesis. Dev Cell *16*, 70-82.

Pinkney, J.H., Stehouwer, C.D., Coppack, S.W., and Yudkin, J.S. (1997). Endothelial dysfunction: cause of the insulin resistance syndrome. Diabetes *46 Suppl 2*, S9-13.

Pittenger, M.F., Mackay, A.M., Beck, S.C., Jaiswal, R.K., Douglas, R., Mosca, J.D., Moorman, M.A., Simonetti, D.W., Craig, S., and Marshak, D.R. (1999). Multilineage potential of adult human mesenchymal stem cells. Science *284*, 143-147.

Pober, J.S., Gimbrone, M.A., Jr., Lapierre, L.A., Mendrick, D.L., Fiers, W., Rothlein, R., and Springer, T.A. (1986). Overlapping patterns of activation of human endothelial cells

by interleukin 1, tumor necrosis factor, and immune interferon. J Immunol *137*, 1893-1896.

Ponce, M.L., Nomizu, M., Delgado, M.C., Kuratomi, Y., Hoffman, M.P., Powell, S., Yamada, Y., Kleinman, H.K., and Malinda, K.M. (1999). Identification of endothelial cell binding sites on the laminin gamma 1 chain. Circ Res *84*, 688-694.

Potier, E., Ferreira, E., Andriamanalijaona, R., Pujol, J.P., Oudina, K., Logeart-Avramoglou, D., and Petite, H. (2007). Hypoxia affects mesenchymal stromal cell osteogenic differentiation and angiogenic factor expression. Bone *40*, 1078-1087.

Prokopi, M., Pula, G., Mayr, U., Devue, C., Gallagher, J., Xiao, Q., Boulanger, C.M., Westwood, N., Urbich, C., Willeit, J.*, .* (2009). Proteomic analysis reveals presence of platelet microparticles in endothelial progenitor cell cultures. Blood *114*, 723-732.

Quillard, T., Devalliere, J., Chatelais, M., Coulon, F., Seveno, C., Romagnoli, M., Barille Nion, S., and Charreau, B. (2009). Notch2 signaling sensitizes endothelial cells to apoptosis by negatively regulating the key protective molecule survivin. PLoS One *4*, e8244.

Rafii, S., Heissig, B., and Hattori, K. (2002). Efficient mobilization and recruitment of marrow-derived endothelial and hematopoietic stem cells by adenoviral vectors expressing angiogenic factors. Gene Ther *9*, 631-641.

Rahimi, N., and Kazlauskas, A. (1999). A role for cadherin-5 in regulation of vascular endothelial growth factor receptor 2 activity in endothelial cells. Mol Biol Cell *10*, 3401-3407.

Rand, M.D., Lindblom, A., Carlson, J., Villoutreix, B.O., and Stenflo, J. (1997). Calcium binding to tandem repeats of EGF-like modules. Expression and characterization of the EGF-like modules of human Notch-1 implicated in receptor-ligand interactions. Protein Sci *6*, 2059-2071.

Rand, M.D., Grimm, L.M., Artavanis-Tsakonas, S., Patriub, V., Blacklow, S.C., Sklar, J., and Aster, J.C. (2000). Calcium depletion dissociates and activates heterodimeric notch receptors. Mol Cell Biol *20*, 1825-1835.

RayChaudhury, A., Elkins, M., Kozien, D., and Nakada, M.T. (2001). Regulation of PECAM-1 in endothelial cells during cell growth and migration. Exp Biol Med (Maywood) *226*, 686-691.

Reddi, A.H. (1994). Bone and cartilage differentiation. Curr Opin Genet Dev *4*, 737-744.

Reddy, K., Zhou, Z., Schadler, K., Jia, S.F., and Kleinerman, E.S. (2008). Bone marrow subsets differentiate into endothelial cells and pericytes contributing to Ewing's tumor vessels. Mol Cancer Res *6*, 929-936.

Ren, H., Cao, Y., Zhao, Q., Li, J., Zhou, C., Liao, L., Jia, M., Cai, H., Han, Z.C., Yang, R.*, .* (2006). Proliferation and differentiation of bone marrow stromal cells under hypoxic conditions. Biochem Biophys Res Commun *347*, 12-21.

Ribatti, D., Nico, B., Vacca, A., and Presta, M. (2006). The gelatin sponge-chorioallantoic membrane assay. Nat Protoc *1*, 85-91.

Ribatti, D. (2007). The discovery of endothelial progenitor cells. An historical review. Leuk Res *31*, 439-444.

Ridgway, J., Zhang, G., Wu, Y., Stawicki, S., Liang, W.C., Chanthery, Y., Kowalski, J., Watts, R.J., Callahan, C., Kasman, I.*, .* (2006). Inhibition of Dll4 signalling inhibits tumour growth by deregulating angiogenesis. Nature *444*, 1083-1087.

Riha, G.M., Lin, P.H., Lumsden, A.B., Yao, Q., and Chen, C. (2005). Review: application of stem cells for vascular tissue engineering. Tissue Eng *11*, 1535-1552.

Rival, Y., Del Maschio, A., Rabiet, M.J., Dejana, E., and Duperray, A. (1996). Inhibition of platelet endothelial cell adhesion molecule-1 synthesis and leukocyte transmigration in endothelial cells by the combined action of TNF-alpha and IFN-gamma. J Immunol *157*, 1233-1241.

Rodriguez, C., Slevin, M., Rodriguez-Calvo, R., Kumar, S., Krupinski, J., Tejerina, T., and Martinez-Gonzalez, J. (2009). Modulation of endothelium and endothelial progenitor cell function by low-density lipoproteins: implication for vascular repair, angiogenesis and vasculogenesis. Pathobiology *76*, 11-22.

Romero, L.I., Zhang, D.N., Herron, G.S., and Karasek, M.A. (1997). Interleukin-1 induces major phenotypic changes in human skin microvascular endothelial cells. J Cell Physiol *173*, 84-92.

Roorda, B.D., ter Elst, A., Kamps, W.A., and de Bont, E.S. (2009). Bone marrow-derived cells and tumor growth: contribution of bone marrow-derived cells to tumor micro-environments with special focus on mesenchymal stem cells. Crit Rev Oncol Hematol *69*, 187-198.

Rozen, S., and Skaletsky, H. (2000). Primer3 on the WWW for general users and for biologist programmers. Methods Mol Biol *132*, 365-386.

Sadler, J.E. (1998). Biochemistry and genetics of von Willebrand factor. Annu Rev Biochem *67*, 395-424.

Sainson, R.C., and Harris, A.L. (2006). Hypoxia-regulated differentiation: let's step it up a Notch. Trends Mol Med *12*, 141-143.

Sales, K.M., Salacinski, H.J., Alobaid, N., Mikhail, M., Balakrishnan, V., and Seifalian, A.M. (2005). Advancing vascular tissue engineering: the role of stem cell technology. Trends Biotechnol *23*, 461-467.

Salmonsson, L., Svensson, L., Pettersson, S., Wiklund, O., and Ohlsson, B.G. (2003). Oxidised LDL decreases VEGFR1 expression in human monocyte-derived macrophages. Atherosclerosis *169*, 259-267.

Santa Maria, L., Rojas, C.V., and Minguell, J.J. (2004). Signals from damaged but not undamaged skeletal muscle induce myogenic differentiation of rat bone-marrow-derived mesenchymal stem cells. Exp Cell Res *300*, 418-426.

Sarugaser, R., Hanoun, L., Keating, A., Stanford, W.L., and Davies, J.E. (2009). Human mesenchymal stem cells self-renew and differentiate according to a deterministic hierarchy. PLoS One *4*, e6498.

Sasaki, M., Abe, R., Fujita, Y., Ando, S., Inokuma, D., and Shimizu, H. (2008). Mesenchymal stem cells are recruited into wounded skin and contribute to wound repair by transdifferentiation into multiple skin cell type. J Immunol *180*, 2581-2587.

Satoh, H., Kishi, K., Tanaka, T., Kubota, Y., Nakajima, T., Akasaka, Y., and Ishii, T. (2004). Transplanted mesenchymal stem cells are effective for skin regeneration in acute cutaneous wounds. Cell Transplant *13*, 405-412.

Sawada, N., Tomomura, A., Sattler, C.A., Sattler, G.L., Kleinman, H.K., and Pitot, H.C. (1987). Effects of extracellular matrix components on the growth and differentiation of cultured rat hepatocytes. In Vitro Cell Dev Biol *23*, 267-273.

Scadden, D.T. (2006). The stem-cell niche as an entity of action. Nature *441*, 1075-1079.

Scaffidi, P., and Misteli, T. (2008). Lamin A-dependent misregulation of adult stem cells associated with accelerated ageing. Nat Cell Biol *10*, 452-459.

Schaffler, A., and Buchler, C. (2007). Concise review: adipose tissue-derived stromal cells--basic and clinical implications for novel cell-based therapies. Stem Cells *25*, 818-827.

Schick, P.K., Walker, J., Profeta, B., Denisova, L., and Bennett, V. (1997). Synthesis and secretion of von Willebrand factor and fibronectin in megakaryocytes at different phases of maturation. Arterioscler Thromb Vasc Biol *17*, 797-801.

Schlingemann, R.O., Rietveld, F.J., Kwaspen, F., van de Kerkhof, P.C., de Waal, R.M., and Ruiter, D.J. (1991). Differential expression of markers for endothelial cells, pericytes, and basal lamina in the microvasculature of tumors and granulation tissue. Am J Pathol *138*, 1335-1347.

Schmeisser, A., Garlichs, C.D., Zhang, H., Eskafi, S., Graffy, C., Ludwig, J., Strasser, R.H., and Daniel, W.G. (2001). Monocytes coexpress endothelial and macrophagocytic lineage markers and form cord-like structures in Matrigel under angiogenic conditions. Cardiovasc Res *49*, 671-680.

Schmeisser, A., Graffy, C., Daniel, W.G., and Strasser, R.H. (2003). Phenotypic overlap between monocytes and vascular endothelial cells. Adv Exp Med Biol *522*, 59-74.

Schuetz, E.G., Li, D., Omiecinski, C.J., Muller-Eberhard, U., Kleinman, H.K., Elswick, B., and Guzelian, P.S. (1988). Regulation of gene expression in adult rat hepatocytes cultured on a basement membrane matrix. J Cell Physiol *134*, 309-323.

Sekiya, I., Larson, B.L., Vuoristo, J.T., Cui, J.G., and Prockop, D.J. (2004). Adipogenic differentiation of human adult stem cells from bone marrow stroma (MSCs). J Bone Miner Res *19*, 256-264.

Shalaby, F., Rossant, J., Yamaguchi, T.P., Gertsenstein, M., Wu, X.F., Breitman, M.L., and Schuh, A.C. (1995). Failure of blood-island formation and vasculogenesis in Flk-1-deficient mice. Nature *376*, 62-66.

Shalaby, F., Ho, J., Stanford, W.L., Fischer, K.D., Schuh, A.C., Schwartz, L., Bernstein, A., and Rossant, J. (1997). A requirement for Flk1 in primitive and definitive hematopoiesis and vasculogenesis. Cell *89*, 981-990.

Shang, Y.C., Wang, S.H., Xiong, F., Zhao, C.P., Peng, F.N., Feng, S.W., Li, M.S., Li, Y., and Zhang, C. (2007). Wnt3a signaling promotes proliferation, myogenic differentiation, and migration of rat bone marrow mesenchymal stem cells. Acta Pharmacol Sin *28*, 1761-1774.

Shanti, R.M., Li, W.J., Nesti, L.J., Wang, X., and Tuan, R.S. (2007). Adult mesenchymal stem cells: biological properties, characteristics, and applications in maxillofacial surgery. J Oral Maxillofac Surg *65*, 1640-1647.

Shay-Salit, A., Shushy, M., Wolfovitz, E., Yahav, H., Breviario, F., Dejana, E., and Resnick, N. (2002). VEGF receptor 2 and the adherens junction as a mechanical transducer in vascular endothelial cells. Proc Natl Acad Sci U S A *99*, 9462-9467.

Shibuya, M. (2006a). Differential roles of vascular endothelial growth factor receptor-1 and receptor-2 in angiogenesis. J Biochem Mol Biol *39*, 469-478.

Shibuya, M. (2006b). Vascular endothelial growth factor receptor-1 (VEGFR1/Flt-1): a dual regulator for angiogenesis. Angiogenesis *9*, 225-230; discussion 231.

Shibuya, M. (2006c). Vascular endothelial growth factor (VEGF)-Receptor2: its biological functions, major signaling pathway, and specific ligand VEGF-E. Endothelium *13*, 63-69.

Shoji, T., Ii, M., Mifune, Y., Matsumoto, T., Kawamoto, A., Kwon, S.M., Kuroda, T., Kuroda, R., Kurosaka, M., and Asahara, T. (2010) Local transplantation of human multipotent adipose-derived stem cells accelerates fracture healing via enhanced osteogenesis and angiogenesis. Lab Invest *90*, 637-649.

Siekmann, A.F., Covassin, L., and Lawson, N.D. (2008). Modulation of VEGF signalling output by the Notch pathway. Bioessays *30*, 303-313.

Silva, G.V., Litovsky, S., Assad, J.A., Sousa, A.L., Martin, B.J., Vela, D., Coulter, S.C., Lin, J., Ober, J., Vaughn, W.K., . (2005). Mesenchymal stem cells differentiate into an endothelial phenotype, enhance vascular density, and improve heart function in a canine chronic ischemia model. Circulation *111*, 150-156.

Slater, B.J., Kwan, M.D., Gupta, D.M., Panetta, N.J., and Longaker, M.T. (2008). Mesenchymal cells for skeletal tissue engineering. Expert Opin Biol Ther *8*, 885-893.

Smadja, D.M., Bieche, I., Helley, D., Laurendeau, I., Simonin, G., Muller, L., Aiach, M., and Gaussem, P. (2007). Increased VEGFR2 expression during human late endothelial progenitor cells expansion enhances in vitro angiogenesis with up-regulation of integrin alpha(6). J Cell Mol Med *11*, 1149-1161.

Solursh, M., and Reiter, R.S. (1975). Determination of limb bud chondrocytes during a transient block of the cell cycle. Cell Differ *4*, 131-137.

Sone, M., Itoh, H., Yamahara, K., Yamashita, J.K., Yurugi-Kobayashi, T., Nonoguchi, A., Suzuki, Y., Chao, T.H., Sawada, N., Fukunaga, Y., . (2007). Pathway for differentiation of human embryonic stem cells to vascular cell components and their potential for vascular regeneration. Arterioscler Thromb Vasc Biol *27*, 2127-2134.

Soriano, P. (1994). Abnormal kidney development and hematological disorders in PDGF beta-receptor mutant mice. Genes Dev *8*, 1888-1896.

Sorrell, J.M., Baber, M.A., and Caplan, A.I. (2009). Influence of adult mesenchymal stem cells on in vitro vascular formation. Tissue Eng Part A *15*, 1751-1761.

Stack, M.S., Gray, R.D., and Pizzo, S.V. (1993). Modulation of murine B16F10 melanoma plasminogen activator production by a synthetic peptide derived from the laminin A chain. Cancer Res *53*, 1998-2004.

Stephan, S., Ball, S.G., Williamson, M., Bax, D.V., Lomas, A., Shuttleworth, C.A., and Kielty, C.M. (2006). Cell-matrix biology in vascular tissue engineering. J Anat *209*, 495-502.

Stojkovic, M., Lako, M., Strachan, T., and Murdoch, A. (2004). Derivation, growth and applications of human embryonic stem cells. Reproduction *128*, 259-267.

Stolberg, S., and McCloskey, K.E. (2009). Can shear stress direct stem cell fate? Biotechnol Prog *25*, 10-19.

Storgard, C., Mikolon, D., and Stupack, D.G. (2005). Angiogenesis assays in the chick CAM. Methods Mol Biol *294*, 123-136.

Studeny, M., Marini, F.C., Champlin, R.E., Zompetta, C., Fidler, I.J., and Andreeff, M. (2002). Bone marrow-derived mesenchymal stem cells as vehicles for interferon-beta delivery into tumors. Cancer Res *62*, 3603-3608.

Stupack, D.G., and Cheresh, D.A. (2004). Integrins and angiogenesis. Curr Top Dev Biol *64*, 207-238.

Suchting, S., Freitas, C., le Noble, F., Benedito, R., Breant, C., Duarte, A., and Eichmann, A. (2007). The Notch ligand Delta-like 4 negatively regulates endothelial tip cell formation and vessel branching. Proc Natl Acad Sci U S A *104*, 3225-3230.

Sweeney, C., Morrow, D., Birney, Y.A., Coyle, S., Hennessy, C., Scheller, A., Cummins, P.M., Walls, D., Redmond, E.M., and Cahill, P.A. (2004). Notch 1 and 3 receptor signaling modulates vascular smooth muscle cell growth, apoptosis, and migration via a CBF-1/RBP-Jk dependent pathway. FASEB J *18*, 1421-1423.

Swijnenburg, R.J., Tanaka, M., Vogel, H., Baker, J., Kofidis, T., Gunawan, F., Lebl, D.R., Caffarelli, A.D., de Bruin, J.L., Fedoseyeva, E.V., . (2005). Embryonic stem cell immunogenicity increases upon differentiation after transplantation into ischemic myocardium. Circulation *112*, I166-172.

Takahashi, T., Yamaguchi, S., Chida, K., and Shibuya, M. (2001). A single autophosphorylation site on KDR/Flk-1 is essential for VEGF-A-dependent activation of PLC-gamma and DNA synthesis in vascular endothelial cells. EMBO J *20*, 2768-2778.

Takahashi, H., and Shibuya, M. (2005). The vascular endothelial growth factor (VEGF)/VEGF receptor system and its role under physiological and pathological conditions. Clin Sci (Lond) *109*, 227-241.

Tang, Y.L. (2005a). Autologous mesenchymal stem cells for post-ischemic myocardial repair. Methods Mol Med *112*, 183-192.

Tang, Y.L., Zhao, Q., Qin, X., Shen, L., Cheng, L., Ge, J., and Phillips, M.I. (2005b). Paracrine action enhances the effects of autologous mesenchymal stem cell transplantation on vascular regeneration in rat model of myocardial infarction. Ann Thorac Surg *80*, 229-236; discussion 236-227.

Tang, J., Xie, Q., Pan, G., Wang, J., and Wang, M. (2006). Mesenchymal stem cells participate in angiogenesis and improve heart function in rat model of myocardial ischemia with reperfusion. Eur J Cardiothorac Surg *30*, 353-361.

Tanimoto, T., Lungu, A.O., and Berk, B.C. (2004). Sphingosine 1-phosphate transactivates the platelet-derived growth factor beta receptor and epidermal growth factor receptor in vascular smooth muscle cells. Circ Res *94*, 1050-1058.

Tateishi-Yuyama, E., Matsubara, H., Murohara, T., Ikeda, U., Shintani, S., Masaki, H., Amano, K., Kishimoto, Y., Yoshimoto, K., Akashi, H., . (2002). Therapeutic angiogenesis for patients with limb ischaemia by autologous transplantation of bone-marrow cells: a pilot study and a randomised controlled trial. Lancet *360*, 427-435.

Taylor, K.L., Henderson, A.M., and Hughes, C.C. (2002). Notch activation during endothelial cell network formation in vitro targets the basic HLH transcription factor HESR-1 and downregulates VEGFR2/KDR expression. Microvasc Res *64*, 372-383.

Tepper, O.M., Capla, J.M., Galiano, R.D., Ceradini, D.J., Callaghan, M.J., Kleinman, M.E., and Gurtner, G.C. (2005). Adult vasculogenesis occurs through in situ recruitment, proliferation, and tubulization of circulating bone marrow-derived cells. Blood *105*, 1068-1077.

Thurston, G., and Kitajewski, J. (2008). VEGF and Delta-Notch: interacting signalling pathways in tumour angiogenesis. Br J Cancer *99*, 1204-1209.

Toma, C., Pittenger, M.F., Cahill, K.S., Byrne, B.J., and Kessler, P.D. (2002). Human mesenchymal stem cells differentiate to a cardiomyocyte phenotype in the adult murine heart. Circulation *105*, 93-98.

Tomita, S., Mickle, D.A., Weisel, R.D., Jia, Z.Q., Tumiati, L.C., Allidina, Y., Liu, P., and Li, R.K. (2002). Improved heart function with myogenesis and angiogenesis after autologous porcine bone marrow stromal cell transplantation. J Thorac Cardiovasc Surg *123*, 1132-1140.

Tuan, R.S., Boland, G., and Tuli, R. (2003). Adult mesenchymal stem cells and cell-based tissue engineering. Arthritis Res Ther *5*, 32-45.

Uccelli, A., Pistoia, V., and Moretta, L. (2007). Mesenchymal stem cells: a new strategy for immunosuppression? Trends Immunol *28*, 219-226.

Urbich, C., and Dimmeler, S. (2004). Endothelial progenitor cells: characterization and role in vascular biology. Circ Res *95*, 343-353.

Uyttendaele, H., Marazzi, G., Wu, G., Yan, Q., Sassoon, D., and Kitajewski, J. (1996). Notch4/int-3, a mammary proto-oncogene, is an endothelial cell-specific mammalian Notch gene. Development *122*, 2251-2259.

van Tuyn, J., Knaan-Shanzer, S., van de Watering, M.J., de Graaf, M., van der Laarse, A., Schalij, M.J., van der Wall, E.E., de Vries, A.A., and Atsma, D.E. (2005). Activation of cardiac and smooth muscle-specific genes in primary human cells after forced expression of human myocardin. Cardiovasc Res *67*, 245-255.

van Vliet, P., Sluijter, J.P., Doevendans, P.A., and Goumans, M.J. (2007). Isolation and expansion of resident cardiac progenitor cells. Expert Rev Cardiovasc Ther *5*, 33-43.

Vecchi, M., Rudolph-Owen, L.A., Brown, C.L., Dempsey, P.J., and Carpenter, G. (1998). Tyrosine phosphorylation and proteolysis. Pervanadate-induced, metalloprotease-dependent cleavage of the ErbB-4 receptor and amphiregulin. J Biol Chem *273*, 20589-20595.

Vestweber, D. (2008). VE-cadherin: the major endothelial adhesion molecule controlling cellular junctions and blood vessel formation. Arterioscler Thromb Vasc Biol *28*, 223-232.

Vestweber, D., Winderlich, M., Cagna, G., and Nottebaum, A.F. (2009). Cell adhesion dynamics at endothelial junctions: VE-cadherin as a major player. Trends Cell Biol *19*, 8-15.

Villa, N., Walker, L., Lindsell, C.E., Gasson, J., Iruela-Arispe, M.L., and Weinmaster, G. (2001). Vascular expression of Notch pathway receptors and ligands is restricted to arterial vessels. Mech Dev *108*, 161-164.

Vincent, P.A., Xiao, K., Buckley, K.M., and Kowalczyk, A.P. (2004). VE-cadherin: adhesion at arm's length. Am J Physiol Cell Physiol *286*, C987-997.

Vogeli, K.M., Jin, S.W., Martin, G.R., and Stainier, D.Y. (2006). A common progenitor for haematopoietic and endothelial lineages in the zebrafish gastrula. Nature *443*, 337-339.

Voyta, J.C., Via, D.P., Butterfield, C.E., and Zetter, B.R. (1984). Identification and isolation of endothelial cells based on their increased uptake of acetylated-low density lipoprotein. J Cell Biol *99*, 2034-2040.

Vukicevic, S., Luyten, F.P., Kleinman, H.K., and Reddi, A.H. (1990). Differentiation of canalicular cell processes in bone cells by basement membrane matrix components: regulation by discrete domains of laminin. Cell *63*, 437-445.

Wakabayashi, K., Nagai, A., Sheikh, A.M., Shiota, Y., Narantuya, D., Watanabe, T., Masuda, J., Kobayashi, S., Kim, S.U., and Yamaguchi, S. Transplantation of human mesenchymal stem cells promotes functional improvement and increased expression of neurotrophic factors in a rat focal cerebral ischemia model. J Neurosci Res *88*, 1017-1025.

Wallez, Y., Vilgrain, I., and Huber, P. (2006). Angiogenesis: the VE-cadherin switch. Trends Cardiovasc Med *16*, 55-59.

Wallez, Y., Cand, F., Cruzalegui, F., Wernstedt, C., Souchelnytskyi, S., Vilgrain, I., and Huber, P. (2007). Src kinase phosphorylates vascular endothelial-cadherin in response to vascular endothelial growth factor: identification of tyrosine 685 as the unique target site. Oncogene *26*, 1067-1077.

Wang, T., Xu, Z., Jiang, W., and Ma, A. (2006). Cell-to-cell contact induces mesenchymal stem cell to differentiate into cardiomyocyte and smooth muscle cell. Int J Cardiol *109*, 74-81.

Wang, T.T., Tio, M., Lee, W., Beerheide, W., and Udolph, G. (2007a). Neural differentiation of mesenchymal-like stem cells from cord blood is mediated by PKA. Biochem Biophys Res Commun *357*, 1021-1027.

Wang, Z.Z., Au, P., Chen, T., Shao, Y., Daheron, L.M., Bai, H., Arzigian, M., Fukumura, D., Jain, R.K., and Scadden, D.T. (2007b). Endothelial cells derived from human embryonic stem cells form durable blood vessels in vivo. Nat Biotechnol *25*, 317-318.

Weibel, E.R., and Palade, G.E. (1964). New Cytoplasmic Components in Arterial Endothelia. J Cell Biol *23*, 101-112.

Westermark, B., Claesson-Welsh, L., and Heldin, C.H. (1990). Structural and functional aspects of platelet-derived growth factor and its receptors. Ciba Found Symp *150*, 6-14; discussion 14-22.

Wilson, A., and Trumpp, A. (2006). Bone-marrow haematopoietic-stem-cell niches. Nat Rev Immunol *6*, 93-106.

Woodard, A.S., Garcia-Cardena, G., Leong, M., Madri, J.A., Sessa, W.C., and Languino, L.R. (1998). The synergistic activity of alphavbeta3 integrin and PDGF receptor increases cell migration. J Cell Sci *111 (Pt 4)*, 469-478.

Woodfin, A., Voisin, M.B., and Nourshargh, S. (2007). PECAM-1: a multi-functional molecule in inflammation and vascular biology. Arterioscler Thromb Vasc Biol *27*, 2514-2523.

Worster, A.A., Nixon, A.J., Brower-Toland, B.D., and Williams, J. (2000). Effect of transforming growth factor beta1 on chondrogenic differentiation of cultured equine mesenchymal stem cells. Am J Vet Res *61*, 1003-1010.

Wu, X., Huang, L., Zhou, Q., Song, Y., Li, A., Jin, J., and Cui, B. (2005). Mesenchymal stem cells participating in ex vivo endothelium repair and its effect on vascular smooth muscle cells growth. Int J Cardiol *105*, 274-282.

Wu, Y., Chen, L., Scott, P.G., and Tredget, E.E. (2007). Mesenchymal stem cells enhance wound healing through differentiation and angiogenesis. Stem Cells *25*, 2648-2659.

Xaymardan, M., Tang, L., Zagreda, L., Pallante, B., Zheng, J., Chazen, J.L., Chin, A., Duignan, I., Nahirney, P., Rafii, S., . (2004). Platelet-derived growth factor-AB promotes the generation of adult bone marrow-derived cardiac myocytes. Circ Res *94*, E39-45.

Xiao, K., Allison, D.F., Kottke, M.D., Summers, S., Sorescu, G.P., Faundez, V., and Kowalczyk, A.P. (2003). Mechanisms of VE-cadherin processing and degradation in microvascular endothelial cells. J Biol Chem *278*, 19199-19208.

Xin, H., Kanehira, M., Mizuguchi, H., Hayakawa, T., Kikuchi, T., Nukiwa, T., and Saijo, Y. (2007). Targeted delivery of CX3CL1 to multiple lung tumors by mesenchymal stem cells. Stem Cells *25*, 1618-1626.

Xu, C., Inokuma, M.S., Denham, J., Golds, K., Kundu, P., Gold, J.D., and Carpenter, M.K. (2001). Feeder-free growth of undifferentiated human embryonic stem cells. Nat Biotechnol *19*, 971-974.

Xu, W., Zhang, X., Qian, H., Zhu, W., Sun, X., Hu, J., Zhou, H., and Chen, Y. (2004). Mesenchymal stem cells from adult human bone marrow differentiate into a cardiomyocyte phenotype in vitro. Exp Biol Med (Maywood) *229*, 623-631.

Xu, J., Liu, X., Chen, J., Zacharek, A., Cui, X., Savant-Bhonsale, S., Liu, Z., and Chopp, M. (2009). Simvastatin enhances bone marrow stromal cell differentiation into endothelial cells via notch signaling pathway. Am J Physiol Cell Physiol *296*, C535-543.

Xu, Y., Meng, H., Li, C., Hao, M., Wang, Y., Yu, Z., Li, Q., Han, J., Zhai, Q., and Qiu, L. (2010) Umbilical Cord Derived Mesenchymal Stem Cells Isolated by a Novel Explantation Technique Can Differentiate Into Functional Endothelial Cells and Promote Revascularization. Stem Cells Dev. Epub ahead of print.

Yamamoto, K., Sokabe, T., Watabe, T., Miyazono, K., Yamashita, J.K., Obi, S., Ohura, N., Matsushita, A., Kamiya, A., and Ando, J. (2005). Fluid shear stress induces differentiation of Flk-1-positive embryonic stem cells into vascular endothelial cells in vitro. Am J Physiol Heart Circ Physiol *288*, H1915-1924.

Yang, C., Zhang, Z.H., Li, Z.J., Yang, R.C., Qian, G.Q., and Han, Z.C. (2004). Enhancement of neovascularization with cord blood CD133+ cell-derived endothelial progenitor cell transplantation. Thromb Haemost *91*, 1202-1212.

Yanjie, J., Jiping, S., Yan, Z., Xiaofeng, Z., Boai, Z., and Yajun, L. (2007). Effects of Notch-1 signalling pathway on differentiation of marrow mesenchymal stem cells into neurons in vitro. Neuroreport *18*, 1443-1447.

Yoshida, T., Sinha, S., Dandre, F., Wamhoff, B.R., Hoofnagle, M.H., Kremer, B.E., Wang, D.Z., Olson, E.N., and Owens, G.K. (2003). Myocardin is a key regulator of CArG-dependent transcription of multiple smooth muscle marker genes. Circ Res *92*, 856-864.

Yue, W.M., Liu, W., Bi, Y.W., He, X.P., Sun, W.Y., Pang, X.Y., Gu, X.H., and Wang, X.P. (2008). Mesenchymal stem cells differentiate into an endothelial phenotype, reduce neointimal formation, and enhance endothelial function in a rat vein grafting model. Stem Cells Dev *17*, 785-793.

Zachos, T.A., Shields, K.M., and Bertone, A.L. (2006). Gene-mediated osteogenic differentiation of stem cells by bone morphogenetic proteins-2 or -6. J Orthop Res *24*, 1279-1291.

Zeng, L., Xiao, Q., Margariti, A., Zhang, Z., Zampetaki, A., Patel, S., Capogrossi, M.C., Hu, Y., and Xu, Q. (2006). HDAC3 is crucial in shear- and VEGF-induced stem cell differentiation toward endothelial cells. J Cell Biol *174*, 1059-1069.

Zhang, G., Zhou, J., Fan, Q., Zheng, Z., Zhang, F., Liu, X., and Hu, S. (2008). Arterial-venous endothelial cell fate is related to vascular endothelial growth factor and Notch status during human bone mesenchymal stem cell differentiation. FEBS Lett *582*, 2957-2964.

Zhang, K., Shi, B., Chen, J., Zhang, D., Zhu, Y., Zhou, C., Zhao, H., Jiang, X., and Xu, Z. (2010) Bone Marrow Mesenchymal Stem Cells Induce Angiogenesis and Promote Bladder Cancer Growth in a Rabbit Model. Urol Int *84*, 94-99.

Zhou, H., Lu, N., Chen, Z.Q., Song, Q.L., Yu, H.M., and Li, X.J. (2009). Osteopontin mediates dense culture-induced proliferation and adhesion of prostate tumour cells: role of protein kinase C, p38 mitogen-activated protein kinase and calcium. Basic Clin Pharmacol Toxicol *104*, 164-170.

Zimmerman, T.S., Dent, J.A., Ruggeri, Z.M., and Nannini, L.H. (1986). Subunit composition of plasma von Willebrand factor. Cleavage is present in normal individuals, increased in IIA and IIB von Willebrand disease, but minimal in variants with aberrant structure of individual oligomers (types IIC, IID, and IIE). J Clin Invest *77*, 947-951.

Zovein, A.C., and Iruela-Arispe, M.L. (2006). My O'Myeloid, a tale of two lineages. Proc Natl Acad Sci U S A *103*, 12959-12960.